

Integrated Regulation of Cardiac Fatty Acid and Glucose Oxidation

by

Tariq Altamimi

A thesis submitted in partial fulfillment of the requirements for the degree of

Doctor of Philosophy

Medical Sciences - Pediatrics
University of Alberta

© Tariq Altamimi, 2018

Abstract

Energy substrate utilization in the heart is both altered by- and contributes to- the pathophysiology of heart disease. For example, there is an increased reliance on fatty acid oxidation for energy production in conditions such as diabetes, diabetic cardiomyopathy, and during reperfusion of ischemic hearts. Fatty acids are less efficient energy substrates than glucose, and an increased use of fatty acids can increase the burden on energetically compromised hearts, contributing to cardiac dysfunction. Therefore, understanding the relationship between metabolism of fatty acids and glucose, the two major substrates competing for energy production in the heart, is essential to providing the knowledge required for developing new metabolic treatments to treat heart disease. Such therapies depend on targeting and modifying regulatory steps in this integrated relationship. To this aim, I explored in this thesis potential points of regulation of glucose and fatty acid oxidation at different levels and through several approaches. These included control of mitochondrial uptake of fatty acyl coenzyme A (CoA), mitochondrial calcium control of cardiac energy metabolism, control of fatty acid supply through endothelial cells, as well as the effects of a liver-secreted energy-modifying peptide hormone, adropin, on the regulation of fatty acid and glucose oxidation.

I first focused on exploring one regulatory process for mitochondrial fatty acid uptake, and hence oxidation, by investigating a potential cytosolic localization of an important metabolic enzyme, carnitine acetyltransferase (CrAT), known to reside in the mitochondrial and peroxisomal matrices. We found evidence of partial localization of CrAT in the cytosol of cardiomyocytes. This cytosolic CrAT could indirectly affect

malonyl-CoA turnover in the cytosol, thereby influencing malonyl-CoA control of mitochondrial uptake of long-chain fatty acyl-CoAs and their subsequent mitochondrial oxidation. These results add to our knowledge of the importance of CrAT in the regulation of cardiac energy metabolism through a previously undiscovered cytosolic activity.

We then assessed what changes in cardiac energy metabolism ensue in response to impairment of mitochondrial calcium uptake, which is presumed to control cellular glucose oxidation. This was studied in a transgenic mouse model with a cardiac-specific deficiency of the mitochondrial calcium uniporter (MCU) channel protein, the primary gate for calcium influx through the inner mitochondrial membrane. Contrary to our expectations, MCU deficient mouse hearts showed higher cardiac work and uninhibited glucose oxidation rates, and when subjected to an inotrope challenge they displayed a normal rise in glucose oxidation but a greater stimulation of fatty acid oxidation. The underlying mechanism involved a stimulatory hyperacetylation of malonyl-CoA carboxylase, the enzyme responsible for degradation of the fatty acid oxidation inhibitor, malonyl-CoA. Our novel findings disagree with the previously proposed importance of MCU activity in the regulation of mitochondrial glucose oxidation.

To explore endothelial transport and supply of fatty acids to cardiomyocytes in the control of myocardial energy metabolism, we tested the recent proposal that impaired endothelial autophagy impairs trans-endothelial trafficking of fatty acids to neighboring cardiomyocytes. The autophagy-related protein 7 (ATG7) is an essential component of cellular autophagosome formation. Based on this, we utilized endothelial-specific ATG7 knockout (EC-ATG7^{-/-}) mice to investigate the effect of impaired endothelial

autophagy on cardiac energy metabolism in hearts subjected to both aerobic and ischemia/reperfusion (I/R) conditions. EC-ATG7^{-/-} mouse hearts exhibited greater insulin-induced reduction of fatty acid oxidation compared to wild-type hearts, which was more marked under I/R conditions. Consistent with impaired fatty acid availability to the myocardial cells, EC-ATG7^{-/-} hearts contained significantly lower triacylglycerol content, the major fatty acid storage form, compared to wild-type littermates. These results support an important role of endothelial autophagy in cardiomyocyte fatty acid metabolism.

We then investigated the effects of a liver-secreted factor, adropin, on cardiac energy metabolism. Intraperitoneal adropin injections both enhanced insulin signaling and cardiac function. Interestingly, acute adropin administration to isolated perfused hearts promoted glucose oxidation and insulin signalling, suggesting a direct and acute action of adropin, possibly through an undiscovered receptor. We propose adropin as a metabolic modulator and a potentially important target for the treatment of cardiac disease associated with impaired insulin sensitivity.

Overall, the results presented in this thesis provide novel insights into the control of cardiac fatty acid and glucose metabolism at different levels. Such information can broaden our scientific knowledge and help devise new therapeutic interventions aiming at optimizing energy homeostasis in heart disease.

Preface

The research projects addressed by this thesis were approved by the University of Alberta Care and Use Committee, Project Name “Energy metabolism in the ischemic and non-ischemic heart”, AUP00000288. This project received its annual renewal on July 31, 2017. The ethics committee follows the Canadian Council on Animal Care guidelines.

Chapter 3 of this thesis has been published as: Tariq R. Altamimi, Panakkezhum D. Thomas, Ahmed M. Darwesh, Natasha Fillmore, Mohammad U. Mahmoud, Liyan Zhang, Abhishek Gupta, Rami Al Batran, John M. Seubert and Gary D. Lopaschuk. “Cytosolic carnitine acetyltransferase as a source of cytosolic acetyl-CoA: a possible mechanism for regulation of cardiac energy metabolism.” *Biochemical Journal* (2018) 475:959–976. I was responsible for all data production (except for what is indicated below), analysis and writing the manuscript. P Thomas performed experiments on hearts vs. livers. A Darwesh assisted in western blots. N Fillmore cultured H9c2 cells. GD Lopaschuk contributed to the experimental design and editing of the manuscript.

I produced the data (excluding those indicated below), performed data analysis, and writing of Chapter 4, 5, and 6. A Fukushima conducted most western blots in Chapter 4 and 6 in addition to acetylation assays in Chapter 4. L Zhang performed triacylglycerol measurements in Chapter 5 and helped with *in vivo* adropin injections in Chapter 6. K Singh performed siRNA transfection experiments in Chapter 5. K Strynadka performed the UPLC measurements in Chapter 3 and 4. G Lopaschuk was involved in study designs and coordination of collaborations.

Acknowledgements

First, I would like to express my genuine gratitude and appreciation to my advisor and mentor, Dr. Gary Lopaschuk, for his continuous support throughout my PhD studies, and for providing me with all necessary guidance and motivation. I truly thank him for the opportunity to be part of his excellent research team and for his patience, understanding and belief in my abilities. The vast knowledge and expertise he has, which he is eager to share, proved priceless in developing my research skills and experience.

I would also like to thank the members of my supervisory committee, Dr. René Jacobs, Dr. John Seubert, and Dr. Dawei Zhang, for their valuable time and enlightening insights and comments throughout the PhD process.

My sincere thanks and appreciation also extend to Dr. Arata Fukushima, Sonia Rawat, and Dr. Golam Mezbah Uddin for all their support and help in conducting this research and to my colleagues in Dr. Lopaschuk's lab for their intellectual input and technical assistance as well as for their good company throughout the years.

Finally, I would like to thank my mother and brother for supporting me during my study and in my life in general as well as my lovely and caring wife and children who fill my life with hope and happiness.

Chapter 1: Introduction	1
1.1 Introduction	2
1.2 Myocardial fatty acid metabolism	3
1.2.1 Malonyl-CoA control of fatty acid oxidation	5
1.3 Myocardial Glucose metabolism	6
1.4 The Randle cycle	8
1.5 The carnitine system	9
1.5.1 Carnitine acetyltransferase: function and location	10
1.5.2 Metabolic roles of carnitine acetyltransferase	13
1.6 Mitochondrial calcium uptake	15
1.6.1 Mitochondrial calcium uniporter (MCU)	15
1.6.2 MCU and cardiac energy metabolism	16
1.6.3 MCU and cardiac function	17
1.7 Endothelial role in fatty acid delivery to the cardiomyocyte	18
1.8 Protein acetylation and myocardial energy metabolism	21
1.8.1 Control of lysine acetylation	21
1.8.2 Regulation of energy metabolism by protein acetylation	23
1.9 Energy metabolism in cardiac ischemia/reperfusion (I/R)	25
1.10 Peripherally secreted factors affecting cardiac energy metabolism	26
1.11 Modulation of energy metabolism as a treatment for heart	
Disease	28

1.12 Hypothesis	30
1.12.1 General Hypothesis	30
1.12.2 Chapter 3 Specific Hypothesis and Experimental Objectives	30
1.12.3 Chapter 4 Specific Hypothesis and Experimental Objectives	31
1.12.4 Chapter 5 Specific Hypothesis and Experimental Objectives	32
1.12.5 Chapter 6 Specific Hypothesis and Experimental Objectives	33
Chapter 2: Materials and Methods	47
2.1 Introduction	48
2.2 Animals	50
2.3 Materials	51
2.4 Methods	54
2.4.1 Cell culture	54
2.4.2 Subcellular fractionation	54
2.4.3 Enzyme activity assays	56
2.4.4 Isolated working heart perfusions	57
2.4.5 Measurement of mechanical function in the isolated working heart	58
2.4.6 Assay of ¹⁴ CO ₂ and ³ H ₂ O	58
2.4.7 Calculation of ATP, Acetyl-CoA, and proton production	60
2.4.8 Tissue content of total triacylglycerol (TAG) and incorporation of palmitate into TAG	60
2.4.9 Western blot analysis	61
2.4.10 Protein acetylation assay	62
2.4.11 Determination of CoA esters	63
2.4.12 NAD ⁺ and NADH determination	63
2.4.13 Intraperitoneal glucose tolerance test	64

2.4.14	HUVECs and real-time Polymerase Chain Reaction	64
2.4.15	Statistical analysis	64
Chapter 3: Cytosolic carnitine acetyltransferase as a source of cytosolic acetyl-CoA: a possible mechanism for regulation of cardiac energy metabolism		65
3.1	Abstract	66
3.2	Introduction	67
3.3	Materials and Methods	69
3.3.1	Materials	69
3.3.2	Animals	69
3.3.3	Cell culture	70
3.3.4	Subcellular fractionation	70
3.3.5	Heart perfusions	72
3.3.6	Enzyme assays	73
3.3.7	Western blotting	74
3.3.8	Determination of CoA esters	75
3.3.9	Determination of free- and acyl-carnitines	75
3.3.10	Statistical analysis	76
3.4	Results	76
3.4.1	Acetyl-CoA production by CrAT in the heart	76
3.4.2	Cytosolic CrAT localization	79
3.4.3	CrAT involvement in malonyl-CoA regulation of cardiac metabolism .	82
3.5	Discussion	85
Chapter 4: Cardiac-Specific Deficiency of the Mitochondrial Calcium Uniporter Augments Fatty Acid Oxidation and Functional Reserve		112
4.1	Abstract	113
4.2	Introduction	114

4.3	Materials and Methods	115
4.3.1	Materials	115
4.3.2	Animals	116
4.3.3	Study protocol and heart perfusions	117
4.3.4	Determination of short-CoA esters	118
4.3.5	Western blotting	118
4.3.6	Acetylation assay	119
4.3.7	NAD ⁺ and NADH assay	120
4.3.8	Statistical analysis	120
4.4	Results	120
4.4.1	MCU ^{fl/fl-MCM} hearts show enhanced cardiac function at similar-to-control heart rates	120
4.4.2	Fatty acid oxidation in MCU ^{fl/fl-MCM} hearts is increased in response to isoproterenol stress	122
4.4.3	Protein levels and phosphorylation of key components of energy metabolism in MCU ^{fl/fl-MCM} hearts display minor variation	124
4.4.4	Protein acetylation is altered in MCU ^{fl/fl-MCM} hearts	125
4.5	Discussion	126
Chapter 5: A Novel Role of Endothelial Autophagy as a Regulator of Myocardial Fatty Acid Oxidation		
		142
5.1	Abstract	143
5.2	Introduction	144
5.3	Materials and Methods	145
5.3.1	Endothelial cell-specific ATG7 knockout mice	145
5.3.2	Ex vivo aerobic heart perfusion protocol	146
5.3.3	Ex vivo ischemic-reperfusion heart perfusion protocol	146

5.3.4	Triacylglycerol assay	147
5.3.5	Real-time polymerase chain reaction	147
5.3.6	Statistical analysis	148
5.4	Results	148
5.4.1	Endothelial specific ATG7 deletion is associated with reduced myocardial fatty acid oxidation in response to insulin	148
5.4.2	Endothelial specific ATG7 deletion is associated with augmented cardiac glucose oxidation, diminished cardiac fatty acid oxidation and reduced cardiac efficiency following I/R insult	149
5.4.3	Endothelial specific ATG7 deletion lowers cardiac TAG stores and expression of endothelial fatty acid binding proteins	151
5.5	Discussion	151
Chapter 6: Adropin Regulates Cardiac Energy Metabolism and Improves Cardiac Function and Efficiency		163
6.1	Abstract	164
6.2	Introduction	165
6.3	Materials and Methods	167
6.3.1	Materials and animals	167
6.3.2	Study protocol	167
6.3.3	Heart perfusions	168
6.3.4	Western blotting	169
6.3.5	Glucose tolerance test	170
6.3.6	Statistical analysis	170
6.4	Results	170
6.4.1	Adropin administration to fasting mice improves cardiac function and efficiency while increasing insulin's inhibitory effect on palmitate oxidation	170

6.4.2	In vivo 24 hr treatment with adropin does not change protein levels of key metabolic enzymes proposed to mediate its effects in skeletal muscles	173
6.4.3	Acute administration of adropin stimulates glucose oxidation with a corresponding inhibition of palmitate oxidation	173
6.4.4	Insulin signaling is enhanced in the hearts of adropin-injected mice and in isolated hearts perfused with adropin	174
6.5	Discussion	176
Chapter 7: Discussion and Conclusions		193
7.1	Summary	194
7.2	Roles of carnitine acetyltransferase in malonyl-CoA control of myocardial fatty acid oxidation	197
7.3	Mitochondrial calcium uptake and the oxidative metabolism	200
7.4	Microvascular and endothelial energy substrate supply to the myocardium	203
7.5	Adropin enhances insulin effects on glucose and fatty acid utilization	207
7.6	Limitations	210
7.6.1	The isolated working heart	210
7.6.2	<i>In vitro</i> enzyme activity assays and subcellular fractionation	211
7.6.3	Representation of cardiomyocyte energy metabolism by H9c2 cells ...	212
7.6.4	The mouse model, strain-specific differences and genotype characterization	213
7.7	Final conclusions	214
7.8	Future directions	215
References		218
Appendices		264
Appendix A: Supplemental Data for Chapter 3		264
Appendix B: Supplemental Data for Chapter 6		272

List of Tables

Page Numbers

Table 3.1. Michaelis–Menten parameters for forward (CrAT) and reverse (RCrAT) activities of carnitine acetyltransferase in the heart and liver of C57BL/6 mice 93

Table 5.1. Cardiac parameters of working hearts from EC-ATG7^{-/-} and WT littermate controls perfused under aerobic conditions 156

List of Figures**Page Numbers**

Figure 1.1. Summary of cellular fatty acid metabolism in the heart.....	34
Figure 1.2. Summary of cellular glucose metabolism in the heart.....	36
Figure 1.3. The updated version of Randle cycle	38
Figure 1.4. A schematic view of the mitochondrial carnitine system	40
Figure 1.5. Proposed role of mitochondrial Ca²⁺ uptake on cardiac energy metabolism	42
Figure 1.6. An overview of lysine acetylation of proteins in glucose and fatty acid metabolic pathways in the heart	44
Figure 3.1. Carnitine acetyltransferase activities and kinetics in the heart compared with the liver	94
Figure 3.2. Enzyme activity of carnitine acetyltransferase presented as percent of V_{max}	96
Figure 3.3. Cytosolic carnitine acetyltransferase in cardiac tissue	98
Figure 3.4. Cytosolic carnitine acetyltransferase activities in homogenized cultured cardiac cells	100
Figure 3.5. Cytosolic carnitine acetyltransferase activities in permeabilized cardiac cells	102
Figure 3.6. Cardiac protein level and total activity of CrAT are decreased in ACC2 deficiency	104
Figure 3.7. Free, short-chain, long-chain acyl-, and total carnitine content in ACC2KO hearts compared to WT controls	106
Figure 3.8. Cardiac protein level and total activity of CrAT are increased in response to a HFD	108
Figure 3.9. Proposed scheme as to how CrAT contributes to regulation of energy metabolism	110

Figure 4.1. MCU deficient hearts show enhanced cardiac function at comparable heart rates	130
Figure 4.2. MCU deficient heart metabolism is altered in response to isoproterenol stress	132
Figure 4.3. Protein levels and phosphorylation of key components of energy metabolism in MCU deficient hearts display minor variation	134
Figure 4.4. Protein levels of additional important proteins involved in energy metabolism, mitochondrial biogenesis and mitochondrial Ca²⁺ homeostasis in MCU^{fl/fl-MCM} and MCU^{fl/fl} control mouse hearts	136
Figure 4.5. Protein acetylation is altered in MCU^{fl/fl-MCM} hearts	138
Figure 4.6. Protein acetylation of PDH and PGC-1α in MCU^{fl/fl-MCM} and MCU^{fl/fl} control mouse hearts	140
Figure 5.1. Endothelial specific ATG7 deletion is associated with reduced myocardial fatty acid oxidation in response to insulin	157
Figure 5.2. Endothelial specific ATG7 deletion is associated with augmented cardiac glucose oxidation, diminished cardiac fatty acid oxidation and reduced cardiac efficiency following an I/R insult	159
Figure 5.3. Endothelial specific ATG7 deletion lowers cardiac TAG stores and expression of endothelial fatty acid binding proteins	161
Figure 6.1. <i>In vivo</i> adropin enhances cardiac efficiency and modulates insulin-induced inhibition of fatty acid oxidation	181
Figure 6.2. Protein levels of key components of cardiac energy metabolism are not changed after three <i>in vivo</i> adropin injections	183
Figure 6.3. <i>Ex vivo</i> adropin enhances cardiac glucose oxidation and inhibits fatty acid oxidation	185
Figure 6.4. <i>In vivo</i> adropin increases cardiac insulin sensitivity	187
Figure 6.5. <i>Ex vivo</i> adropin increases cardiac insulin sensitivity	189
Figure 6.6. A diagram of proposed adropin metabolic effects	191

Figure A1. Percentage of mitochondrial breakage in mouse heart ventricular tissue homogenized by either a Polytron or a Potter-Elvehjem homogenizer 264

Figure A2. Confocal microscopy images of a frozen section of left ventricular C57BL/6 mouse heart tissue 266

Figure A3. Percentage of mitochondrial breakage in cultured H9c2 cells permeabilized by either a Potter-Elvehjem homogenizer (A), or by digitonin plasma membrane permeabilization (B) 268

Figure A4. Succinyl CoA levels in heart ventricles of ACC2KO mice as compared to WT controls 270

Figure B1. Glucose tolerance test of fasting lean C57BL/6 mice which received three injections of 450 nmol/kg adropin³⁴⁻⁷⁶ or vehicle over 24 hours 272

Figure B2. Total protein acetylation (A) and PGC1- α (B) in mouse hearts perfused with ex vivo adropin³⁴⁻⁷⁶ (2nM). 274

List of Abbreviations

-/-	Knockout
ACC	Acetyl-CoA carboxylase
ACL	ATP-citrate lyase
ADP	Adenosine diphosphate
Adr	Adropin
Akt	Protein kinase B
AMP	Adenosine monophosphate
AMPK	5' AMP-activated protein kinase
ANOVA	Analysis of variance
AS160	Akt substrate of 160 kDa
ATG7	Autophagy-related protein 7
ATP	Adenosine triphosphate
AU	Arbitrary unit
BCAA	Branched-chain amino acid
BSA	Bovine serum albumin
Ca ²⁺	Calcium
CACT	Carnitine/acylcarnitine translocase
CBP	CREB-binding protein
CD36	Cluster of differentiation 36
cDNA	Complementary deoxyribonucleic acid
CO ₂	Carbon dioxide
CoA	Coenzyme A

COT	Carnitine octanoyltransferase
CPT	Carnitine palmitoyltransferase
Cr	Creatine
CrAT	Carnitine acetyltransferase
CS	Citrate synthase
DAG	Diacylglycerol
<i>db/db</i>	Leptin receptor deficient
DM	Diabetes mellitus
DMEM	Dulbecco's modified eagle medium
DNA	Deoxyribonucleic acid
DTNB	5, 5'-dithio-bis-[2-nitrobenzoic acid]
DTT	Dithiothreitol
EC	Endothelial cell
ECL	Enhanced chemiluminescence
EDTA	Ethylene diamine tetra-acetic acid
Enho	Energy homeostasis associated gene
ETC	Electron transport chain
FABP	Fatty acid binding protein
FABPpm	Plasma membrane fatty acid binding protein
FACS	Fatty acyl CoA synthetase
FAD	Flavin adenine dinucleotide
FADH ₂	Flavin adenine dinucleotide, reduced
FAT/CD36	Fatty acid translocase

FATP	Fatty acid transport protein
FBS	Fetal bovine serum
g	Gram
GAPDH	Glyceraldehyde 3-phosphate dehydrogenase
GCN5	General control of amino acid synthesis 5
GCN5L1	GCN5- like enzyme 1
GIK	Glucose-insulin-potassium
GLUT	Glucose transporter
GPIHBP1	Glycosylphosphatidylinositol-anchored high density lipoprotein-binding protein 1
GPR19	G-protein coupled receptor 19
GSK3 β	Glycogen synthase kinase 3 beta
H ⁺	Proton
HDAC	Histone deacetylase
HFD	High-fat diet
HK	Hexokinase
HR	Heart rate
hr	Hour(s)
HUVEC	Human umbilical vein endothelial cells
I/R	Ischemic/reperfusion
IC ₅₀	The half maximal inhibitory concentration
ICDH	Isocitrate dehydrogenase
IRS-1	Insulin receptor substrate 1

ISO	Isoproterenol
JNK	c-Jun NH ₂ -terminal kinase
kDa	Kilodalton
kg	Kilogram
KO	Knock-out
LCAD	Long-chain acyl CoA dehydrogenase
LDH	Lactate dehydrogenase
LDL	Low density lipoprotein
LFD	Low-fat diet
LPL	Lipoprotein lipase
LVDP	Left ventricular developed pressure
MCD	Malonyl-CoA decarboxylase
MCU	Mitochondrial calcium uniporter
MEBM	Mitochondrial Extraction Buffer mix
mg	Milligram
MI	Myocardial infarction
min	Minute(s)
mito-NCLX	Mitochondrial sodium-calcium exchanger
MPC	Mitochondrial pyruvate carrier
mPTP	Mitochondrial permeability transition pore
mRNA	Messenger ribonucleic acid
mTOR	Mechanistic target of rapamycin
Na ⁺	Sodium

NAD ⁺	Nicotinamide adenine dinucleotide
NADH	Nicotinamide adenine dinucleotide, reduced
NFDM	Non-fat dry milk
NMN	Nicotinamide mononucleotide
OCTN2	Organic cation Na ⁺ -dependent transporter 2
PBS	Phosphate buffered saline
PBST	Phosphate buffered saline with tween
PCA	Perchloric acid
PCr	Phospho-creatine
PCR	Polymerase chain reaction
PDC	Pyruvate dehydrogenase complex
PDH	Pyruvate dehydrogenase
PDHP	Pyruvate dehydrogenase phosphatase
PDK	Pyruvate dehydrogenase kinase
PFK-1	Phosphofructosekinase-1
PGC-1 α	Peroxisome proliferator-activated receptor gamma coactivator 1-alpha
Pi	Inorganic phosphate group
PI3K	Phosphatidyl inositol 3 kinase
PKC	Protein kinase C
PLS	Peroxidase-labeled streptavidin
PPAR α	Peroxisome proliferator-activated receptor alpha
PTM	Post-translational modifications
RCrAT	Reverse carnitine acetyltransferase

RyR2	Ryanodine receptor 2
SDS-PAGE	Sodium dodecylsulfate polyacrylamide gel electrophoresis
SEM	Standard error of the mean
siRNA	Small interfering RNA
SIRT	Sirtuin
SR	Sarcoplasmic reticulum
TAG	Triacylglycerol
TCA	Tricarboxylic acid
U	Unit
UPLC	Ultra-performance liquid chromatography
VDAC	Voltage dependent anion channel
VLDL	Very low density lipoprotein
Vol	Volume
WB	Western blotting
wt	Weight
WT	Wild-type
α -KGDH	α -Ketoglutarate dehydrogenase
β -HAD	β -Hydroxyacyl CoA dehydrogenase

CHAPTER 1

Introduction

CHAPTER 1

Introduction

1.1 Introduction

Understanding cardiac energy metabolism is essential for our perception of how the heart functions in health and disease. For instance, an increased reliance on fatty acid oxidation for energy production can impair cardiac efficiency whenever oxygen is limited or in situations when cardiac function is compromised (1-3). This leads to further impairment of cardiac function (1,4,5). One example where alterations in energy metabolism contribute to poor contractile function is cardiac ischemia. Ischemia decreases cardiac energy production, compromises cardiac efficiency and leads to conditions that augment fatty acid utilization during the reperfusion period (2,5). The increase in fatty acid oxidation is accompanied by suppression of glucose oxidation while glycolysis is not proportionally suppressed, leading to lactate and proton production which contributes to the observed contractile dysfunction (1,2,5). Another condition where cardiac efficiency is perturbed is insulin resistance occurring in the hearts of diabetics and obese individuals. Insulin resistance is associated with impaired uptake and metabolism of glucose with increased reliance on fatty acid oxidation as a source of energy due to several factors including elevated levels of circulating fatty acids and up-regulation of proteins involved in fatty acid uptake, transport and oxidation (1). While some of these metabolic alterations occur secondary to defective insulin signaling (6), some are a result of local myocardial derangements (4). This thesis

focuses on control of glucose and fatty acid oxidation in the heart with experimental investigation of novel approaches to positively alter energy metabolism in the heart and consequently enhance cardiac efficiency. This chapter introduces energy metabolism in the heart and some points at which cardiac glucose and fatty acid oxidation can be regulated.

1.2 Myocardial fatty acid metabolism

The heart has a high energy demand and under normal conditions the mitochondrial oxidation of fatty acids accounts for about 70% of energy production in the heart (1). Fatty acid oxidation is the process of degrading fatty acids into acetyl-CoA molecules that eventually lead to the production of ATP through mitochondrial oxidative phosphorylation (Figure 1.1). Fatty acids gain access to cardiomyocytes either through passive diffusion (short to medium carbon chain) or through facilitated transport by protein carriers in the cell membrane, which consist mainly of fatty acid translocase (FAT/CD36), plasma membrane fatty acid binding protein (FABPpm), and fatty acid transporter protein (FATP) 1/6 (7). Endogenous triacylglycerol (TAG) functions as stores that provide another source of fatty acids (8). Once in the cytosol, fatty acids are esterified to free coenzyme A (CoA) by a family of fatty acyl CoA synthetase (FACS) enzymes, a process that requires the hydrolysis of two high energy phosphate bonds from ATP. Fatty acyl-CoAs are then ready to be used in the synthesis of several lipid intermediates (e.g. diacylglycerol (DAG), triacylglycerol (TAG), ceramides, and membrane lipids) or to be directed to the outer mitochondrial membrane where, if their carbon chain is short to medium, they can directly diffuse into the mitochondria or, if

having a long carbon chain, carnitine palmitoyltransferase I (CPT I) catalyzes what is considered the first step in long-chain fatty acid oxidation (1). CPT I transfers long chain acyl moieties to carnitine creating acylcarnitines, which are able to traverse the inner mitochondrial membrane through the carrier protein, carnitine/acylcarnitine translocase (CACT) to the mitochondrial matrix (9,10). Noteworthy, CPT I is susceptible to potent allosteric inhibition by malonyl-CoA and this step constitutes a bottle neck in the process of fatty acid oxidation (11-14). In turn, malonyl-CoA is produced by acetyl-CoA carboxylase (ACC) and degraded by malonyl-CoA decarboxylase (MCD) in the cytosol and its levels depend on a balance between the two processes (9,10,13,14).

Following admittance to the mitochondria, carnitine palmitoyltransferase II (CPT II) located on the inner mitochondrial membrane with its active site facing the matrix, transfers the long-chain fatty acyl moiety back to CoA (10). Thereafter in the mitochondrial matrix, the acyl CoA is subjected to β -oxidation. This process involves a series of sequential reactions catalyzed by enzymes with isoforms targeting very long-, long, medium, and short-chain acyl-CoA molecules. These are generally named: acyl-CoA-dehydrogenase; enoyl-CoA hydratase; 3-L-hydroxyacyl-CoA dehydrogenase; and 3-ketoacyl-CoA thiolase. Mono- and poly-unsaturated fatty acids require auxiliary enzymes, 2,4-dienoyl-CoA reductase and enoyl-CoA isomerase to produce a trans double-bond before the above enzymes are able to process the acyl-CoA (15). The net products for each cycle of fatty acid oxidation are one molecule of each of the following: acetyl-CoA, the reduced form of flavin adenine dinucleotide (FADH₂), the reduced form of nicotinamide dinucleotide (NADH), and an acyl-CoA molecule that is

two carbons shorter. The electron energy stored in FADH₂ and NADH can be directly used by the electron transport chain (ETC) to produce ATP by the process of oxidative phosphorylation, while acetyl-CoA can enter the tricarboxylic acid (TCA) cycle for further processing and FADH₂/NADH production (1). There are several factors affecting the rates of fatty acid oxidation including plasma concentrations of fatty acids, intracellular malonyl-CoA levels, allosteric, transcriptional, and post-translational control of the enzymes of uptake and transport through cellular membranes as well as mitochondrial β -oxidation enzymes, all of which are governed by many interplaying processes and factors (16).

1.2.1 Malonyl-CoA control of fatty acid oxidation

Allosteric inhibition of CPT I by malonyl-CoA is a key mechanism by which mitochondrial fatty acid uptake, and hence oxidation, is regulated (10-13,17-19). Two isoforms of ACC are expressed in the myocardium, ACC 1 and ACC 2, with the latter predominating (20-24). There is direct evidence that ACC activity is inversely related to cardiac fatty acid oxidation (25-29). Similarly, ACC activity and malonyl-CoA levels regulate skeletal muscle fatty acid oxidation (30-32). AMP kinase (AMPK) phosphorylation of ACC inactivates it and thus leads to reduction of malonyl-CoA levels and increased fatty acid oxidation (33-35). AMPK is a serine/threonine kinase that is activated by increased AMP levels and thus acts as a sensor of metabolic stresses associated with ATP degradation to AMP, as well as declines in the phosphocreatine/creatine (Cr/PCr) ratio (33,35,36). AMPK not only plays a key role in the regulation of fatty acid oxidation, but also in regulating glucose uptake and glycolysis (26,37-43). Other factors in the absence of changes in AMP/ATP and Cr/PCr

ratios can affect myocardial AMPK activity, including the inhibitory action of insulin on AMPK (44,45). The myocardium also displays high expression and activity of MCD (46). Several studies have demonstrated an association between increased MCD activity and acceleration of fatty acid oxidation rates in different physiological and pathological conditions, including fasting, diabetes, ischemia, and newborn heart development (37,46-48). In this thesis, I propose a role of another cellular enzyme, carnitine acetyltransferase (CrAT), in the ACC- malonyl-CoA axis control of fatty acid oxidation. This will be discussed below.

1.3 Myocardial Glucose metabolism

Glucose represents the second major substrate used by the heart to produce energy through the process of glycolysis and glucose oxidation (Figure 1.2). The first step in this process involves the uptake of glucose by the cell through the two main glucose transporter proteins, GLUT 1 and GLUT 4, with the latter being recruited to the sarcolemmal membrane by insulin to promote glucose metabolism (49). Once inside the cytosol, glucose is phosphorylated and thus sequestered inside the cell, by the action of hexokinase I or II, to produce glucose-6-phosphate (50,51). Hexokinase II is the predominant isoform of hexokinase in the mature heart (50,51). Afterwards, glucose-6-phosphate is either directed towards glycogen storage, is catabolized by the process of glycolysis, or enters the pentose phosphate pathway. In glycolysis, phosphofructokinase 1 (PFK1) catalyzes an irreversible step after which glucose must continue through glycolysis (51). It also represents a key regulatory site for glycolysis, as the enzyme is sensitive to control by several metabolites, nucleotides, and ions. Stimulators include

AMP, ADP, Pi, and fructose 2,6-bisphosphate, whereas inhibitors include citrate, ATP, and protons (51,52). The net products of glycolysis for one mole of glucose metabolized are 2 moles of each of ATP, NADH, protons, and pyruvate. Thereafter, pyruvate has two main fates, either to enter the mitochondria and be oxidized or to be converted to lactate in the cytosol by the action of lactate dehydrogenase which simultaneously regenerates the oxidized form of nicotinamide dinucleotide (NAD^+) necessary for glycolysis to continue (53). A third minor pathway is carboxylation to form oxaloacetate or malate through anaplerotic reactions (54). Conversion of pyruvate to lactate occurs under anaerobic conditions or in cases of inhibited mitochondrial pyruvate oxidation, such as what occurs in diabetes (53,55).

Pyruvate is transported into the mitochondria by means of the pyruvate mitochondrial carrier (56,57). Subsequently, most of the mitochondrial pyruvate is oxidatively decarboxylated by the pyruvate dehydrogenase (PDH) complex, producing acetyl-CoA which mainly then feeds into the TCA cycle (51,52). PDH catalyzes the irreversible and primary regulatory step in glucose oxidation (58,59). In humans, the enzyme complex consists of a total of 96 subunits arranged in three enzymes: pyruvate decarboxylase (E1), dihydrolipoamide acetyltransferase (E2), and dihydrolipoamide dehydrogenase (E3) (60). The activity of PDH is regulated by product/substrate levels (i.e. NADH/NAD^+ and/or acetyl-CoA/CoA inhibits PDH) and by two enzymes: a kinase (PDH kinase, PDK) and a phosphatase (PDH phosphatase, PDHP) that are tightly and loosely bound, respectively, to the E2 unit and exert inactivating phosphorylation and activating de-phosphorylation, respectively, on any of three specific serine residues in the E1 α subunit (59,60). NADH, acetyl-CoA and ATP stimulate PDK, whereas NAD^+ ,

CoA, ADP, and pyruvate inhibit it. PDHP, in turn, is stimulated by Ca^{2+} and Mg^{2+} (52,59,61). If glycolysis is fully coupled to glucose (pyruvate) oxidation, an average of 31 ATP molecules is generated by the complete oxidation of one molecule of glucose (62).

1.4 The Randle cycle

The Randle cycle is a reciprocal inhibitory relationship between glucose and fatty acid oxidation (63) (Figure 1.3). According to the Randle cycle, fatty acids and glucose compete as energy substrates for the production of ATP. Increasing fatty acid oxidation can inhibit glucose oxidation through at least two mechanisms. First, the cytosolic glycolytic enzyme phosphofructokinase is under inhibitory control by citrate produced in the TCA cycle. Cellular citrate levels, in turn, are proportional to the rate of acetyl-CoA production mainly by fatty acid oxidation. Second, PDH is inhibited by NADH produced by fatty acid oxidation and an increase in the acetyl-CoA/CoA ratio, both through product inhibition (acetyl-CoA being a product of PDH) and through stimulating the inhibitory phosphorylation by PDK (52,63). Conversely, glucose oxidation-derived NADH can inhibit both acyl-CoA dehydrogenase and 3-hydroxyacyl-CoA dehydrogenase, enzymes of β -oxidation (52). Furthermore, the acetyl-CoA generated by glucose oxidation can also control β -oxidation through inhibition of 3-ketoacyl-CoA thiolase (52). Therefore, fatty acids and glucose oxidation rates appear to have an inverse relationship in many cell types, particularly cardiomyocytes. In this context, it is worth mentioning that although fatty acid oxidation has a greater ability to produce ATP compared to glucose, this comes at the expense of using more oxygen and

the futile wasting of ATP energy on non-contractile processes such as TAG synthesis and hydrolysis (1,3,52). Accordingly, fatty acids are considered less efficient energy substrates than glucose and a great reliance on their oxidation can decrease mechanical efficiency in the heart.

1.5 The carnitine system

The reversible transformation of free carnitine to acylcarnitines, and hence the localization or transport of acyl moieties among intracellular compartments and intracellular trafficking of fatty acids, is dependent on the activities of several transferase enzymes that are widely but unevenly distributed throughout the cytosol and cellular organelles (64). These distinct proteins are members of the carnitine acyltransferase family or the carnitine system, which play central and integrative roles in cell metabolism (Figure 1.4). The enzymes CPT I and CPT II, as well as the transporter protein CACT, are briefly discussed above in the context of fatty acid metabolism. The inability of cardiomyocytes to effectively synthesize L-carnitine (65), the essential metabolite/substrate of these enzymes and transport proteins, necessitates an efficient muscular extraction of carnitine from the blood against a high concentration gradient. This is provided by a sarcolemmal transporter namely, the organic cation Na^+ -dependent transporter 2 (OCTN2) (66). Each of the acyltransferase enzymes shows properties that fit the specific reaction it performs in terms of its localization, the length of acyl group it transfers, and the regulatory mechanism of its activity. Carnitine octanoyltransferase (COT) is another member of this system. It is known to exist only in peroxisomes and preferentially interacts with medium chain acyl-CoA esters and is

assumed to provide a mechanism through which acyl moieties are transported out of the peroxisomal core (67).

1.5.1 Carnitine acetyltransferase: function and location

An important component of the carnitine system is CrAT. It is structurally and functionally related to the other carnitine acyltransferases with a molecular weight of about 70 kDa and specificity toward short chain acyl groups (68,69). Although identified early, it is the least characterized of the carnitine acyltransferases. The main action of CrAT is to catalyze the reversible transfer of acetyl group between free CoA and carnitine (70). Substrate specificity of mitochondrial CrAT includes short- and medium-chain acyl-CoAs (C2 to C10) and some branched-chain amino acid (BCAA) oxidation intermediates to produce acylcarnitines that are exported out of cells and appear in the blood of patients of different inborn errors of metabolism displaying impaired fatty acid and BCAA oxidation (71). As the mitochondrial and peroxisomal membranes are impermeable to acetyl-CoA, CrAT in peroxisomes and mitochondria is thought to assist in exporting short chain acyl groups (e.g. acetyl- and propionyl- groups produced by peroxisomal or mitochondrial fatty acid oxidation and mitochondrial pyruvate and ketone oxidation) out of these organelles by transferring these acyl groups from CoA esters to carnitine (72). In this regard, it is proposed to provide an alternative means of exporting acetyl moieties (as acetylcarnitine) in addition to the acetate form (produced by peroxisomal acyl-CoA thioesterases or TCA cycle) to the cytosol eventually supporting malonyl-CoA production (71,72).

CrAT is known to be localized in the mitochondrial matrix and peroxisomes. However, it has also been proposed to exist in the endoplasmic reticulum and nucleus (67). In a

study on *Aspergillus nidulans*, a fungus widely used in studying eukaryotic cell biology, a cytoplasmic CrAT encoded by the *facC* gene was found to produce cytosolic acetyl-CoA while another gene: *acuJ* gene was found to encode another CrAT localized either in mitochondria or peroxisomes depending on its N- or C-terminal targeting sequence (73). This finding appears particularly interesting as a putative mammalian cytosolic CrAT can complete the circle after exporting excess acetyl moieties produced in mitochondria to the cytosol by regenerating acetyl-CoA in the cytosol which can serve as a substrate for the production of the potent fatty acid oxidation inhibitor, malonyl-CoA (Figure 1.3).

In humans, mitochondrial and peroxisomal CrAT are encoded by the same gene, with alternative splicing resulting in different variants targeted to either of the subcellular organelles (74). According to the protein knowledge base UniProtKB (UniProt # P43155) (75), three CrAT variants exist in humans as a result of three different mRNA splice variants that encode slightly different amino acid sequences (75). Only two of these form functional isoenzymes and are localized to either mitochondria or peroxisomes depending on the presence of an N-terminal mitochondria signal sequence in the larger variant (canonical CrAT, 626 amino acids) or the influence of the C-terminal peroxisomal signal sequence (AKL) in the shorter isoenzyme (splice variant, 605 amino acids) lacking the mitochondrial signal sequence (74,75). The 21 a.a N-terminal mitochondrial targeting sequence: MLFAAARTVVKPLGFLKPFSL in human CrAT isoform 1 is similar (but not identical) to that in the canonical murine CrAT isoform: MLFAAARTVVKPLGLLKPSSL (UniProt # P47934, also total 626 amino acids). Accordingly, this murine CrAT isoform is also expected to be localized to the

mitochondria. Similarly, another murine CrAT sequence (UniProt # H7BX88, total 605 a.a) is very similar to the human isoform 2 mentioned above and contains the same C-terminal peroxisomal signal sequence (AKL) while lacking the 1-21 N-terminal mitochondrial targeting sequence explained earlier. The two murine CrAT isoforms, similar to the human's corresponding isoforms, are encoded by the same gene. Interestingly, the mitochondrial signal seems to dominate and prevent peroxisomal localization which implies that the peroxisomal signal is relatively weak and may not be totally efficient thus leaving some "peroxisomal" CrAT behind in the cytosol. However, such a theory requires sufficient investigation.

Previous studies from our research group proposed regeneration of cytosolic acetyl-CoA from acetylcarnitine by means of a proposed cytosolic CrAT which can lead to a rise in malonyl-CoA levels and CPT I inhibition, regulating the rates of fatty acid oxidation with corresponding changes in glucose oxidation (29,76). However in order to play this role, CrAT must exist in the cytosol of the cardiomyocyte without being contained in a membranous vesicle and to have free access to cytosolic acetylcarnitines. However, the presence of a cytosolic CrAT activity was previously questioned in a study on rat cardiomyocytes (77). The results of that study attributed 5-11% of the total cellular activity of CrAT to the cytosolic fraction and that activity was considered insignificant and insufficient to sustain flux of acetyl-CoA to the ACC-mediated malonyl-CoA production (77). In contrast, we find the above activity to be sufficient to supply the substrate for the production of malonyl-CoA bearing in mind the turnover rates of malonyl-CoA and the sensitivity of the predominant ACC isoform in the heart (ACC2) to acetyl-CoA concentrations (29,76). Moreover, heart CPT I is extremely

sensitive to the smallest change in malonyl-CoA concentration. The IC_{50} of CPT I for malonyl-CoA $\approx 100\text{nM}$ (29,78). Therefore, small changes in cytosolic acetyl-CoA concentration could theoretically lead to a strong inhibition of CPT I and fatty acid oxidation (29).

1.5.2 Metabolic roles of carnitine acetyltransferase

Recently, CrAT is increasingly being viewed as a key component of energy metabolic regulation in skeletal muscles and seems to be actively involved in energy substrate selection, insulin sensitivity and carbohydrate metabolism. The interplay between carnitine and CoA pools and the modulation of acetyl-CoA/CoA ratio in myocytes have been discussed by studies in our, as well as other, laboratories. This included studies involving carnitine supplementation to isolated mitochondria, myocytes, hearts or skeletal muscles, or more recently by using modulation of CrAT expression in skeletal muscle cells through knocking down or knocking out the enzyme (29,79-87). It is now widely accepted that CrAT plays a key role in the modulation of the mitochondrial acetyl-CoA/CoA ratio by acting as a buffer system that prevents the accumulation of acetyl-CoA which can inhibit PDH activity and pyruvate (or glucose) oxidation (Figure 1.3) (80,87). Furthermore, the continuous regeneration of free CoA is essential for supporting many mitochondrial enzymatic processes (88). To emphasize a role for CrAT in acetyl-CoA buffering, a hyperpolarized ^{13}C magnetic resonance study investigated the immediate fate of infused $[2-^{13}\text{C}]$ pyruvate in rat hearts (80). The data suggested that half of the PDH-derived acetyl-CoA quickly (within 50 s.) cycles through CrAT into the acetylcarnitine pool prior to re-conversion to acetyl-CoA and incorporation into the TCA cycle. This indicates that the acetylcarnitine pool acts like a

storage pool that can accommodate any excess in acetyl-CoA production by PDH, and can also quickly provide acetyl-CoA to the TCA cycle when needed, all through the dynamic actions of CrAT (80).

This important regulatory action of CrAT on myocardial glucose oxidation was shown by early experimental studies conducted in our lab on isolated working rat hearts. Carnitine loading to normal, ischemic, carnitine-deficient, and diabetic rat hearts increased glucose oxidation at the expense of fatty acid oxidation, and improved contractile function in those hearts (84-87). Although carnitine is a substrate of CPT I, the first enzyme responsible for fatty acid oxidation, the peculiar action of carnitine stated above is explained by the concept of variable affinities for carnitine of CrAT and CPT I and the equilibrium between free CoA and acetyl-CoA, which regulates PDH activity. Being also a substrate of CrAT, high free carnitine levels in mitochondria would stimulate CrAT-mediated transfer of acetyl groups from acetyl-CoA to carnitine thus decreasing the acetyl-CoA/CoA ratio. As explained above, this would translate into relieving the constituent inhibition of PDH and pyruvate oxidation (84).

Metabolic inflexibility is a concept that refers to the impaired ability of the cell to switch from using fatty acids to glucose for energy production in response to metabolic cues (89). CrAT knock-out mice display glucose intolerance, insulin resistance, and impaired postprandial metabolic switch to glucose (metabolic inflexibility) (79). Here again, CrAT may be acting as an outlet for acetyl-CoA in states of superfluity (as in transition from fasting to feeding). Loss of CrAT function raises cardiac and skeletal muscle long chain acylcarnitines levels (mostly by enhancing fatty acid oxidation rates) and blunts the carnitine-mediated stimulation of PDH activity and pyruvate competition

with fatty acids as a fuel (79). Interestingly, this previous study also found a severely depressed CrAT mRNA expression in patients with type 2 DM (79). Glucose tolerance was improved upon carnitine supplementation in diabetic patients whereas CrAT expression levels in isolated skeletal muscles was directly correlated to glucose uptake, fuel selection and acetylcarnitine efflux (79). Related to these beneficial effects of carnitine administration, several clinical trials have shown that L-carnitine improves metabolic and functional profiles in the ischemic heart, as evident by improved exercise tolerance and ventricular function in angina patients, decreased plasma levels of markers of cell injury, reduced incidence of arrhythmia, and improved recovery and survival after a myocardial infarction (90-95). These beneficial effects are mostly attributed to carnitine's activation of CrAT, resulting in an increase in glucose oxidation in these diseased hearts as it is known that stimulating fatty acid oxidation (presumably by carnitine stimulation of CPT I) in those cardiac debilities is not favorable.

1.6 Mitochondrial calcium uptake

1.6.1 Mitochondrial calcium uniporter (MCU)

Mitochondrial uptake of calcium in vertebrates has been documented since the early 1960s (96). This process has central roles in cell physiology by stimulating ATP production, shaping cytosolic calcium transients, and regulating cell death (97). It had been attributed to a putative yet undiscovered mitochondrial calcium uniporter (MCU), until eventually identified in 2011 (98). The gene for MCU contains a sequence coding for two trans-membrane domains embedded in the inner mitochondrial membrane (98). In addition, several other proteins associated with this channel have been identified as

regulatory components (99-102). The significance of MCU involvement in Ca^{2+} homeostasis is substantiated by its distribution and concentration at mitochondria-sarcoplasmic reticulum (SR) associations near ryanodine receptors (RyR2) to better serve local Ca^{2+} signaling and the excitation-energetic coupling (103).

1.6.2 MCU and cardiac energy metabolism

A rise in mitochondrial Ca^{2+} is believed to actively contribute to the increase in energy production needed to sustain contractile function following adrenergic stimulation by increasing the activity of mitochondrial dehydrogenases (Figure 1.5) (104,105). This includes activation of PDH, resulting in an increase in glucose oxidation, due to a Ca^{2+} stimulation of PDH phosphatase (22,106). Ca^{2+} crosses the inner mitochondrial membrane primarily through the MCU channel (98). Therefore, a deficiency in the MCU would be expected to decrease energy production and compromise contractile function of the heart, especially in response to an adrenergic stimulation.

Early studies on metabolic effects of increasing workload by epinephrine showed an increased glucose uptake and oxidation upon treatment of isolated perfused hearts (107). The increase in glucose oxidation rates was associated with increased glycolysis and enhanced PDH activity even at the presence of high fatty acid levels (22,106). This was mainly attributed to the stimulatory effect of Ca^{2+} on PDH phosphatase (52). Increasing the workload of the heart seems to also increase oxidation of endogenous and exogenous fatty acids, but with a lower magnitude than increases in glucose oxidation (glycogenolysis and PDH stimulation) (48). Changes in the cytosolic concentration of Ca^{2+} could be relayed into mitochondria and hence influence the activity of the intramitochondrial Ca^{2+} -sensitive dehydrogenases, including PDH,

isocitrate dehydrogenase, and α -ketoglutarate dehydrogenase (Figure 1.5) (106). A recent study suggested a correlation between reduced levels of MCU and insulin resistance as found in type-1 diabetic mice and in mouse neonatal cardiomyocytes cultured in hyperglycemic conditions (108). In those cells, reduced MCU levels correlated with decreased glucose oxidation associating with higher phosphorylation and lower activity of PDH. However, MCU deficiency models have shown mixed results regarding PDH phosphorylation and activity (109,110) as explained below.

1.6.3 MCU and cardiac function

It has been suggested that MCU is essential for rapidly increasing mitochondrial Ca^{2+} in pacemaker cells and that MCU-enhanced oxidative phosphorylation is required to accelerate reloading of an intracellular Ca^{2+} compartment before each heartbeat (111). Studies on functional consequences of modified expression/activity of MCU have shown mixed results. For example, ruthenium red (an inhibitor of MCU) was shown to improve left ventricle function while spermine (an opener of MCU) elicited opposite responses in hearts subjected to ischemic post- conditioning (112). Conversely, in another study using *ex vivo* perfused mouse hearts, both Ru360 and spermine (an inhibitor and stimulator of MCU, respectively) induced negative and positive inotropic effects, respectively with antagonistic effects (113). In the latter study, inotropic stimulation with isoproterenol elevated oxygen consumption, Ca^{2+} -dependent activation of PDH, and mitochondrial Ca^{2+} content while these effects were abolished by Ru360, indicating uncoupling between workload and ATP production upon MCU inhibition (113). Another recent study showed that whole body MCU knock-out mice, although normally displaying reduced cardiomyocyte mitochondrial matrix Ca^{2+} , interestingly

had normal cardiac function, ATP levels, and respiratory control ratio in response to transverse aortic constriction comparing to controls (114). Other studies exploiting myocardial MCU deficiency through transgenic expression of a dominant-negative MCU or cardiac MCU deletion, showed normal resting heart rates despite being incapable of physiological fight or flight heart rate acceleration (109,111). Mitochondria isolated from inducible cardiac-specific MCU knockout mouse hearts show lack of evidence for Ca^{2+} -induced mitochondrial permeability transition pore (mPTP) opening and thus these hearts were protected against ischemia/reperfusion (I/R) injury (109,115). However in other studies using different animal models of MCU deficiency, this was not translating into protection of the cells and myocardial tissue against cell death (110,116).

From the above, mitochondrial Ca^{2+} currents are believed to be closely associated with mitochondrial energy metabolism and cardiac function and an understanding of what actually occurs in the heart in the context of modified mitochondrial Ca^{2+} uptake may provide a basis for utilizing this regulatory point in the future in finding novel tools to modify cardiac energy metabolism. Chapter 4 of this thesis sheds the light on some aspects of the relationship of MCU and cardiac energy metabolism.

1.7 Endothelial role in fatty acid delivery to the cardiomyocyte

Unesterified fatty acids used by the heart are released from circulating albumin, or originate from the hydrolysis of TAG contained within low density lipoproteins (LDL) and chylomicrons. The hydrolysis of this TAG occurs by the action of lipoprotein lipase

(LPL) located at the luminal side of endothelial cells (EC) (1). Glycosylphosphatidylinositol-anchored high density lipoprotein-binding protein 1 (GPIHBP1) in capillary endothelial cells appears critical in this process, through its actions of shuttling LPL to the capillary lumen, where it can hydrolyze lipoprotein TAG (117). However, after that, fatty acids are thought to be transported across the EC as most of these molecules are too large to squeeze in between ECs. The details of such transport are not clear and little is known about the contribution of endothelium-mediated delivery of energy substrates to cardiomyocytes in the regulation of cardiac energy metabolism (118). Recent insights have suggested that activation of the AMPK pathway increases fatty acid metabolism in ECs during nutrient starvation (119,120). Whether this affects the trans-endothelial fatty acid transport is unclear. ECs dynamically form and degrade lipid droplets with corresponding changes in enzymes and proteins involved in TAG synthesis and degradation in response to changes of free fatty acid and TAG levels in the blood or cell culture media (121). This indicates active lipid metabolism in ECs that not only maintains a buffering mechanism of excess fatty acids in the blood and lipid homeostasis inside the EC, but may also have a key role in trans-cellular transport of fatty acids across the endothelial layer to adjacent cells such as cardiomyocytes. A recent study revealed a role of endothelial Notch signaling in the inter-endothelial transport of fatty acids to cardiomyocytes, thus adding to its roles as a regulator of metabolism and angiogenesis during cell development and in regeneration and repair of tissues (122). Impaired delivery of fatty acids was observed in cultured endothelial cells and transgenic mice with inhibition of Notch signaling, which preceded the impairment of cardiac function. The decreased fatty acid transport across

the endothelium was accompanied by lipid accumulation in the plasma and liver and an augmented myocardial glucose uptake and utilization with activation of mTOR (mechanistic target of rapamycin) signaling leading to cardiac hypertrophy and failure (122).

Autophagy (literally ‘self-eating’) is an essential catabolic pathway that degrades cellular components, including damaged protein and organelles, within the lysosome to maintain cellular homeostasis and assist cellular survival mechanisms during stress (123). Recent research points towards an important role of autophagy in the paracrine regulation of vasoactive substances from the endothelium (124) and in the regulation of cholesterol homeostasis (125). *In vitro* studies have shown that oxidized lipids can trigger endothelial and smooth muscle cell autophagy (126). In primary ECs, LDL stimulates autophagosome formation (125). The autophagic flux within the endothelial layer of blood vessels appears to play a role in managing exogenous lipids by engulfment within autophagic structures (125). These observations along with the growing evidence that intracellular lipids can be degraded by lysosomal lipases (127), suggest that lipids may be directly or indirectly trafficked into and through autophagosomes. A relevant term, lipophagy, refers to the specific degradation of lipids by the autophagic machinery (128). A recent study discussed a dynamic relationship between lipolysis, autophagy, and mitochondrial fusion existing in mouse embryonic fibroblasts to coordinate the fate of fatty acids as to be either stored in lipid droplets or transported to mitochondria for oxidation or to autophagosomes for degradation and transport to the surrounding fluid (129). Interruption of the balance seems to cause mishandling of these fatty acids and possible lipotoxicity (129). I have attempted in the

research highlighted by Chapter 5 to study some aspects of this autophagy-related fatty acid transport through the EC to feed cardiomyocytes with these important energy substrates.

1.8 Protein acetylation and myocardial energy metabolism

Lysine acetylation was originally identified in early 1960s as a regulatory mechanism of gene transcription through the modification of histones (130). It largely contributes to the dynamicity of chromatin that is required for the transcriptional factors to selectively function on the gene(s) of interest (131). It is now known that acetylation affects many cellular processes including gene expression, the cell cycle, apoptosis, cancer, mitochondrial autophagy, ageing, and energy metabolism (132-137). In recent years, there has been an increasing interest in the role of acetylation in the regulation of expression and activity of non-histone proteins including energy metabolic enzymes. This reversible post-translational modification (PTM) can occur to single or multiple lysine residues in as many as 65% of total mitochondrial proteins. Interestingly, almost every enzyme in glycolysis, the TCA cycle, fatty acid metabolism, gluconeogenesis, glycogen metabolism, and PDH can be acetylated in human liver tissue (138,139). Therefore, acetylation may rival major protein modifications including phosphorylation or ubiquitination (140).

1.8.1 Control of lysine acetylation

Reversible lysine acetylation is mediated by the action of several acetyltransferase and deacetylase enzymes (141). Four classes of histone deacetylases (HDACs) are known,

among which are sirtuins that are classified as class III HDACs (142,143). Sirtuins are NAD⁺-dependent deacetylases, and therefore are responsive to cellular energy and redox status (144-147). Mammals have seven known sirtuins, (SIRT 1-7) with different subcellular localization displaying distinct activities and protein targets (148,149). SIRT 1, 6, and 7 are primarily nuclear, deacetylating transcriptional factors and metabolic enzymes. SIRT2 is mainly localized to the cytoplasm, whereas SIRT 3, 4, and 5 reside in the mitochondrial matrix and are of particular interest in the regulation of mitochondrial energy metabolism (150,151). Being involved in fuel sensing and metabolic responses to caloric restriction and starvation, SIRT3 has been extensively studied (147,152). SIRT3 deacetylates and thus regulates important mitochondrial metabolic enzymes including LCAD, β -HAD, and PDH (153-159). SIRT4 deacetylates and inhibits MCD, leading to increases levels of malonyl-CoA, an endogenous inhibitor of mitochondrial fatty acid uptake (160). On the other hand, histone acetyltransferases such as CREB-binding protein (CBP), p300, general control of amino acid synthesis 5 (GCN5), and GCN5 like-1 (GCN5L1) are involved in the acetylation process. For example, GCN5 acetylates PGC-1 α , reducing its transcriptional function (161,162). GCN5L1 is the only known mitochondrial lysine acetyltransferase and has been shown to counteract the deacetylation actions of SIRT3 (163).

Protein acetylation is mainly dependent on the enzymatic activity of acetyltransferases and deacetylases (133,139,153). However, the subcellular compartmental levels of acetyl-CoA, being a substrate of acetylation reaction, and NAD⁺, as a co-factor and a stimulator of sirtuins, may also be important contributors to the regulation of acetylation (144,145,164,165). This can be particularly important in the mitochondria, since it has

high levels of both acetyl-CoA and NAD^+ . Consistent with these facts, lysine acetylation is affected by altered nutritional status, as occurs after high-fat feeding or caloric restriction (166,167). Acetyl-CoA produced by fatty acid oxidation was found to drive mitochondrial protein acetylation under fasting conditions (168). As such, acetylation of metabolic proteins may function as a nutrient sensor that leads to modification of energy metabolism.

1.8.2 Regulation of energy metabolism by protein acetylation

Dysregulated lysine acetylation of metabolic enzymes has been associated with impairment of cardiac energy metabolism in obesity, diabetes, and heart failure (139,154,155,169,170) (Figure 1.6). A state of hyperacetylation prevails with heart failure affecting enzymes and transcriptional factors involved in fatty acid oxidation, the TCA cycle, and the ETC (171). This coincides with increased levels of acetyl-CoA in heart samples from patients with end-stage heart failure (172). Consistently, cardiac dysfunction in complex I-deficient mouse hearts shows reduced NAD^+/NADH ratios associated with enhanced protein acetylation (173). A previous study from our lab showed hyperacetylation of fatty acid oxidation enzymes that correlated with the metabolic remodeling in mouse hearts with experimental obesity and heart failure (154). PDH, the rate-limiting enzyme of glucose oxidation, was shown in another study from our lab to be hyperacetylated and inhibited in hypertrophied hearts, leading to impaired insulin sensitivity in those hearts (158).

The effects of enhanced lysine acetylation of fatty acid oxidation enzymes on the net rate of fatty acid oxidation are not fully agreed upon, as some studies suggest an inhibitory effect, while others suggest it to be stimulatory. Hirschey *et al.* found in

livers of SIRT3 knockout mice an accumulation of long-chain acylcarnitines, suggestive of impaired fatty acid oxidation (153). This was linked to a reduced activity of LCAD, a key enzyme of fatty acid oxidation, through its increased acetylation status. In accordance with this, a site-specific mutagenesis study suggested two acetylated LCAD amino acids, K318 and K322, to suppress its activity through affecting the enzyme's conformation (157). However, this concept is challenged by many observations as well as experimental evidence particularly in the heart. For instance, a state of enhanced acetylation of mitochondrial proteins secondary to downregulation of SIRT3 is seen in hearts from obese and diabetic mice, accompanied by the well-established stimulation of fatty acid oxidation. This is supported by a recent study from our lab that demonstrated higher cardiac fatty acid oxidation rates in mice on high-fat diet, accompanied by reduced SIRT3 protein levels and enhanced acetylation of LCAD and β -HAD, key enzymes of fatty acid oxidation, that positively correlated with fatty acid oxidation rates and LCAD activity (154). In accordance with this, mice with diet-induced obesity and pressure-overload heart failure displayed increased cardiac protein levels of GCN5L1, a mitochondrial acetyltransferase, accompanied by hyperacetylation and stimulated activity of LCAD, as well as increased fatty acid oxidation rates (169). Similarly, hyperacetylation of the fatty acid oxidation enzyme complex enoyl-CoA hydratase/3-hydroxyacyl-CoA was shown to stimulate its activity in HEK293 cells (139). Diabetic hearts, which demonstrate higher fatty acid oxidation, show hyperacetylation of mitochondrial proteins particularly the α subunit of the trifunctional protein complex, which contains the key enzymes of β -oxidation (174). In line with this, SIRT3 knockout mouse skeletal muscles display both protein hyperacetylation and

enhanced fatty acid oxidation rates (159). Additionally, acetylation of key metabolic enzymes appear to play a critical role in the maturation of cardiac energy metabolism in the newborn that is featured by promotion of fatty acid oxidation within the first 3 weeks of age (175). Accordingly, it is more plausible that increased acetylation of fatty acid oxidation enzymes enhances the flux of fatty acyl-CoAs through this pathway.

1.9 Energy metabolism in cardiac ischemia/reperfusion (I/R)

Myocardial ischemia is a major cause of death and disability in developed countries (2). It is associated with serious and deleterious perturbations in biochemical and functional characteristics of the heart. Particularly, energy metabolism is markedly altered (2). In response to the acute decline in oxygen availability, the ischemic heart increases its reliance on anaerobic glycolysis, resulting in the accumulation of lactate and protons, thus contributing to the waste of the already depleted ATP in rectifying ionic imbalances (53,176). On the other hand, during reperfusion (e.g. by thrombolysis or revascularization), fatty acid oxidation increases and becomes the predominant energy source, significantly outmatching glucose oxidation (2,5). This is mainly attributed to increased availability of circulating fatty acids accompanied by decreased myocardial oxidation of glucose. These changes are produced by the sympathetic discharge accompanying ischemic insults, which stimulates lipolysis from adipose tissue and decreases insulin secretion and muscle insulin sensitivity (2,63,177,178). Furthermore, during ischemia the concentration of malonyl-CoA, the endogenous inhibitor of mitochondrial fatty acid oxidation, dramatically declines. This occurs as a result of decreased synthesis of malonyl-CoA by ACC (secondary to the enhanced inhibitory

phosphorylation by AMPK) accompanied by continuous MCD activity that maintains malonyl-CoA degradation (13,14). In addition, increased fatty acid oxidation can inhibit glucose oxidation by virtue of the Randle cycle, through suppressing the activity of the rate limiting enzyme of glucose oxidation, PDH (63). This occurs while glycolysis is not proportionally suppressed (2). Protein acetylation is globally increased in I/R mouse hearts (179). This can be attenuated by pharmacological activation of sirtuins (180,181). As explained above, when key mitochondrial enzymes involved in fatty acid oxidation are hyperacetylated, an increase in their activities, and thus in total fatty acid oxidation rates, is expected (154).

As discussed earlier in the context of the Randle cycle, although fatty acid oxidation has a greater ability to produce ATP as compared to glucose, this comes at the expense of using more oxygen (1,3). Consequently, in I/R hearts, a greater reliance on the oxidation of the less efficient energy substrate, fatty acids, would increase the burden on an already injured heart (2,3). To summarize, I/R insult is featured by accelerated anaerobic glycolysis during ischemia followed during reperfusion by enhanced fatty acid oxidation and inhibited glucose oxidation with the resultant futile use of oxygen and ATP and compromised cardiac efficiency.

1.10 Peripherally secreted factors affecting cardiac energy metabolism

Several secreted peptides from extra-cardiac organs and tissues are known to actively regulate energy homeostasis and alter insulin sensitivity in the heart and skeletal muscles (182-185). The majority of research in this area has focused on factors secreted

by adipocytes (i.e. adipokines). These factors function locally at the adipose tissue, as well as having hormone-like endocrine effects on the liver, heart, skeletal muscles (184). For instance, adiponectin enhances insulin sensitivity and stimulates fatty acid metabolism in liver and muscle tissues (184,185), while promoting lipid storage in white adipose tissue as TAG (186). Leptin is another adipokine that regulates hypothalamic control of food intake and satiety, as well as altering muscle fatty acid metabolism and insulin sensitivity (182,187). In contrast to leptin, ghrelin is a hormone released mainly by the gastro-intestinal tract to stimulate hypothalamic control of appetite and promote fatty acid storage (188-190). Dysregulated adiponectin and leptin secretion and function contribute to the insulin resistance seen in obesity, which is also associated with other factors secreted from adipose tissue that promote insulin resistance, such as resistin and pro-inflammatory cytokines (184,185). However, liver-secreted factors have received less attention as modulators of energy homeostasis in extrahepatic tissues (183). Such factors act as paracrine and endocrine hormones affecting carbohydrate, lipid, and amino acid metabolism in response to nutritional changes (183,191). Adropin is an example of a liver-secreted metabolic factor (that is encoded by the Energy Homeostasis Associated gene, *Enho*) with important roles in the regulation of skeletal muscle energy metabolism especially in post-prandial conditions (192,193) and in obesity (194). Transgenic overexpression or exogenous adropin administration has been shown to improve the metabolic profiles including better glucose tolerance and oxidation and insulin sensitivity in animals with diet-induced obesity (193,194). Accordingly, adropin provides a promising target in devising therapies for the metabolic syndrome, obesity, and diabetes and may prove beneficial in

modulation of myocardial energy metabolism. However, what role adropin has, if any, in mediating cardiac fatty acid and glucose oxidation is not known. This will be addressed in Chapter 6 of this thesis.

1.11 Modulation of energy metabolism as a treatment for heart disease

Since the introduction of glucose-insulin-potassium (GIK) therapy for myocardial infarction (MI) around 50 years ago (195), there has been an increasing interest in the modulation of myocardial energy metabolism as a therapeutic approach for heart disease. Some success has been reached in laboratory and clinical research, and a few medications are either already in clinical use or under development. For example, the therapeutic effects of the clinically used (or once used) medications as etomoxir, perhexiline, ranolazine, trimetazidine, and dichloroacetate or those under development such as newer PDK and MCD inhibitors are all attributable to altering the balance between fatty acid and glucose oxidation in such a way that it favors glucose oxidation (2,196). Increasing cardiac NAD^+ levels through administering medically available precursors of NAD^+ , such as nicotinamide riboside (NR) and nicotinamide mononucleotide (NMN) (197,198) which are currently the subject of clinical trials, can modify protein acetylation (by activating sirtuins) (181). This has been shown to offer heart protection against I/R injury either through effects on SIRT1 (181), or through stimulating glycolysis and preventing mPTP opening (199).

Finding new targets for the modulation of heart metabolism represents an attractive research goal. However, until now the subject of cardiac energy metabolism control

appears far from being fully understood, and there are several known and presumably unknown regulatory checkpoints that could potentially be therapeutically targeted in the complex network of cardiac energy metabolism. These may include regulatory points such as CrAT and MCU activity, or secreted liver factors such as adropin, as well as modulation of endothelial delivery of fatty acids to cardiomyocytes, subjects that I address in the research included in this thesis.

1.12 Hypothesis

1.12.1 General Hypothesis

In hearts subjected to increased workload, fasting, or acute ischemic stress, changes in cardiac energy metabolism occur and may compromise cardiac energy efficiency. Impaired energy substrate utilization is associated with reduced cardiac function. A general increase in fatty acid oxidation with concomitant decrease in glucose oxidation is observed in reperfused hearts after ischemia, in hearts of fasting individuals, and in hearts with impaired calcium homeostasis, especially with increased workloads. Additionally, in conditions with increased adiposity and circulating fatty acid (such as seen in type-2 diabetes and obesity), the endothelial delivery of fatty acid contributes to the increased rates of myocardial fatty acid oxidation. The enhanced reliance on fatty acid oxidation for energy production relative to glucose oxidation decreases cardiac efficiency. I hypothesize that these changes in energy metabolism will result in impaired cardiac function as observed under the utilized experimental conditions imposing the specific cardiac stress/challenge. I also hypothesize that increasing the reliance on glucose oxidation as an efficient energy source is important in maintaining cardiac function. Optimizing the balance of energy substrate utilization can improve cardiac function in the stressed heart.

1.12.2 Chapter 3 Specific Hypothesis and Experimental Objectives

The continuous energy production and utilization by the heart requires effective regulatory points that can fine-tune energy metabolic rates. In the mitochondria, CrAT can directly affect glucose oxidation rates by buffering the excess acetyl-CoA and thus maintain continuous flux through PDH. I hypothesize that, in addition to the

mitochondria, CrAT is partially localized to the cytosol of cardiomyocytes. I also hypothesize that through its cytosolic activity, CrAT can provide an additional checkpoint for the control of fatty acid oxidation by regenerating acetyl-CoA that can constitute a substrate for the production of the fatty acid inhibitor malonyl-CoA, through the action of cytosolic acetyl-CoA carboxylase (ACC).

This hypothesis will be tested by measuring the activity and assessing the protein levels of CrAT in subcellular fractions in the heart compared to the liver, which possess lipogenic abilities and is believed to mostly depend on another cytosolic enzyme, namely ATP-citrate lyase, to provide acetyl-CoA as the building block of fatty acid synthesis. I will then investigate CrAT cytosolic localization in undifferentiated versus differentiated H9c2 cells, a regenerative myocardial cell line, to further understand CrAT relation with the different metabolic profiles of these cells as they proceed to metabolic maturation. This will add to our understanding of the roles of CrAT in myocardial energy metabolism.

1.12.3 Chapter 4 Specific Hypothesis and Experimental Objectives

Mitochondrial Ca^{2+} has been historically attributed to having important roles in the regulation of energy substrate metabolism. I hypothesize that hearts from mice with impairment of mitochondrial calcium uptake will show dysregulated energy metabolism, especially upon subjecting them to isoproterenol (catecholamine) challenge. This impairment is expected to be manifested by decreased glucose oxidation as PDH is expected to be inhibited as a result of presumably decreased mitochondrial calcium levels.

This hypothesis will be addressed by utilizing a mouse model with cardiac-specific knocked-out mitochondrial calcium uniporter (MCU) channel to study energy substrate metabolism and preference under normal and high-workload conditions. Changes in glucose oxidation and fatty acid oxidation will be examined in isolated perfused working hearts at baseline, in response to insulin, and during an isoproterenol challenge. This will broaden our understanding of the importance of mitochondrial calcium homeostasis in the regulation of cardiac energy metabolism.

1.12.4 Chapter 5 Specific Hypothesis and Experimental Objectives

I hypothesize that impaired fatty acid delivery to the cardiomyocyte through the endothelial layer may decrease cardiac fatty acid oxidation rates. This may benefit the heart in ischemia reperfusion injury by improving cardiac efficiency.

This hypothesis will be tested by determining if impaired endothelial autophagy, which was previously ascribed some roles in fatty acid trafficking across the endothelial cell, can result in decreased delivery and thus oxidation of fatty acids in the myocardium. I will utilize a mouse model with endothelial-specific ATG7 knock-out, which is an essential component of autophagosome formation. I will investigate this under conditions of normal aerobic *ex vivo* perfusion and relate metabolic changes in response to insulin in these hearts. Additionally, I will test whether the proposed metabolic consequences can provide protection from, or amelioration of, I/R injury.

1.12.5 Chapter 6 Specific Hypothesis and Experimental Objectives

I hypothesize that a liver-secreted peptide, namely adropin, can affect cardiac energy metabolism through enhancement of glucose oxidation. This will be associated with enhanced cardiac function and/or response to insulin.

This hypothesis will be examined by determining what changes occur in cardiac energy metabolism in healthy mouse hearts that are subjected to a fasting protocol and three injections of the adropin peptide (or its vehicle) over one day. Energy metabolism will be assessed using isolated working heart perfusions and correlated with investigation of protein translational mechanisms that were previously ascribed metabolic effects of adropin in skeletal muscles. Further, acute metabolic and functional effects of perfusing mouse hearts with adropin as well as assessment of components of insulin signaling will be assessed.

Figure 1.1. Summary of cellular fatty acid metabolism in the heart. CD36/FAT, fatty acid translocase; FACS, fatty acyl-CoA synthetase; CPT, carnitine palmitoyltransferase; CACT, carnitine/acylcarnitine translocase; MCD, malonyl-CoA decarboxylase; ACC, acetyl-CoA carboxylase; NAD⁺, nicotinamide adenine dinucleotide; TCA, tricarboxylic acid cycle; ETC, electron transport chain; NAD⁺, nicotinamide adenine dinucleotide; FAD, Flavin adenine dinucleotide;

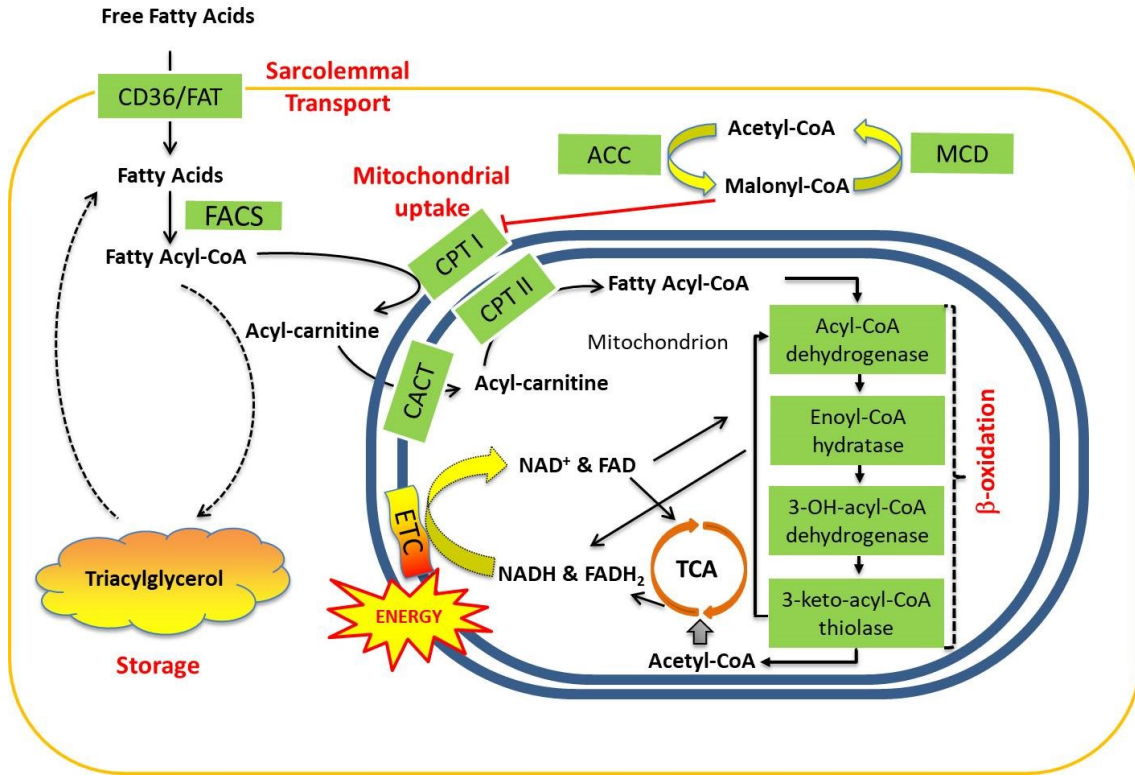


Figure 1.1

Figure 1.2. Summary of cellular glucose metabolism in the heart. GLUT1/4, glucose transporter-1 or 4; NAD⁺, nicotinamide adenine dinucleotide; FAD, Flavin adenine dinucleotide; TCA, tricarboxylic acid cycle; MPC, mitochondrial pyruvate carrier; ETC, electron transport chain.

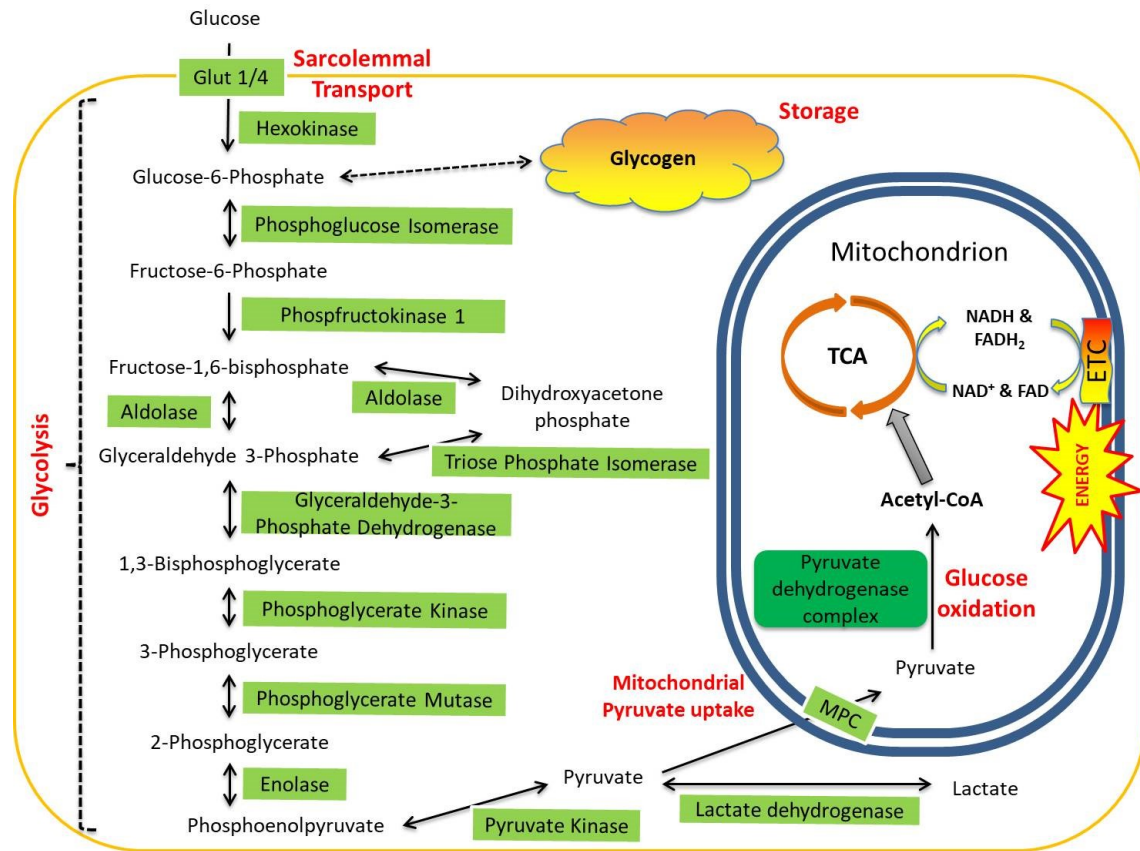


Figure 1.2

Figure 1.3. The updated version of Randle cycle. The reciprocal relationship between fatty acid and glucose oxidation is evident at several steps in both pathways thus introducing another level for the regulation of cellular metabolism of these substrates. NAD⁺, nicotinamide adenine dinucleotide; PFK-1, phosphofructokinase-1; TCT, tri-carboxylate transporter; MPC, mitochondrial pyruvate carrier; CoA, coenzyme A; PDH, pyruvate dehydrogenase; PDHP and PDK, pyruvate dehydrogenase phosphatase and kinase, respectively; CrAT carnitine-acetyltransferase; CACT, carnitine/acylcarnitine translocase; ACC, acetyl-CoA carboxylase; MCD, malonyl-CoA decarboxylase; CPT I and II, carnitine palmitoyltransferase 1 and 2, respectively.

Figure 1.4. A schematic view of the mitochondrial carnitine system. Carnitine is the common substrate for all components of this system. The carnitine system is involved in several metabolic functions of the cell including fatty acid flux into the mitochondria, modulation of Coenzyme A (CoA) pools, and efflux of acylcarnitines out of mitochondria and cells into the extracellular fluid. CACT, carnitine/acylcarnitine translocase; FACS, fatty acyl CoA synthase; CrAT, carnitine acetyltransferase; CPT I, CPT II, carnitine palmitoyltransferase I and II, respectively; TAG, triacylglycerol; LC-acyl-CoA, long-chain acyl-CoA; LC- acylcarnitine, long-chain acylcarnitine.

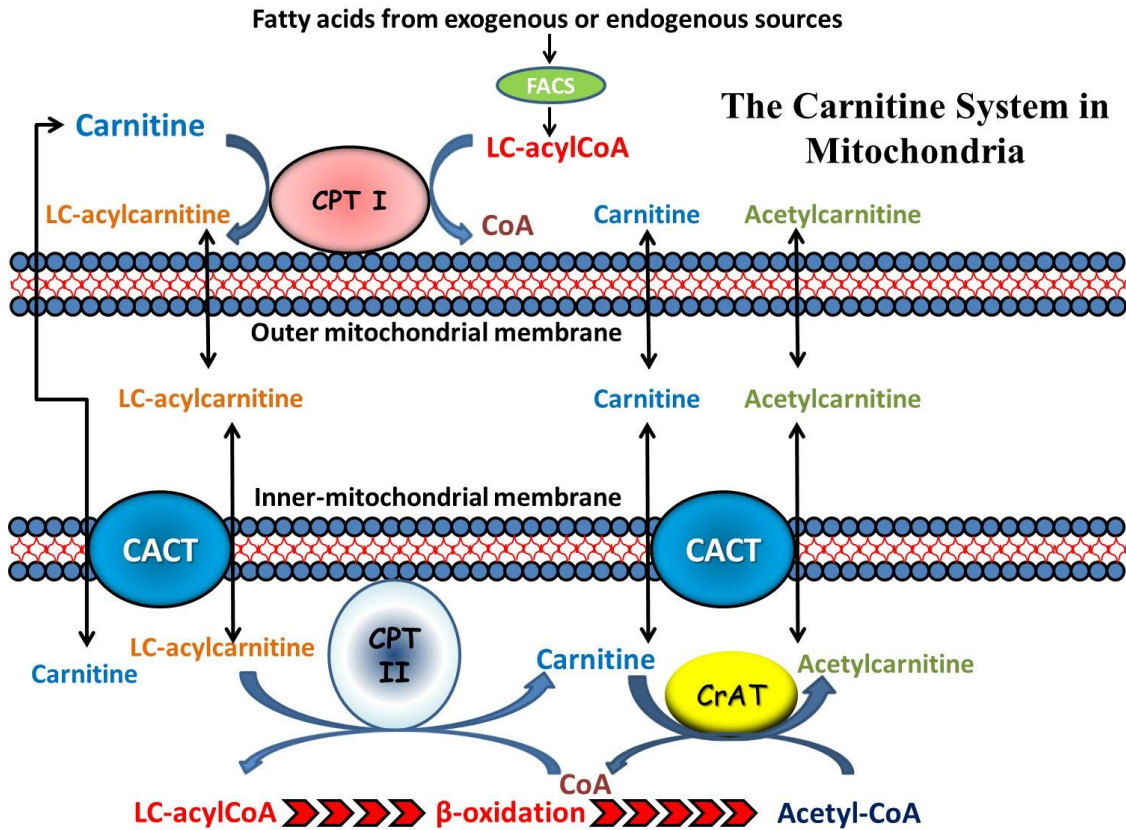


Figure 1.4

Figure 1.5. Proposed role of mitochondrial Ca^{2+} uptake on cardiac energy metabolism. The mitochondrial Ca^{2+} uniporter (MCU) is responsible for the mitochondrial uptake of Ca^{2+} and thus influence Ca^{2+} homeostasis inside the mitochondrial matrix, which is proposed to affect the activity of calmodulin-dependent phosphatases and influence dehydrogenases such as pyruvate dehydrogenase complex (PDH) and TCA cycle enzymes of isocitrate and α -ketoglutarate dehydrogenases (ICDH and α -KGDH, respectively).

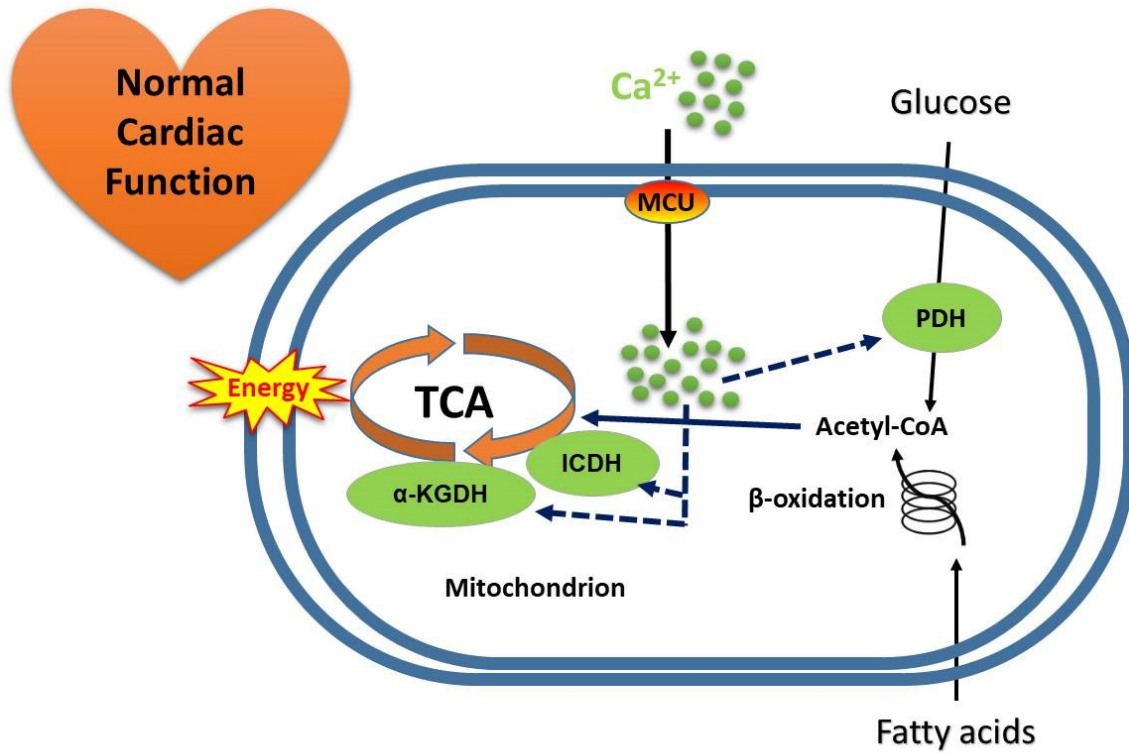


Figure 1.5

Figure 1.6. An overview of lysine acetylation of proteins in glucose and fatty acid metabolic pathways in the heart. In conditions of increased acetylation such as obesity, diabetes, and heart failure, decreased SIRT3 and increased GCN5L1 activity/expression can induce hyperacetylation of fatty acid oxidation enzymes, stimulating their activities. Decreased SIRT4 deacetylation activity as a result of low NAD^+ levels can potentially enhance the acetylation and thereby activity of malonyl-CoA decarboxylase, leading to a decline in malonyl-CoA levels, and an increase in mitochondrial fatty acid uptake and oxidation. Defects in electron transport chain or acetylation of its components result in decreased NAD^+ levels in mitochondria, thereby inhibiting SIRT3 and SIRT4 activities. In addition to enzymatic acetylation, non-enzymatic acetylation through increased mitochondrial acetyl-CoA levels, through accelerated fatty acid oxidation, accompanied by a decrease in SIRT3 activity secondary to low NAD^+ levels, can all render the diverse mitochondrial proteins susceptible to hyperacetylation. In addition, acetylated CrAT can reduce acetyl-CoA buffering capacity and lead to expansion of acetyl-CoA pool in mitochondria, while acetylation of succinate dehydrogenase is proposed to inhibit the flux through TCA cycle and ETC. GLUT4, glucose transporter-4; CD36/FAT, fatty acid translocase; Ac, acetylation; CPT, carnitine palmitoyltransferase; MCD, malonyl-CoA decarboxylase; ACC, acetyl-CoA carboxylase; NAD^+ , nicotinamide adenine dinucleotide; TCA, tricarboxylic acid; CACT, carnitine/acylcarnitine translocase; CrAT, carnitine acetyltransferase; LDH, lactate dehydrogenase; SIRT, sirtuin; PDH, pyruvate dehydrogenase; MPC, mitochondrial pyruvate carrier; GCN5L1, general control of

amino acid synthesis 5 like 1; ETC, electron transport chain; SDH, succinate dehydrogenase.

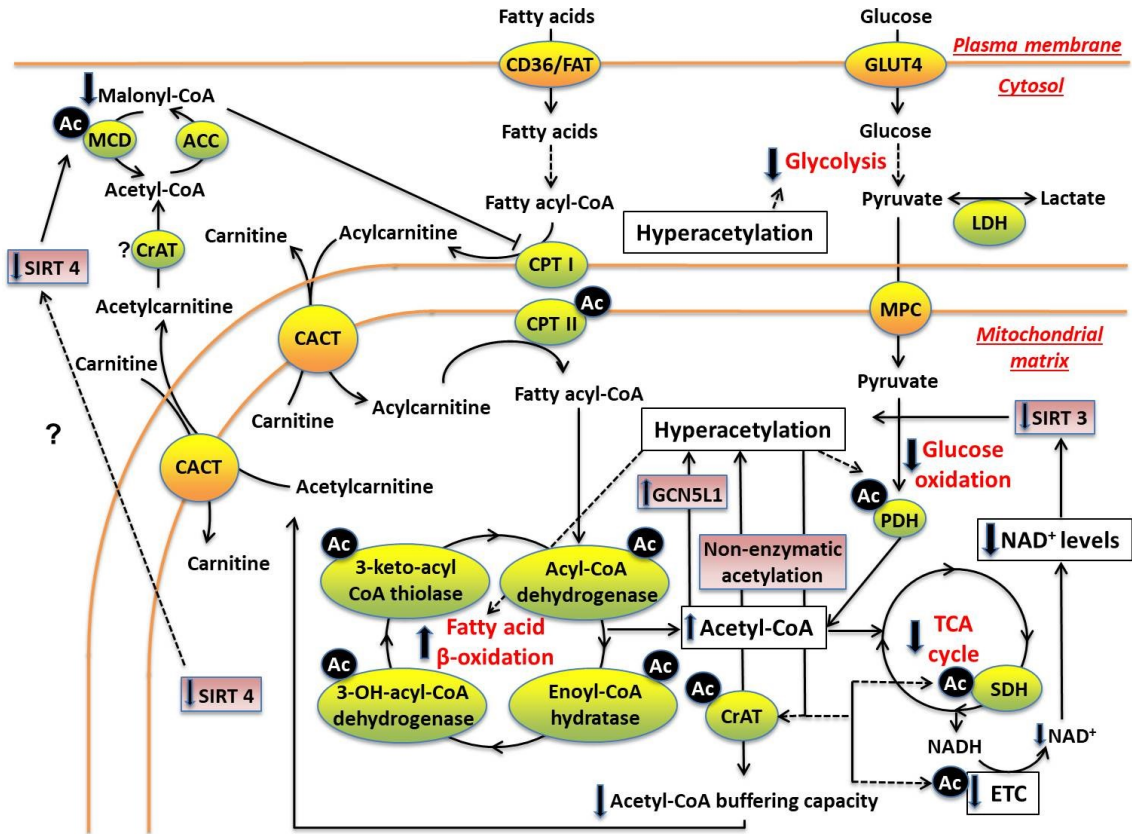


Figure 1.6

CHAPTER 2

Materials and Methods

CHAPTER 2

Materials and Methods

2.1 Introduction

In this thesis I focused on investigating biochemical regulatory processes and pharmacological interventions proposed to modulate glucose and fatty acid oxidation in either cultured cardiac cells or the intact heart, under non-stressful conditions, increased workload, or when subjected to I/R injury. For the study in Chapter 3, *in vitro* experiments were conducted in differentiated and undifferentiated cultured H9c2 cells to characterize CrAT, an important enzyme for short acyl group trafficking in myocardial cells. The methods that were used to investigate CrAT's cytosolic localization, cell culture and differentiation process are provided below. To assess CrAT localization in whole hearts, C57BL/6 mouse hearts were utilized. Enzymatic assays of CrAT as well as other enzymes were conducted alongside western blotting investigations. Also to further investigate the relationship between CrAT and cardiac energy metabolism, two mouse models were utilized. The first model was the ACC2 knock-out mouse where the malonyl-CoA production is genetically modified and is associated with increased rates of fatty acid oxidation. The second model was a diet-induced obesity model created by 10-weeks of high-fat diet consumption by C57BL/6 mice inducing enhanced rates of fatty acid oxidation. Relationships were studied through correlating energy metabolic rates measured by radiolabeled-energy substrate tracing and acetyl-CoA/CoA ratios to CrAT protein levels and activity in these

particular mice after subjecting them to *ex vivo* isolated working heart aerobic perfusions.

In the study discussed in Chapter 4, I conducted a series of experiments to examine whether compromised calcium uptake to the mitochondria can influence myocardial metabolism. The experiments were conducted with an initial assumption of impaired glucose oxidation through inhibition of PDH secondary to decreased calcium-dependent PDH phosphatase stimulation. This study utilized a mouse model of inducible cardio-specific deficiency of the mitochondrial calcium uniporter, the major calcium transporter recently identified in mitochondria. I used an isolated heart perfusion protocol that tested cardiac fatty acid and glucose oxidation in these hearts (and controls) in addition to function at baseline and in response to insulin alone, followed by increasing the workload by infusing isoproterenol.

To assess the role of endothelial mediated delivery of fatty acids, the project discussed in Chapter 5, a protocol of global no-flow I/R injury to isolated hearts was adopted to examine whether the genetic ablation of endothelial ATG7, and hence autophagy, would presumably modulate myocardial fatty acid oxidation and would have an effect on preservation of cardiac function after an ischemic insult. Energy metabolism was examined under aerobic conditions as well as in I/R. The assumption of inhibition of fatty acid delivery and oxidation in the myocardium was tested as a possible mechanism for combating the I/R stress. This was afterwards correlated with data obtained on TAG in hearts from knockout and control mice as well as data from transfection of human umbilical vein endothelial cells (HUVECs) with scrambled (control) or anti-ATG7 siRNA on endothelial cell expressed FABP.

Finally, as for the project assessing adropin discussed in details in Chapter 6, an initial set of experiments included 3 intraperitoneal injections of this peptide or vehicle into C57BL/6 mice over 24 hours, the last 12-16 of which involved fasting the animals before conducting *ex vivo* isolated working heart perfusion. These experiments were named *in vivo* adropin study. A subsequent set of perfusions were performed on hearts from non-fasting mice without injections. Here, adropin or vehicle was added directly to the perfusate and hearts were aerobically perfused where I could follow direct and prompt metabolic and functional effects of the intervention. These experiments were labelled *ex vivo* adropin study. Insulin sensitivity was tested in both studies by addition of insulin at mid-time of perfusions.

In these research projects, there was an emphasis on the relationship between *ex vivo* cardiac function and energy metabolism of the two major substrates (that are fatty acids represented by palmitate bound to albumin and glucose dissolved in the perfusate). The description of the methods used in this thesis is provided below. Details specific to individual studies will be provided in the “Materials and Methods” sections of Chapters 3 to 6.

2.2 Animals

Male mice were used in all studies included in this thesis. Wild-type C57Bl/6 mice were purchased from Charles River Laboratories (Wilmington, Massachusetts) while ACC2^{-/-} mice and littermates were obtained from Dr. Gary Lopaschuk’s colony (originally generated by Dr. David Olson at the Beth Israel Deaconess Medical Center Boston,

Massachusetts as previously described (16)). The inducible cardiac-specific MCU knock-out model was previously described (109). Briefly $Mcu^{fl/fl}$ mice were achieved by creating mice with a loxP flanked exons 5 and 6 of the *Mcu* locus. These mice were either crossed (or not, as controls) with mice expressing a tamoxifen-inducible Cre recombinase (MerCreMer) under α -myosin heavy chain promoter to produce the knock-out genotype ($Mcu^{fl/fl-MCM}$) (109). The MCU deficiency was induced by feeding 8-week old animals with tamoxifen laden chow (Harlan, 400mg/kg), including $MCU^{fl/fl}$ control mice for four weeks, then the mice were studied 3 months later. In experiments conducted on mice fed a standard chow diet or a high-fat diet (details of diets are explained in the Materials section below), the mice were given *ad libitum* either of the two diets for 10 weeks after weaning. The endothelial specific ATG7 KO mouse model (EC-ATG7^{-/-}) has been previously described and characterized (125,200,201). Briefly, EC-ATG7^{-/-} mice were produced by crossing ATG7^{fllox/fllox} and VE-Cadherin-Cre transgenic mice (The Jackson Laboratory, Bar Harbor, Maine; Stock # 006137). All animal studies were approved by the University of Alberta Health Sciences Animal Welfare Committee and comply with the guidelines of the Canadian Council of Animal Care, Alberta.

2.3 Materials

L-Carnitine, O-acetyl carnitine, CoA, acetyl-CoA, oxaloacetate, DTNB, ATP, malic dehydrogenase, digitonin, and citrate synthase were purchased from Sigma Aldrich (St Louis, Missouri). Fatty acid free bovine serum albumin (BSA) was purchased from Equitech-Bio Inc (Kerrville, Texas). [5-³H] glucose, [U-¹⁴C] glucose, [9, 10- ³H]

palmitate, and enhanced chemiluminescence (ECL) substrate were obtained from Perkin Elmer (Waltham, Massachusetts). Hyamine hydroxide was obtained from Curtis Laboratories (Bensalem, Pennsylvania). Adropin³⁴⁻⁷⁶ was obtained from ChinaPeptides Co., Ltd. (Shanghai, China). Mitochondria/Cytosol Fractionation Kit was purchased from Abcam (Cambridge, UK). EnzyChrom NAD⁺/NADH Assay Kit (E2ND-100) was obtained from Bioassays systems (Hayward, California). Free fatty acid assay kit was obtained from Wako Pure Chemicals Industries Ltd. (Osaka, Japan). Insulin (Novolin ge Toronto) was obtained from University of Alberta hospital stores and originally from Novo Nordisk (Mississauga, Ontario). For measurement of short chain CoAs, Waters UPLC system was used containing Supelco C8 10cm x 2.1mm 2.2 μ m column that was purchased from Waters Company (Milford, Massachusetts). Cell culture supplies were obtained from Sigma Aldrich (St Louis, Missouri) and Life Technologies (Carlsbad, California). GCN5-like protein 1 (GCN5L1) and β -actin primary antibodies, A/G-agarose beads, goat anti rabbit, goat anti mouse, and donkey anti goat secondary antibodies were all obtained from Santa Cruz (Santa Cruz, California). Carnitine acetyltransferase (CrAT) antibody was obtained from Aviva Systems Biology (San Diego, California). Long chain acyl CoA dehydrogenase (LCAD), β -hydroxyacyl CoA dehydrogenase (β -HAD), peroxisome proliferator activated receptor (PPAR) α , total OXPHOS rodent AB cocktail, citrate synthase (CS), α -tubulin, peroxisome proliferator-activated receptor gamma coactivator 1- alpha (PGC-1 α), sirtuin 3 (SIRT3), sirtuin 4 (SIRT4), cluster of differentiation 36 (CD36), carnitine palmitoyltransferase isoform B (CPT I B), PDK4, and mitochondrial Na⁺/Ca²⁺ exchanger (mito-NCLX or SLC24A6) primary antibodies were obtained from Abcam (Toronto, Ontario). 5'AMP-activated

protein kinase (AMPK), p-AMPK T172, pyruvate dehydrogenase (PDH), glyceraldehyde 3-phosphate dehydrogenase (GAPDH), forkhead box protein O1 (FoxO1), protein kinase B (Akt), p-Akt S473, glycogen synthase kinase (GSK)3 β , p-GSK3 α/β S21/9, mitochondrial Ca²⁺ uniporter (MCU), sirtuin 1 (SIRT1), Akt substrate of 160 kDa (AS160), p-AS160 T642, voltage dependent anion channel (VDAC), c-Jun NH2-terminal kinase (JNK), and p-JNK T183/Y185 primary antibodies were obtained from Cell Signaling (Danvers, Massachusetts). Malonyl-CoA decarboxylase (MCD) primary antibody was available through the University of Alberta. p-PDH S293 primary antibody was obtained from Calbiochem (San Diego, California). Acetyl-lysine, p-ACC S79/1200, insulin receptor substrate (IRS-1), p-IRS-1 Y628, and p-IRS-1 S307 primary antibody was obtained from Millipore (Darmstadt, Germany). Prohibitin was obtained from Fitzgerald Industries (Acton, Massachusetts). Peroxidase labeled streptavidin was obtained from Jackson ImmunoResearch (West Grove, Pennsylvania). ScintiSafe scintillation fluid, Pierce protease and phosphatase inhibitor mini tablets and all other chemicals were obtained from Thermo-scientific/Fisher Scientific (Fair Lawn, New Jersey). Nitrocellulose membrane was obtained from BioRad Laboratories (Munich, Germany). Western blotting Medical x-ray film was obtained from FUJIFILM (Tokyo, Japan). Standard chow diet (cat # 8656, Harlan Teklad), referred to as LFD, contained 34% calories from protein, 13% calories from fat, and 53% calories from carbohydrate and was obtained from Envigo (Madison, Wisconsin). HFD (cat# D12492, Research Diets) provided 20% calories from protein, 60% calories from fat (54.4% lard, 5.6% soybean oil), and 20% of calories from carbohydrate (12.2% maltodextrin, and 6.8% sucrose) and was obtained from Research Diets, (New Brunswick, New Jersey).

2.4 Methods

2.4.1 Cell culture

H9c2 cells (ATCC, Rockville, Maryland, USA) were cultured under standard conditions (202). Culture media contained high glucose Dulbecco's modified eagle medium (DMEM), 10% fetal bovine serum (FBS), 1% penicillin/streptomycin, and 0.25 mM carnitine. To induce differentiation once confluency reached 90%, the media was switched to cardiomyocyte differentiation media (high glucose- DMEM, 10% FBS, 1% penicillin/streptomycin, 0.25 mM carnitine, and 10 nM retinoic acid). Then cells were differentiated for 7 days. Cell culture media was changed every 48 to 72 hr during the differentiation period.

2.4.2 Subcellular fractionation

A. For heart/liver comparison: Tissue lysate differential centrifugation was used based on methods reported for the heart and liver with buffer conditions adapted for CrAT activity (203-205). Briefly, freshly extracted 8 to 10 week-old C57BL/6 mouse heart ventricles and livers were quickly washed and minced in ice cold homogenization buffer containing 20 mM Tris-HCl buffer (pH 7.5), 130 mM KCl, and 1 mM EDTA then homogenized using a Polytron homogenizer at medium speed for 25 s on ice. After centrifugation of homogenates at 800g for 10 min and discarding the pellet (cellular debris), the supernatant was centrifuged again at 8500g for 15 min. The pellet was re-suspended and centrifuged again at 8500g for 15 min. Thereafter, the pellet was re-suspended and used as the mitochondrial fraction. The supernatant from the first 8500g spin was centrifuged at 105,000g for 60 min, and the supernatant used as the cytosolic fraction. For preliminary experiments, a peroxisome-enriched fraction

(17,000g for 15 min, pellet) and microsomal fraction (105,000g for 60 min pellet) were also used.

B. For heart tissue CrAT localization: 8 to 10 week-old C57BL/6 mouse hearts were quickly removed from euthanized animals then immediately perfused for 5 min in a retrograde aortic Langendorff perfusion system with fatty acid free-, radiolabel free-Krebs-Henseleit solution to wash out blood and then the ventricles were excised and further washed with ice-cold phosphate buffer saline (PBS). After that, these tissues were either used for either CrAT activity or western blotting experiments. For activity assays, the ventricles were minced in 1 ml Cytosolic Extraction Buffer Mix prepared from a Mitochondria/Cytosol Fractionation Kit (Abcam plc, Cambridge, UK) and homogenized manually by Potter-Elvehjem PTFE pestle and glass tube (Sigma-Aldrich) by 10 strokes. Thereafter, the fractionation process was according to the kit's manufacturer protocol producing mitochondrial and cytosolic enriched subcellular fractions. For western blot fractionation assays, heart ventricles were minced on ice in a homogenization buffer containing: 10 mM tris HCL, 250mM sucrose, and 1 protease and phosphatase inhibitor tablet per 10 ml and homogenized by 25 strokes in Potter-Elvehjem. Thereafter, the fractionation process was the same as A, producing mitochondrial and cytosolic enriched subcellular fractions.

C. For cultured cell CrAT activity localization: After differentiating for 7 days, H9c2 cells along with undifferentiated controls were trypsinized and washed three times in PBS and then either manually homogenized after transferring to 1 ml ice-cold CrAT buffer (as used in A section) with Potter-Elvehjem homogenizer by 30 strokes, or permeabilized by incubation in CrAT buffer with pre-added digitonin (0.025 mg/ml)

for 10 min at 4°C on a shaker. Thereafter, the fractionation process followed the same differential centrifugation protocol used in section A.

Homogenate and mitochondrial fraction lysates were sonicated at medium power for 10 intermittent seconds on ice to disrupt the mitochondrial membranes or in case of using the fractionation kit, the Mitochondrial Extraction Buffer mix (MEBM) served that purpose. In preliminary experiments, the sonication approach and MEBM produced similar activity results to those produced using 0.1% Triton X-100 permeabilization.

2.4.3 Enzyme activity assays

The forward CrAT activity (acetyl-CoA to acetylcarnitine) was assayed spectrophotometrically using a DTNB reaction (412 nm absorbance) (77,206) with modification. Briefly, the reaction mixture for the spectrophotometric assay contained 0.1 M Tris-HCl (pH 8.0), 125 μ M DTNB, 0.1 mM acetyl-CoA (for localization and specific activity) or 0-100 μ M acetyl-CoA (for kinetics), 1.1 mM L-carnitine (for localization and specific activity) or 0-1.1 mM L-carnitine (for kinetics), and an aliquot of the enzyme source. Reverse CrAT activity (RCrAT) was assayed by a malic dehydrogenase-citrate synthase coupled assay (205,207) with some modifications. The assay mixture contained 100 mM Tris pH 8, 10 mM L-malate, 1 mM dithioerythritol, 0.2 mM NAD⁺, 2 mM acetyl-L-carnitine, 1 mM CoA (for localization and specific activity) or 0-200 CoA μ M (for kinetics), 20 units of malic dehydrogenase, 1 unit citrate synthase, and the fraction to be assayed. The reaction was monitored (NADH production) spectrophotometrically at 340nm. ATP- citrate lyase (ACL) activity was measured by malic dehydrogenase coupled assay (208) with minor modifications. The assay mixture contained 100 mM Tris pH 8, 0.2 mM NADH, 10 mM DTT, 5 mM ATP,

5 mM MgCl₂, 0.4 mM CoA, 10 mM potassium citrate, 20 units malic dehydrogenase and the sample to be assayed. The reaction was followed by monitoring absorbance changes at 340 nm. Citrate synthase activity was measured by a DTNB reaction (209) with 0.2 mM acetyl-CoA and 0.5 mM oxaloacetate in 100 mM Tris pH7.5 buffer. Protein concentration of subcellular fractions/ total homogenates was measured using Bradford assay (210).

2.4.4 Isolated working heart perfusions

Aged-matched male mice were used along with appropriate littermate controls. Isolated working heart perfusions were as described previously (21,211). Mice were anesthetized with a 12 mg intraperitoneal injection of sodium pentobarbital USP. Hearts were quickly extracted and the aorta cannulated and perfused in a retrograde manner in the Langendorff mode with Krebs-Henseleit buffer (KHB) containing in mM (118.5 NaCl, 25 NaHCO₃, 4.7 KCl, 1.2 MgSO₄, 1.2 KH₂PO₄, 2.5 CaCl₂, and 5 glucose) that is saturated with a gas mixture of 95% O₂ and 5% CO₂. Once the excess tissue was trimmed and the left atrium cannulated, the heart was switched to the working mode by opening the left atrial inflow (11.5 mmHg) and aortic outflow (against an afterload of 50 mmHg) lines while closing the Langendorff line. Thereafter, the perfusate flowed normally through the aorta in an antegrade manner. The working heart buffer consisted of a modified Krebs Henseleit solution that contained in addition to the above either 0.8, or 1.2 mM palmitate bound to 3% bovine serum albumin and either 0 or 100µU/ml insulin depending on the specific study protocol. Trace amounts of a combination of two appropriate radiolabeled molecules of [5-³H] glucose, [U-¹⁴C] glucose, [9, 10-³H] palmitate were added to assess rates of glycolysis, glucose oxidation, and palmitate

oxidation, respectively. Two metabolic rates were determined simultaneously by quantitative collection of $^{14}\text{CO}_2$ and $^3\text{H}_2\text{O}$ produced by the hearts (21,211). A linear time course was created from sampling every 10 min (7 min in experiments on MCU knock-out hearts) of the working buffer and hyamine hydroxide (used to capture CO_2) throughout the duration of perfusion in an air-sealed system. At the end of the perfusion protocol, hearts were clamp-frozen in liquid nitrogen and stored at $-80\text{ }^\circ\text{C}$ for subsequent biochemical studies. The dry/wet tissue ratio was calculated and metabolic rates were normalized to the total dry mass of the heart.

2.4.5 Measurement of mechanical function in the isolated working heart

Cardiac functional parameters were recorded using an MP100 acquisition system from AcqKnowledge (BIOPAC Systems, Inc.) that assessed heart rate and aortic pressure from signals produced by a Harvard apparatus pressure transducer connected to the aortic outflow line. Transonic flow probes were attached to left atrial and aortic lines to assess cardiac output and aortic outflow, respectively, through a T206 flow module (Transonic Systems, Inc). Cardiac work is calculated as the product of peak systolic pressure (minus 11.5 mmHg preload pressure) and cardiac output. Efficiency is represented as the ratio of cardiac work to total calculated acetyl-CoA production rates (from glucose and fatty acid oxidation rates). Coronary flow was calculated by subtracting aortic flow from cardiac output.

2.4.6 Assay of $^{14}\text{CO}_2$ and $^3\text{H}_2\text{O}$

Steady-state glycolysis or palmitate oxidation rates were calculated based on the amount of $^3\text{H}_2\text{O}$ produced by the isolated working heart from $[5\text{-}^3\text{H}]$ glucose or $[9, 10\text{-}^3\text{H}]$ palmitate, respectively. This was assessed by a $^3\text{H}_2\text{O}$ extraction assay using an

evaporation/condensation method on perfusate samples to separate $^3\text{H}_2\text{O}$ from un-metabolized [$5\text{-}^3\text{H}$] glucose or [$9, 10\text{-}^3\text{H}$] palmitate. Duplicate samples of 200 μl were pipetted out from larger perfusate samples, previously withdrawn at consecutive time points of perfusions and kept under mineral oil, then pipetted into 1.5 ml capless Eppendorf tubes placed inside scintillation vials containing 500 μl of double distilled H_2O (to help in heat transduction and to dilute the $^3\text{H}_2\text{O}$). Duplicate 200 μl samples of a standard solution of $^3\text{H}_2\text{O}$ were similarly prepared in parallel. These scintillation vials were capped and incubated at 50°C for 24 hr to promote $^3\text{H}_2\text{O}$ evaporation from inside the capless tube to its outer surfaces and the surrounding closed vial. Vials were then transferred to 4°C overnight to induce condensation. Thereafter, all water droplets on the outer wall of each capless tube, including $^3\text{H}_2\text{O}$, were carefully returned to the scintillation vials before properly discarding the capless tube with its remaining content. Duplicates of 200 μl of either $^3\text{H}_2\text{O}$ standard solution or un-metabolized buffer were placed inside empty scintillation vials to calculate transfer efficiency and specific activity, respectively. Scintillation fluid was added and radioactivity counted for all samples and standards in a liquid scintillation analyzer (Tri-carb 2800TR, Perkin Elmer).

Glucose oxidation rates calculated based on $^{14}\text{CO}_2$ production from [$\text{U-}^{14}\text{C}$] glucose. Any air exiting the air-sealed working heart system including $^{14}\text{CO}_2$ in the gaseous state had only one port of exit through a metal tube which tip is submerged and bubbling into hyamine hydroxide (a CO_2 scavenger) in a glass tube. Hyamine captures CO_2 and is sampled into scintillation vials filled with scintillation fluid to be counted later. The $^{14}\text{CO}_2$ dissolved in perfusate samples was released as a gas by mixing part of the sample

with sulfuric acid in an air-sealed glass vial except for a small whole leading to a scintillation vial at the top containing a hyamine-soaked filter paper to capture the released CO₂ overnight until scintillation fluid is added the next day and radioactivity counted.

2.4.7 Calculation of ATP, acetyl-CoA, and proton production

The metabolic rates determined by the methods described above were used to calculate ATP, acetyl-CoA, and proton production rates. For ATP produced by glycolysis and glucose oxidation, I used the assumption that 2 ATP and 31 ATP, respectively, are produced from metabolizing one molecule of glucose. For palmitate, a net of 106 ATP molecules is produced. As for TCA cycle acetyl-CoA production, 2 and 8 molecules of acetyl-CoA are produced from oxidizing 1 molecule of glucose and palmitate, respectively. Proton production was calculated by subtracting the glucose oxidation rate from glycolysis rate and then multiplying the result by 2.

2.4.8 Tissue content of total triacylglycerol (TAG) and incorporation of palmitate into TAG

TAG content was determined in heart ventricular tissue as previously described (212). Lipids were extracted from frozen tissue according to the method of Bligh & Dyer (213) with modifications. Tissue (10 mg) was homogenized in 20-fold volume (mg : μ l) of 2:1 chloroform-methanol then a 20% volume of methanol was added, and the lysate centrifuged at 3500g for 10 min. Subsequently, 20% volume of 0.04% CaCl₂ was added to the supernatant before centrifugation at 2400g for 20 min. The upper phase was discarded and the interface washed 3 times with a solution consisting of chloroform, methanol, and water (at a 3:48:47 volume ratio). Afterwards, methanol (50 μ l) was

added to form one phase before drying the samples under N₂ at 60°C and re-dissolving in a mixture of tert-butyl alcohol, triton X-100, and methanol (3:1:1 ratio) to form the final TAG extract. Cardiac TAG content was then measured colorimetrically using an enzymatic assay kit (Wako Pure Chemical Industries) according to manufacturer instructions. For perfused hearts, a portion of TAG extract was counted in a liquid scintillation analyzer (Tri-carb 2800TR, Perkin Elmer) to calculate the incorporation of perfused (exogenous) palmitate into TAG stores based on the specific activities of [9,10-³H]palmitate in un-metabolized perfusate samples. TAG content and palmitate incorporation were expressed as μmol/g dry tissue weight.

2.4.9 Western blot analysis

Protein levels in mouse hearts were assessed using immunoblotting as previously described (214). Briefly, mouse heart tissue was either homogenized on ice by Potter-Elvehjem homogenizer and then fractionated as explained above or frozen and later Polytron homogenized on ice for 25 s (depending on protocol) in a solution containing 50 mM Tris HCl, 0.02% Brij-35, 1 mM EDTA, 10% glycerol, 1 mM DTT, and protease and phosphatase inhibitors (Sigma). After sitting on ice for 10 min tissue homogenates were centrifuged at 800 g for 10 min and supernatants (lysates) were stored at -80°C. Protein contents of the lysates were determined using the Bradford protein assay (210). Samples were diluted and boiled in sample digestion buffer and 15-60 ug protein/well was run on 5%, 8%, 10% or 15% SDS-polyacrylamide gel electrophoresis (SDS-PAGE). Electrophoresis was run initially for 10 min at 60 Volts and then increased to 120 Volts until samples had completely run through. Proteins in gel were then transferred to a 0.45 μm nitrocellulose membrane overnight at 22-35 V. The membranes

were then blocked for 1 hr in 5% non-fat dry milk (NFDM) dissolved in 0.1% (vol/vol) tween 20- phosphate buffer saline (PBST) and then probed overnight at 4°C with the appropriate antibody in 3% BSA in PBST. The antibodies used and their vol:vol concentration in buffer was 1:1000 except for the following: CrAT (1:2000), GAPDH (1:3000), IRS-1 (1:500), pIRS-1 S307 (1:500), pIRS-1 Y628 (1:500), and peroxidase labeled streptavidin (1:2000). After washing the primary antibody 4 times x 10 min with PBST, the membranes were incubated with the appropriate peroxidase-conjugated secondary antibody 1% non-fat dry milk in PBST (Santa Cruz, 1:5000) for 1 hr at room temperature and washed again 4 times x 10 min before the immunoblot bands were detected using ECL and autoradiography. Peroxidase-labeled streptavidin (PLS) was used directly without secondary AB for the detection of ACC2 protein levels. Densitometry analysis of immunoblots was performed using ImageJ software (National Institutes of Health, USA) and normalized for value of the appropriate loading control.

2.4.10 Protein acetylation assay

Specific protein acetylation was assessed using an immunoprecipitation (IP) method as previously described (175) with minor modification. Frozen heart tissue was homogenized in IP buffer containing 50mM Tris HCl (pH 7.5), 150 mM NaCl, 5 mM EDTA, 0.5% NP-40, 1% Triton-X, and freshly added 1uM TSA, 5 mM nicotinamide, and 10 mM sodium butyrate, and protease inhibitor cocktail. Supernatants of 10,000 g for 10 min at 4°C were assayed for protein and a total of 100 µg protein was pre-cleared with 20 µl A/G-agarose beads then incubated with 3 µg acetyl-lysine antibody overnight at 4°C. The following day, 50 µl of A/G-agarose beads were added to each sample and incubated at 4°C on a rotator for 6 hr. Samples were then washed three times and spun

down at 5,000 g for 5 min keeping the pellet which was then mixed with 20ul 4x sample digestion buffer and boiled at 95°C for 5 min. Samples were then centrifuged at 15,000g for 15 min and all supernatant taken which could then be detected by western blotting as explained above. One separate sample was not incubated with agarose beads and antibody to serve as a positive control while a negative control was represented by a lysate processed with normal (control) rabbit IgG instead of acetyl-lysine antibody. The magnitude of acetylation was quantified by normalizing acetylated protein for total protein (input) band intensities.

2.4.11 Determination of CoA esters

CoA esters including free CoA, malonyl-, succinyl-, and acetyl-CoA were measured using a UPLC (ultra-performance liquid chromatography) procedure adapted from a method previously described with modification (215). Frozen heart tissue (15-20 mg) was homogenized for 25 seconds in 150 ul 6% PCA and left on ice for 10 min. Samples were centrifuged for 5 min at 12,000g and 4° C. Supernatants were then run on a Waters UPLC system that included a binary solvent manager (model 646M), sample manager (model 326M) and PDA detector (model 155M) using a Supelco C8 10cm x 2.1mm 2.2µm column, as described previously (216).

2.4.12 NAD⁺ and NADH determination

NAD⁺ and NADH content was measured in frozen heart ventricular tissue using EnzyChrom NAD⁺/NADH Assay kit (Bioassay Systems) according to the manufacturer's protocol.

2.4.13 Intraperitoneal glucose tolerance test

Mice fasted for 12 hr were assessed for whole body glucose tolerance. Body weight was assessed and blood glucose levels were measured using a commercial glucometer just before intraperitoneal injection of 2 g glucose/kg body weight. Blood glucose levels were then assessed at 15, 30, 45, 60, 75, 90, and 120 min from glucose administration.

2.4.14 HUVECs and real-time Polymerase Chain Reaction

Human umbilical vein endothelial cells (HUVECs) were cultured as previously described (200). The ATG7 knockdown experiments were performed by using small interfering RNA (siRNA) and scrambled siRNA as controls. Total RNA was isolated 48 hr post-transfection and cDNAs were synthesized using quantitect kit (Qiagen). Real-time PCR was performed for ATG7, CD36, fatty acids binding proteins (FABP 4 and 5) and GAPDH as loading control.

2.4.15 Statistical analysis

Data are expressed as means \pm SEM. Statistical significance of the means was determined using paired or unpaired t test, one-way analysis of variance (ANOVA) or two-ANOVA with repeated measures followed by Bonferroni post-hoc test where appropriate. Differences were considered significant if $p < 0.05$. GraphPad Prism 5 software was used for enzyme kinetics and statistical analysis.

CHAPTER 3

Cytosolic carnitine acetyltransferase as a source of cytosolic acetyl-CoA: a possible mechanism for regulation of cardiac energy metabolism

This chapter has been published: Tariq R. Altamimi, Panakkezhum D. Thomas, Ahmed M. Darwesh, Natasha Fillmore, Mohammad U. Mahmoud, Liyan Zhang, Abhishek Gupta, Rami Al Batran, John M. Seubert and Gary D. Lopaschuk. “Cytosolic carnitine acetyltransferase as a source of cytosolic acetyl-CoA: a possible mechanism for regulation of cardiac energy metabolism.” *Biochemical Journal* (2018) **475** 959–976.

Panakkezhum Thomas performed comparative experiments on hearts vs. livers. Ahmed M. Darwesh conducted subcellular localization western blotting. Natasha Fillmore provided cell cultures. I performed the rest of the experiments as well as experimental design, statistical analysis, and writing of the manuscript.

CHAPTER 3

Cytosolic carnitine acetyltransferase as a source of cytosolic acetyl-CoA: a possible mechanism for regulation of cardiac energy metabolism

3.1 Abstract

The role of carnitine acetyltransferase (CrAT) in regulating cardiac energy metabolism is poorly understood. CrAT modulates mitochondrial acetyl-CoA/CoA (coenzyme A) ratios, thus regulating pyruvate dehydrogenase activity and glucose oxidation. Here, we propose that cardiac CrAT also provides cytosolic acetyl-CoA for the production of malonyl-CoA, a potent inhibitor of fatty acid oxidation. We show that in the murine cardiomyocyte cytosol, reverse CrAT activity (RCrAT, producing acetyl-CoA) is higher compared with the liver, which primarily uses ATP-citrate lyase to produce cytosolic acetyl-CoA for lipogenesis. The heart displayed a lower RCrAT K_m for CoA compared with the liver. Furthermore, cytosolic RCrAT accounted for $4.6 \pm 0.7\%$ of total activity in heart tissue and $12.7 \pm 0.2\%$ in H9c2 cells, while highly purified heart cytosolic fractions showed significant CrAT protein levels. To investigate the relationship between CrAT and acetyl-CoA carboxylase (ACC), the cytosolic enzyme catalyzing malonyl-CoA production from acetyl-CoA, we studied ACC2-knockout mouse hearts which showed decreased CrAT protein levels and activity, associated with increased palmitate oxidation and acetyl-CoA/CoA ratio compared with controls. Conversely,

feeding mice a high-fat diet for 10 weeks increased cardiac CrAT protein levels and activity, associated with a reduced acetyl-CoA/CoA ratio and glucose oxidation. These data support the presence of a cytosolic CrAT with a low K_m for CoA, favoring the formation of cytosolic acetyl-CoA, providing an additional source to the classical ATP-citrate lyase pathway, and that there is an inverse relation between CrAT and the ratio of acetyl-CoA/CoA as evident in conditions affecting the regulation of cardiac energy metabolism.

3.2 Introduction

Cardiac disease is a major cause of death around the world (217). Multiple mechanisms lead to cardiac dysfunction and disability in heart disease, including alterations in myocardial energy metabolism (1,2). In recent years there has been an increasing interest in the modulation of myocardial energy metabolism as a therapeutic approach to treat heart disease (2). A state of competition exists between glucose and fatty acids as the main energy substrates used by the myocardium (63). However, compared to glucose oxidation and due to several factors, fatty acids are considered a less efficient source of energy (1,3). Accordingly, the therapeutic effects of metabolic modulatory medications are primarily aimed at tilting the balance toward glucose oxidation (2,196). Being a potent inhibitor of carnitine palmitoyltransferase I (CPT I), which controls mitochondrial fatty acid uptake, cytosolic malonyl-CoA constitutes a key regulatory point of fatty acid oxidation, and provides a potentially important target for therapeutic intervention (11-14). Malonyl-CoA is produced by acetyl-CoA carboxylase (ACC) and degraded by malonyl-CoA decarboxylase (MCD) in the cytosol and its levels depend on

a balance between the two processes and possibly its utilization for malonylation of proteins (13,14,218).

Carnitine acetyltransferase (CrAT) (also known as Carnitine O-acetyltransferase, EC number: 2.3.1.7) is a key member of the carnitine acyltransferase family. This enzyme family is essential for intracellular trafficking of fatty acids and thus for fatty acid oxidation (88). Although identified early, CrAT functions are the least studied among the carnitine acyltransferases. CrAT catalyzes the reversible transfer of acetyl group between CoA and carnitine:



CrAT is localized in the mitochondrial matrix and peroxisomes, but has also been proposed to exist in the endoplasmic reticulum and nucleus (67,219). However, a cytosolic localization of CrAT has not yet been shown. In the mitochondria, CrAT plays a key role in the modulation of mitochondrial acetyl-CoA/CoA ratios and can act as a buffer system preventing the accumulation of acetyl-CoA that would inhibit pyruvate dehydrogenase (PDH) activity (and thus pyruvate or glucose oxidation) and 3-ketoacyl CoA thiolase activity (and thus fatty acid oxidation) (80,86). The acetylcarnitine produced by mitochondrial CrAT can be shuttled out of the mitochondria and into the cytosol by carnitine translocase (16). The subsequent fate of the cytosolic acetylcarnitine has not been well characterized. We propose a pathway that involves regeneration of cytosolic acetyl-CoA from acetylcarnitine by means of a putative cytosolic CrAT, which then serves as a substrate for ACC to produce the potent fatty acid oxidation inhibitor, malonyl-CoA (29,76).

The aim of this study was to determine if CrAT is partially localized in the cytosol of the cardiomyocyte and whether CrAT is capable of functioning in the reverse direction (producing acetyl-CoA) to affect the regulation of fatty acid oxidation via the malonyl-CoA axis. We also investigated the relationship between CrAT and the malonyl-CoA axis in hearts from two mouse models known to have alterations in malonyl-CoA control of fatty acid oxidation.

3.3 Materials and Methods

3.3.1 Materials

Fatty acid free bovine serum albumin (BSA) was purchased from Equitech-Bio Inc. (Kerrville, Texas). [U-¹⁴C] glucose, [9, 10-³H] palmitate, and enhanced chemiluminescence substrate were obtained from Perkin Elmer (Waltham, Massachusetts). Antibodies used for western blotting (WB) were obtained from sources specified below. All other chemicals were purchased from Sigma Aldrich (St Louis, Missouri). Standard chow diet (8656, Harlan Teklad, Madison, WI, USA) referred to as LFD contained 34% calories from protein, 13% calories from fat, and 53% calories from carbohydrate. The high-fat diet (HFD) (D12492, Research Diets, New Brunswick, NJ, USA) provided 20% calories from protein, 60% calories from fat (54.4% lard, 5.6% soybean oil), and 20% of calories from carbohydrate (12.2% maltodextrin, and 6.8% sucrose).

3.3.2 Animals

Hearts and livers from euthanized C57BL/6 male mice (*Charles River* laboratories, Wilmington, MA) or hearts from euthanized ACC2^{-/-} (ACC2KO) male mice (originally

obtained from Dr. David Olson at the Beth Israel Deaconess Medical Center in Boston, Massachusetts and generated as previously described (16)) and their wild-type (WT) littermates were extracted and immediately used for mitochondrial and cytosolic isolations, or perfused before freezing and performing biochemical analysis. To assess the effect of high-fat feeding, two groups of C57BL/6 male mice underwent 10 weeks of feeding after weaning with either a regular chow diet (LFD) or a 60% fat diet (HFD) before euthanizing the animals and subjecting the hearts to *ex vivo* heart perfusions, as described below. All studies were approved by the University of Alberta Health Sciences Animal Welfare Committee and conform to the guidelines of the Canadian Council of Animal Care.

3.3.3 Cell culture

H9c2 cells (ATCC, Rockville, Maryland, USA) were cultured under standard conditions (202). Once confluency reached 90% media was switched to cardiomyocyte differentiation media (high glucose Dulbecco's Modified Eagle Medium (DMEM), 10% fetal bovine serum (FBS), 1% penicillin/streptomycin, 0.25 mM carnitine, and 10 nM retinoic acid). Then cells were differentiated for 7 days. The media was changed every 48 to 72 hr during the differentiation period.

3.3.4 Subcellular fractionation

Heart/liver comparison

Tissue lysate differential centrifugation was used based on methods reported for heart and liver with buffer conditions adapted for CrAT activity (203-205). Briefly, freshly extracted 8 to 10 week-old C57BL/6 mouse heart ventricles and livers were quickly washed and minced in ice cold homogenization buffer containing 20 mM Tris-HCl

buffer (pH 7.5), 130 mM KCl, and 1 mM EDTA then homogenized using a Polytron homogenizer at medium speed for 25 seconds on ice. After discarding the 800g x 10 min centrifugation pellet of homogenates (cellular debris), the supernatant was centrifuged again at 8500g x 15 min. The pellet was re-suspended and centrifuged again at 8500g x 15 min. Thereafter, the pellet was re-suspended and used as the mitochondrial fraction. The supernatant from the first 8500g spin was centrifuged at 105,000g x 60min, and the supernatant used as the cytosolic fraction. For preliminary experiments, a peroxisome-enriched fraction (17,000g x 15min, pellet) and microsomal fraction (105,000g x 60 min pellet) were also used.

Heart tissue CrAT localization

Eight- to 10-week-old C57BL/6 mouse hearts were quickly removed from euthanized animals then immediately perfused for 5 min in a Langendorff system to wash out blood and then the ventricles were excised and washed in ice-cold phosphate buffer saline (PBS). After that, these tissues were used for either CrAT activity or western blot experiments. For activity assays, the ventricles were minced in 1 ml Cytosolic Extraction Buffer Mix prepared from a Mitochondria/Cytosol Fractionation Kit (Abcam) and homogenized manually by Potter-Elvehjem PTFE pestle and glass tube (Sigma- Aldrich) by 10 strokes. Thereafter, the fractionation process was according to the kit's manufacturer protocol producing mitochondrial and cytosolic enriched subcellular fractions. For western blot fractionation assays, heart ventricles were minced on ice in a homogenization buffer containing: 10 mM Tris-HCl, 250mM sucrose, protease and phosphatase inhibitors and homogenized by 25 strokes in Potter-Elvehjem

homogenizer. Thereafter, the fractionation process was the same as in the ‘heart/liver comparison’ section.

Cultured cell CrAT activity localization

After differentiating for 7 days, H9c2 cells along with undifferentiated control cells were trypsinized and washed three times in PBS and then either manually homogenized after transferring to 1 ml ice-cold CrAT buffer (as used in the section ‘heart/liver comparison’) with Potter-Elvehjem homogenizer by 30 strokes, or permeabilized by incubation in CrAT buffer with pre-added digitonin (0.025 mg/ml) for 10 min at 4°C on a shaker. Subsequently, the fractionation process followed the same differential centrifugation protocol used in the ‘heart/liver comparison’ section.

Homogenate and mitochondrial fraction lysates produced by ‘heart/liver comparison’ and ‘cultured cell CrAT activity localization’ methods were sonicated at medium power for 10 intermittent seconds on ice to disrupt the mitochondrial membranes. Mitochondrial activity fractions in the ‘heart tissue CrAT localization’ method were lysed using the Mitochondrial Extraction Buffer mix (MEBM) provided in the fractionation kit mentioned above. In preliminary experiments, the sonication approach and MEBM produced similar activity results to those produced using 0.1% Triton X-100 permeabilization.

3.3.5 Heart perfusions

Fourteen week old male HFD mice or 16 to 28 week old ACCKO mice were used and compared to LFD mice or age-matched WT littermates, respectively. Mice were euthanized and hearts isolated and aerobically perfused using the *ex vivo* working heart

model for 60 min in a Krebs-Henseleit buffer containing 5mM glucose, 0.8 mM palmitate and 100 μ U/ml insulin, as described previously (21,211). Oxidation rates of glucose and palmitate were determined simultaneously by quantitative collection of $^{14}\text{CO}_2$ and $^3\text{H}_2\text{O}$ produced by the hearts consuming traces of [U- ^{14}C]glucose and [9, 10- ^3H]palmitate, respectively (21,211). Cardiac functional parameters were recorded using an MP100 system from AcqKnowledge (BIOPAC Systems, Inc.). Cardiac work was calculated as a function of peak systolic pressure and cardiac output. Efficiency is represented as the ratio of cardiac work to total calculated acetyl-CoA production rates (from glucose and fatty acid oxidation rates). At the end of the perfusion protocol, hearts were clamp-frozen in liquid nitrogen and stored at $-80\text{ }^\circ\text{C}$ for subsequent biochemical studies. The dry/wet tissue ratio was calculated and metabolic rates were normalized to the total dry mass of the heart.

3.3.6 Enzyme assays

The forward CrAT activity (acetyl-CoA to acetylcarnitine) was assayed spectrophotometrically using a DTNB (5, 5'-dithio-bis-[2-nitrobenzoic acid]) reaction (412 nm absorbance) (77,206) with modification. Briefly the reaction mixture for the spectrophotometric assay contained 0.1 M Tris-HCl (pH 8.0), 125 μM DTNB, 0.1 mM acetyl-CoA (for localization and specific activity) or 0-100 μM acetyl-CoA (for kinetics), 1.1 mM L-carnitine (for localization and specific activity) or 0-1.1 mM L-carnitine (for kinetics), and an aliquot of the enzyme source. Reverse CrAT activity (RCrAT) was assayed by a malic dehydrogenase-citrate synthase coupled assay (205,207) with some modifications. The assay mixture contained 100 mM Tris pH 8, 10 mM L-malate, 1 mM dithioerythritol, 0.2 mM NAD^+ , 2 mM acetyl-L-carnitine, 1 mM

CoA (for localization and specific activity) or 0-200 CoA μ M (for kinetics), 20 units of malic dehydrogenase, 1 unit citrate synthase, and the fraction to be assayed. The reaction was monitored (NADH production) spectrophotometrically at 340nm. ATP-citrate lyase (ACL) activity was measured by malic dehydrogenase coupled assay (208) with minor modifications. The assay mixture contained 100 mM Tris pH 8, 0.2 mM NADH, 10 mM DTT, 5 mM ATP, 5 mM $MgCl_2$, 0.4 mM CoA, 10 mM potassium citrate, 20 units malic dehydrogenase and the sample to be assayed. The reaction was followed by monitoring absorbance changes at 340 nm. Citrate synthase activity was measured by a DTNB reaction (209) with 0.2 mM acetyl-CoA and 0.5 mM oxaloacetate in 100 mM Tris pH7.5 buffer. Protein concentration of subcellular fractions/ total homogenates was measured using Bradford assay.

3.3.7 Western blotting

CrAT protein levels in mouse hearts were assessed using immunoblotting as described previously (214). Briefly, mouse heart tissue was either homogenized then fractionated as explained above or frozen and later Polytron-homogenized producing lysates and loading samples that were run on SDS-polyacrylamide gel electrophoresis then transferred to nitrocellulose membranes. The membranes were then blocked and probed with anti-CrAT antibody (AB) (Aviva Systems Biology, Cat# ARP53559_P050), anti-GAPDH antibody (Cell Signaling Technology, Cat# 2118), anti-prohibitin antibody (Fitzgerald Industries Cat# 10R-P140a), or anti- α -tubulin (Abcam Cat# 7291). Thereafter, standard western blotting procedures were conducted as previously described (214). Peroxidase-labeled streptavidin (PLS) (Jackson ImmunoResearch Laboratories, Cat# 016-030-084) was used for detection of ACC2 protein levels.

Densitometry analysis of immunoblots was performed using ImageJ software (National Institutes of Health, USA) and normalized for value of the appropriate loading control.

3.3.8 Determination of CoA esters

Free CoA and its short esters including free CoA, malonyl-, succinyl- and acetyl-CoA were measured using an ultra-performance liquid chromatography (UPLC) procedure adapted from a method previously described with modification (215). Heart tissue (15-20 mg) was homogenized for 25 seconds in 150 μ l 6% perchloric acid (PCA) and put on ice for 10 min. Samples were centrifuged for 5 min at 12,000g and 4° C. Supernatants were then run on a Waters UPLC system that included a binary solvent manager (model 646M), sample manager (model 326M) and PDA detector (model 155M) using a Supelco C8 10cm x 2.1mm 2.2 μ m column as described previously (216).

3.3.9 Determination of free- and acyl- carnitines

Frozen 20-30mg samples from heart ventricular tissue were homogenized in 6% PCA and placed on ice for 5 min before centrifugation for 10 min at 10000 g and 4 °C. Free L-carnitine was determined directly in neutralized supernatant, whereas short-acylcarnitines (along with free carnitine) were determined in neutralized samples after alkaline extraction (pH 11.5 at 55°C for 15min) of a portion of the supernatant. Long-acylcarnitines were determined in neutralized samples from the purified pellet after alkaline extraction (pH 13 and at 70°C for 60 min). The extracted free carnitine in all three sets of samples was then determined by a radiometric assay (220). Total carnitine was calculated as the sum of free, short- and long-acylcarnitines in each heart.

3.3.10 Statistical analysis

Data are expressed as means \pm SEM. Statistical significance of the means was determined using unpaired t test, one-way analysis of variance (ANOVA) or two-ANOVA with repeated measures followed by Bonferroni post-hoc test where appropriate. Differences were deemed significant if $P < 0.05$. GraphPad Prism 5 software was used for enzyme kinetics and statistical analysis.

3.4 Results

3.4.1 Acetyl-CoA production by CrAT in the heart

To determine if cardiac CrAT was a source of cytosolic acetyl-CoA, we first investigated the reverse CrAT activity in the heart and whether a cytoplasmic CrAT activity could be detected. We compared the activities and kinetics of CrAT in the heart to those in the liver, in order to delineate the metabolic role(s) that this enzyme may play in a highly catabolic tissue, the heart where fatty acid oxidation is essential, compared to a lipogenic metabolically active organ, the liver to serve the metabolic requirements of either tissue. In preliminary studies, CrAT activity was measured in peroxisome and microsomal-enriched fractions from mouse heart tissue and was found to be minimal in both fractions. Hence, further studies were confined to mitochondrial and cytosolic fractions or to whole tissue lysates. The strictly cytosolic ATP-citrate lyase (ACL) represents a major source of cytosolic acetyl-CoA for the synthesis of fatty acids and different lipid stores in the liver (221). It is proposed to play at least a partial role in the regeneration of acetyl-CoA in the cytosol of muscle cells (222). Citrate synthase (CS), on the other hand, is strictly a mitochondrial enzyme and its activity in

the cytosolic fraction indicates the percent of mitochondrial breakage. Therefore, it was used for that purpose (i.e. a mitochondrial marker).

The specific activities of CrAT, RCrAT, CS and ACL of C57BL/6 mouse heart and liver tissues are presented in Figure 3.1. Mouse heart mitochondria had a much higher CrAT activity (9 fold) compared to liver mitochondria (Figure 3.1A) in agreement with previously reported activities in rat and mouse heart and liver mitochondria (203,223). Heart mitochondria also had a 6 fold greater RCrAT activity compared to the liver (Figure 3.1A). A similar pattern was seen in CrAT activities measured in cytosolic fractions (Figure 3.1B). Noteworthy, a significant proportion of the measured cytosolic CrAT activity (apparent CrAT activity) is attributed to contamination with mitochondrial CrAT due to breakage of mitochondrial membranes during the isolation process (Figure 3.1D) (as evident by the detectible CS activity in cytosolic fractions, Figure 3.1C). However, even after accounting for mitochondrial content leakage into the cytosolic fraction using the equation:

$$\text{Corrected CrAT}_{\text{cyto}} = \text{apparent CrAT}_{\text{cyto}} - (\text{CrAT}_{\text{mito}} \times \text{CS}_{\text{cyto}} / \text{CS}_{\text{mito}}) \dots\dots\dots (1),$$

the residual cytosolic RCrAT activity in the heart was significantly higher than that in the liver (Figure 3.1E). Conversely, cytosolic ACL activity, an alternative source of cytosolic acetyl-CoA in liver, was >2.5 fold higher in the liver than the heart (Figure 3.1F). Being a lipogenic tissue and in light of the relatively low cytosolic RCrAT activity, the higher ACL activity in the liver is consistent with the requirement of acetyl-CoA for fatty acid synthesis. These data suggest an important role of CrAT in the

cytosol of myocardial cells, particularly through the reverse reaction which, at least in part and parallel to ACL, could constitute a source of cytosolic acetyl-CoA.

In order to further understand differences between heart and liver CrAT, we then performed forward and reverse enzyme kinetics. These assays were run in lysates from mouse heart and liver mitochondrial fractions and total homogenates (Figure 3.1G-J and Table 3.1). Cytosolic activities were not utilized due to the inability to reliably detect the low activities of CrAT at low substrate levels. Again, cardiac CrAT activities in the heart exceeded those in the liver tissue by several folds in both the forward and reverse direction (Figure 3.1G-J). In fact, total CrAT protein level in liver homogenates is considerably lower than those in heart homogenates that we could not detect it at protein content as high as 54 μg per well in SDS-polyacrylamide gel (Figure 3.1K). Due to the relatively small CrAT activity in the liver and to clearly display the hyperbolic nature of CrAT and RCrAT activity curves we present in Figure 3.2 the activity curves shown in Figure 3.1G-J as percent of V_{max} . Our kinetic data fit Michaelis-Menten kinetics with significant correlation (Table 3.1). The K_m for carnitine of heart mitochondrial CrAT was significantly higher than the liver ($P<0.05$) (Table 3.1). Interestingly, the K_m for CoA showed the opposite trend, which was lower in the heart compared to the liver ($P<0.05$) (Table 3.1). Although CrAT is assumed to exist at a smaller concentration in the total cytoplasmic protein pool than in the mitochondria alone and thus expected to exert lower activity in total homogenates compared to mitochondrial fractions, it showed numerically higher but statistically comparable V_{max} in heart homogenates compared to mitochondria (102.6 ± 7.0 vs. 80.6 ± 7.5 $\text{nmol} \cdot \text{min}^{-1} \cdot \text{mg protein}^{-1}$, respectively, $P=0.09$). This may further supports the hypothesis of

localization of an active CrAT in the cytosol of cardiomyocytes that keeps its total cytoplasmic concentration high enough to display this V_{\max} value. Since earlier CrAT studies were done on rats, we also measured CrAT activity in rat heart homogenates (Figure 3.1L). Velocity-substrate curves were obtained for carnitine as the variable substrate. The K_m and V_{\max} values for carnitine were generally comparable to those obtained from mouse heart homogenates (Table 3,1 and Figure 3,1H, P value not significant for either between the two species). Together, these results show that CrAT is capable of functioning in the reverse direction to produce acetyl-CoA; they also attribute a higher importance to cardiac CrAT as opposed to ACL in the cytosol of cardiac cells which could provide cytosolic acetyl-CoA, at least in collaboration with ACL.

3.4.2 Cytosolic CrAT localization

To focus on investigating possible cytosolic CrAT localization, we next performed subcellular fractionation on ventricular tissue excised from mouse hearts and subjected to mild homogenization with a Potter-Elvehjem homogenizer. This method applies shearing forces to disrupt the sample including cell membranes and induces less mitochondrial breakage than does Polytron homogenization as evident by reduced mitochondrial CS leaking out to cytosolic fractions (Appendix A, Figure A1). As expected, specific activities of CrAT and CS were higher in the mitochondrial fraction (Figure 3.3A-C). Interestingly, however, the ratios between CrAT and CS activities were significantly higher in the cytosolic preparation compared to the mitochondrial fraction when performing assays in either directions of CrAT activity (Figure 3.3D and 2G). Using equation (1) with CS and CrAT forward and reverse activities in subcellular

fractions, we calculated the residual cytosolic activities of the enzyme yielding 3.5 ± 0.5 , and $4.0 \pm 0.6 \text{ nmol} \cdot \text{min}^{-1} \cdot \text{mg protein}^{-1}$ (Figure 3.3E and H), representing percentages of total cellular CrAT and RCrAT that are shown in Figure 3.3F and I, respectively. For visual evidence of a cytosolic localization of CrAT, we performed immunohistochemistry experiments on heart slides. However, we achieved inconclusive data (Appendix A, Figure A2) which may reflect the hypothesized small proportion of cytosolic CrAT and thus the high mitochondrial/peroxisomal background. Therefore, we moved on to utilize an immunoblotting approach using mitochondrial and cytosolic markers in highly purified subcellular fractions of mouse heart ventricular tissues (Figure 3.3J). We utilized immunoblotting of prohibitin to confirm our successful fractionation procedure. Although prohibitin is a structural protein in the inner mitochondrial membrane, previous research studies have shown that prohibitin can leak into the cytosol in cases of mitochondrial injuries and therefore was used as a marker of mitochondrial contamination of cytosolic fractions (224-226). The undetectable prohibitin (mitochondrial marker) in cytosolic fractions indicates a highly pure fraction with minimum mitochondrial contamination. Here again we could detect significant CrAT protein levels in the cytosol with expectedly lower amounts than in mitochondria.

To determine if CrAT functions are modified by cardiomyocyte maturation and to further decrease mitochondrial breakage, we examined the cytosolic localization of CrAT in cultured H9c2 cells using both a Potter-Elvehjem homogenization (Figure 3.4) and a digitonin-based permeabilization (Figure 3.5) of cell plasma membrane. H9c2 are myoblasts derived from embryonic rat heart ventricle that can be differentiated into a more metabolically mature form (227,228). Using Potter homogenization, apparent CS

cytosolic activity was minimal reflecting a mitochondrial break of as low as 10.2 to 6.8% in undifferentiated and differentiated H9c2 cells, respectively (Appendix A, Figure A3). Similar to cardiac tissue, CrAT and RCrAT to CS activities were significantly higher in mitochondria compared to the cytosol (Figure 3.4A-C), whereas CrAT/CS and RCrAT/CS activity ratios in cytosolic fractions were significantly higher than in mitochondria (Figure 3.4D and G). These indicate actual cytosolic activities of 1.4 ± 0.2 and 1.1 ± 0.6 $\text{nmol} \cdot \text{min}^{-1} \cdot \text{mg protein}^{-1}$ in undifferentiated cells and 1.8 ± 0.2 and 2.8 ± 0.5 $\text{nmol} \cdot \text{min}^{-1} \cdot \text{mg protein}^{-1}$ in differentiated cells of CrAT and RCrAT, respectively (Figure 3.4E and H). These cytosolic activities represent averages of 6.9% and 7.2% in undifferentiated cells and 8.3% and 14.1% in differentiated cells of total CrAT and RCrAT, respectively (Figure 3.4F and I).

A mild digitonin lysis of cell membranes produced even lower mitochondrial breakage, averaging 7.4% to 5.5% in undifferentiated and differentiated H9c2 cells, respectively (Appendix A, Figure A3). Here again, an actual residual activity of CrAT in either reaction direction was reflected by clear difference in CrAT/CS activity ratios between the cell suspension medium (cytosolic fraction) and the extracted mitochondria (Figure 3.5D and G). Corrected cytosolic activities were 10.1 ± 2.4 and 4.2 ± 0.2 $\text{nmol} \cdot \text{min}^{-1} \cdot \text{mg protein}^{-1}$ in undifferentiated cells and 3.7 ± 0.7 and 4.0 ± 0.3 $\text{nmol} \cdot \text{min}^{-1} \cdot \text{mg protein}^{-1}$ in differentiated cells of CrAT and RCrAT, respectively (Figure 3.5E and H). Corrected cytosolic activity percentages were 51% and 27% in undifferentiated cells and 21% and 12% in differentiated cells of total CrAT and RCrAT, respectively (Figure 3.5F and I). Both mitochondrial CS and RCrAT activities were significantly higher in differentiated cells reflecting a higher protein content and maturity of mitochondria compared to

undifferentiated controls (Figure 3.5A and 4C). Together, these results indicate a cytosolic localization of CrAT in the mouse hearts and in a cultured cardiac cell-line where it can provide cytosolic acetyl-CoA from acetylcarnitine even in glycolytic undifferentiated H9c2 myoblasts.

3.4.3 CrAT involvement in malonyl-CoA regulation of cardiac metabolism

The comparison between CrAT and RCrAT kinetics in heart homogenates and mitochondrial fractions (Table 3.1) suggested that mitochondrial CrAT substrate affinity (at least in the forward reaction) was not affected by exposure to the cytosol contents (K_m 's for carnitine are not statistically different) and thus the mixed CrAT enzyme pool in homogenates may fairly represent (or mirror) the largest pool, that is in mitochondria. This assumption was used when assessing CrAT activities in homogenates of frozen tissues (e.g. after perfusions as explained below), from which purely separated mitochondrial- and cytosolic- enriched fractions are difficult to achieve and thus for practical purposes, homogenate activities were utilized in the working-perfused heart studies. We investigated how CrAT activity and protein levels are modified in mouse hearts with metabolic phenotypes that show alterations of the glucose/fatty acid oxidation balance. The first model chosen was one that is directly related to the malonyl-CoA axis, the ACC2-knockout mouse (ACC2KO) with whole body genetic ablation of ACC2, the predominant isoform of ACC in the heart (29). The second model was C57BL/6 mice fed for 10 weeks with a 60% high-fat diet (HFD) which show increased reliance of the heart on fatty acid oxidation for energy production compared to their regular diet controls (referred to here as low-fat diet, LFD) (214).

CrAT protein levels and activity in ACC2KO mouse hearts were compared to the acetyl-CoA/CoA ratio and malonyl-CoA levels, in order to determine if a relationship exists between these parameters as well as the metabolic profile of these hearts. Immunoblot analysis confirmed ACC2 deletion in the hearts of ACC2KO mice (Figure 3.6G). Being not subjected to stresses, these ACC2KO hearts showed cardiac work and efficiency, parameters of *ex vivo* cardiac function and efficiency of energy utilization, not different from WT controls (Figure 3.6A and F). However, these hearts did show significant differences in glucose and fatty acid oxidation rates compared to WT controls (Figure 3.6B and C). While the contribution of the oxidation of either substrates to the production of TCA cycle acetyl-CoA showed a higher reliance on fatty acid oxidation in ACC2KO hearts, the total acetyl-CoA production rate (from both substrates combined) was comparable to controls (Figure 3.6E and D). There was a significant decrease in CrAT protein levels in ACC2KO hearts (Figure 3.6G). Similarly, CrAT activity was also decreased (Figure 3.6H) in ACC2KO hearts. Interestingly, the acetyl-CoA/CoA ratio was significantly higher in ACC2KO heart than in control hearts (Figure 3.6I) without a difference in total malonyl-CoA between the two groups (Figure 3.6J). The reduced CrAT protein level and activity in ACC2KO hearts, which we mostly attribute to the larger pool of CrAT in the mitochondria, have incited us to measure the levels of free carnitine as well as short- and long- acylcarnitines in these hearts. ACC2KO hearts displayed higher free carnitine and lower levels of short-acylcarnitines compared to controls (Figure 3.7), consistent with a declined CrAT-mediated acetyltransferase activity from acetyl-CoA to free carnitine. In summary, ACC2KO mouse hearts showed a decrease in CrAT level and activity associated with a

high acetyl-CoA/CoA ratio, which was accompanied by an increase in the reliance on fatty acid oxidation.

To determine whether physiologically induced conditions associated with changes in acetyl-CoA levels in the heart can correlate with CrAT activity and protein levels, we next studied the effect of a 10-week HFD feeding on cardiac fatty acid and glucose oxidation in mice and correlated those metabolic effects to changes in CrAT. Again here in these unstressed hearts, cardiac work and efficiency were not statistically different between the two groups (Figure 3.8A and F). However, glucose oxidation rate in HFD hearts decreased to almost 28% of controls, (Figure 3.8B), whereas palmitate oxidation was not significantly different between the two groups (Figure 3.8C). This severe drop in glucose oxidation with HFD without a corresponding increase in fatty acid oxidation compromised the total production of TCA cycle acetyl-CoA (Figure 3.8D), in addition to decreasing the contribution of glucose oxidation to acetyl-CoA production (Figure 3.8E). On the other hand, CrAT protein levels and activity (Figure 3.8G and H, respectively) were both higher in hearts from HFD compared to LFD mice. This was accompanied by a significantly lower acetyl-CoA/CoA ratio in HFD hearts compared to LFD (Figure 3.8I). Here again, malonyl-CoA content was not different from controls (Figure 3.8J). In summary, hearts from 10-week HFD mice showed a higher CrAT levels and activity which were associated with a reduced acetyl-CoA/CoA ratio and a decrease in acetyl-CoA production secondary to low rates of glucose oxidation.

3.5 Discussion

As early as the 1960's, mitochondrial CrAT has been ascribed an important role in “buffering” excess acetyl-CoA, by transferring the acetyl- groups from acetyl-CoA to acetylcarnitine and thus contributing to the regulation of glucose oxidation (80,86,229). It is widely believed that acetylcarnitine is subsequently shuttled out of the mitochondria (16). However, what happens to acetylcarnitine in the cytosol has not been unequivocally determined. In this study, we provide findings that suggest partial localization of CrAT to the cytosol of cardiomyocytes, which works hand-in-hand with the mitochondrial CrAT in the regulation of cardiac energy metabolism through the regeneration of cytosolic acetyl-CoA from mitochondrial acetylcarnitine. We show that in whole hearts and in cultured H9c2 cells, a significant reverse CrAT activity exists and that this activity is present in the cytosol. We propose that the cytosolic acetyl-CoA produced by the reverse CrAT activity can then be used for malonyl-CoA synthesis, thereby regulating mitochondrial fatty acid uptake and oxidation (Figure 3.9). We show here that total CrAT levels and activity are lower in hearts with an attenuated ability to synthesize malonyl-CoA (i.e. ACC2KO mice hearts), whereas they are increased in hearts showing lower acetyl-CoA/CoA ratio (i.e. mice on a HFD).

For CrAT to support production of cytosolic acetyl-CoA and thus indirectly control malonyl-CoA inhibition of fatty acid oxidation, it must exist in the cytosol of cardiomyocytes without being contained in a membranous vesicle, unlike, for example, peroxisomal CrAT, to be allowed free access to cytosolic acetylcarnitine. It should also possess sufficient capacity to function in the reverse direction (RCrAT) to produce cytosolic acetyl-CoA. We show here that compared to the liver, the heart has >2.5 fold

higher cytosolic localized RCrAT activity. This has a special implication as the heart is not a lipogenic organ and a higher acetyl-CoA producing capacity is mostly directed towards the supply of malonyl-CoA production for fatty acid oxidation control. The citrate - ACL pathway is well-established in the liver as a source of cytosolic acetyl-CoA used in fatty acid synthesis (230). ACL is also suggested by previous studies to generate cytosolic acetyl-CoA in muscle cells (77). Poirier *et al.* proposed that ACL uses citrate molecules exported from the mitochondria to the cytosol as its substrate to provide cytosolic acetyl-CoA for the production of malonyl-CoA (222). Nonetheless, that study did not rule out a role for CrAT and acetylcarnitine as an alternative or supportive source and strong experimental evidence excluding CrAT contribution is still lacking. Our current results show relatively low cytosolic RCrAT activity in the liver accompanied by higher ACL activity which is consistent with the requirement of acetyl-CoA for fatty acid synthesis. Interestingly, these two enzyme activities in the liver differ from the heart with a similar proportion (i.e. about 2.5 folds) but in opposite directions. This may indicate complementary roles of these enzymes in heart and liver tissues to provide backup metabolic pathways.

One limitation in our study is that the incubation conditions used in our enzymatic assays, as with most *in vitro* assays, do not completely duplicate what is seen *in vivo* at the cellular/tissue level. This includes not using the exact concentration of carnitine that may inhibit cytosolic RCrAT activity *in vivo*. However, our assays do utilize buffers offering optimal pH, solubility and unlimited substrates and cofactors, and assess the activity at a linear steady-state velocity that produces considerable concentrations of products in the process, thus at least partly simulate *in vivo* product inhibition. There

has been very little research investigating the concentration of individual esters of carnitine in different subcellular compartments. However, despite that total carnitine content is known to be greater in the cytosol compared to the mitochondria on a per-gram-tissue basis, the concentration gradient is estimated to be minimum (231). The majority of the cytosolic, as well as the mitochondrial, carnitine is in the acid-soluble form which includes free and short-carnitines, whereas long-chain acylcarnitines concentrations are relatively low (231). The proportion of free versus acetylated form (acetylcarnitine) is unknown (232). Relevant to this, the mitochondrial membrane carnitine/acylcarnitine translocator (CACT) catalyzes the exchange of carnitine across the inner mitochondrial membrane as well as the unidirectional transport of carnitine down its concentration gradient (233). This process eventually results in the equilibration of carnitine concentrations across the mitochondrial membrane and also suggests that cytosolic and mitochondrial concentrations of free carnitine and acylcarnitines should be similar (232,234). Taking all of that into consideration and the fact that the equilibrium constant of CrAT is close to 1 (≈ 0.6) toward producing acetyl-CoA (205,206), we predict cytosolic CrAT to function near its equilibrium in the reverse direction when concentrations of acetylcarnitine change under different metabolic conditions.

The significantly higher CrAT K_m for carnitine in the heart compared to the liver suggests different physiological regulation of CrAT activity under variable concentrations of carnitine in the cardiomyocyte versus the hepatocyte. Accordingly, the liver enzyme may be working under saturating concentrations of carnitine, rendering it insensitive to minor changes in carnitine concentration as opposed to a more

responsive cardiac enzyme. Conversely, the lower cardiac CrAT K_m for CoA compared to liver favors the formation of cytosolic acetyl-CoA (by RCrAT direction) provided that the cytosolic variant of CrAT has similar kinetic characteristics to the mitochondrial enzyme, which we could not validate under our experimental conditions.

High mitochondrial breakage constitutes a major technical disadvantage of Polytron homogenization. Reported values for mitochondrial breakage vary from 5 to 30% (231,235). Therefore, we adopted different cell permeabilization techniques in the experiments subsequent to Polytron homogenization to increase specificity. Undifferentiated H9c2 myoblasts show proliferative capacity with a more glycolytic metabolic phenotype that is remodeled upon differentiation to become relatively more reliant on oxidative mitochondrial metabolism with higher energetic efficiency resembling mature cardiomyocytes (228). Mitochondrial break was lower in homogenized H9c2 cells and further lower with the milder digitonin permeabilization. Using these cardiomyocytes, we established that cytosolic localization of CrAT is essential even before differentiation of these myoblasts. The generally higher mitochondrial activities of CrAT and CS in differentiated cells are consistent with mitochondrial maturity and biogenesis occurring with H9c2 differentiation (228). In general, as long as the proportion of CrAT released from the mitochondria is comparable to or lower than that of CS, then the ratios presented in Figure 3-5 are valid predictors of actual cytosolic activity. Both CrAT and CS associate with the inner mitochondrial membrane with variable degrees. CrAT has a higher binding propensity, which reaches as high as 90% of the mitochondrial enzyme in a non-saturable manner, whereas CS association to the membrane is less strong and shows saturability

(236,237). Accordingly, there is a higher probability that less proportion of mitochondrial CrAT than that of CS is released from broken mitochondria during homogenization and centrifugation. Thus one can assume that the calculated (corrected) cytosolic CrAT herein is actually an underestimate of the actual value or that at least the estimation is safely valid.

Using the K_m and V_{max} values in Table 3.1, we calculate an RCrAT activity of 10.6 nmol acetyl-CoA per min per mg protein at 25 mM CoA, which is a normal cytoplasmic concentration. This activity is sufficient to supply the substrate for the production of malonyl-CoA bearing in mind the high turnover rates of malonyl-CoA and sensitivity of the predominant ACC isoform in the heart (ACC2) to acetyl-CoA concentration (29,76). Moreover, heart CPT I is extremely sensitive to the smallest change in malonyl-CoA concentration with an IC_{50} for malonyl-CoA \approx 100nM (29,78). Therefore, small changes in cytosolic acetyl-CoA concentration could theoretically lead to a strong inhibition of CPT I and fatty acid oxidation (29).

The ACC reaction in the heart is essential to the malonyl-CoA axis due to the low levels of the substrate, acetyl-CoA in the cytosol and the tighter regulation by kinases such as 5'adenosine monophosphate-activated protein kinase (AMPK) and hormones like insulin (238-241). In ACC2KO mouse hearts, a relationship between the lower CrAT protein levels and activity and an increased production of fatty acid-derived acetyl-CoA and its accumulation (high acetyl-CoA/CoA ratio) may exist. Although the TCA cycle consumes acetyl-CoA and thus may affect the acetyl-CoA/CoA ratio and although we did not measure actual TCA cycle enzyme activities, however we did measure succinyl-CoA levels which is an intermediate of the TCA cycle and they were not different

between WT and ACC2KO hearts (Appendix A, Figure A4). Accordingly and in light of unchanged total acetyl-CoA production (Figure 3.6D), it is highly plausible that in ACC2KO hearts the reduced mitochondrial CrAT buffering of acetyl-CoA, where most CrAT and acetyl-CoA exist, due to lower CrAT levels/activity has contributed to the increased ratio. However to explain why CrAT levels went down, we propose that the abolished ACC2-driven malonyl-CoA production may have decreased the requirement of acetylcarnitine originating from the mitochondria thus causing a product inhibition or a negative feedback resulting in a reduced requirement and protein levels of mitochondrial CrAT (down-regulation). This mitochondrial CrAT represents the majority of cellular CrAT and thus a drop in its levels will translate into lower total protein levels and activity of CrAT. Consistent with this drop in CrAT levels are the lower levels of cardiac short-acylcarnitines and higher free carnitine we found in ACC2KO hearts compared to controls (Figure 3.7).

Conversely, 10-week HFD feeding showed an opposite pattern with respect to CrAT protein levels and activities which were both higher compared to LFD control hearts. This is similar to what was recently reported in skeletal muscles of Zucker diabetic fatty rats showing increased activity and protein level of CrAT with a higher proportion of the latter (242). However that same study showed in 20-week high-fat diet that increased CrAT protein levels were not matched by increased activity in skeletal muscles (242). In HFD hearts, acetyl-CoA/CoA ratio was low contrary to what was found in ACC2KO mice. However, the fact that the inverse relationship between CrAT activity and acetyl-CoA/CoA was maintained in both models is intriguing. We propose that the increased activity of CrAT enhances the transfer of acetyl groups from acetyl-

CoA to carnitine in the mitochondria leaving behind a lower ratio of acetylated vs. free CoA. A status of depressed acetyl-CoA production in these HFD hearts secondary to significantly compromised glucose oxidation (diet-induced insulin resistance) with unaltered palmitate oxidation rate may have up-regulated mitochondrial CrAT (at transcriptional or post-translational level) to sustain constant supply of acetylcarnitine to the cytosol and/or out of the cell thus regenerating mitochondrial free CoA for continuous metabolic processes. In this sense, CrAT variability in both models could be resulting from up-regulation/down-regulation processes suggesting a missing link between acetyl-CoA/CoA ratio and the regulation of CrAT levels and/or activity.

Adding to the complexity of this paradigm is the fact that in both ACC2KO and HFD hearts, malonyl-CoA was not different from respective controls. In fact, it is intriguing that ACC2KO hearts show a normal level of malonyl-CoA. However, this was previously shown in the same animal model in skeletal muscles and may suggest compensatory mechanism counteracting the deletion of ACC2, the major ACC isoform in the heart (16). Whether this malonyl-CoA production is mediated by ACC1 is not clear but highly possible (29,243). The two isoforms are encoded by two separate genes, with ACC2 having capacity to bind the outer mitochondrial membrane and most likely provide a pool of malonyl-CoA directed toward CPT I inhibition and fatty acid oxidation regulation unlike ACC1 that is free in the cytosol and is mostly involved in the synthesis of fatty acids (243,244). Consequently, accepting the value of total tissue content of malonyl-CoA as a predictor of malonyl-CoA inhibition of CPT I and fatty acid oxidation is questionable even in a non-lipogenic organ like the heart. In fact, the inhibition of fatty acid oxidation by malonyl-CoA has been challenged before and holds

some uncertainty (245,246). Additionally in both models investigated here, measurements of malonyl-CoA levels were performed in insulin-treated hearts. Insulin is known to up-regulate ACC activity through inhibiting its phosphorylation by AMPK and cause an acute increase in malonyl-CoA levels (26,247). Therefore, insulin may have turned available ACC “on” producing “maximum” levels of malonyl-CoA and hence the lack of differences. Although our ACC2KO and WT cardiac levels of malonyl-CoA are in accordance with previously measured values in rat hearts ($\approx 10 \text{ nmol} \cdot \text{g dry weight}^{-1}$) (29), the levels were about two times higher in LFD and HFD hearts which could have resulted from the different genetic background or age of these mice (FVB vs. C57BL/6). The discrepancy in metabolic rates between the two control groups (WT ACC2 and C57BL/6 controls) may as well, have resulted from the different age and/or genetic background of these mice.

In conclusion, we provide evidence for cytosolic CrAT protein localization and activity in whole ventricular tissue and H9c2 cells that is able to supply acetyl-CoA for malonyl-CoA synthesis by ACC. In addition, CrAT functions appear to actively interact with enzymes of the malonyl-CoA axis, particularly ACC, and respond to metabolic clues such as dietary fat to fine-tune the regulation of energy metabolism. Understanding some of CrAT roles in the cardiomyocyte (summarized in Figure 3.9) will add to our knowledge of cardiac energy metabolism aiming at finding potential metabolic therapies for treatment of heart disease.

Table 3.1 Michaelis–Menten parameters for forward (CrAT) and reverse (RCrAT) activities of carnitine acetyltransferase in the heart and liver of C57BL/6 mice. $n = 3–4$ in triplicate technical samples.

CrAT			
Fraction	K_m (μM carnitine)	R^2 goodness of fit	V_{\max} ($\text{nmol} \cdot \text{min}^{-1} \cdot \text{mg protein}^{-1}$)
Heart			
Homogenate	53.7 \pm 1.1*	0.94	102.6 \pm 7.0*
Mitochondria	56.2 \pm 9.4*	0.94	80.6 \pm 7.5*
Liver			
Homogenate	3.5 \pm 0.3†	0.92	9.0 \pm 0.4
Mitochondria	11.0 \pm 1.8	0.85	10.2 \pm 1.1
RCrAT			
Fraction	K_m (μM CoA)	R^2 goodness of fit	V_{\max} ($\text{nmol} \cdot \text{min}^{-1} \cdot \text{mg protein}^{-1}$)
Heart			
Homogenate	66.4 \pm 1.6*,†	0.75	26.8 \pm 6.2*
Mitochondria	32.8 \pm 2.4*	0.91	24.5 \pm 1.8*
Liver			
Homogenate	113.4 \pm 8.1	0.93	3.1 \pm 0.3
Mitochondria	88.8 \pm 9.0	0.61	7.0 \pm 2.1
* $P < 0.05$, vs. corresponding fraction from liver tissue. † $P < 0.05$, vs. mitochondrial value of same tissue type, unpaired t-test.			

Figure 3.1. Carnitine acetyltransferase activities and kinetics in the heart compared with the liver. Carnitine acetyltransferase activity in the heart and in the liver in both mitochondrial (**A**) and cytosolic fractions (**B**). CS activity in the heart and the liver (**C**). Mitochondria breakage represented as CS leakage into cytosolic fractions (**D**). Corrected cytosolic acetyl-CoA-producing (RCrAT) activity in the heart and the liver (**E**). ATP-citrate lyase activity in the heart and the liver (**F**). Enzyme kinetics of carnitine acetyltransferase in the forward direction at variable carnitine concentrations in mitochondrial fractions (**G**) and homogenates (**H**) and in the reverse direction at variable free CoA concentrations in mitochondrial fractions (**I**) and homogenates (**J**) from heart ventricular and liver tissue. Total CrAT protein levels in homogenates of liver and cardiac ventricular tissues using α -tubulin as loading control (**K**). C57BL/6 mouse tissues were used in experiments from **A** to **K**. Enzyme kinetics for CrAT in homogenates of rat hearts (**L**). $^*P < 0.05$ compared with that of liver in the same direction of activity. $^{\#}P < 0.05$ compared with the mitochondrial fraction. $n = 3-5$ in triplicate technical samples. CrAT and RCrAT: forward and reverse directions of the carnitine acetyltransferase reaction, respectively. ACL: ATP-citrate lyase.

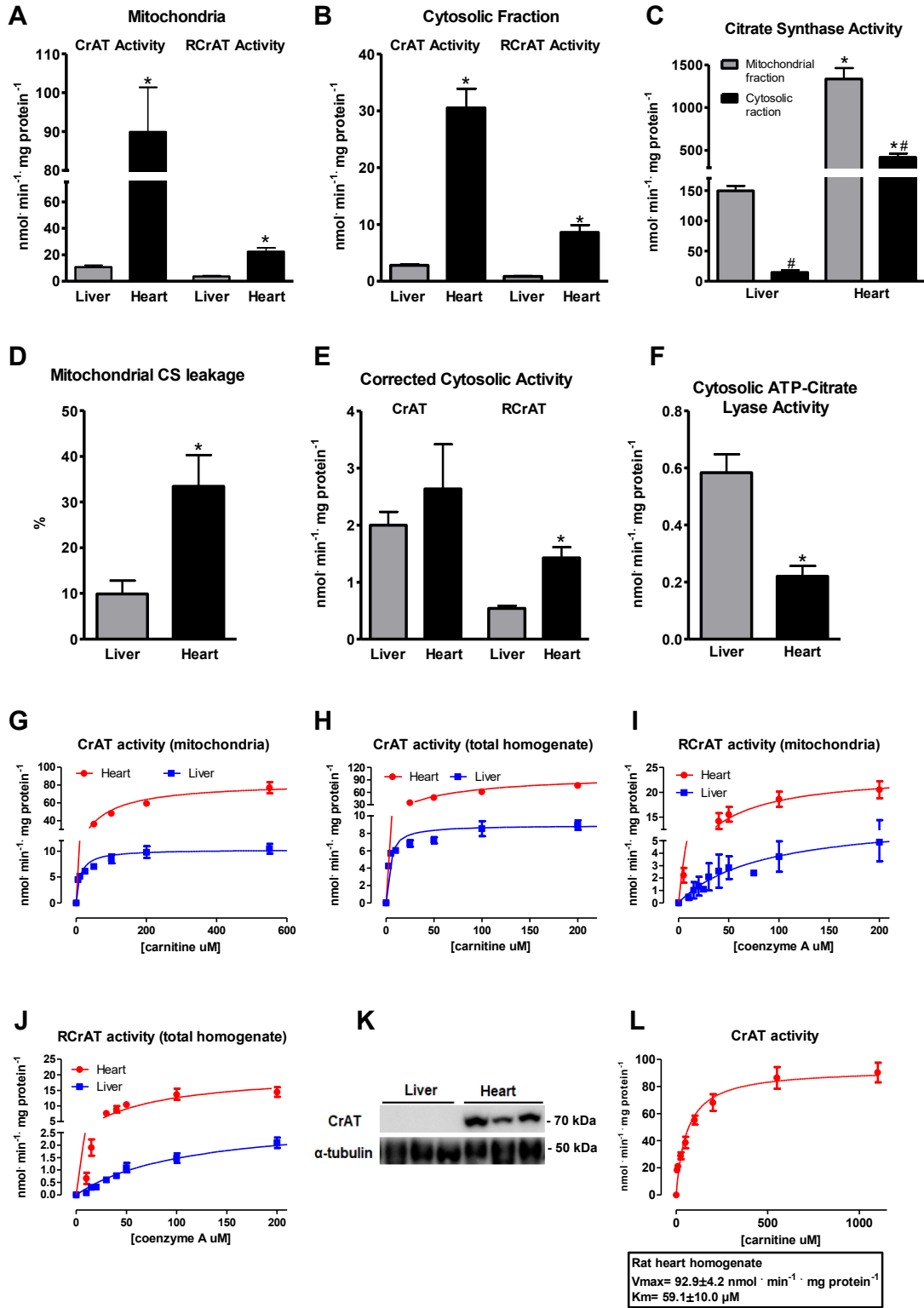


Figure 3.1

Figure 3.2. Enzyme activity of carnitine acetyltransferase presented as percent of V_{max} in the forward direction (**A-D**) at variable carnitine concentrations in mitochondrial fractions (**A, B**) and homogenates (**C, D**) and in reverse direction (**E,-H**) at variable free CoA concentrations in mitochondrial fractions (**E, F**) and homogenates (**G, H**) from heart ventricular and liver tissue, respectively.

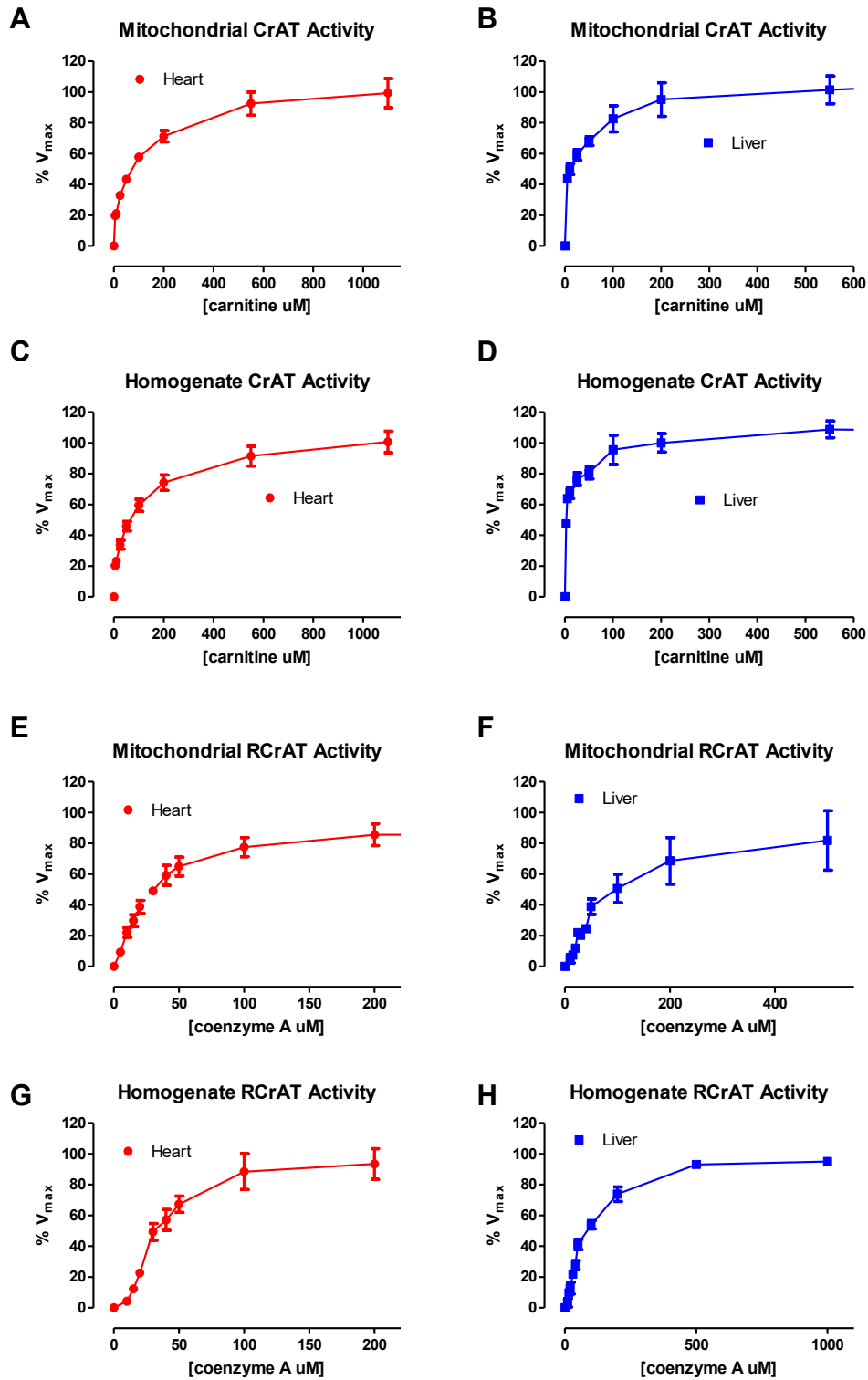


Figure 3.2

Figure 3.3. Cytosolic carnitine acetyltransferase in cardiac tissue. Enzyme activities of CS (**A**), forward CrAT (**B**), and reverse RCrAT carnitine acetyltransferase (**C**), in cytosolic and mitochondrial fractions. CrAT/CS and RCrAT/CS ratios (**D** and **G**, respectively) in cytosolic fractions compared with the mitochondrial fraction. Calculated residual cytosolic activities of CrAT (**E,F**) and RCrAT (**H,I**). * $P < 0.05$ vs. mitochondria, $n = 10-14$ in triplicate technical samples. Immunoblots of CrAT protein in highly purified cytosolic fractions (**J**), $n = 6$. Lysates were obtained from C57BL/6 mouse heart ventricles homogenized by Potter-Elvehjem.

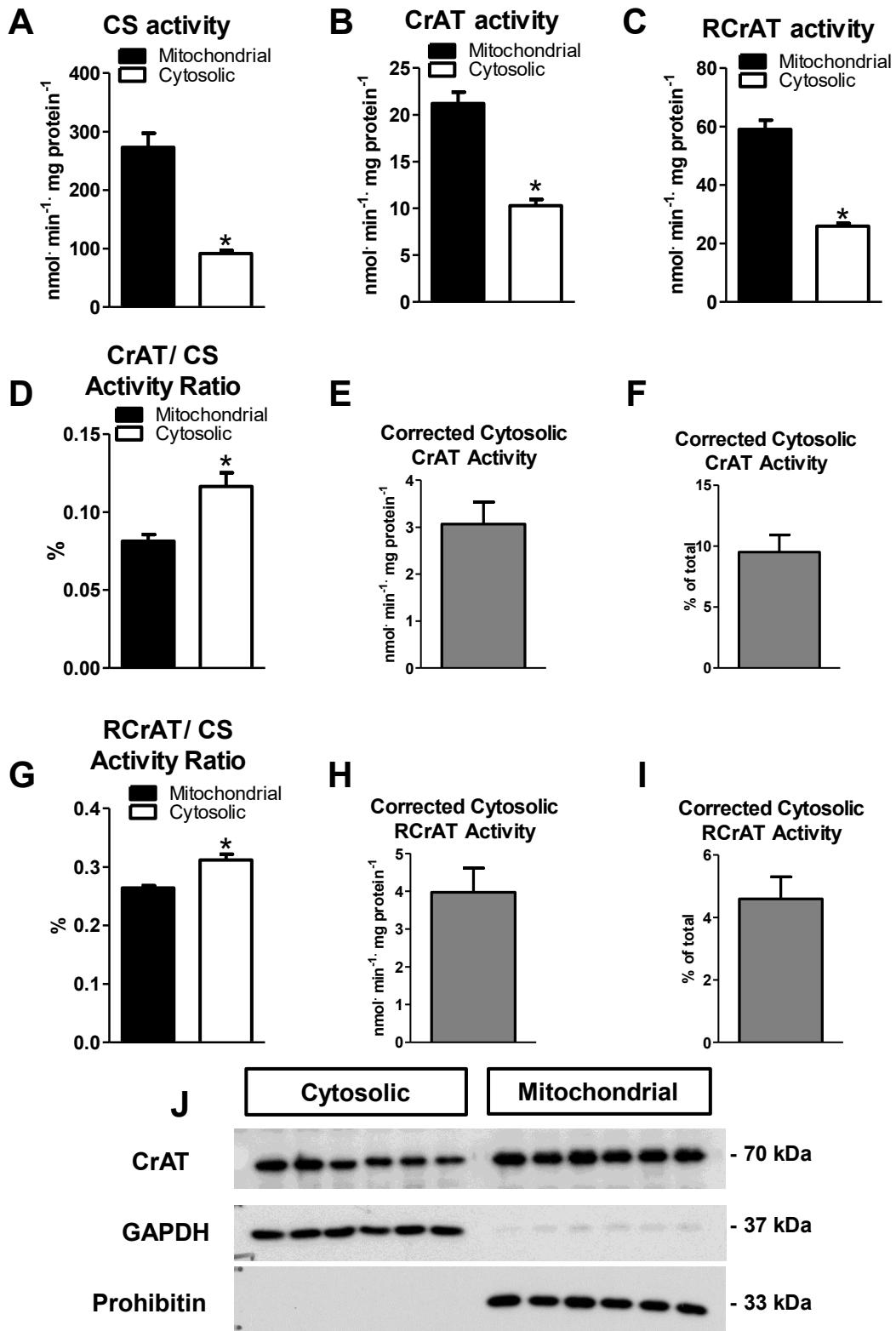


Figure 3.3

Figure 3.4. Cytosolic carnitine acetyltransferase activities in homogenized cultured cardiac cells. Enzyme activities of CS (**A**), forward CrAT (**B**), and reverse RCrAT carnitine acetyltransferase (**C**), in cytosolic and mitochondrial fractions of cultured H9c2 cells. CrAT/CS and RCrAT/CS ratios (**D** and **G**, respectively) in cytosolic fractions compared with the mitochondrial fraction. Calculated residual cytosolic activities of CrAT (**E,F**) and RCrAT (**H,I**). Lysates were obtained from homogenized undifferentiated and differentiated H9c2 cells using Potter-Elvehjem. * $P < 0.05$ vs. mitochondria, $n = 3$ in triplicate technical samples.

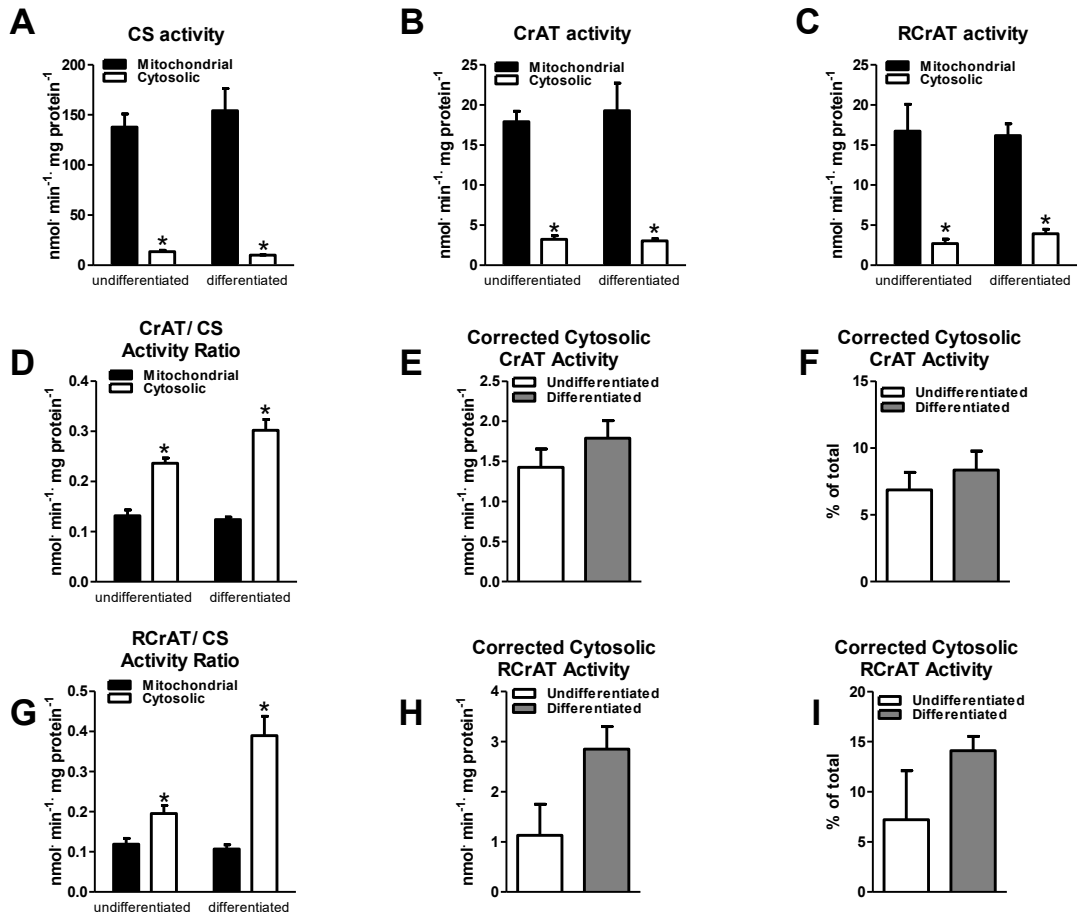


Figure 3.4

Figure 3.5. Cytosolic carnitine acetyltransferase activities in permeabilized cardiac cells. Enzyme activities of CS (**A**), forward CrAT (**B**), and reverse RCrAT carnitine acetyltransferase (**C**), in cytosolic and mitochondrial fractions of cultured H9c2 cells. CrAT/CS and RCrAT/CS ratios (**D** and **G**, respectively) in cytosolic fractions compared with the mitochondria fraction. Calculated residual cytosolic activities of CrAT (**E,F**) and RCrAT (**H,I**). Lysates were obtained from undifferentiated and differentiated H9c2 cells permeabilized by digitonin as explained in methods. * $P < 0.05$ vs. mitochondria, # $P < 0.05$ vs. undifferentiated cells in the respective fraction. $n = 3$ in triplicate technical samples.

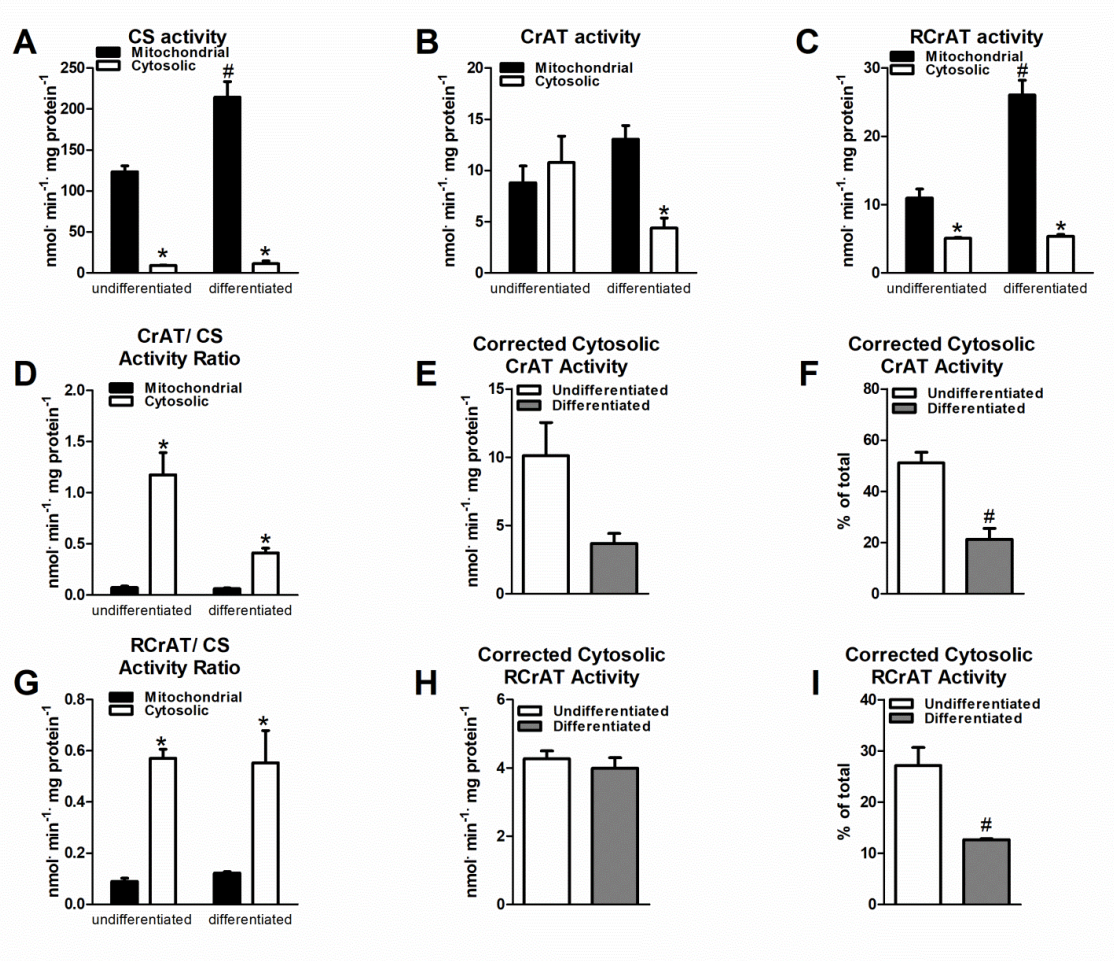


Figure 3.5

Figure 3.6. Cardiac protein level and total activity of CrAT are decreased in ACC2 deficiency. *Ex vivo* cardiac work (**A**); glucose oxidation (**B**); palmitate oxidation (**C**); total acetyl-CoA production (**D**); percentage contribution of glucose and palmitate oxidation to acetyl-CoA production (**E**); cardiac efficiency (**F**); CrAT western blots (**G**) ($n = 6$); CrAT activity (**H**); and acetyl-CoA/CoA ratio (**I**) of ACC2KO and WT control mice. Confirmation of ACC2 gene deletion in hearts of ACC2KO animals is shown in panel **G** using WB with peroxidase-labeled streptavidin that binds the biotin cofactor of carboxylases. ACC2 band is missing in ACC2KO hearts in contrast with WT controls showing both ACC1 and 2. (**J**) Malonyl-CoA levels measured by UPLC as explained in methods and normalized for g dry weight of tissue. $n = 5-18$. Duplicate technical samples were used to yield data in **B-F** and triplicates for **H**. * $P < 0.05$ vs. WT.

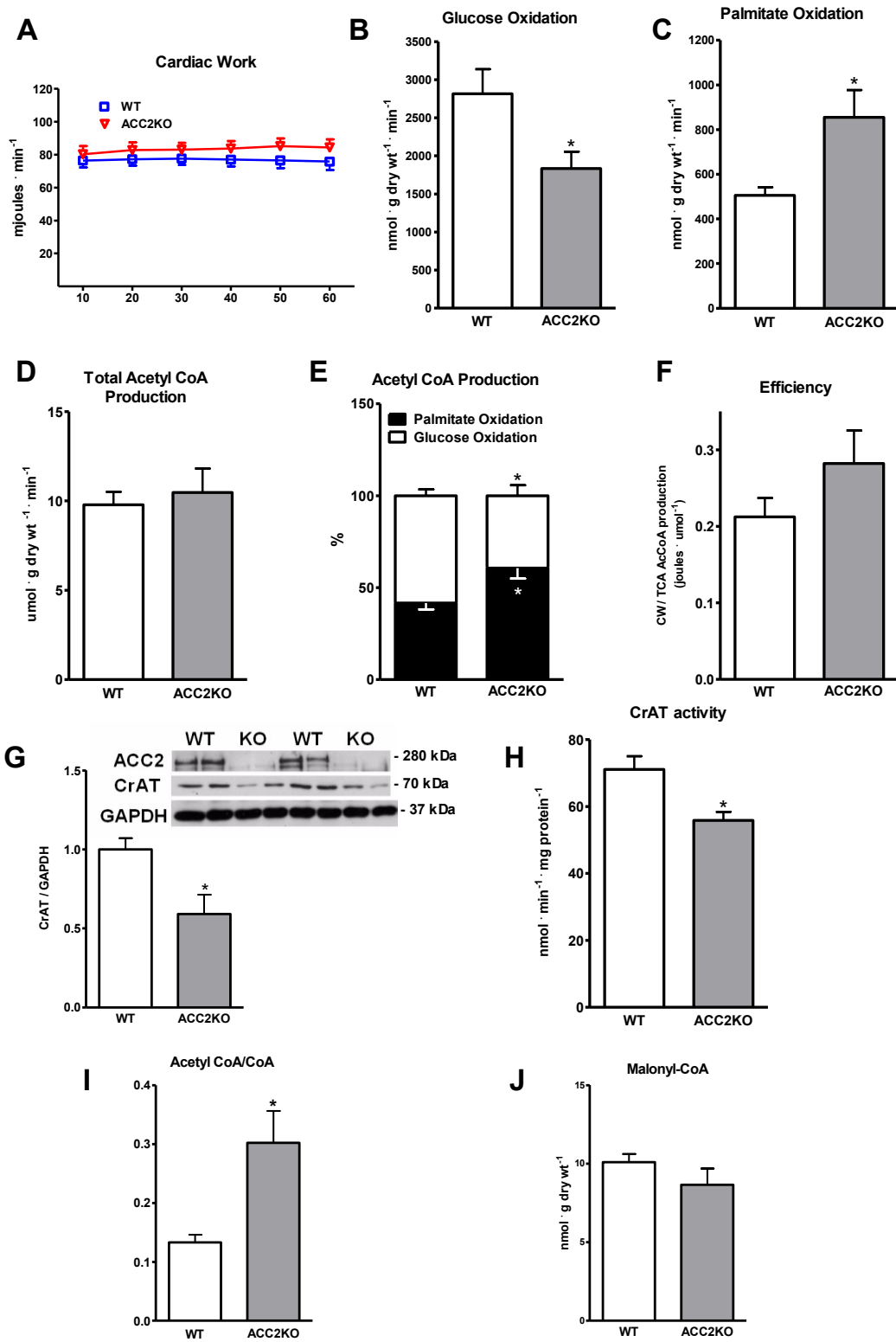


Figure 3.6

Figure 3.7. Free, short-chain, long-chain acyl-, and total carnitine content in ACC2KO hearts compared to WT controls. $n=4-14$. $*P<0.05$ vs. WT.

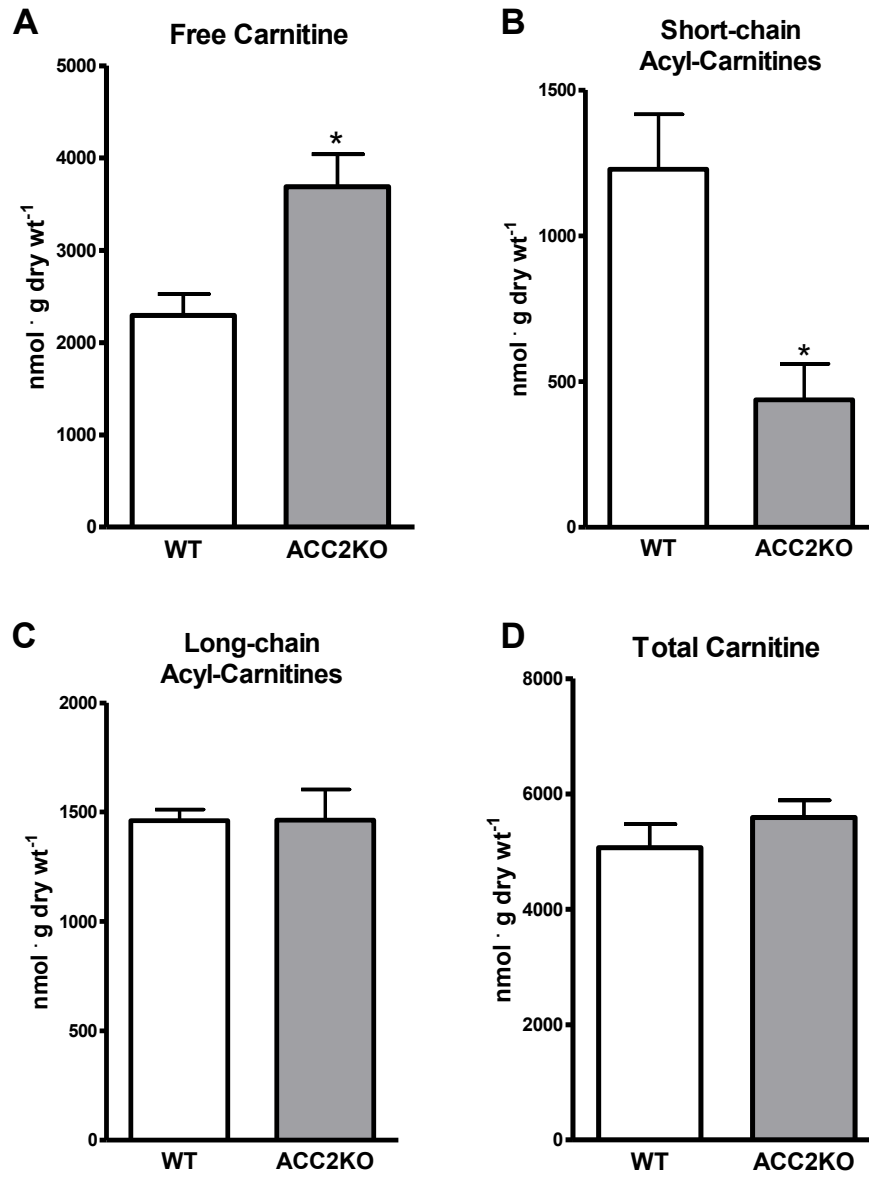


Figure 3.7

Figure 3.8. Cardiac protein level and total activity of CrAT are increased in response to a HFD. *Ex vivo* cardiac work (**A**); glucose oxidation (**B**); palmitate oxidation (**C**); total acetyl-CoA production (**D**); percentage contribution of glucose and palmitate oxidation to acetyl-CoA production (**E**); cardiac efficiency (**F**); CrAT western blots (**G**) ($n = 6$); CrAT activity (**H**); and acetyl-CoA/CoA ratio (**I**) of hearts from mice fed a 60% HFD for 10 weeks when compared with LFD controls. (**J**) Malonyl-CoA levels measured by UPLC as explained in methods and normalized for g dry weight of tissue. Duplicate technical samples were used to yield data in **B–F** and triplicates for **H**. $n = 3–7$. * $P < 0.05$ vs. LFD.

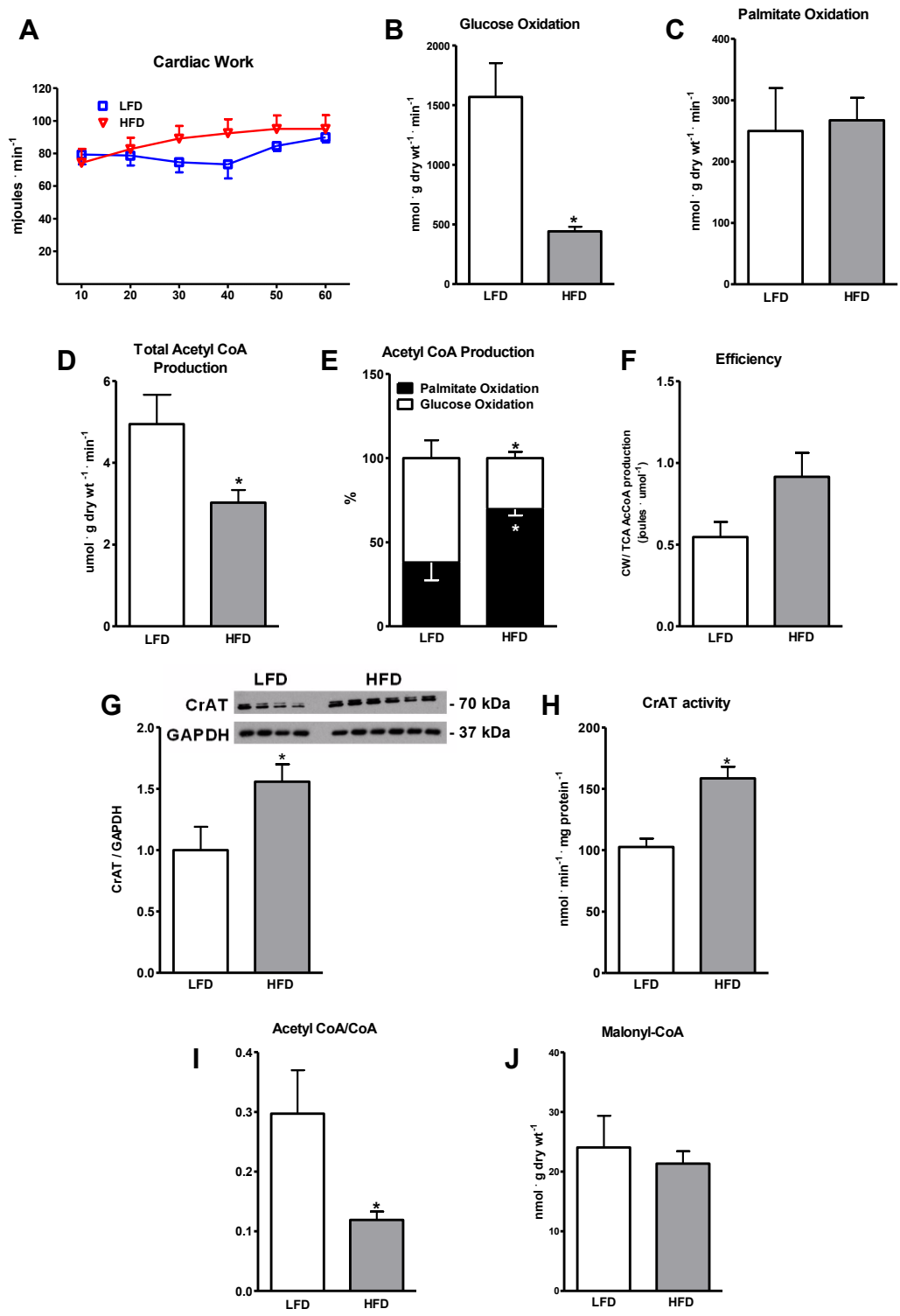


Figure 3.8

Figure 3.9. Proposed scheme as to how CrAT contributes to regulation of energy metabolism. To sustain the activity of the pyruvate dehydrogenase and hence glucose oxidation, mitochondrial CrAT (mCrAT) lowers acetyl-CoA by producing acetylcarnitine, which is exported to the cytosol where cytosolic CrAT (cCrAT) produces acetyl-CoA to supply malonyl-CoA production, thereby regulating fatty acid oxidation. CD36/FAT, fatty acid translocase; FACS, fatty acyl-CoA synthetase; CPT, carnitine palmitoyltransferase; GLUT, glucose transporter; CACT, carnitine/acetylcarnitine translocase; MCD, malonyl-CoA decarboxylase; ACC, acetyl-CoA carboxylase; ACL, ATP-citrate lyase; PDC, pyruvate dehydrogenase complex; TCA, tricarboxylic acid cycle.

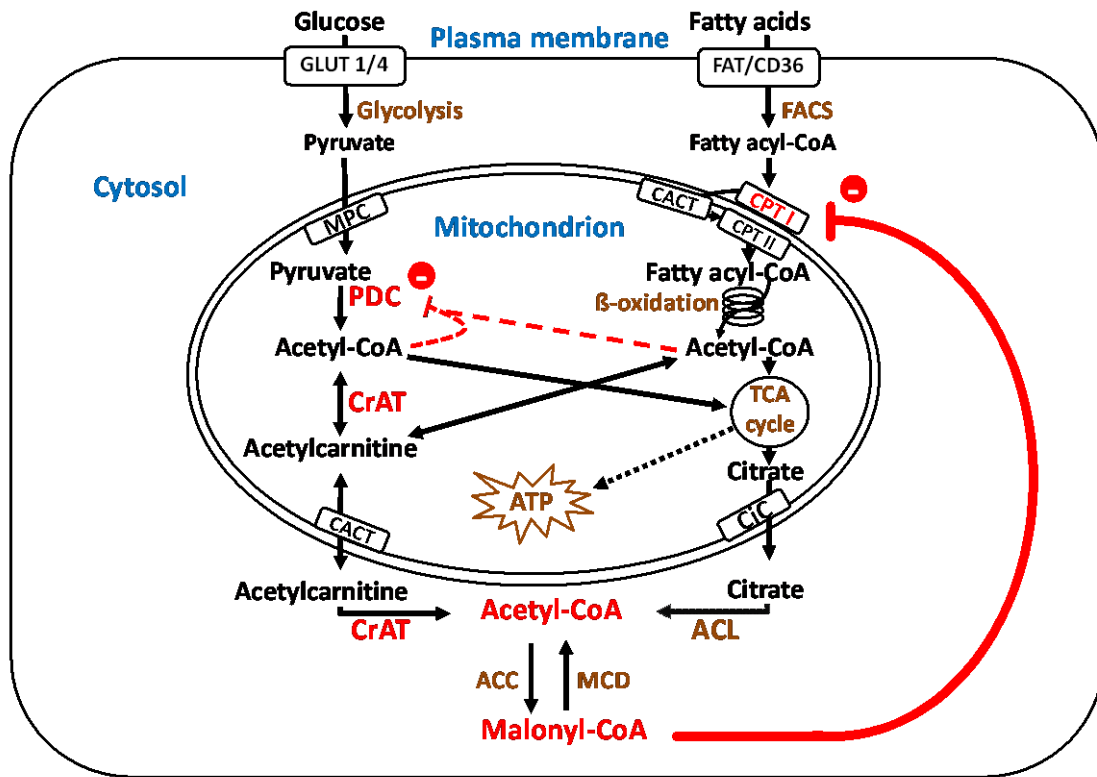


Figure 3.9

CHAPTER 4

Cardiac-Specific Deficiency of the Mitochondrial Calcium Uniporter Augments Fatty Acid Oxidation and Functional Reserve

A manuscript is currently in preparation to be submitted to *Journal of Molecular and Cellular Cardiology*.

Arata Fukushima helped with western blotting and acetylation experiments. Golam Mezbah Uddin conducted some western blotting experiments. I designed the study, conducted all remaining experiments, analyzed the results, and wrote the manuscript.

CHAPTER 4

Cardiac-Specific Deficiency of the Mitochondrial Calcium Uniporter Augments Fatty Acid Oxidation and Functional Reserve

4.1 Abstract

The mitochondrial calcium uniporter (MCU) relays cytosolic Ca^{2+} transients to the mitochondria. We examined whether energy metabolism was compromised in hearts from mice with a cardiac-specific deficiency of MCU subjected to an isoproterenol challenge. Surprisingly, isolated working hearts from cardiac MCU deleted mice showed higher cardiac work, both in the presence or absence of isoproterenol. These hearts were not energy-starved, with isoproterenol inducing a similar increase in glucose oxidation rates compared to control hearts, but a greater increase in fatty acid oxidation rates. This correlated with lower levels of the fatty acid oxidation inhibitor malonyl-CoA, and to an increased stimulatory acetylation of its degrading enzyme malonyl-CoA decarboxylase and of the fatty acid oxidation enzyme β -hydroxyacyl CoA dehydrogenase. We conclude that impaired mitochondrial Ca^{2+} uptake does not compromise cardiac energetics due to a compensatory stimulation of fatty acid oxidation that provides a higher energy reserve during acute adrenergic stress.

4.2 Introduction

Mitochondrial uptake of Ca^{2+} in vertebrates has been documented since the early 1960s (96). This process has a central role in cell physiology by stimulating ATP production, shaping cytosolic Ca^{2+} transients, and regulating cell death (97). Mitochondrial Ca^{2+} uptake has been attributed to a putative mitochondrial Ca^{2+} uniporter (MCU), with the channel eventually being identified in 2011 (98). The gene for MCU contains a sequence coding for two trans-membrane domains embedded in the inner mitochondrial membrane (98). In addition, several other proteins associated with this channel have been identified as regulatory components (99-102).

Early studies examining the metabolic effects of increasing heart work showed an increased myocardial glucose uptake and glucose oxidation with epinephrine treatment (107). This increase in glucose oxidation rates is associated with increased glycolysis and enhanced pyruvate dehydrogenase (PDH) activity even at the presence of high fatty acid levels (22,106). This was mainly attributed to the stimulatory effect of an increase in mitochondrial Ca^{2+} on PDH phosphatase (52). While increasing workload also increases fatty acid oxidation, this occurs with a lower magnitude than glucose oxidation (glycogenolysis and PDH stimulation) (22,48). This presumably occurs due to adrenergic-induced increases in cytosolic Ca^{2+} that are relayed into mitochondria by the MCU and hence influence the activity of the intramitochondrial Ca^{2+} -sensitive dehydrogenases and PDH phosphatase (106).

Mitochondria derived from $\text{MCU}^{-/-}$ mice have no apparent capacity to rapidly uptake Ca^{2+} (109,110). Despite this, basal metabolism in the skeletal muscle of $\text{MCU}^{-/-}$ mice

seems unaffected despite alterations in the phosphorylation and activity of PDH (110). In addition, MCU^{-/-} mice exhibit marked impairment in their ability to perform strenuous work and respond to acute exercise stimulation (109,110). However, it is not clear what effect increasing workload has on cardiac function and energetics if cardiac mitochondrial Ca²⁺ uptake is compromised. Therefore, we conducted our study on MCU cardiac-specific and inducible knock-out mice hypothesizing that subjecting these mice to an increased workload (i.e. isoproterenol stress) will result in an impaired glucose oxidation and reduced efficiency due to a higher phosphorylation status of PDH resulting from a decreased Ca²⁺-dependent PDH phosphatase activity.

4.3 Materials and Methods

4.3.1 Materials

Fatty acid free bovine serum albumin (BSA) was obtained from Equitech-Bio Inc. (Kerrville, Texas). [U-¹⁴C] glucose, [9, 10-³H] palmitate, and enhanced chemiluminescence substrate were obtained from Perkin Elmer (Waltham, Massachusetts). Hyamine hydroxide was obtained from Curtis Laboratories (Bensalem, Pennsylvania). EnzyChrom NAD⁺/NADH Assay kit (E2ND-100) was obtained from Bioassays Systems (Hayward, California). Insulin (Novolin ge Toronto) was obtained from University of Alberta hospital stores and originally from Novo Nordisk (Mississauga, Ontario). For measurement of short chain CoAs, Waters UPLC system was used containing Supelco C8 10cm x 2.1mm 2.2µm column that was purchased from Waters Company (Milford, Massachusetts). A/G-agarose beads, Goat anti rabbit, goat

anti mouse, and donkey anti goat secondary antibodies were obtained from Santa Cruz (Santa Cruz, California). Specific primary antibodies were obtained from the indicated following sources: CS, α -tubulin, LCAD, β -HAD, PGC-1 α , SIRT3, SIRT4, Total OXPHOS Rodent AB Cocktail (for complex I to V), and mito-NCLX (SLC24A6) (Abcam Toronto, Ontario). MCD (University of Alberta). GCN5L1 (Santa Cruz, California). AMPK, p-AMPK T172, MCU, FOXO1, SIRT1, VDAC, and PDH (Cell Signaling, Danvers, Massachusetts). p-PDH S293 (Calbiochem, San Diego, California). Acetyl-lysine, and p-ACC S79, (Millipore, Darmstadt, Germany). Peroxidase labeled streptavidin (Jackson ImmunoResearch, West Grove, Pennsylvania). Nitrocellulose membrane was obtained from BioRad Laboratories (Munich, Germany). Western blotting Medical x-ray film was obtained from FUJIFILM (Tokyo, Japan). ScintiSafe scintillation fluid, Pierce protease and phosphatase inhibitor mini tablets and all other chemicals were obtained from thermo-scientific/Fisher Scientific (Fair Lawn, New Jersey).

4.3.2 Animals

The generation of the inducible cardiac specific MCU knock-out mouse was previously described (109). Briefly, MCU^{fl/fl} mice were generated by targeting the *Mcu* locus with loxP flanking exons 5 and 6. MCU^{fl/fl} animals were crossed (or not, as controls) with mice expressing a tamoxifen-inducible Cre recombinase (MerCreMer) under α -myosin heavy chain promoter to produce MCU^{fl/fl-MCM} animals. MCU deficiency was induced by feeding 8-week old male mice with tamoxifen laden chow (Harlan, 400mg/kg) along with MCU^{fl/fl} controls (109) for 4 weeks, then analyzed 3 months later. All animal studies were approved by the University of Alberta Health Sciences Animal Welfare

Committee and comply with the guidelines of the Canadian Council of Animal Care, Alberta, as well as Cincinnati Children's Hospital Medical Center and Emory University's Institutional Animal Care and Use Committees.

4.3.3 Study protocol and heart perfusions

Hearts from male $MCU^{fl/fl-MCM}$ and $MCU^{fl/fl}$ control mice (20-22 week old) were perfused in an *ex vivo* working heart system to evaluate cardiac functional and metabolic changes. Mice were anesthetized using 12 mg sodium pentobarbital administered intraperitoneally then the hearts were isolated and perfused as described previously (21,211) with modification. The perfusion protocol consisted of 63 min aerobic perfusion divided into 3 consecutive periods of: 21 min without insulin, followed by 21 min with insulin (100 μ U/ml), and another 21 min with both insulin and isoproterenol (ISO, 10nM), to induce a condition of increased workload on these hearts. Perfusion buffer consisted of a modified Krebs–Henseleit Bicarbonate (KHB) solution containing in mM (118.5 NaCl, 25 NaHCO₃, 4.7 KCl, 1.2 MgSO₄, 1.2 KH₂PO₄, 2.5 CaCl₂, 5 glucose, 0.8 palmitate bound to 3% bovine serum albumin with trace amounts of radioactive [U-¹⁴C]glucose, and [9, 10-³H]palmitate. The buffer was continuously oxygenated with 95% O₂ and 5% CO₂ gas mixture. Glucose and palmitate oxidation rates were measured simultaneously by quantitative collection of ¹⁴CO₂ and ³H₂O produced by the heart from metabolizing glucose and palmitate, respectively, and expressed as nmol per g dry weight per min (nmol · g dry wt⁻¹ · min⁻¹) (21,211).

Cardiac functional parameters were recorded using an MP100 system from AcqKnowledge (BIOPAC Systems, Inc.). Cardiac work was calculated as a function of

peak systolic pressure and cardiac output. Efficiency is represented as the ratio of cardiac work to total calculated acetyl-CoA production rates (from glucose and fatty acid oxidation rates). At the end of the perfusion protocol, hearts were clamp-frozen in liquid nitrogen and stored at -80 °C for subsequent biochemical studies. The dry/wet tissue ratio was calculated and metabolic rates were normalized to the total dry mass of the heart.

4.3.4 Determination of short-CoA esters

Free CoA and its short esters including free CoA, malonyl-, and acetyl-CoA were measured using an ultra-performance liquid chromatography (UPLC) procedure adapted from a method previously described with modification (215). Heart tissue (15-20 mg) was homogenized for 25 seconds in 150 µl 6% PCA and put on ice for 10 min. Samples were centrifuged for 5 min x 12,000g and 4° C. Supernatants were then run on a Waters UPLC system that included a binary solvent manager (model 646M), sample manager (model 326M) and PDA detector (model 155M) using a Supelco C8 10cm x 2.1mm 2.2µm column as described previously (216).

4.3.5 Western blotting

Protein levels in mouse hearts were assessed using immunoblotting as described previously (214). Briefly, frozen mouse heart ventricular tissue was homogenized using Polytron-homogenized. The tissue lysates were used to produce loading samples that were run on SDS-polyacrylamide gel electrophoresis then transferred to nitrocellulose membranes. The membranes were then blocked and probed with specific primary antibody and afterwards, standard western blotting procedures were conducted as

previously described (214). Peroxidase-labeled streptavidin (PLS) (Jackson ImmunoResearch Laboratories, Cat# 016-030-084) was used for detection of ACC2 protein levels. Densitometry analysis of immunoblots was performed using ImageJ software (National Institutes of Health, USA) and normalized for value of the appropriate loading control.

4.3.6 Acetylation assay

Specific protein acetylation was determined using an immunoprecipitation (IP) assay as previously described (175) with some modifications. Frozen heart tissue was homogenized in immunoprecipitation buffer containing 50mM Tris HCl (pH 7.5), 150mM NaCl, 5mM EDTA, 0.5% NP-40, 1% Triton-X, and freshly added 1uM TSA, 5mM nicotinamide, and 10mM sodium butyrate, and protease inhibitor cocktail. Supernatants of 10,000 g for 10 min at 4°C were assayed for protein and a total of 100 µg protein was precleared with 20 µl A/G-agarose beads then incubated with 3 µg acetyl-lysine antibody (Millipore) overnight at 4°C. The following day, 50 µl of A/G-agarose beads were added to each sample and incubated at 4°C on a rotator for 6 hr. Samples were then washed three times and spun down at 5,000 g for 5 min keeping the pellet which was then mixed with 20ul 4x sample digestion buffer and boiled at 95°C for 5 min. Samples were then centrifuged at 15,000g for 15 min and all supernatant taken which could then be detected by Western blotting as explained above. One separate sample was not incubated with agarose beads and antibody to serve as a positive control while a negative control was represented by a lysate processed with normal (control) rabbit IgG instead of acetyl-lysine antibody. The magnitude of

acetylation was quantified by normalizing acetylated protein for total protein (input) band intensities.

4.3.7 NAD⁺ and NADH assay

NAD⁺ and NADH content was assessed in tissue samples from frozen ventricles of the perfused hearts using EnzyChrom NAD⁺/NADH Assay kit (E2ND-100) according to the manufacturer's protocol.

4.3.8 Statistical analysis

Data are presented as mean \pm SEM. Statistical significance was determined using an unpaired t-test, one-way analysis of variance (ANOVA) or two-ANOVA with repeated measures, followed by Bonferroni post-hoc test as appropriate. Differences were deemed significant if $p < 0.05$.

4.4 Results

4.4.1 MCU^{fl/fl-MCM} hearts show enhanced cardiac function at similar-to-control heart rates

The animal model of cardiac-specific MCU deficient mouse (MCU^{fl/fl-MCM}) which displays a normal healthy phenotype along with the accompanying impairment of mitochondrial Ca²⁺ uptake was previously described (109). To evaluate functional consequences of MCU deficiency, we investigated in MCU^{fl/fl-MCM} and in MCU^{fl/fl} control hearts several functional parameters before (basal) and after the addition of insulin, as well as after the introduction of ISO to create a considerably increased

workload representing an acute stress challenge to these hearts. In this regard, we utilized a unique *ex vivo* approach that provides actual workload to the mouse heart through a perfusion system offering a normal directional (ante-grade) aortic and coronary flow of an energy-substrate containing perfusate with physiologically relevant concentrations and the ability to pump against actual afterloads. The system provides homeostatic and cardiac work data in parallel with ongoing assessment of energy metabolism.

In addition to previous confirmation of the cardiac-specific MCU deficient ($MCU^{fl/fl-MCM}$) mice (109), we also confirmed the MCU deficiency by immunoblotting. There was a significant drop in MCU protein levels in the MCU deficient hearts to below 40% of control levels (Figure 4.1A). The reason behind the incomplete deletion of MCU, which was previously seen in the same mouse model (109), is unclear but may have resulted from variable activity of Cre recombinase in different cells in what is known as “Cre mosaicism” that is reported in some strains producing incomplete recombination in some cells (248). In accordance with our previous experience with *ex vivo* working heart perfusions, we did not see changes in cardiac function upon the addition of insulin and henceforth, our assessment and statistical tests were based on pre- and post- ISO perfusions.

Despite the rapid increase of heart rate after administration of ISO in all hearts, there was no statistical difference between the two genotypes throughout the perfusion protocol (Figure 4.1B). However, and in contrast to our expectations, $MCU^{fl/fl-MCM}$ hearts showed an enhanced cardiac function throughout the protocol even at baseline. This is displayed as higher left ventricular developed pressure (LVDP), cardiac output,

peak systolic pressure, as well as cardiac work (Figure 4.1C-F). In summary, despite a decrease of cardiac MCU protein, hearts showed an enhanced cardiac function that persisted after ISO challenge.

4.4.2 Fatty acid oxidation in MCU^{fl/fl-MCM} hearts is increased in response to isoproterenol stress

To investigate the energy substrate preference in hearts with impaired MCU function, we utilized a radioisotope-based method tracing the oxidation of fatty acids and glucose, the two major energy substrates for the heart. This method provides an actual quantitative assessment of the contribution of fatty acid and glucose oxidation to the tricarboxylic acid (TCA) cycle over the time course of perfusion in the heart. Unexpectedly, the basal (without insulin) metabolic rates in MCU^{fl/fl-MCM} hearts of both fatty acid oxidation and glucose oxidation were comparable to controls rates (Figure 4.2A and 2B). This suggests that the decrease in mitochondrial Ca²⁺ seen in MCU deficient hearts is not impairing flux through the TCA cycle dehydrogenases (isocitrate dehydrogenase and α -ketoglutarate dehydrogenase).

As expected, addition of insulin increased glucose oxidation (Figure 4.2A) and decreased fatty acid oxidation (Figure 4.2B) in the control hearts. Interestingly, in the presence of insulin MCU deficient hearts showed an unexpected enhanced response in the rate of glucose oxidation as compared to controls (Figure 4.2A). This suggests that MCU deficiency was not decreasing PDH activity (the rate-limiting enzyme for glucose oxidation) due to a decrease in Ca²⁺-activation of PDH phosphatase. The decline in fatty acid oxidation rates seen in the presence of insulin also occurred in the MCU deficient

hearts, with no statistical difference between the two genotypes (Figure 4.2B). These responses disagree with previous suggestions of a correlation between MCU deficiency and a metabolic inflexibility (108). Although glucose oxidation was enhanced in both groups upon the administration of ISO, interestingly only the MCU^{fl/fl-MCM} hearts showed accelerated fatty acid oxidation rates that was unmatched by the controls (Figure 4.2 A and 2B). This was translated into higher contribution of fatty acid oxidation to TCA cycle acetyl-CoA production in MCU deficient hearts compared to controls (Figure 4.2C) and resulted in a reduced cardiac efficiency (Figure 4.2D). It is important here to note that cardiac efficiency was not different between the two animal groups at any specific treatment. However with ISO, MCU^{fl/fl-MCM} hearts became more reliant on the less efficient energy substrate, fatty acids to produce considerable amount of cardiac work and consequently, this led to a decreased efficiency compared to pre-ISO (1).

The increase in fatty acid oxidation in MCU deficient hearts in response to ISO was associated with lower levels of malonyl-CoA (Figure 4.2E). Malonyl-CoA is a potent biological inhibitor of carnitine palmitoyltransferase I (CPT I), the gatekeeper of mitochondrial fatty acid uptake and subsequent oxidation (14). The accelerated fatty acid oxidation was also correlated with improved energy reserve as shown by a higher acetyl-CoA/CoA ratio in the MCU deficient hearts (Figure 4.2F). Therefore, MCU deficient hearts did not show compromised energy production or metabolic inflexibility in the absence or presence of insulin. Rather, the higher cardiac work displayed by these hearts correlated well with enhanced energy production and reserve, with a greater reliance on fatty acid oxidation in response to ISO stimulation.

4.4.3 Protein levels and phosphorylation of key components of energy metabolism in MCU^{fl/fl-MCM} hearts display minor variation

Since MCU deficiency was not associated with poor cardiac function or restricted energy metabolism, we aimed at explaining these unexpected findings by investigating important mitochondrial biogenesis and metabolic proteins. No changes were seen in the phosphorylation of PDH, AMP-activated protein kinase (AMPK), or acetyl-CoA carboxylase (ACC) (Figure 4.3A and B). Similarly, protein levels of malonyl-CoA decarboxylase (MCD) responsible of malonyl-CoA degradation and those of the fatty acid oxidation enzymes long-chain acyl-CoA dehydrogenase (LCAD) and β -hydroxyacyl CoA dehydrogenase (β -HAD) were not different (Figure 4.3C and D). Peroxisome proliferator-activated receptor gamma coactivator 1-alpha (PGC-1 α), the voltage-dependent anion channel (VDAC), and citrate synthase (CS) (relevant to mitochondrial biogenesis and abundance, Figure 4.3C and D, and Figure 4.4A and B) were not different than MCU^{fl/fl} control mouse hearts. In addition, total PDH and FOXO1 associated with glucose oxidation and insulin signaling pathways (1,249) protein levels did not differ between MCU deficient mice and controls (Figure 4.4A and B).

As previously reported (109), protein levels of mitochondrial sodium-calcium exchanger (NCLX) showed a compensatory decrease paralleling the partial deficiency of MCU in MCU^{fl/fl-MCM} hearts (Figure 4.4A and B). Interestingly, both electron transport chain (ETC) complex I and II protein levels were decreased in MCU^{fl/fl-MCM} (Figure 4.3C and D). However, the decline appears to be mild and is unlikely impeding oxidative phosphorylation processes based on the unrestricted metabolic rates discussed

above. In summary, the protein levels and phosphorylation of several components of cardiac energy metabolic pathways appear unaltered in MCU deficient mice, with the exception of mild decrease in ETC complex I and II protein levels.

4.4.4 Protein acetylation is altered in MCU^{fl/fl-MCM} hearts

As complex I and II protein content was decreased in MCU deficient hearts, we hypothesized that NAD⁺/NADH turnover could be affected. Therefore, we measured NAD⁺ and NADH levels and the ratio between the oxidized to reduced NAD forms. The NAD⁺/NADH ratio has important implications on the activity of sirtuins which are NAD⁺-dependent deacylases distributed among cellular compartments and involved in lysine deacylation processes. Post-translational modifications (PTM) involving acetylation are known to regulate cellular energy metabolism (139). NAD⁺ levels were significantly lower, whereas NADH content in MCU deficient hearts was not different than controls (Figure 4.5A). Consequently, the NAD⁺/NADH ratio was lower in MCU^{fl/fl-MCM} hearts compared to MCU^{fl/fl} (Figure 4.5A).

Since increased NAD⁺ levels, such as seen with Complex I deficiency, activate sirtuins (173), we examined what effect MCU deficiency has on total cardiac lysine acetylation and of specific key metabolic proteins/enzymes. Although total protein acetylation (Figure 4.5B) and the protein levels of SIRT1, SIRT3, and SIRT4 (nuclear and mitochondrial deacetylases), as well as GCN5L1 (mitochondrial acetyltransferase), were not different from controls (Figure 4.5C and D), the acetylation status of β -HAD (a fatty acid oxidation enzyme) was increased, which we have previously shown to increase fatty acid oxidation rates (154,175), although LCAD acetylation was not

altered (Figure 4.5E and F). Acetylation of MCD (involved in malonyl-CoA degradation) was also increased (Figure 4.5E and F), which increases MCD activity (160) and may therefore explain the decrease in malonyl-CoA we observed. PGC-1 α (a target of SIRT1, Figure 4.5C and D) was also increased in MCU^{fl/fl-MCM} hearts. This was not seen with PDH (Figure 4.6A and B). Our data suggests that increased acetylation of β -HAD and MCD (resulting in a decrease in malonyl-CoA levels) may be responsible for the increase in fatty acid oxidation seen in the MCU deficient hearts.

4.5 Discussion

The heart has a large energy demand in order to maintain continuous contractile function, with this energy demand intensifying during fight or flight stressful situations (1,109). A rise in mitochondrial Ca²⁺ is believed to actively contribute to the increase in energy production needed to sustain contractile function following adrenergic stimulation by increasing the activity of mitochondrial TCA cycle dehydrogenases and PDH (secondary to activation of PDH phosphatase) (104,105). Since Ca²⁺ crosses the inner mitochondrial membrane primarily through the MCU channel (98), a deficiency in MCU would be expected to decrease energy production and compromise contractile function of the heart, especially in response to an adrenergic stimulation. However, we directly demonstrate that MCU deficiency does not compromise energy production or contractile function in the heart. This is primarily due to a compensatory increase in fatty acid oxidation and higher energy reserve in the heart.

Of interest, we demonstrate a higher than normal cardiac work in mice with a cardiac specific MCU deficiency, even after the induction of an ISO stress. Although this finding appears unexpected, this increased work was probably the result of a compensatory increase in energy production originating from fatty acid oxidation. In addition, the contribution of glucose oxidation to energy production was also not compromised in MCU deficient hearts. We also did not see a decrease in overall TCA cycle activity, suggesting that the demonstrated decrease in mitochondrial Ca^{2+} seen with MCU deficiency (109) is not impairing either the TCA cycle dehydrogenases or PDH activity.

The lack of a functional deficit in the MCU deficient hearts subjected to an adrenergic stress is supported by other approaches in which MCU activity was altered. For example, ruthenium red (an inhibitor of MCU) increased cardiac function, while spermine (an opener of MCU) decreased cardiac function in hearts subjected to ischemic post- conditioning (112). Conversely, in another study using *ex vivo* perfused mouse hearts, both Ru360 and spermine (an inhibitor and stimulator of MCU, respectively) induced negative and positive inotropic effects, respectively with antagonistic effects (113). In this latter study, inotropic stimulation with ISO elevated oxygen consumption, increased Ca^{2+} -dependent activation of PDH, and increased mitochondrial Ca^{2+} content. These effects were abolished by Ru360, suggesting an uncoupling between workload and ATP production upon MCU inhibition (113). It should be recognized, however, that hearts in this study were perfused in the absence of physiologically relevant concentrations of fatty acids, which would not allow for a compensatory increase in fatty acid oxidation, such as we observed in our study.

Another recent study showed in whole body MCU knock-out mice that although cardiomyocyte mitochondrial matrix Ca^{2+} levels were reduced, normal levels of cardiac function, ATP, and respiratory control ratio under basal conditions were seen in addition to normal responses to ISO stress and transverse aortic constriction (114). Other studies using myocardial MCU inhibition by transgenic expression of a dominant-negative MCU or cardiac deletion also showed normal resting heart rates despite incapability of the animals of physiological “fight or flight” heart rate acceleration (109,111).

The insulin-stimulated increases in glucose oxidation in our MCU deficient hearts are particularly interesting. A recent study suggested a correlation between reduced levels of MCU and insulin resistance as found in type-1 diabetic mice and in mouse neonatal cardiomyocytes cultured under hyperglycemic conditions (108). In those cells, reduced MCU levels correlated with decreased glucose oxidation associating with higher phosphorylation and lower activity of PDH. This variability in phosphorylation of PDH was not reproduced in our study perhaps as a result of the obscuring effect of ISO stimulation on PDH phosphorylation. Here again, however, MCU deficiency models have shown mixing results regarding PDH phosphorylation/activity (109,110). As for the glucose oxidation rates in the MCU deficient hearts that were comparable to controls after ISO administration, we believe that the rates have leveled up to a maximum in all perfused hearts due to the augmented energy demands under the increased workload.

The increase in fatty acid oxidation seen in the MCU deficient hearts was likely due, in part, to a decrease in malonyl-CoA levels, which would result in an increase in

mitochondrial fatty acid uptake. Our data suggests that this decrease in malonyl-CoA was not due to a reduction in ACC activity, but rather an increase in malonyl-CoA degradation. MCD acetylation was increased in the MCU deficient hearts (Figure 4.5E and F), which is associated with stimulation of its malonyl-CoA degradation activity (160). In addition, an increased acetylation of the fatty acid oxidation enzyme, β -HAD occurred (Figure 4.5E and F) which is correlated with enhanced activity of fatty acid oxidation (154,175). Therefore, alterations in acetylation of these enzymes may explain the increase in fatty acid oxidation we observed in MCU deficient hearts. We propose that the drop in NAD^+ levels seen in the MCU deficient hearts decreased SIRT3 activity (which deacetylates β -HAD) and decreased SIRT4 (which deacetylates MCD), leading to an increase in β -HAD activity and a decrease in malonyl-CoA levels. Combined, this resulted in activation in fatty acid oxidation in the MCU deficient hearts.

In conclusion, MCU deficiency in the heart is not associated with energy starvation or decreased cardiac function. This is because fatty acid oxidation increases to meet the extra energy demand. These hearts showed improved energetic reserve. Mechanisms of metabolic alterations include enhancement of lysine acetylation of key regulatory metabolic proteins. Understanding the roles of mitochondrial Ca^{2+} uptake in heart metabolism may provide better insights on future therapeutic approaches for heart disease.

Figure 4.1. MCU deficient hearts show enhanced cardiac function at comparable heart rates. (A) Western blotting confirmation of MCU protein deficiency in MCU^{fl/fl-MCM} mouse hearts compared to MCU^{fl/fl} control after 8-week tamoxifen treatment. α -tubulin was used as a protein loading control. * P <0.05 versus MCU^{fl/fl} control, unpaired t-test (n =4-6). Functional parameters of 63 min *ex vivo* working heart perfusions of MCU^{fl/fl} and MCU^{fl/fl-MCM} hearts showing (B) heart rate, (C) left ventricular developed pressure (LVDP), (D) cardiac output (CO), (E) peak systolic pressure, and (F) cardiac work. Insulin (100 μ U/ml) was added at 21 min, followed by addition of ISO (10nM) at 42 min as described in methods. Cardiac functional parameters data (B to E) were recorded using an MP100 system from AcqKnowledge (BIOPAC Systems, Inc.), while cardiac work was calculated as explained in experimental procedures. Statistical significance over the time course of pre- and post- ISO between MCU^{fl/fl-MCM} and MCU^{fl/fl} control in B to F was determined using 2-way ANOVA with repeated measures and, if significant, is indicated below the specific functional figure. For data in B-F, n =10-13, * P <0.05 compared to MCU^{fl/fl} at the specific time point using Bonferroni post-hoc test. All values represented as mean \pm SEM. MCU: mitochondrial calcium uniporter; ISO: isoproterenol.

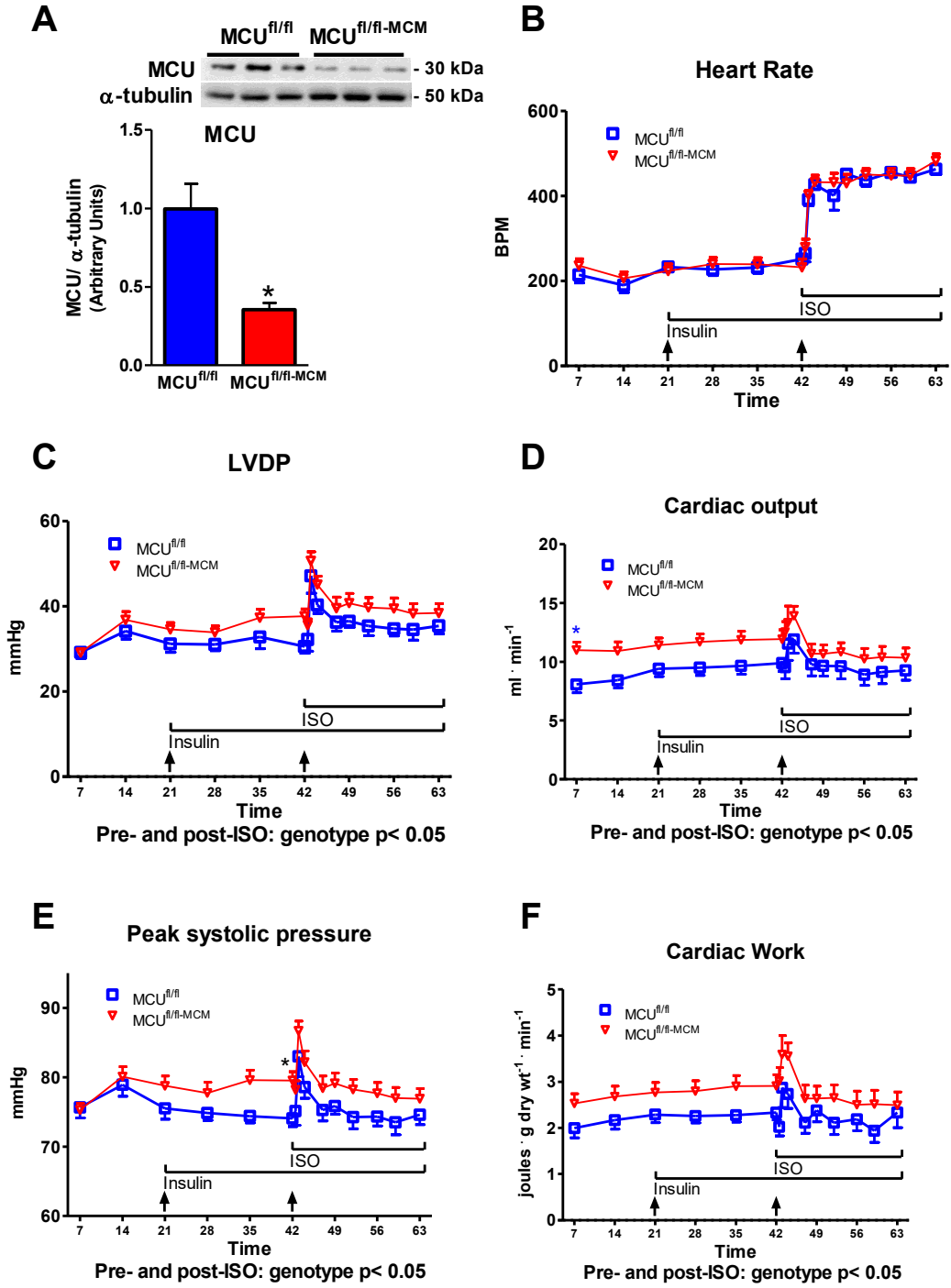


Figure 4.1

Figure 4.2. MCU deficient heart metabolism is altered in response to isoproterenol stress. Energy substrate metabolic rates during *ex vivo* working heart perfusions of MCU^{fl/fl} and MCU^{fl/fl-MCM} showing (A) glucose oxidation, and (B) palmitate oxidation rates at baseline (21 min), with insulin (100 μ U/ml) (21 min), and after ISO (10nM) administration (21 min). (C) Specific contributions of oxidized palmitate versus glucose in MCU^{fl/fl} and MCU^{fl/fl-MCM} hearts in the production of TCA cycle acetyl-CoA during the three different perfusion periods mentioned in A and B. (D) Cardiac efficiency of MCU^{fl/fl} and MCU^{fl/fl-MCM} calculated as the cardiac work normalized for total TCA cycle acetyl-CoA production during the three different perfusion periods mentioned in A and B. In A to D * $P < 0.05$ versus MCU^{fl/fl} control at the same treatment period, unpaired t-test. # $P < 0.05$ versus baseline of same genotype group, 1-way ANOVA ($n=10-13$). (E) Malonyl-CoA levels, expressed as nmol per g dry weight of tissue, and (F) Acetyl-CoA/CoA ratio measured in samples from heart ventricles clamp-frozen at the end of the 63 min heart perfusion protocol of MCU^{fl/fl} and MCU^{fl/fl-MCM}. In E and F * $P < 0.05$ versus MCU^{fl/fl} control, unpaired t-test. ($n=8-12$). All values represented as mean \pm SEM. MCU: mitochondrial calcium uniporter; ISO: isoproterenol.

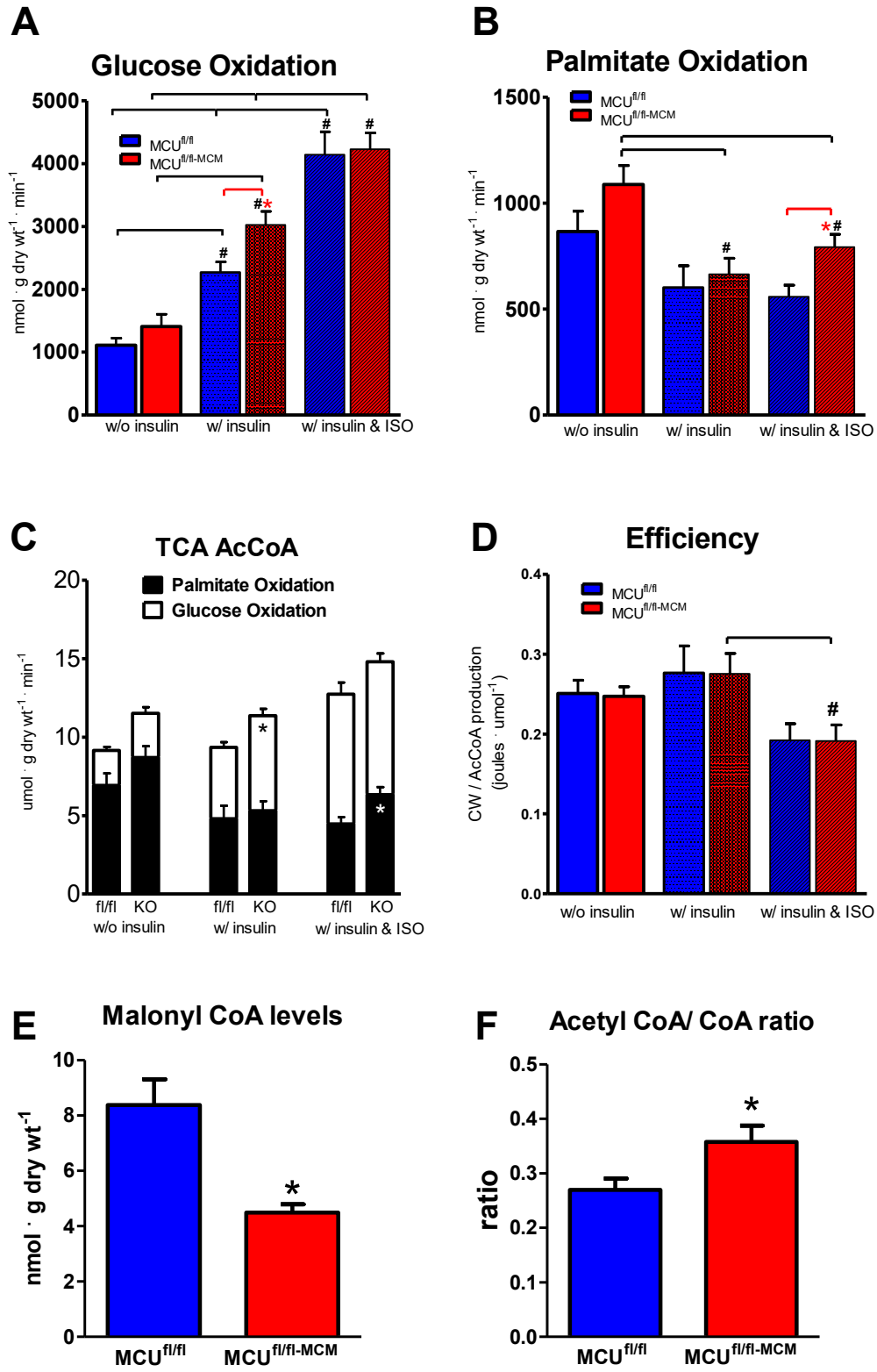


Figure 4.2

Figure 4.3. Protein levels and phosphorylation of key components of energy metabolism in MCU deficient hearts display minor variation. (A) Western blotting analysis of the phosphorylation of key enzymes involved glucose and fatty acid oxidation, S293 p-PDH, T172 p-AMPK, and S79/1200 p-ACC, which are associated with their activity. Each phosphorylated form of these enzymes is normalized for the total protein level of the respective enzyme. (B) Quantification of data presented in (A). (C) Western blotting analysis of the protein levels of key enzymes and proteins involved in energy metabolism and oxidative phosphorylation as well as mitochondria biogenesis. Blots of the following proteins are presented: MCD; LCAD; β -HAD; PGC-1 α ; VDAC; ETC complexes I, II, III, and V. α -tubulin was used as a protein loading control. (D) Quantification of data presented in (C). WB samples were made from heart ventricles clamp-frozen at the end of the 63 min heart perfusion protocol of MCU^{fl/fl} and MCU^{fl/fl-MCM}. * $P < 0.05$ versus MCU^{fl/fl}, unpaired t-test ($n=5-6$). All values represented as mean \pm SEM.

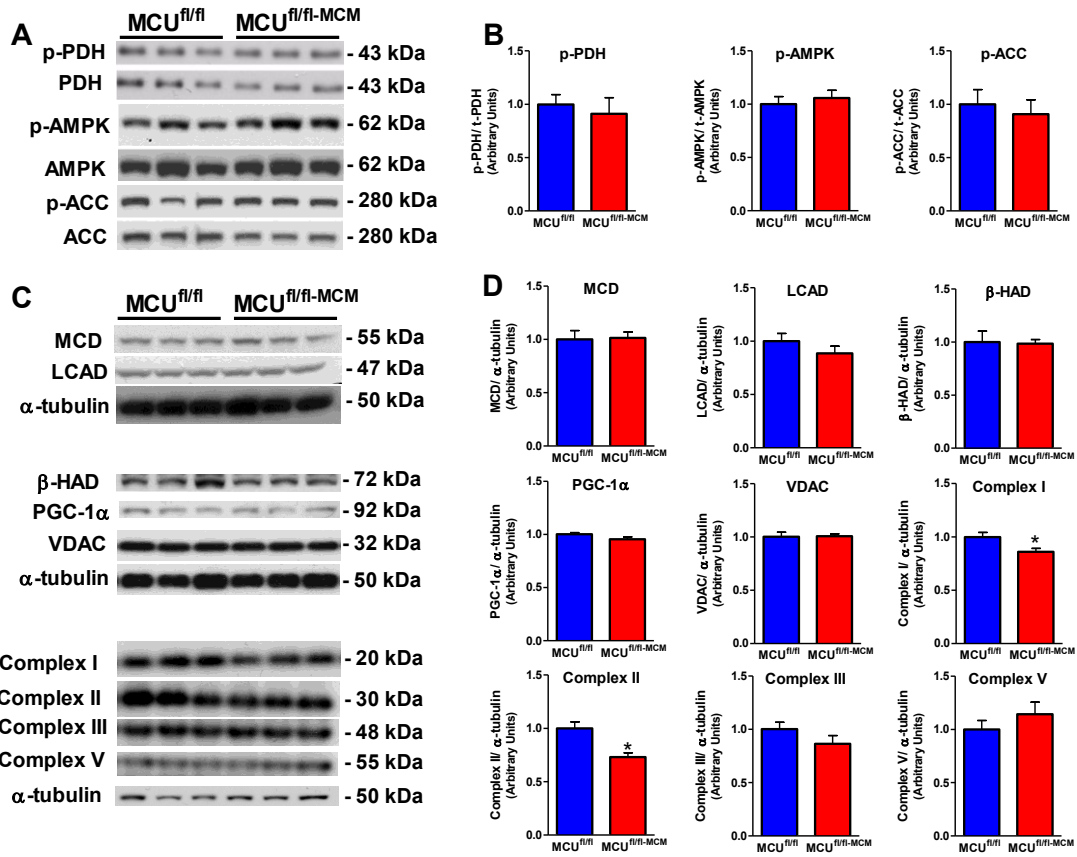


Figure 4.3

Figure 4.4. Protein levels of additional important proteins involved in energy metabolism, mitochondrial biogenesis and mitochondrial Ca²⁺ homeostasis in MCU^{fl/fl-MCM} and MCU^{fl/fl} control mouse hearts. (A) Western blotting analysis mitochondrial NCLX (mitochondrial Ca²⁺ efflux), PDH (glucose oxidation), CS (TCA cycle), and FOXO1 (transcriptional factor for metabolic pathways). α -tubulin was used as a protein loading control. (B) Quantification of data presented in (A). * $P < 0.05$ versus MCU^{fl/fl}, unpaired t-test ($n=4-6$). Western blotting and immunoprecipitation samples were prepared from heart ventricles clamp-frozen at the end of the 63 min heart perfusion protocol of MCU^{fl/fl} and MCU^{fl/fl-MCM}. All values represented as mean \pm SEM.

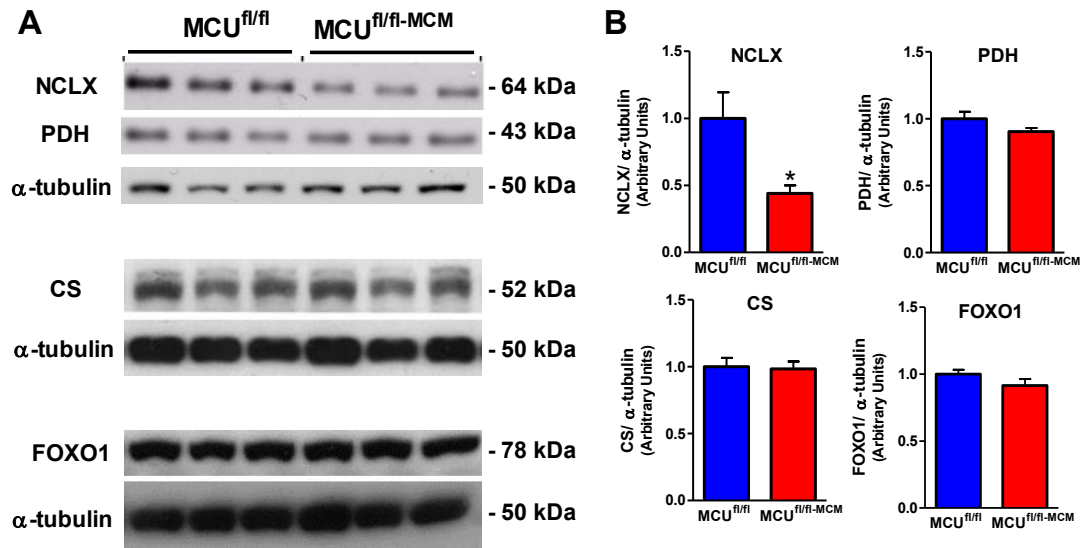


Figure 4.4

Figure 4.5. Protein acetylation is altered in MCU^{fl/fl-MCM} hearts. (A) NAD⁺, NADH levels, expressed as nmol per g dry weight of tissue, and NAD⁺/ NADH ratio in heart tissue from MCU^{fl/fl} and MCU^{fl/fl-MCM} mice (*n*=10). (B) Western blotting analysis and quantification of total protein acetylation in MCU^{fl/fl} and MCU^{fl/fl-MCM} mouse hearts. α -tubulin was used as a protein loading control. (C) Western blotting analysis of SIRT1, SIRT3, SIRT4, and GCN5L1, important enzymes regulating lysine acetylation of key metabolic proteins. α -tubulin was used as a protein loading control. (D) Quantification of data presented in (C). (E) Acetylation status of β -HAD, LCAD, and MCD enzymes involved in fatty acid oxidation assessed by reverse immunoprecipitation (IP) acetylation assay explained in methods. (F) Quantification of data presented in (E) by normalizing for IP input of the respective total protein levels. NAD⁺, NADH, western blotting, and immunoprecipitation samples were prepared from heart ventricles clamp-frozen at the end of the 63 min heart perfusion protocol of MCU^{fl/fl} and MCU^{fl/fl-MCM}. For data in **B-F** *n*=4-6. **P*< 0.05 versus MCU^{fl/fl} unpaired t-test. All values represented as mean \pm SEM.

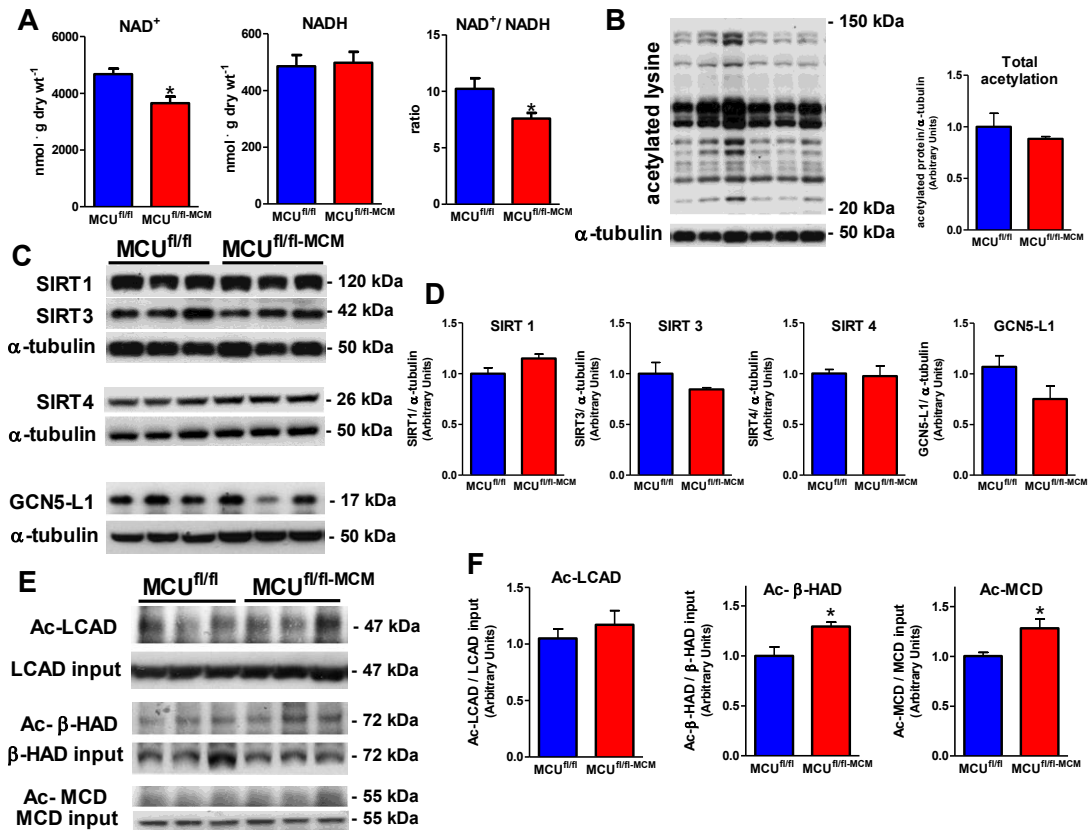


Figure 4.5

Figure 4.6. Protein acetylation of PDH and PGC-1 α in MCU^{fl/fl-MCM} and MCU^{fl/fl} control mouse hearts. (A) Acetylation status of PGC-1 α and PDH, proteins involved in mitochondrial biogenesis and glucose oxidation, respectively, assessed by reverse immunoprecipitation (IP) acetylation assay explained in methods. (B) Quantification of data presented in (A) by normalizing for IP input of the respective total protein levels. * $P < 0.05$ versus MCU^{fl/fl}, unpaired t-test ($n=4-6$). Western blotting and immunoprecipitation samples were prepared from heart ventricles clamp-frozen at the end of the 63 min heart perfusion protocol of MCU^{fl/fl} and MCU^{fl/fl-MCM}. All values represented as mean \pm SEM.

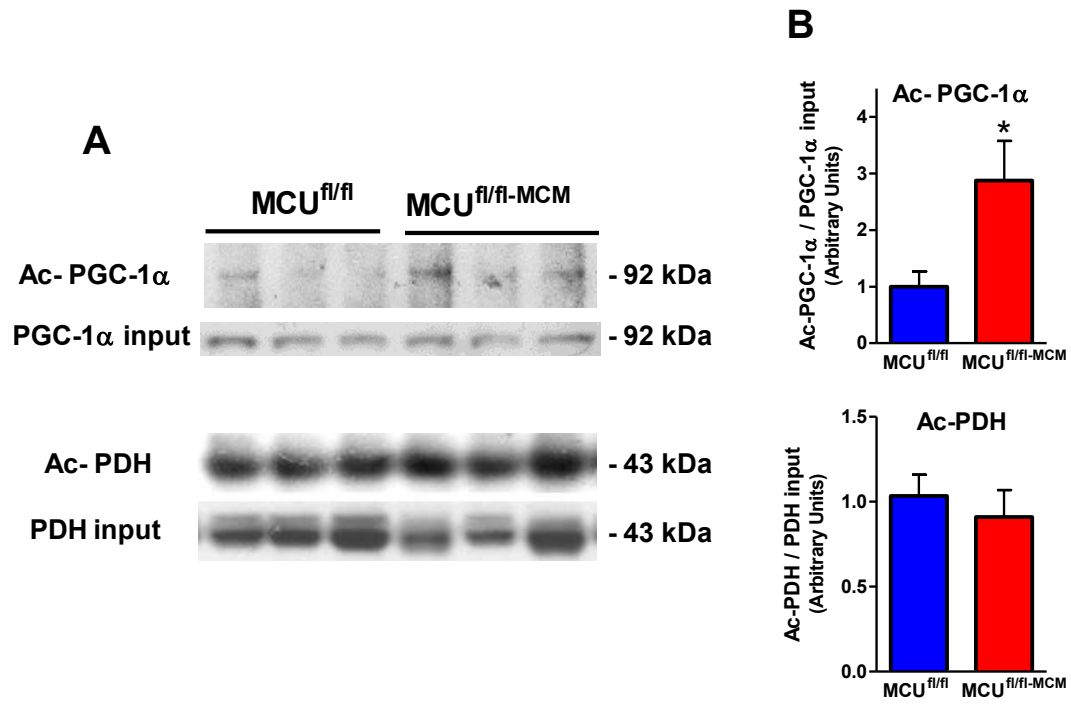


Figure 4.6

CHAPTER 5

A Novel Role of Endothelial Autophagy as a Regulator of Myocardial Fatty Acid Oxidation

A manuscript was recently submitted to *The Journal of Thoracic and Cardiovascular Surgery*, and is presently under revision.

Krishna Singh performed siRNA transfection experiments. Liyan Zhang assisted in Triacylglycerol assay. I conducted the majority of experiments, as well as the experimental design, analyzed the results, and wrote the manuscript.

CHAPTER 5

A Novel Role of Endothelial Autophagy as a Regulator of Myocardial Fatty Acid Oxidation

5.1 Abstract

We sought to determine if endothelial autophagy impacts fatty acid delivery to the myocardium and hence energy metabolism of the heart. We utilized isolated working mouse hearts to compare cardiac function, energy metabolism and ischemic response of hearts from endothelial cell-specific ATG7 knockout (EC-ATG7^{-/-}) mice to hearts from their wild-type littermates. We also conducted gene analyses on human umbilical vein endothelial cells (HUVECs) incubated with scrambled siRNA or siATG7. In the presence of insulin, working hearts from EC-ATG7^{-/-} mice, relative to those from wild-type littermates, exhibited greater reductions in insulin-associated palmitate oxidation ($P < 0.05$) indicating a diminished reliance on fatty acids as a fuel source. Likewise, palmitate oxidation was markedly lower in the hearts of EC-ATG7^{-/-} mice vs. wild-type mice during reperfusion of ischemic hearts ($P < 0.05$). While hearts from EC-ATG7^{-/-} mice revealed significantly lower triacylglycerol content compared to those from wild-type mice ($P < 0.05$), ATG7-silenced human umbilical vein endothelial cells demonstrated appreciably lower fatty acid binding protein 4 and 5 expression relative to those treated with scrambled siRNA ($P < 0.05$). We conclude that the disruption of endothelial autophagy reduces cardiac fatty acid storage and dampens reliance on fatty

acid oxidation as a cardiac fuel source. The autophagy network represents a novel target for designing new strategies aimed at resetting perturbed myocardial bioenergetics.

5.2 Introduction

Myocardial contractile function imposes a significant metabolic demand on the body. Under physiological conditions, approximately 70% of the energy requirements of hearts are fueled by fatty acid oxidation with much of the remaining 30% derived from glucose oxidation (1). While, in the normal heart, fatty acid and glucose metabolism are intricately entwined and tightly regulated, this relationship can become progressively perturbed in the settings of ischemia and heart failure when there is an imbalance in the oxygen supply-demand axis (2).

Given that substrate utilization is a critical component for sustaining the metabolic demands of the myocardium, it is perhaps not surprising that much attention has to date focused on gaining a better understanding of both the myocardial metabolome and the cross-talks that occur within the myocardial cell (250). In contrast, despite our appreciation that endothelial cells (ECs) and cardiomyocytes have an intimate relationship (251) and that ECs play a fundamental role in the pathophysiology of ischemia/reperfusion (I/R) (252), there has been relatively little reported on the EC-cardiomyocyte bioenergetic relationship and how derangements of this partnership could impact the energy demands of the myocardium and in turn myocardial contractility.

Autophagy, an essential and evolutionary well conserved catabolic pathway that recycles cellular components to maintain cellular homeostasis and promote cellular survival, has been implicated in the pathophysiology of various cardiovascular diseases (253-255). Our collaborating group previously reported that autophagy-related protein 7 (ATG7), and accordingly autophagy, is not only key in the paracrine regulation of EC-released vasoactive substances (124), but also that impaired ATG7 expression and consequently, the autophagic machinery contributes to the pathophysiology of thrombosis (200) and I/R injury (256). Findings from our collaborating group and others have further demonstrated a bidirectional regulatory relationship between autophagy and cholesterol homeostasis, thus implicating a role for autophagy in potentially regulating the metabolic network (125,127).

In consideration of the evidence described above, we sought to determine if endothelial autophagy may be a yet unrecognized regulator of myocardial energy metabolism. To this aim, functional and biochemical assessments were conducted on hearts isolated from EC-specific ATG7 knockout (EC-ATG7^{-/-}) mice. To provide a molecular context, concomitant gene analyses were performed on ATG7-silenced human umbilical vein endothelial cells (HUVECs).

5.3 Materials and methods

5.3.1 Endothelial cell-specific ATG7 knockout mice

The EC-ATG7^{-/-} mice used in the studies described herein have been previously described and characterized (125,200,201). In short, EC-ATG7^{-/-} mice were the progeny

of ATG7^{flox/flox} and VE-Cadherin-Cre transgenic mice (The Jackson Laboratory, Bar Harbor, Maine; Stock # 006137). *Ex vivo* experiments were conducted on hearts isolated from anesthetized (12 mg sodium pentobarbital, intraperitoneal) age-matched (22- to 36-week old) male EC-ATG7^{-/-} and wild-type (WT) littermate controls. All animal-related protocols were approved by the University of Alberta Health Sciences Animal Welfare Committee and the St. Michaels Hospital Animal Care Committee prior to conduct, and the procedures performed were in full compliance with the guidelines of the Canadian Council of Animal Care.

5.3.2 *Ex vivo* aerobic heart perfusion protocol

Isolated working hearts were perfused as described previously (21,211) with an aerated (95% O₂/ 5%CO₂) modified Krebs–Henseleit bicarbonate solution maintained at 37° C and containing (in mmol/L) 118.5 NaCl, 25 NaHCO₃, 4.7 KCl, 1.2 MgSO₄, 1.2 KH₂PO₄, 2.5 CaCl₂, and 5 glucose with 0.8 palmitate bound to 3% bovine serum albumin as well as trace amounts of [U-¹⁴C]glucose and [9,10-³H]palmitate. At the end of 30 min, insulin (100 μU/ml) was added the perfusate after which the hearts were continually perfused for a further 30 min. Steady state glucose and palmitate oxidative rates were concurrently measured via quantitative collection of ¹⁴CO₂ and ³H₂O, both products of glucose and palmitate metabolism (21,211).

5.3.3 *Ex vivo* ischemic-reperfusion heart perfusion protocol

Isolated working hearts were perfused under aerobic conditions for 30 min with palmitate-supplemented (final concentration 1.2 mmol/L) Krebs–Henseleit bicarbonate solution kept at 37 °C. This was followed by 20 min of global no-flow ischemia then 40 min of aerobic reperfusion. The palmitate levels added served to simulate the enhanced

fatty acid levels typically observed under pathological I/R conditions (1,2). Cardiac functional parameters were continuously sampled with an MP100 system coupled to the AcqKnowledge software from BIOPAC Systems, Inc. Cardiac work was calculated from the corresponding peak systolic pressure and cardiac output values. Cardiac efficiency was assessed by normalizing cardiac work to the rate of acetyl-CoA synthesis. At the end of the perfusion protocols, the hearts were freeze-clamped in liquid nitrogen and stored at -80°C until they were processed for biochemical analyses.

5.3.4 Triacylglycerol assay

Lipids were extracted from frozen ventricle samples (10 mg) of murine hearts using a modified version of the Bligh and Dyer method (213). In brief, the samples were homogenized in a 2:1 chloroform-methanol mixture then mixed with a 20% volume of methanol. The suspension was centrifuged at 3500g for 10 min at 4 °C and the supernatant mixed with a 20% volume of 0.04% CaCl₂. Following a second spin of 2400g for 20 min at 4 °C, the upper phase was discarded and the interface washed 3 times with a (by volume ratio) chloroform (3): methanol (48): water (47) mixture. Each sample was mixed with 50 µL methanol then dried under nitrogen at 60 °C for 5-10 min as necessary. The resultant pellet was dissolved in a mixture of (by volume ratio) tert-Butyl alcohol (3): Triton X-100 (1): methanol (1) and levels of myocardial triacylglycerol (TAG) measured with a colorimetric assay kit (Wako Chemicals, Richmond, VA).

5.3.5 Real-time polymerase chain reaction

HUVECs (Lonza, Walkersville, MD), cultured as previously described, were treated for 48 hours with either small interfering RNA (siRNA) targeted at ATG7 (siATG7) or

scrambled siRNAs (both from Ambion, Foster City, CA) (201). cDNAs, synthesized from total RNA using the Quantitect kit (Qiagen, Germantown, MD), were processed for quantitative analyses of ATG7, *CD36*, fatty acid-binding proteins (FABPs) and glyceraldehyde 3-phosphate dehydrogenase (GAPDH) by real-time polymerase chain reaction (RT-PCR) using the StepOnePlus™ Real-Time PCR System (Applied Biosystems, Foster City, CA).

5.3.6 Statistical analysis

Data are presented as mean \pm SEM. Statistical significance was determined with the Student's t-test (either paired or unpaired) or the two-way analysis of variance (ANOVA) with repeated measures, followed by Bonferroni post-hoc analysis wherever appropriate. Differences were considered significant under conditions of $P < 0.05$).

5.4 Results

5.4.1 Endothelial specific ATG7 deletion is associated with reduced myocardial fatty acid oxidation in response to insulin

Under basal aerobic conditions, the cardiac parameters of working hearts from EC-ATG7^{-/-} mice appeared indistinguishable from those of their WT littermate controls and remained stable during the 60 min observation window (Table 5.1 and Figure 5.1A). Insulin perfusion led to marked and significant increases in glucose oxidation rates to ~2.6-fold for hearts from WT mice and ~3-fold for hearts from EC-ATG7^{-/-} mice (Figure 5.1B; both $P < 0.05$). In contrast, palmitate oxidation rates fell in response to insulin (Figure 5.1C) although only the change observed with the hearts of EC-ATG7^{-/-} mice reached statistical significance ($P < 0.05$). TCA cycle acetyl-CoA production

rates, in the absence and presence of insulin, did not differ between the hearts from EC-ATG7^{-/-} mice and those from their WT littermates (Figure 5.1D). Further investigations revealed that in the absence of insulin, the acetyl-CoA for the TCA cycle in the two groups of hearts was fed to similar extents by the intrinsic glucose and fatty oxidation pathways (Figure 5.1E). In the presence of insulin, however, hearts from the two groups of mice exhibited different substrate utilization preferences. Specifically, glucose oxidation in the hearts of EC-ATG7^{-/-} mice contributed relatively more, and accordingly palmitate oxidation relatively less, to driving the TCA cycle than that in the hearts from the WT littermate controls (Figure 5.1E). Of note, despite the differences in energy substrate composition observed, cardiac efficiency for both groups of hearts when exposed to insulin was similar (Figure 5.1F).

5.4.2 Endothelial specific ATG7 deletion is associated with augmented cardiac glucose oxidation, diminished cardiac fatty acid oxidation and reduced cardiac efficiency following I/R insult

Cardiac work measured in the hearts from EC-ATG7^{-/-} and WT mice, before, during and after I/R, were similar with ~50% recovery detected in both cases (Figure 5.2A). Notably, there were no functional differences between the two groups of hearts (Figure 5.2A) although their metabolic profiles displayed distinct differences. Intact autophagy has been correlated with better recovery in cardiac I/R models (257). Although the impairment of autophagy was confined to endothelial cells, it may have somehow hindered post-ischemic recovery even in these metabolically efficient hearts. The salutary effect of decreased palmitate oxidation and increased glucose oxidation in EC-

ATG7^{-/-} compared to their WT controls was most likely masked by the fact that in control hearts, palmitate oxidation was unchanged or even tending to decrease during reperfusion instead of increasing as we normally see. The reason behind this variation is unclear but may stem from some collateral effects accompanying the genetic manipulation in these mice. Glucose oxidation rates for the hearts from EC-ATG7^{-/-} mice were approximately 3-fold those of the WT mice during both the pre-ischemia (EC-ATG7^{-/-} 3433 ± 734 vs. WT 1242 ± 184 nmol · g dry wt⁻¹ · min⁻¹; *P* < 0.05) and reperfusion (3287 ± 655 vs. 1036 ± 160 nmol · g dry wt⁻¹ · min⁻¹; *P* < 0.05) phases (Figure 5.2B). Although palmitate oxidation rates for the two groups of mice were comparable during ischemia and reperfusion (Figure 5.2C), a statistical difference was achieved only for the difference in palmitate oxidation rates between the ischemic and reperfusion phases for the hearts from EC-ATG7^{-/-} mice (Figure 5.2C; *P* < 0.05).

Prior to ischemia, TCA cycle acetyl-CoA production rates in the hearts from EC-ATG7^{-/-} mice were approximately 50% greater than those for the hearts from WT mice (Figure 5.2D). This heightened energy drive appeared to be fueled by elevations in glucose oxidation rates since the palmitate oxidation rates of the hearts from EC-ATG7^{-/-} and WT mice were similar (Figure 5.2E). During the reperfusion phase, hearts from EC-ATG7^{-/-} mice continued to exhibit increased TCA cycle acetyl-CoA production rates, which were accompanied by lower palmitate oxidation rates (Figure 5.2E; *P* < 0.05). The greater energy consumption measured in the hearts from EC-ATG7^{-/-} vs. WT mice during the I/R protocol correlated with the lower cardiac efficiency calculated for the former group (Figure 5.2F; *P* < 0.05).

5.4.3 Endothelial specific ATG7 deletion lowers cardiac TAG stores and expression of endothelial fatty acid binding proteins

Inasmuch as the TAG levels in the heart ventricles from EC-ATG7^{-/-} mice were approximately half of those detected in the WT littermates (Figure 5.3A; $P < 0.05$), we hypothesized that endothelial specific deletion of ATG7 (Figure 5.3B and C) may be associated with dysfunctional lipid transport. HUVECs are among the most widespread cultured cell type for *in vitro* studying of endothelial biology in vascular and angiogenesis pathologies. These cells have been previously utilized in Dr. Verma's lab for studying endothelial autophagy relationship on lipid homeostasis (125) and offer several advantages by being relatively easy to retrieve and isolate from the umbilical vein, be driven to proliferate under *in vitro* conditions, and by responding to exogenous stimuli such as cytokines and siRNA transfection, producing predictable knockdown of the mRNA of interest in addition to be suitable for metabolism research (258). RT-PCR analyses indicated that CD36 expression in ATG7-silenced HUVECs did not differ appreciably from that in scrambled siRNA-transfected HUVECs (Figure 5.3D). The expression of fatty acid binding protein 4 (FABP4) and 5 (FABP5), on the other hand, were significantly lower in siATG7-treated HUVECs relative to that in the scrambled siRNA-transfected HUVECs (Figure 5.3E and F; $P < 0.05$ for both).

5.5 Discussion

Normal functioning hearts have high energy demands that are supported mainly by fatty acid and glucose oxidation (2). Evidence to date suggest that the pathophysiology of several chronic cardiac disorders may stem from, or are exacerbated, by anomalies in

myocardial energy substrate metabolism (259). We report in this work that disruption of normal EC autophagic flux decreases EC FABP expression and suggest that this molecular anomaly may account in part for the lower TAG levels detected in hearts from EC-ATG7^{-/-} mice relative to those from their WT littermate controls. The smaller myocardial TAG pool may also partially explain why hearts isolated from EC-ATG7^{-/-} mice appeared less reliant on palmitate oxidation as a fuel source during both insulin stimulation and following ischemia induction in our I/R model.

The crosstalk between ECs and cardiomyocytes forms a critical regulatory pathway for normal cardiac development and growth (251). Accordingly, deviations from the norm, no matter how small, could have significant implications on cardiomyocyte phenotype, metabolism, growth, contractility, rhythmicity, and survival (251). Indeed, dysfunctional autocrine and paracrine signals at the endothelial level are known to play a role in triggering and promoting I/R-associated irregularities (252). It is therefore somewhat surprising that given the basic high energy needs of the heart and our evolving understanding of the pathological foundation of multiple coronary and vascular diseases, the delivery of energy substrates from ECs to cardiomyocytes remains a poorly explored and understood biological entity.

Cellular 5' adenosine monophosphate-activated protein kinase (AMPK) is a phylogenetically conserved energy sensor that has attracted much interest as a potential therapeutic target to elevate muscle glucose uptake in diabetes, while favoring fatty acid oxidation over fatty acid synthesis (260). Nutrient starvation in HUVECs has been previously associated with AMPK activation and increases in fatty acid metabolism (119,120). Milieu changes in free fatty acid and TAG levels trigger lipid droplet

formation and degradation which ensure EC metabolic homeostasis while also serving as fatty acid reservoirs for the cells nearby (121). These observations collectively suggest that ECs possess the necessary machinery to regulate intracellular lipid levels, buffer the circulatory fatty acid content and assist in the translocation of fatty acids from ECs to the neighboring cardiomyocytes. However, unlike cardiomyocytes which impose the greatest energy demands among the cells of the heart, ECs rely primarily on glycolysis as their fuel source (261) and it is highly likely that the impact ECs have on cardiac energy metabolism is limited to that necessary for substrate delivery. Accordingly, the metabolic rates that we report herein most likely represent cardiomyocyte utilization of coronary EC-delivered substrates.

As mentioned earlier, our collaborating group has reported extensively on how abnormalities in the autophagic network are associated with functional, biochemical and molecular changes that have been implicated in a wide range of cardiovascular anomalies (124,200,253-256). This includes showing that EC autophagy plays a critical role in restricting lipid accrual within the vasculature and consequently can alter the downstream atherosclerotic burden (125). These results linking autophagy to lipid homeostasis and atherogenesis not only align well with those previously reported (126,262-264), but also extend the findings of Rambold and colleagues (129) who described the significance of autophagy in fatty acid trafficking and toxicity. The observations made in the current body of experiments add to the existing literature by demonstrating that an intact endothelial autophagy network is essential for keeping up with the energy demands of the heart.

FABPs are lipid chaperones that are ubiquitously expressed in cells and tissues acutely involved in fatty acid trafficking, signaling and metabolism (265). Compared to hearts and skeletal muscles of WT mice, the corresponding samples from FABP4/5 double-knockout mice exhibited significantly lower uptake of the fatty acid analogue ^{125}I -15-(p-iodophenyl)-3-(R,S)-methyl pentadecanoic acid and markedly greater uptake of the glucose analogue ^{18}F -fluorodeoxyglucose (266). This coupled with supporting protein assessments led the investigators of the study to conclude that FABP4 and FABP5 may be potential therapeutic targets for correcting dysregulated lipid metabolism and signaling. Inasmuch as ATG7 silencing appreciably dampened cardiac TAG content as well as lowered EC FABP4 and FABP5 expression, it would not be unreasonable to posit that the absence of autophagy leads to a decline in fatty acid translocation and in turn a diminished TAG reservoir resulting in less fatty acid oxidation-associated energy production. However, we cannot exclude the possibility that alternative roles of the ATG7 protein in ECs that extend beyond its known role in autophagy may have led to the altered cardiac energy substrate preference. Although our I/R model did not show beneficial effects on recovery in EC-ATG7^{-/-}, possibly due to the importance of autophagy in mitigation of I/R injury, the benefits of inhibiting palmitate and stimulating glucose oxidation in other cardiac disease settings such as failing or insulin resistant hearts by targeting endothelial lipid handling through autophagosomes or FABP4/5 may still exist and require further investigation.

In summary, the results reported herein demonstrate that fatty acid metabolism within the heart is reliant on an intact endothelial autophagy network. To the best of our knowledge, this is the first demonstration linking disrupted endothelial autophagy with

dysregulated cardiac energy metabolism via altered FABP expression. Our findings support the notion that the endothelial autophagy network in conjunction with FABPs may offer novel therapeutic targets for normalizing deranged myocardial mitochondrial bioenergetics.

Table 5.1. Cardiac parameters of working hearts from EC-ATG7^{-/-} and WT littermate controls perfused under aerobic conditions. Data shown are mean values for *n*= 5-8 mice. P value not significant, 2-way ANOVA with repeated measures (time).

Parameter	Time (min)											
	10		20		30		40		50		60	
	WT	EC-ATG7 ^{-/-}										
Cardiac Output (ml/min)	7.3± 1.6	7.2± 0.8	7.7± 1.4	7.4± 0.6	8.2± 1.2	7.4± 0.6	7.7± 1.3	7.6± 0.9	8.5± 0.9	8.0± 0.9	8.8± 0.8	7.8± 1.0
Left Ventricle Developed Pressure (mmHg)	31.6± 2.4	34.5± 2.8	28.0± 2.8	34.8± 2.1	27.5± 1.8	32.8± 2.1	29.8± 3.1	30.8± 2.5	30.3± 1.8	30.9± 2.3	29.4± 2.0	29.5± 2.4
Aortic Outflow (ml/min)	5.6± 1.2	5.8± 0.7	5.7± 1.0	5.5± 0.6	6.9± 0.6	5.4± 0.6	6.2± 0.8	5.5± 0.8	7.1± 0.4	5.7± 0.9	7.1± 0.5	5.4± 1.1
Coronary Flow (ml/min)	2.6± 0.5	1.5± 0.2	2.9± 0.5	1.9± 0.2	2.4± 0.6	2.0± 0.2	2.5± 0.6	2.0± 0.2	2.6± 0.8	2.3± 0.2	2.8± 0.9	2.4± 0.3
Heart Rate (beats per min)	227± 33	191± 16	240± 29	181± 13	241± 11	195± 14	234± 22	211± 14	246± 18	217± 13	252± 11	214± 17
Peak Systolic Pressure (mmHg)	76.9± 2.3	80.1± 2.2	72.6± 2.5	80.0± 1.7	72.2± 1.7	78.5± 1.4	72.9± 2.8	76.8± 1.6	73.6± 2.2	76.1± 1.5	72.3± 2.4	75.2± 1.9

Figure 5.1. Endothelial-specific ATG7 deletion is associated with reduced myocardial fatty acid oxidation in response to insulin. The functional and metabolic capacities of hearts from EC-ATG7^{-/-} mice and their WT littermates were measured under aerobic conditions using the isolated working heart system. **(A)** Cardiac work under basal conditions. The following parameters were measured or calculated in the absence and presence of insulin: **(B)** glucose and **(C)** palmitate oxidation rates **(D, E)** metabolic rates relative to cardiac work; **(F)** acetyl-CoA production and **(G)** the corresponding proportional derivation from glucose (upper part of the bar) and palmitate oxidation (lower part of the bar); **(H)** cardiac efficiency. $n = 6-8$ for each group; * $P < 0.05$ vs corresponding data collected in the absence of insulin.

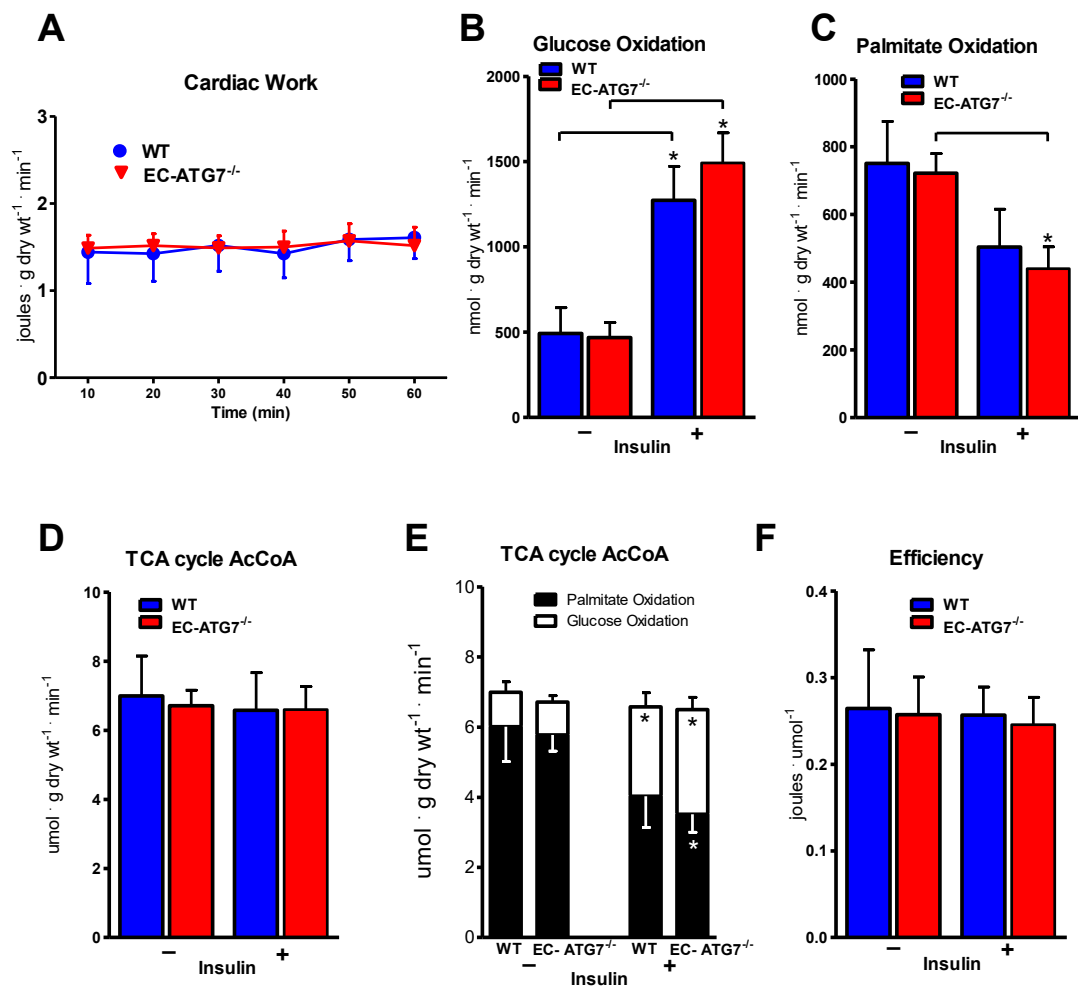


Figure 5.1

Figure 5.2. Endothelial specific ATG7 deletion is associated with augmented cardiac glucose oxidation, diminished cardiac fatty acid oxidation and reduced cardiac efficiency following an I/R insult. The functional and metabolic capacities of hearts from EC-ATG7^{-/-} mice and their WT littermates were measured under I/R conditions in isolated working hearts. The specific pre- and post-ischemia parameters measured were: **(A)** Cardiac work; **(B)** glucose and **(C)** palmitate oxidation rates; **(D)** TCA acetyl-CoA production, and the **(E)** corresponding proportional derivation from glucose (upper part of the bar) and palmitate oxidation (lower part of the bar); **(F)** cardiac efficiency. *n*=14-23 for each group; **P* < 0.05 vs corresponding data from the hearts of the WT group; #*P* < 0.05 vs corresponding pre-ischemia data.

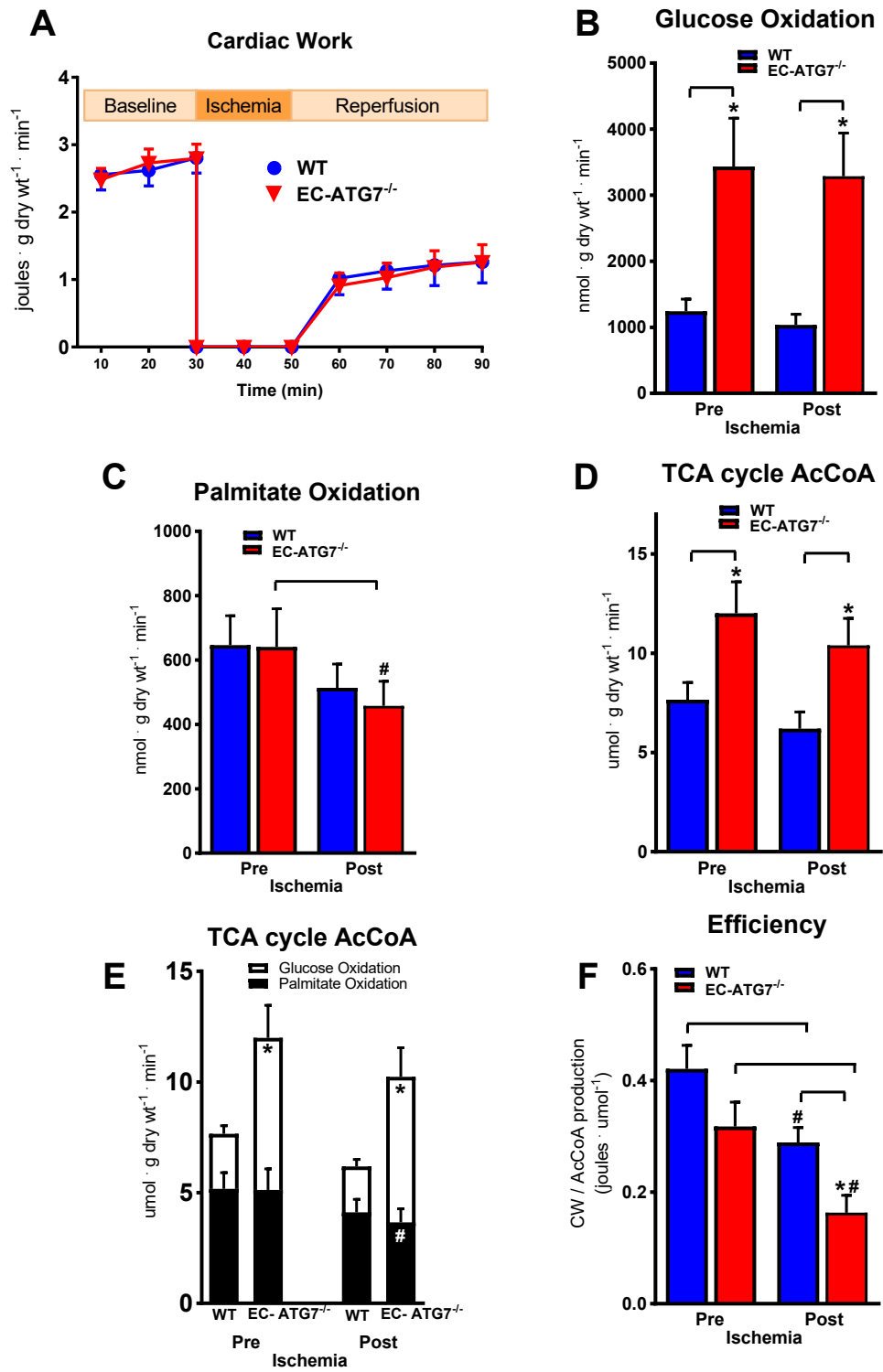


Figure 5.2

Figure 5.3. Endothelial specific ATG7 deletion lowers cardiac TAG stores and expression of endothelial fatty acid binding proteins.

(A) TAG levels in freshly harvested, flash-frozen ventricles from EC-ATG7^{-/-} mice and their WT littermates, n=7-8. (B) Agarose gel electrophoresis of RT-PCR from total RNA of HUVEC cells treated with siRNA showing successful knock-down of ATG7 in cells treated with siATG7. (C) ATG7, (D) *CD36*, (E) *FABP4*, and (F) *FABP5*, expression in siATG7- and scrambled (control) siRNA-treated HUVECs. *GPADH* served as the housekeeping gene. RT-PCR results represent the mean of 3 independent experiments conducted in triplicates. Data in A, C-F are presented as box-and-whiskers plots where the upper and lower borders of the box represent the upper and lower quartiles, the horizontal line inside the box represents the median, the upper and lower whiskers represent the maximum and minimum values of non-outliers, and the + sign represents the mean. **P* < .05 vs corresponding WT or scrambled siRNA-treated group, unpaired t-test.

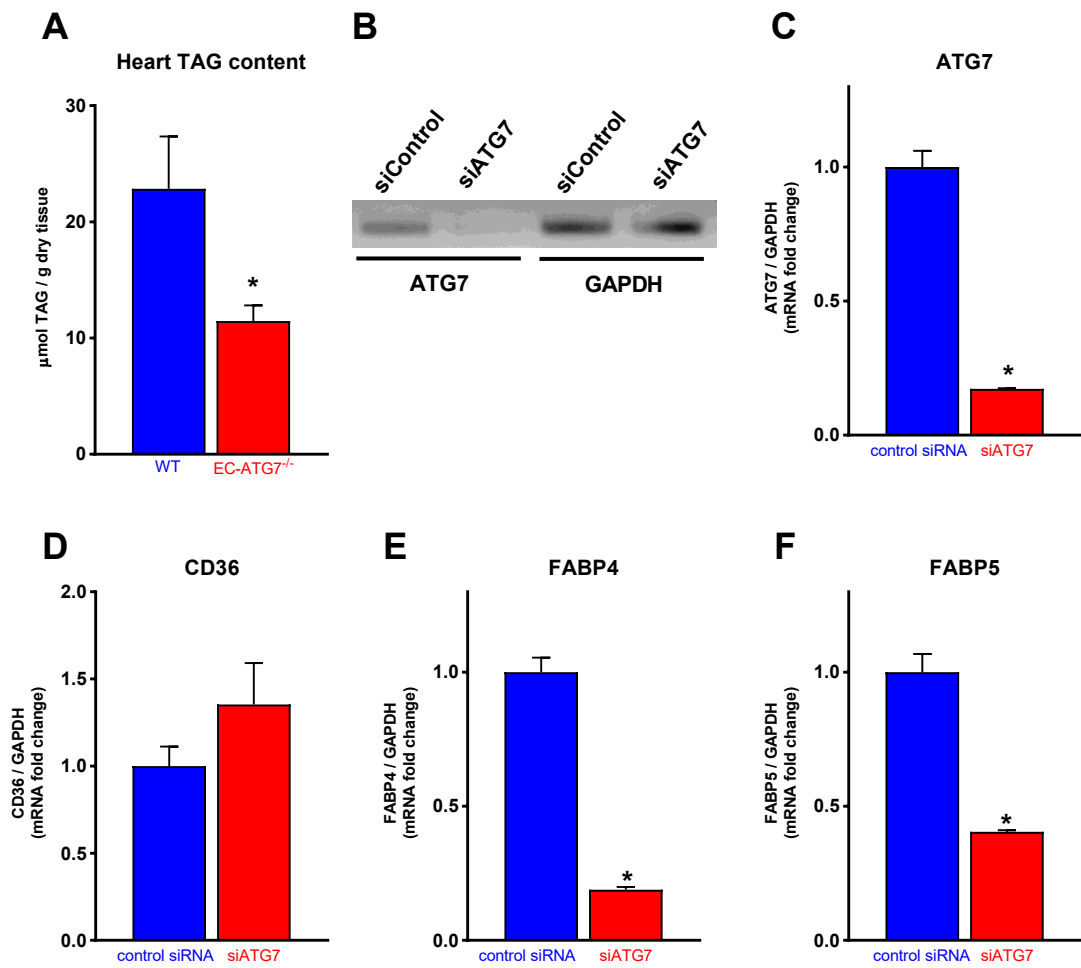


Figure 5.3

CHAPTER 6

Adropin Regulates Cardiac Energy Metabolism and Improves Cardiac Function and Efficiency

A manuscript is currently under preparation to be submitted to the *Journal of Molecular and Cellular Cardiology*

Arata Fukushima and Abhishek Gupta performed part of western blotting, Liyan Zhang assisted in the *in vivo* adropin injections in the mice. I designed and performed all the remaining experiments, analyzed the results, and wrote the manuscript.

CHAPTER 6

Adropin Regulates Cardiac Energy Metabolism and Improves Cardiac Function and Efficiency

6.1 Abstract

Impaired cardiac insulin signaling and high cardiac fatty acid oxidation rates are characteristics of obesity-induced and diabetic-induced cardiomyopathies. The potential role of liver-derived factors in mediating these obesity and diabetes mediated changes in cardiac energy metabolism are underappreciated. Plasma levels of adropin, a liver secreted peptide, declines under conditions of insulin resistance and during fasting. In skeletal muscle, adropin preferentially promotes glucose oxidation over fatty acid oxidation. We therefore determined what effect adropin has on cardiac energy metabolism, insulin signaling and cardiac efficiency. C57Bl/6 mice were fasted to accentuate the differences in adropin plasma levels between animals, and were then intraperitoneally injected with either vehicle or adropin (3 doses of 450 nmol/kg at 6-hr intervals). Despite a fasting-induced predominance of fatty acid oxidation measured in isolated working control hearts, insulin inhibition of fatty acid oxidation was preserved by adropin compared with control ($p < 0.05$). Adropin-treated mouse hearts also showed a higher cardiac work over the course of perfusion ($p < 0.05$), which was accompanied by improved cardiac efficiency and enhanced phosphorylation of insulin signaling

enzymes (p-IRS-1 at Y⁶²⁸, AS160 at T⁶⁴², and GSK3 β at S⁹ p<0.05). Interestingly, acute addition of adropin to isolated working hearts from non-fasting mice also resulted in an inhibition of fatty acid oxidation, accompanied by a robust stimulation of glucose oxidation compared with vehicle-treated hearts. Acute administration of adropin also increased insulin-induced phosphorylation of Akt (Akt S⁴⁷³), IRS-1 (p-IRS-1 Y⁶²⁸), and GSK3 β (p-GSK3 β S⁹) (p<0.05). Both *in vivo* and *in vitro* treatment protocols induced a reduction in the insulin-signalling mitigating phosphorylation of JNK (p-JNK T¹⁸³/Y¹⁸⁵) and IRS-1 (p-IRS-1 S³⁰⁷) phosphorylation, suggesting acute receptor- and/or post-translational modification-mediated mechanisms. These results demonstrate that adropin has important effects on energy metabolism in the heart, and may be a putative candidate for the treatment of cardiac disease associated with impaired insulin sensitivity.

6.2 Introduction

Several secreted peptides have been shown to mediate whole body energy homeostasis, lipid metabolism and maintenance of insulin sensitivity (182,267-269). For instance, adipokines, secreted by the adipose tissue, act as paracrine/endocrine hormones to mediate energy metabolism and have been extensively studied in the setting of obesity and diabetes (270). However, less attention has been given to the potential metabolic actions of liver-secreted metabolic factors such as adropin (193). Adropin is a secretable peptide initially identified in the liver and is encoded by the Energy Homeostasis Associated gene (*Enho*) (193). Circulating adropin levels are closely related to nutritional and metabolic cues in the body. For example, liver adropin expression

decreases with diet- or genetically-induced obesity (193). Additionally, the expression and plasma levels of adropin are increased by feeding and suppressed by fasting (193,271). In skeletal muscles, adropin has been proposed to have a role in mediating energy metabolism through preferentially promoting glucose oxidation over fatty acid oxidation (192). This is associated with improved insulin sensitivity in mice with diet-induced obesity (194). This insulin sensitizing effect of adropin is thought to be mediated by an increase in glucose oxidation through activation of pyruvate dehydrogenase (PDH), by lowering the protein levels of its inhibitory kinase PDH kinase 4 (PDK4), while also inhibiting sarcolemmal and mitochondrial fatty acid uptake at a transcriptional level through decreasing the protein levels of the fatty acid transporter CD36, and carnitine palmitoyltransferase 1 (CPT I) (192,194).

Myocardial energy metabolism is profoundly altered in many heart pathologies including heart failure and diabetic cardiomyopathy (272). Diabetic hearts are more reliant on fatty acid oxidation for energy production and display impairment of glucose uptake and metabolism, whereas failing hearts show general impairment of mitochondrial oxidative phosphorylation with increased dependence on glycolysis (1). These alterations in cardiac energy metabolism contribute to the severity of heart disease (1,4). Clinically, reduced serum levels of adropin are associated with several cardiovascular conditions including endothelial dysfunction, heart failure, acute myocardial infarction, coronary atherosclerosis, and cardiac syndrome X, and represent an independent risk factor and predictor of most of these conditions (273).

Whether adropin alters cardiac energy metabolism in the heart is unknown, as are the potential mechanisms by which it mediates energy metabolism. Understanding the

metabolic effects of adropin may not only provide diagnostic tools for early detection of cardiac pathologies, but may also help devise novel therapies aiming at alleviating the metabolic disturbances contributing to the progression of heart disease. Therefore, the aim of this study was to investigate the effects of adropin administration on cardiac energy metabolism and function with the hypothesis that adropin causes a switch of myocardial energy metabolism towards glucose oxidation, while improving insulin sensitivity.

6.3 Materials and methods

6.3.1 Materials and animals

The materials used in this study are detailed in Chapter 2. Male C57BL/6 mice (7-10 weeks of age) were obtained from Charles River laboratories (Wilmington, MA, USA) and used in the study. The animals were given free access to regular chow diet (Harlan Teklad, Madison, WI, USA) unless a fasting protocol was applied as explained below. All animal studies were approved by the University of Alberta Health Sciences Animal Welfare Committee and conform to the guidelines of the Canadian Council of Animal Care, Alberta.

6.3.2 Study protocol

The animals utilized in this study to evaluate cardiac functional and metabolic changes of adropin were subjected to one of either of the following protocols:

1. *In vivo adropin*: mice received three intra-peritoneal (IP) injections of 450 nmol/kg Adropin³⁴⁻⁷⁶ (ChinaPeptides, Shanghai, China) dissolved in 0.1% BSA normal

saline or vehicle, over a 20-24 hr period. This adropin administration protocol was previously used to induce metabolic actions in whole-body and skeletal muscles in mice (192,194). All mice were fasted after 4 hours of the first treatment injection just before their dark cycle, and for a total of 16-20 hr. This fasting protocol was adopted to accentuate the differences in plasma levels of adropin between the animals of the two experimental groups. At the end of fasting period, the mice were euthanized using 12 mg intraperitoneal sodium pentobarbital followed by isolating and perfusing the heart using a working heart preparation as described previously (21,211) for 30 min without insulin, followed by 30 min with 100 μ U/ml insulin. A schematic view of the *in vivo* protocol is shown in Figure 6.1A.

2. *Ex vivo adropin*: To examine if adropin had acute metabolic/functional effects on the heart, we also acutely perfused hearts from normally fed animals. These animals did not receive treatments before euthanasia. Hearts were perfused using the *ex vivo* working heart system as described above, with the modification that during the whole perfusion protocol, 100 μ U/ml insulin was present in the perfusate as well as either Adropin³⁴⁻⁷⁶ (2 nM, equivalent to 10 ng/ml), an elevated yet physiologically relevant concentration, or vehicle. A schematic view of the *ex vivo* protocol is shown in Figure 6.3A.

6.3.3 Heart perfusions

In addition to the specific treatment as explained above, the isolated working-heart perfusate consisted of a modified Krebs–Henseleit bicarbonate (KHB) solution containing in mM (118.5 NaCl, 4.7 KCl, 2.5 CaCl₂, 25 NaHCO₃, 1.2 KH₂PO₄, 1.2 MgSO₄, 5 glucose, and 0.8 palmitate bound to 3% bovine serum albumin. Trace

amounts of a combination of two appropriate radiolabeled molecules of [5-³H] glucose, [U-¹⁴C] glucose, [9, 10-³H] palmitate were added to perfusate to assess rates of glycolysis, glucose oxidation, and palmitate oxidation, respectively. The perfusate was continuously oxygenated with a gas mixture of 95% O₂ and 5% CO₂. Two metabolic rates were determined simultaneously by quantitative collection of ¹⁴CO₂ and ³H₂O produced by the hearts from metabolizing the respective energy substrates. Rates were expressed as nmol per g dry weight per min (nmol · g dry wt⁻¹ · min⁻¹) (21,211). Proton production from uncoupled glycolysis and glucose oxidation was calculated based on knowledge of the lactate dehydrogenase reaction.

Cardiac function was assessed in isolated working hearts using a MP100 system from AcqKnowledge (BIOPAC Systems, Inc.). This included assessing heart rate, peak systolic pressure, left ventricular developed pressure, cardiac output, and aortic output. Cardiac work was determined as a function of cardiac output and peak systolic pressure. Cardiac efficiency was calculated as the ratio of cardiac work to total acetyl-CoA production rates, which in turn was obtained from energy substrate metabolic rates. At the end of each perfusion, the heart ventricles were clamp-frozen in liquid nitrogen then stored at -80 °C for subsequent biochemical examination. The dry/wet tissue ratio was determined and metabolic rates were represented as per total dry mass of the heart.

6.3.4 Western blotting

Protein levels and phosphorylation were assessed in heart tissue using immunoblotting, as described previously (214). Western blotting samples were prepared from lysates of homogenized heart ventricular tissue and then subjected to western blotting procedures using specific antibodies against the proteins of interest as well as the appropriate

loading controls. The phosphorylation of specific proteins was assessed using an antibody detecting a phosphorylated sequence of the respective protein. More details of these procedures are presented in Chapter 2.

6.3.5 Glucose tolerance test

An intraperitoneal (IP) glucose tolerance test was conducted on fasted mice administered adropin or vehicle using a dose of 2 g glucose/kg as previously described (274). The procedure was performed 60 min after the third IP injection of adropin (450nmol/kg), as explained above, after fasting the animal for 14-18 hr and at least 2 hours prior to heart perfusion. Body weight and blood glucose levels were measured using a commercial glucometer just before the IP glucose injection. Blood glucose levels were then reassessed at 15, 30, 45, 60, 75, 90, and 120 min from glucose administration.

6.3.6 Statistical analysis

Data are expressed as mean \pm SEM. Statistical significance was determined using paired, unpaired t-test, 2-ANOVA, or 2-ANOVA with repeated measures, followed by Bonferroni post-hoc test whenever appropriate. Differences were considered significant if $p < 0.05$.

6.4 Results

6.4.1 Adropin administration to fasting mice improves cardiac function and efficiency while increasing insulin's inhibitory effect on palmitate oxidation

To evaluate the consequences of increased circulating levels of the secretable form of adropin (i.e. adropin³⁴⁻⁷⁶), on cardiac function and metabolism, we injected C57BL/6

mice with either 450 nmol/kg adropin or vehicle three times during a 24 hr period in accordance with previously used protocols that reportedly ensured a physiological response (192,193). A 16-20 hr fasting protocol was adopted to augment the differences in plasma levels of adropin between the two experimental groups and to investigate adropin's metabolic effects under conditions of increased metabolic inflexibility and increased reliance of the heart on fatty acid oxidation for energy production (192,194) that is seen with fasting (1) (Figure 6.1A). Thereafter, several functional parameters were assessed using an isolated working heart system. This approach provides a tool to investigate homeostatic and cardiac work data in parallel with ongoing assessment of energy metabolism. The hearts were subjected to actual workloads through a perfusion system that offered a normal (ante-grade) aortic and coronary flow. It also allowed simultaneous measurement of absolute catabolic rates of two energy substrates in isolation from whole body effects through perfusing the animal heart with a solution containing physiologically relevant concentrations of such substrates, along with traces amounts of radiolabeled substrates, in addition to the ions necessary for normal excitation-contraction processes.

As expected in these lean mice, that were not suffering from impaired insulin sensitivity or glucose homeostasis, whole body glucose tolerance was not different between the two groups (Appendix B, Figure B1). Interestingly, as little as one day treatment with adropin improved *ex vivo* cardiac function, as evidenced by enhanced cardiac work especially upon the introduction of insulin to the perfusate (Figure 6.1B). There was also a significant increase in coronary flow, which may have contributed to the enhanced cardiac work (Figure 6.1C).

Despite fasting, the effect of insulin on stimulating cardiac glucose oxidation rates was seen in both vehicle and adropin-treated mice (Figure 6.1D). In contrast, hearts from vehicle-treated fasted mice, lacked the inhibitory effect of insulin on palmitate oxidation (Figure 6.1E), that normally exist in fed mice. However, the inhibitory effects of insulin on fatty acid oxidation were clearly preserved in hearts from the adropin-treated mice (Figure 6.1E). This suggests enhanced myocardial insulin sensitivity with adropin even in the fasted mice. The lack of effect of adropin on glucose oxidation rates may have stemmed from the relatively inhibited glucose oxidation in such fasting animals, rendering it suppressed and less responsive to adropin. Glycolysis rates were also not different between hearts from adropin-treated mice and vehicle-treated mice (Figure 6.1F). In light of the similar glucose oxidation in both groups, glycolysis-glucose oxidation coupling, and therefore proton production rates, were comparable to control hearts (Figure 6.1G).

By considering the three different sources of ATP production used in our model, it is clear that the contribution of fatty acid oxidation to ATP was decreased by insulin in hearts from adropin-treated mice (Figure 6.1H) which resulted in a moderate decrease in ATP produced to provide the higher cardiac work exerted by these hearts, thus leading to a raise in cardiac efficiency (Figure 6.1I) as defined by the amount of cardiac work per ATP produced. Together, these results suggest that adropin enhances *ex vivo* cardiac function with a stimulatory effect on insulin's inhibition of fatty acid oxidation, associated with higher cardiac efficiency.

6.4.2 *In vivo* 24 hr treatment with adropin does not change protein levels of key metabolic enzymes proposed to mediate its effects in skeletal muscles

Based on our functional and metabolic data, we investigated possible variations in levels and phosphorylation status of proteins known to regulate energy metabolic pathways. We first explored the mechanisms previously suggested to mediate adropin effects on skeletal muscles at a transcriptional levels (192,194). Contrary to previously proposed mechanisms in skeletal muscles, we did not see changes in protein levels of CD36, CPT I b, or PDK (Figure 6.2 A and B). Phosphorylation of PDH E1-alpha subunit at S²⁹³ was also not different between adropin and control groups (Figure 2 A and B). Moreover, phosphorylation of AMP Kinase (p-AMPK T¹⁷²) and acetyl-CoA carboxylase (p-ACC 2 S¹²⁰⁰) were not changed, nor were the protein levels of PPAR α or PGC1- α (Figure 2 A and B). These results suggest that in the heart the metabolic effects associated with adropin administration over a 24 hr period are not explained by variable protein expression of components proposed to mediate the metabolic effects of adropin in skeletal muscle.

6.4.3 Acute administration of adropin stimulates glucose oxidation with a corresponding inhibition of palmitate oxidation

Since we did not see effects of adropin injections on protein levels of the metabolic regulatory components previously suggested to mediate the effects on skeletal muscle energy metabolism (192,194), we examined whether adropin has any acute metabolic/functional effects on the heart that are not dependent on protein expression. This involved directly perfusing isolated working mouse hearts with 2nM adropin or vehicle (Figure 6.3A). Acute adropin-treatment did not have major effects on cardiac

function (Figure 6.3B), although there was a tendency towards improved cardiac work and a significant increase in rate-pressure product (RPP). Despite these minor effects on cardiac function, hearts perfused with adropin showed a significant enhancement of glucose oxidation accompanied by a corresponding decrease in palmitate oxidation (Figure 6.3D and E, respectively) compared with control. Here again, there was no change in glycolysis or proton production rates (Figure 6.3F and G). This resulted in a significant increase in the contribution of glucose oxidation as opposed to palmitate oxidation to the production of ATP (Figure 6.3H). Since these non-stressed hearts produced comparable total amount of ATP and magnitude of cardiac work, their cardiac efficiency did not differ from controls (Figure 6.3I).

6.4.4 Insulin signaling is enhanced in the hearts of adropin-injected mice and in isolated hearts perfused with adropin

The acute and profound effect of acute adropin administration in stimulating cardiac glucose oxidation and inhibiting fatty acid oxidation, and the inhibition of fatty acid oxidation and the lack of changes in the expression of several proteins involved in energy metabolism following *in vivo* adropin administration, led us to the hypothesis that a PTM mechanism(s) may actually be responsible for the effects of adropin on cardiac energy metabolism in the heart. We therefore measured several components of the cardiac insulin signaling pathway following both *in vivo* and *ex vivo* adropin-treatment. As shown in Figure 6.4, tissue lysates of heart ventricles from mice treated with *in vivo* adropin showed enhanced stimulatory phosphorylation of AS160 (p-AS160 T⁶⁴²) and insulin receptor substrate-1 (p- IRS-1 Y⁶²⁸) and an inhibitory phosphorylation

of GSK3 β (p-GSK3 β S⁹), with only a tendency for increased phosphorylation of Akt (p-Akt S⁴⁷³), upstream of GSK3 β and AS160, compared with vehicle controls (p<0.05). Similarly, *ex vivo* adropin also promoted insulin signaling compared with vehicle controls, as evidenced by increased stimulatory phosphorylation of IRS-1 (p-IRS-1 Y⁶²⁸) and Akt (p-Akt S⁴⁷³), as well as by downstream inhibitory phosphorylation of GSK3 β (p-GSK3 β S⁹) in *ex vivo* adropin hearts (p<0.05), although not significantly changing AS160 phosphorylation (p-AS160 T⁶⁴²) status (Figure 6.5).

A negative regulator of IRS-1 is its phosphorylation at S³⁰⁷ residues in mouse tissue (S³¹² in human) which is located at a domain involved in the binding of IRS-1 to the insulin receptor (IR), and when phosphorylated hinders this binding and subsequent insulin signalling (275). We observed a decline in IRS-1 S³⁰⁷ phosphorylation with both *in vivo* and *ex vivo* adropin administration (Figure 6.4 and Figure 6.5). This is consistent with stimulation of insulin signalling and improved cardiac insulin sensitivity evident in the above molecular and metabolic effects of adropin. One upstream kinase responsible for IRS-1 S³⁰⁷ phosphorylation is c-Jun NH₂-terminal kinase (JNK) (276), which displayed decreased phosphorylation (p-JNK T¹⁸³/Y¹⁸⁵) with both *in vivo* and *ex vivo* adropin administration associated with inhibited activity of this kinase and consequently in line with decreased IRS-1 S³⁰⁷ phosphorylation (Figure 6.4 and 6.5). To summarize, *in vivo* adropin injections as well as acute *ex vivo* adropin in isolated hearts was associated with stimulation of insulin signalling pathways that was accompanied by inhibitory effects on JNK/ IRS-1 S³⁰⁷ phosphorylation axis.

6.5 Discussion

Several peptides secreted by non-muscular tissues are known to affect energy homeostasis and insulin sensitivity in heart and skeletal muscle (182-185). The majority of research in this area has focused on factors secreted by adipocytes (i.e. adipokines) including adiponectin and leptin, which have hormone-like endocrine effects on the liver, heart, and skeletal muscles (184). Dysregulated plasma levels and functions of certain adipokines including adiponectin, leptin as well as pro-inflammatory cytokines and resistin are associated with insulin resistance seen in obesity (184,185). However, liver-secreted factors have only gained sufficient attention as potential modulators of energy homeostasis in extrahepatic tissues, particularly the heart (183). Here we show that a secreted form of adropin (i.e. Adropin³⁴⁻⁷⁶), which is naturally synthesized and secreted by the liver, induces significant modification of cardiac energy metabolism by increasing glucose oxidation and inhibiting fatty acid oxidation. We also demonstrate that this is mediated, at least in part, by enhancement of insulin signalling and therefore increased glucose oxidation and inhibition of fatty acid oxidation (1,177). As a result, we demonstrate that the liver can significantly regulate cardiac energy metabolism through the release of adropin.

Decreased adropin plasma levels are associated with markers of insulin resistance (277). Adropin has been recently proposed to have an important role in regulating skeletal muscle energy metabolism particularly in post-prandial conditions (192,193) and in obesity (194). In these previous studies, either transgenic overexpression or exogenous administration of adropin improved the overall metabolic profile in animals with diet-induced obesity through better glucose tolerance and oxidation and insulin sensitivity

(193,194). However, assessment of direct regulatory effects of adropin on cardiac energy substrate metabolism has not been performed prior to our current study.

The expression and plasma levels of adropin are increased during feeding and suppressed by fasting (193,271). Accordingly and in order to increase the contrast in adropin levels between the two treatments and possible effects on cardiac function and energy metabolism, we utilized a fasting protocol applied to mice injected with adropin or vehicle. Although we did not utilize in this initial study an experimental model of diabetes, this approach allowed us to simulate the metabolic status of diabetic hearts by creating a fasting-induced elevation of fatty acid oxidation and inhibited glucose oxidation. This proved useful in evaluating adropin for possible effects counteracting the fasting-associated energy metabolism profile akin to the insulin resistant heart.

The improved cardiac function seen in adropin-treated hearts, particularly the *in vivo* study, is of particular significance and uniqueness to this study. Direct functional consequences were not investigated in previously studied tissue, namely skeletal muscle, and therefore our demonstration of direct beneficial effects of adropin on cardiac function may suggest useful implications and benefit in conditions of cardiac disease associated with impaired insulin sensitivity. However, this study represents a preliminary evaluation of actions of adropin on cardiac function and future investigations on diseased hearts are required. The exact mechanism of improved cardiac function, especially with insulin stimulation, is not clear, although this may be related to an increased cardiac efficiency with *in vivo* adropin (Figure 6.1G), a finding consistent with inhibition of fatty acid oxidation, which is a less efficient energy substrate compared to glucose (1,278).

The mechanism by which adropin was proposed to stimulate glucose oxidation in skeletal muscles involved stimulating PDH activity by down-regulating the protein expression of its inhibitory kinase PDK4 (192,194). Similarly, inhibition of fatty acid oxidation was proposed to occur through decreasing the protein expression of the sarcolemmal fatty acid translocase, CD36, and of CPT I, the enzyme responsible for mitochondrial uptake and hence oxidation of activated long fatty acids (192,194). In addition, it was suggested that these effects are mediated through the inhibitory acetylation control of the transcriptional coactivator PGC-1 α , through SIRT1, with subsequent effects on PDK4 and CPT levels (192,194). Interestingly, although these molecular effects of adropin were accompanied by modulation of energy metabolism in skeletal muscle similar to what we report here in the heart, we could not reproduce such transcriptional, protein level or acetylation changes (Appendix B, Figure B2) with adropin in the heart. This suggests that the cardiac response to adropin may involve different mechanisms depending on the tissue affected and/or duration of treatment. Nonetheless, several components of insulin signaling were stimulated by adropin in our mouse hearts, associated with the increase in glucose oxidation and/or decline in fatty acid oxidation (Figure 6.6). These are consistent with the aforementioned studies on normal and insulin-resistant mouse skeletal muscles (192,194).

The impressive acute adropin metabolic response in the absence of alterations in the expression of key metabolic proteins suggest a mechanism of action involving possible ligand (adropin)-receptor interaction resulting in the post-translational modifications of components of the insulin signalling pathway. Adipokines such as adiponectin and leptin induce their metabolic actions on the heart through binding to specific receptors

on the cell membrane (279,280). For example, different isoforms of adiponectin and leptin receptors are expressed in the heart of humans and rodents mediating direct actions on cardiac energy metabolism (280,281). However, to date the identity of a proposed receptor of adropin remains to be determined. A recent study suggested adropin's effects on the brain to inhibit the water drinking behavior to be mediated through GPR19, a G-protein coupled receptor (GPCR) in neuronal cells (282). This protein is also expressed in the heart although in lower levels (283). A more recent study by Thapa et al. (284), proposed GPR19 as the receptor for adropin in H9c2 cells by mediating its metabolic actions on PDH activation through suppression of PDK4 expression in a p44/42 MAPK – dependent mechanism, Whether this mechanism has played a part in our mouse hearts is challenged by the fact that PDK4 protein levels were not altered by our adropin administration protocol. Further investigation is required to determine the exact receptor/mechanism of action of adropin on the myocardium.

The signaling pathways mediating adropin's metabolic effects in the heart appear to involve modulating JNK activity. Sustained JNK activity is known to contribute to endoplasmic reticulum stress (285). Contrary to our findings, JNK involvement in the actions of adropin on skeletal muscle metabolism was excluded in the recent study discussed above (194) adding to the discrepancies between our results and those of that study. The JNK inhibitory serine phosphorylation of IRS-1 is known to underline inflammatory- as well as free fatty acid- induced insulin resistance (276,286). Binding of insulin to its receptor at the extracellular α subunits elicits the intracellular tyrosine autophosphorylation of the β subunits, which enhances the tyrosine kinase activity of

the receptor to its downstream adaptor proteins including IRS-1 (287,288). The phosphorylated tyrosine residues of IRS initiate the activation of downstream kinases and proteins of the insulin signalling pathway including Akt, which in turn phosphorylates and activates AS160 leading to increased GLUT4 translocation to the cell membrane and thus enhance glucose uptake, as well as phosphorylating and inhibiting GSK3 β to increase glycogen synthesis (Figure 6.6) (287,289). As such, attenuation by adropin of JNK phosphorylation, a surrogate marker of JNK activity, is consistent with de-inhibiting IRS-1 mediation of insulin signalling and the observed enhancement of glucose utilization. However, it remains unclear how administration of adropin could lead to decreased JNK phosphorylation in the heart, and whether these effects are mediated downstream of a cardiac adropin receptor.

In conclusion, we demonstrate that adropin has an important role in regulating cardiac energy substrate preference, secondary to inhibiting fatty acid oxidation and stimulating glucose oxidation. This action of adropin may provide a promising target in devising therapies for metabolic syndrome, obesity, and diabetes by modulating myocardial energy metabolism.

Figure 6.1. *In vivo* adropin enhances cardiac efficiency and modulates insulin-induced inhibition of fatty acid oxidation. (A) A diagram showing the experimental protocol of *in vivo* adropin/vehicle injections followed by isolated working hearts perfusions. Functional and metabolic assessment of working heart perfusions (60 min) of hearts isolated from fasting C57BL/6 mice that were injected three times with intraperitoneal 450 nmol/kg Adropin³⁴⁻⁷⁶ or vehicle over a 20-24 hr period: (B) cardiac work, (C) coronary flow, (D) glucose oxidation; (E) palmitate oxidation; (F) glycolysis; (G) proton production; (H) contribution of the respective catabolic pathway to ATP production and (I) cardiac efficiency. Insulin (100 μ U/ml) was added at 30 min during heart perfusions as described in methods. Cardiac functional parameters data were recorded using an MP100 system from AcqKnowledge (BIOPAC Systems, Inc.), to provide data to calculate cardiac work as explained in experimental procedures. For data in **D-I**, *P< 0.05 (insulin), ^ψP< 0.05 (interaction), 2-way ANOVA. All values represented as mean \pm SEM, n= 5-8.

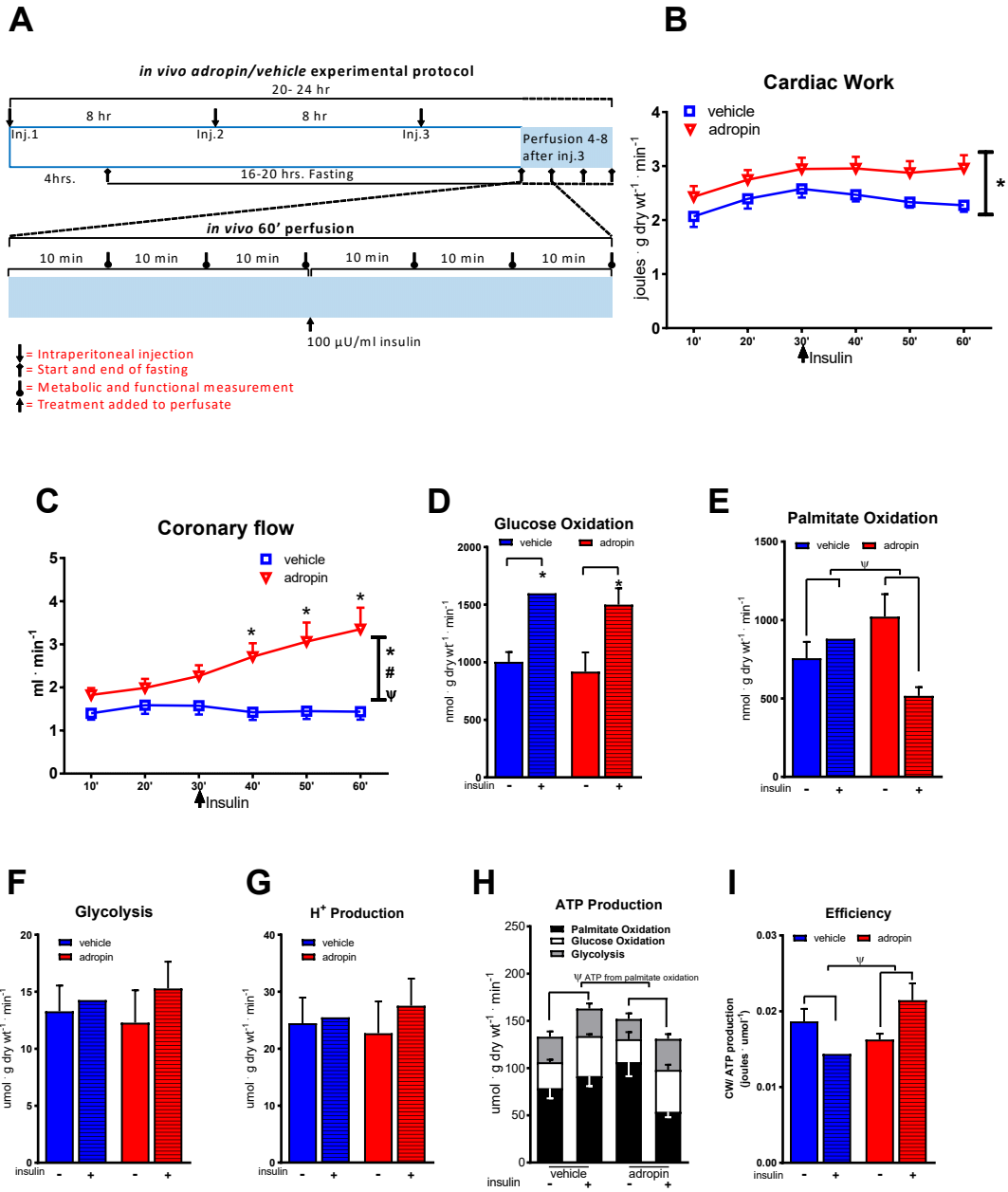


Figure 6.1

Figure 6.2. Protein levels of key components of cardiac energy metabolism are not changed after three *in vivo* adropin injections (A) Western blots of key enzymes involved glucose and fatty acid oxidation, CD36, CPT I B, PDK4, p-PDH S²⁹³, p-AMPK T¹⁷², and p-ACC 2 S¹²⁰⁰, PPAR α , and PGC-1 α , indicating protein levels or activity. α -tubulin or β -actin was used as a protein loading control of the respective protein. Phosphorylated forms of PDH, AMPK, and ACC2 are normalized for the total protein level of the respective enzyme. (B) Quantification of data presented in (A). Western blot samples were prepared from heart ventricles clamp-frozen at the end of the 60 min isolated heart perfusion of hearts isolated from fasting C57BL/6 mice that were injected three times with intraperitoneal 450 nmol/kg Adropin³⁴⁻⁷⁶ or vehicle over a 20-24 hr period. All values represented as mean \pm SEM, n=5. veh, vehicle; adr, adropin.

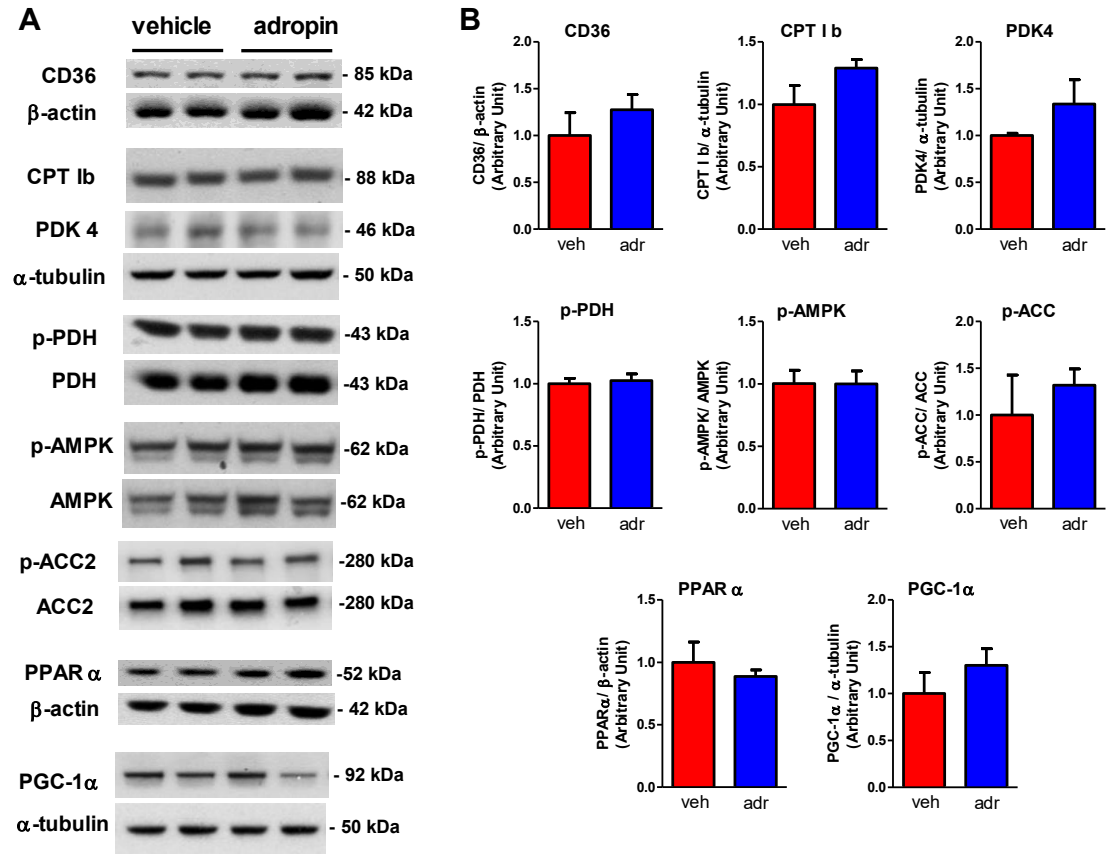


Figure 6.2

Figure 6.3. *Ex vivo* adropin enhances cardiac glucose oxidation and inhibits fatty acid oxidation. (A) A diagram showing the experimental protocol of *ex vivo* adropin/vehicle working hearts perfusions as explained in the methods. Functional and metabolic assessment of working heart perfusions (60 min) of hearts isolated from non-fasting C57BL/6 mice and then perfused with 2nM Adropin³⁴⁻⁷⁶ or vehicle: (B) cardiac work; (C) rate pressure product, (D) glucose oxidation; (E) palmitate oxidation; (F) glycolysis; (G) proton production; (H) contribution of the respective catabolic pathway to ATP production and; (I) cardiac efficiency. Insulin (100 μ U/ml) was present from the beginning of heart perfusions as described in methods. Cardiac functional parameters data were recorded using an MP100 system from AcqKnowledge (BIOPAC Systems, Inc.), to provide data to calculate cardiac work as explained in experimental procedures. For data in **D-I**, * $P < 0.05$ compared to vehicle controls, unpaired t-test. $^{\Psi}P < 0.05$ (interaction), 2-way ANOVA. All values represented as mean \pm SEM, n= 6-14.

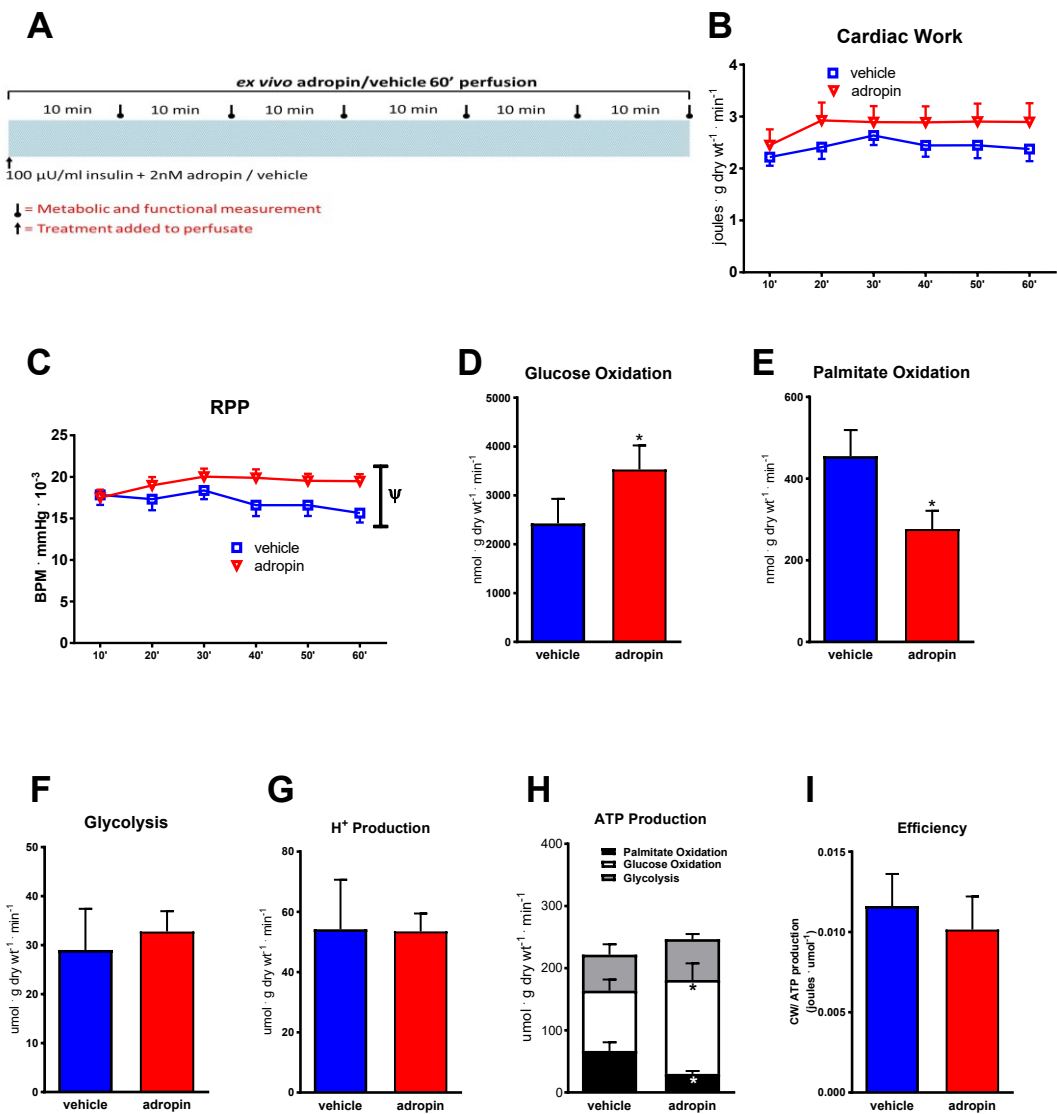


Figure 6.3

Figure 6.4. *In vivo* adropin increases cardiac insulin sensitivity. (A) Western blots showing phosphorylation of key enzymes in the insulin signalling pathway: Akt (p-Akt S473), GSK3 β (p-GSK3 β S9), AS160 (p-AS160 T642), IRS-1 (p- IRS-1 Y628), IRS-1 (p- IRS-1 S307), and JNK (p- JNK T183/Y185) as surrogate markers of their activity. The phosphorylated form of each enzyme is normalized for the total protein level of the respective enzyme. (B) Quantification of data presented in (A). Western blot samples prepared from heart ventricles clamp-frozen at the end of the 60 min isolated heart perfusion of hearts isolated from fasting C57BL/6 mice that were injected three times with intraperitoneal 450 nmol/kg Adropin³⁴⁻⁷⁶ or vehicle over a 20-24 hr period. * $P < 0.05$ versus vehicle control, t-test. All values represented as mean \pm SEM, n=3-5. veh, vehicle; adr, adropin.

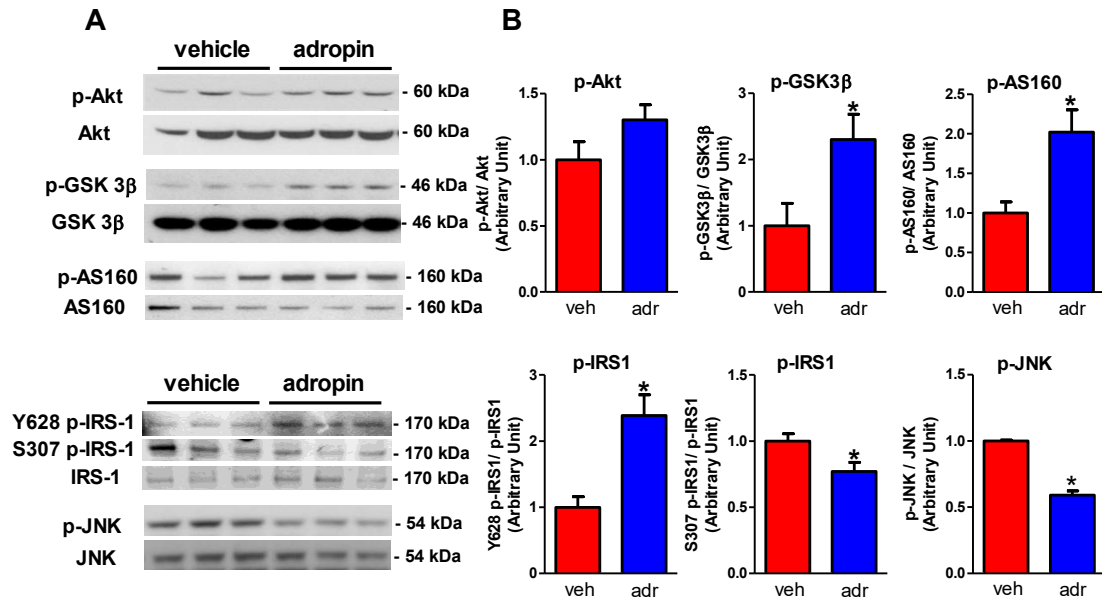


Figure 6.4

Figure 6.5. *Ex vivo* adropin increases cardiac insulin sensitivity. (A) Western blots showing phosphorylation of key enzymes in the insulin signalling pathway: Akt (p-Akt S473), GSK3 β (p-GSK3 β S9), AS160 (p-AS160 T642), IRS-1 (p- IRS-1 Y628), IRS-1 (p- IRS-1 S307), and JNK (p- JNK T183/Y185) as surrogate markers of their activity. The phosphorylated form of each enzyme is normalized for the total protein level of the respective enzyme. (B) Quantification of data presented in (A). WB samples were made from heart ventricles clamp-frozen at the end of the 60 min isolated heart perfusion of hearts isolated from non-fasting C57BL/6 mice and then perfused with 2nM Adropin³⁴⁻⁷⁶ or vehicle. * $P < 0.05$ versus vehicle control, t-test. All values represented as mean \pm SEM, n=4-9. veh, vehicle; adr, adropin.

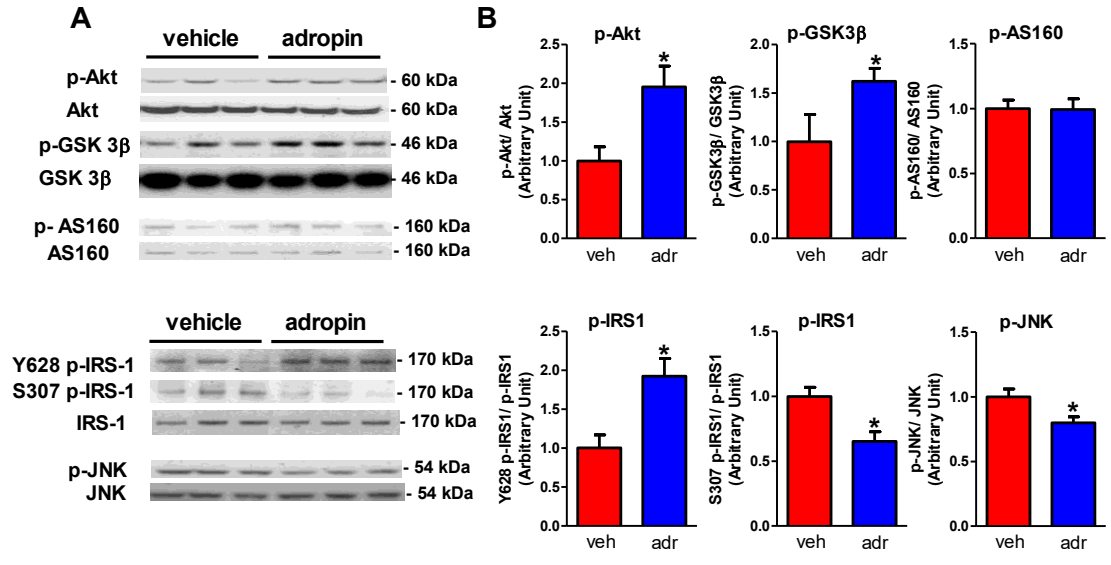


Figure 6.5

Figure 6.6. A diagram of proposed adropin metabolic effects.

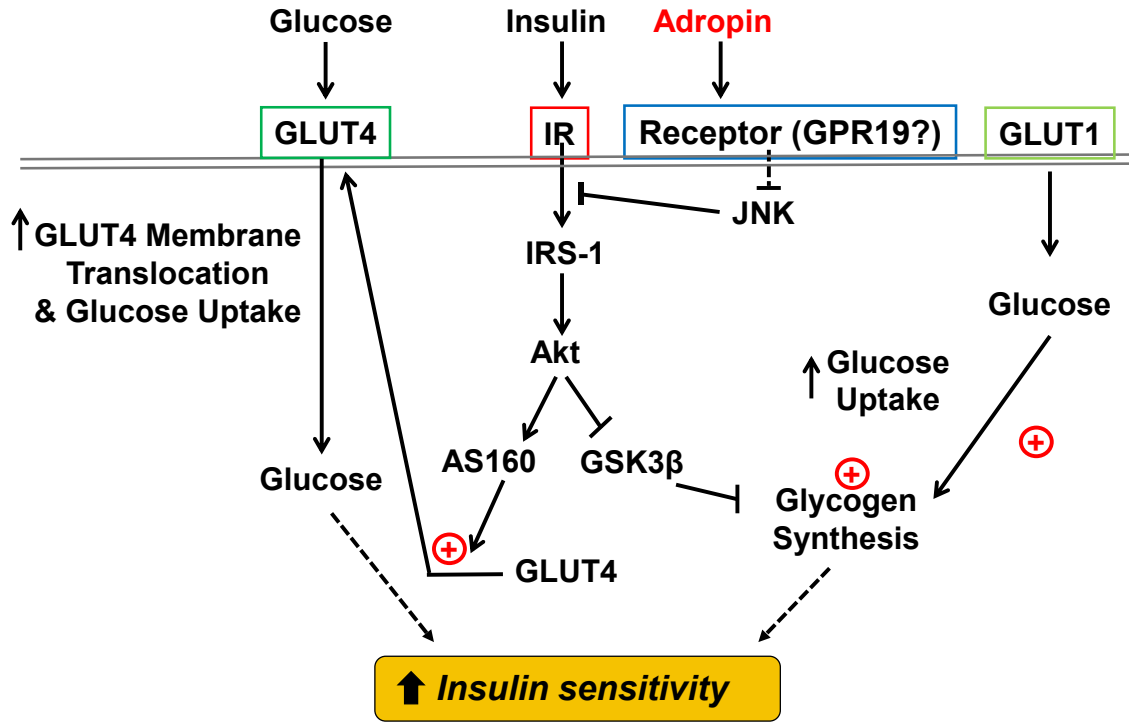


Figure 6.6

CHAPTER 7

Discussion and Conclusions

CHAPTER 7

Discussion and Conclusions

7.1 Summary

The integrated relationship between glucose and fatty acid oxidation in the heart constituted the general scope of this thesis. We examined potential points of regulation that may represent future targets for the modification of cardiac energy metabolism to better match the continuous functional requirements of the contracting heart. Several levels and aspects of control of energy substrate utilization in the heart were explored by our experimental approaches. These included substrate supply, transcriptional, post-translational control, as well as allosteric control of some of key proteins and enzymes actively involved in the regulation of energy substrate preference in the heart. As part of studying some aspects in the transcriptional and allosteric control of cardiac energy metabolism, we invested some efforts to investigate the potential cytosolic localization of an important metabolic enzyme of the carnitine system, namely CrAT, which has been relatively undervalued in research and has been almost exclusively studied in mammals as a mitochondrial or peroxisomal enzyme and thus was shown to play roles in acetyl-CoA/CoA balance in those organelles. We, however, have shown evidence that CrAT is partially localized to the cytosol of cardiac cells, and thus can functionally affect the fate of acetylcarnitine exported out of mitochondria and peroxisomes. Consequently cytosolic CrAT could influence acetyl-CoA and malonyl-CoA levels in the cytosol, which eventually lead to allosteric control of CPT I-mediated mitochondrial

uptake and oxidation of long-chain fatty acyl-CoAs. In the studies described in Chapter 3 we drew a relationship between CrAT protein levels and activity and acetyl-CoA and malonyl-CoA cellular biology in two animal models of genetic and nutritional perturbation of cardiac energy metabolism. Accordingly, CrAT may represent a potentially target for future therapeutic modification of energy metabolism in cardiac disease.

Still in the context of transcriptional control, we explored the effects of a recently recognized liver-secreted factor, adropin, on protein levels of several cellular metabolic components. This was based on a previously proposed mechanism for adropin in the regulation of skeletal muscle energy metabolism. However, based on our findings we discovered that in the heart this proposed mechanism is not likely to be the way adropin produces its metabolic effects, at least within the short-term 24 hr-treatment period we utilized. Alternatively, we provide evidence for a mechanism of action of adropin in the post-translational control of cardiac metabolism by means of an unknown mediator that result in phosphorylation of protein components in the insulin signaling pathway and therefore enhancement of insulin-stimulated glucose metabolism and insulin-inhibited fatty acid oxidation. Accordingly, adropin may be an attractive approach to modulate cardiac metabolism, especially when insulin resistance is present.

The post-translational control was also well articulated in the metabolic changes occurring as a result of myocardial MCU deficiency and impaired mitochondrial Ca^{2+} homeostasis. We have characterized decreased NAD^+ cellular levels and the resulting lysine hyperacetylation of MCD as major determinants of malonyl-CoA levels producing the metabolic profile in MCU deficient hearts under isoproterenol stress. In

our attempt to explore energy substrate supply to cardiomyocytes as one level of the regulation of myocardial metabolism and based on available literature that impaired autophagy in the endothelium impairs its lipid handling, we hypothesized that coronary endothelial trans-cellular trafficking of fatty acids to neighboring cardiomyocytes will be affected by impairment of endothelial autophagy. The mechanism by which fatty acids, particularly the long-chain molecules that are not small enough to travel through inter-endothelial cell junctions, has been a matter of debate for decades. Interestingly, we found a considerable effect of ATG7 ablation, an essential component in the formation of autophagosomes, in the endothelium of mouse hearts on cardiac fatty acid storage and oxidation rates. This suggests a role of this biological process in endothelial cells in their cross-transport of lipids to cardiomyocytes. In almost all of these aforementioned projects, insulin constituted a significant contributor to energy substrate preference in collaboration with the specific intervention we provided. Cardiac insulin resistance is one of the metabolic aberrations accompanying several heart diseases and it is generally believed that improving cardiac insulin sensitivity can improve cardiac function in such hearts.

Overall, this research provides novel findings regarding the tight connection between energy metabolism in the heart and its function as well as the dynamic relationship between the two major energy substrates, fatty acids and glucose, in cardiac energy homeostasis. Such information may provide insights into how energy metabolism can be regulated at different levels and through modifying the activity of several endogenous components. Such ‘tuning’ points can be targeted by researchers and clinicians to optimize cardiac energy homeostasis in health and disease. The remaining

of this chapter will discuss our findings in more detail as well as some associated limitations and potential future directions for this research.

7.2 Roles of carnitine acetyltransferase in malonyl-CoA control of myocardial fatty acid oxidation

The ACC reaction in the heart is essential to the malonyl-CoA axis due to the low levels of the substrate acetyl-CoA in the cytosol, as well as the tight regulation of ACC by kinases such as AMPK and hormones such as insulin (238-241). Changes in mitochondrial acetyl-CoA levels are an important mechanism by which cardiac fatty acid oxidation and glucose oxidation are controlled in the heart. Mitochondrial CrAT has an important role in “buffering” this acetyl-CoA, by transferring the acetyl- groups from acetyl-CoA to acetylcarnitine (80,86). Acetylcarnitine is then shuttled out of the mitochondria through the carnitine/acylcarnitine translocase (16). However, what happens to acetylcarnitine in the cytosol has not been previously determined. In our study presented in Chapter 3, we provide evidence that a cytosolic CrAT functioning in the reverse direction converts acetylcarnitine back to acetyl-CoA. We show in whole hearts and in isolated H9c2 cells that a significant reverse CrAT activity exists, and that this activity is present in the cytosol. We propose that the cytoplasmic acetyl-CoA produced by the reverse CrAT activity can then be used for malonyl-CoA synthesis, thereby regulating mitochondrial fatty acid uptake and oxidation. In the heart, a very large concentration difference exists between cytosolic and mitochondrial CoA content. Around 95% of CoA pool (including acetyl-CoA) is in the mitochondria (in the mM

range) compared to cytosolic CoA (including acetyl-CoA) (low μM range) (231). This has a particular significance as the cytosolic enzyme ACC2 displays a K_m for acetyl-CoA of 117 μM (29), which is much higher than the total cytosolic CoA concentration. Consequently, ACC2 is not saturated with its acetyl-CoA substrate, and slight changes in cytosolic acetyl-CoA should affect its activity to produce malonyl-CoA and thus inhibit mitochondrial fatty acid uptake and oxidation. Moreover, heart CPT I is extremely sensitive to malonyl-CoA inhibition. The IC_{50} of CPT I for malonyl-CoA is $\approx 100\text{nM}$ (29,78). Therefore, small changes in cytosolic acetyl-CoA concentration could theoretically lead to a strong inhibition of CPT I and fatty acid oxidation (29).

We showed that compared to the liver the heart has >2.5 fold higher cytosolic RCrAT activity. This is consistent with a putative role of CrAT in the production of cytosolic acetyl-CoA in the heart and has a special implications, as the heart is not a lipogenic organ and a higher acetyl-CoA producing capacity would most likely be directed towards increased malonyl-CoA production for fatty acid oxidation control. ATP-citrate lyase is another potential source of acetyl-CoA, and has previously been suggested to generate cytosolic acetyl-CoA in muscle cells (77). While ATP-citrate lyase remains as a strong candidate for the regeneration of cytosolic acetyl-CoA, our data suggest that reverse cytosolic CrAT and acetylcarnitine is an alternative and perhaps a complementary source of acetyl-CoA.

In humans, both mitochondrial and peroxisomal CrAT are encoded by the same gene, with alternative splicing resulting in different variants targeted to either subcellular organelle (74). CrAT isoenzyme localization is governed by the presence of an N-terminal mitochondria signal sequence in the larger variant (626 amino acids) or the

influence of the C-terminal peroxisomal signal sequence (AKL) in the shorter isoenzyme (605 amino acids) which lacks the mitochondrial signal sequence (74,75). The mitochondrial signal seems to dominate and prevent peroxisomal localization, which implies that the peroxisomal signal is weaker than the mitochondrial signal and may not be totally efficient, thus leaving some “peroxisomal” CrAT behind in the cytosol. However, under our experimental conditions, we could not confirm this theory.

In hearts of mice with a cardiac specific ACC2KO and in mice fed a HFD, we observed a CrAT protein levels that displayed a pattern related to the measured acetyl-CoA/CoA ratio values and metabolic profiles. CrAT expression is under transcriptional control of the transcriptional factor PPAR α as well as L-carnitine itself (290). This is in agreement with the fact that in HFD hearts, which showed higher CrAT protein levels, there is a higher content of fatty acids in the diet that is normally transported to cardiomyocytes and functions as activators of PPAR α to induce transcription of its target genes (1). In ACC2KO mouse hearts, however, CrAT content was reduced. Similarly, type 2 diabetes patients display reduced CrAT protein and malonyl-CoA levels (79). Whether the resemblance between the two metabolic conditions in ACC2KO and diabetes in terms of increased reliance on fatty acid oxidation and decreased production of malonyl-CoA, is relevant in such comparison is a possibility. Of note, in our post- *ex vivo* perfused hearts, malonyl-CoA levels were not different in ACC2KO than their WT controls. In fact, it is intriguing that ACC2KO hearts show a normal level of malonyl-CoA. However, this was previously shown in the same animal model in skeletal muscles (16), and may indicate some compensatory mechanism counteracting the deletion of ACC2, the major ACC isoform in the heart. Whether this malonyl-CoA

production is mediated by ACC1 is not clear, but is still a possibility (29,243). The two isoforms are encoded by two separate genes, with ACC2 having capacity to bind to the outer mitochondrial membrane and most likely provide a pool of malonyl-CoA directed toward CPT I inhibition and fatty acid oxidation regulation. This contrasts ACC1 that is located in the cytosol and is mostly involved in the synthesis of fatty acids (243,244). Consequently, accepting the value of total tissue content of malonyl-CoA as a predictor of malonyl-CoA inhibition of CPT I and fatty acid β -oxidation rates is questionable. Additionally in both models investigated here, measurements of malonyl-CoA levels were performed in insulin-treated hearts. Insulin is known to up-regulate ACC activity through inhibiting its phosphorylation by AMPK and cause an acute increase in malonyl-CoA levels (26,247). Therefore, theoretically, insulin may have turned all the ACC “on” producing “maximum” levels of malonyl-CoA and hence the insignificant differences.

7.3 Mitochondrial calcium uptake and the oxidative metabolism

Mitochondrial Ca^{2+} currents have been proposed to play important regulatory roles in oxidative energy metabolism, particularly following adrenergic stimulation. This occurs by increasing the activity of mitochondrial TCA cycle dehydrogenases and PDH (secondary to activation of PDH phosphatase) (104,105). As Ca^{2+} crosses the inner mitochondrial membrane primarily through the MCU channel (98), a deficiency in myocardial MCU is expected to compromise energy production and contractile function. However, we demonstrate in our study presented in Chapter 4 that MCU deficiency in murine hearts does not lead to compromised energetics or contractility.

The cardiac-specific MCU deficient mice showed an unexpectedly higher than normal cardiac work, even after the induction of adrenergic (isoproterenol, ISO) stress. This increased work was probably the result of a compensatory increase in energy production originating from fatty acid β -oxidation. Interestingly, the contribution of glucose oxidation to energy production was also not compromised in MCU deficient hearts. This lack of inhibition of overall TCA cycle activity including glucose oxidation suggested that impaired mitochondrial Ca^{2+} uptake in these hearts, which was previously confirmed by our collaborators in cardiomyocytes from these animals (109), is not leading to an impairment of either the TCA cycle dehydrogenases or PDH activity.

The unexpected preserved cardiac function in MCU deficient hearts even after adrenergic stimulation appears to agree with a previous study using a MCU activity inhibitor (112). Another recent study showed in whole body MCU knock-out mice that although cardiomyocyte mitochondrial matrix Ca^{2+} levels were reduced, normal levels of cardiac function, ATP, and respiratory control ratio under basal conditions were seen, in addition to normal responses to ISO stress and transverse aortic constriction (114). Other studies using myocardial MCU inhibition by transgenic expression of a dominant-negative MCU or cardiac deletion also showed normal resting heart rates despite incapability of the animals of physiological “fight or flight” heart rate acceleration (109,111). Conversely, in another study using *ex vivo* perfused mouse hearts, both Ru360 and spermine (an inhibitor and stimulator of MCU, respectively) induced negative and positive inotropic effects, respectively with antagonistic effects (113). Additionally, inotropic stimulation with ISO increased mitochondrial Ca^{2+}

content, elevated oxygen consumption, and increased Ca^{2+} -dependent activation of PDH. These effects were abolished by Ru360, suggesting an uncoupling between the workload and ATP production upon MCU inhibition (113). Noteworthy, is that these studies did not utilize physiologically relevant concentrations of fatty acids, which would not allow for a compensatory increase in fatty acid β -oxidation, such as we observed in our research.

The insulin-stimulated increases in glucose oxidation in our MCU deficient hearts are particularly interesting. A recent study suggested a correlation between reduced levels of MCU and insulin resistance in type-1 diabetic mice and in mouse neonatal cardiomyocytes cultured under hyperglycemic conditions (108). In those cells, reduced MCU levels correlated with decreased glucose oxidation associated with higher phosphorylation and lower activity of PDH. This altered phosphorylation of PDH was not reproduced in our study perhaps as a result of the obscuring effect of ISO stimulation that may have boosted PDH phosphorylation. Here again, however, MCU deficiency models have shown mixed results regarding PDH phosphorylation/activity (109,110). The comparable-to-control glucose oxidation rates we observed in MCU deficient hearts after ISO administration may have resulted from the maximized energy demands under such increased workload. On the other hand, the increase in fatty acid β -oxidation seen in MCU deficient hearts was likely due, at least in part, to a decrease in malonyl-CoA levels, which would increase mitochondrial fatty acid uptake. Our data suggests that this decrease in malonyl-CoA levels was not due to a reduction in ACC activity, but rather due to an increase in malonyl-CoA degradation. MCD acetylation was increased in the MCU deficient hearts, which is associated with stimulation of its

malonyl-CoA degradation activity (160). In addition, an increased acetylation of the fatty acid oxidation enzyme, β -HAD occurred, which is correlated with enhanced activity of fatty acid oxidation (154,175). Therefore, alterations in acetylation of these enzymes may explain, at least in part, the increase in fatty acid β -oxidation we observed in MCU deficient hearts. We propose that the drop in NAD^+ levels seen in the MCU deficient hearts decreases SIRT3 activity (which deacetylates β -HAD) and decreases SIRT4 (which deacetylates MCD), leading to an increase in β -HAD activity and a decrease in malonyl-CoA levels. Combined, this resulted in activation in fatty acid oxidation in the MCU deficient hearts.

7.4 Microvascular and endothelial energy substrate supply to the myocardium

One important step in regulating myocardial, and consequently total heart, energy metabolism is the circulatory supply and delivery of energy substrates to cardiomyocytes (291). A recent study on coronary arteriole occlusion using microspheres underlined the importance of microvascular substrate delivery to the heart, by showing a 50% decline in palmitate oxidation rates in isolated rat hearts upon microsphere infusion that was accompanied by a 70% attenuation of cardiac performance (292). The diabetic myocardium, for instance, can be particularly vulnerable to oxygen deprivation and energy substrate availability. The disrupted micro- and macro-vascular circulation occurring in the diabetic heart, including thicker capillary basement membranes, decreased capillary density and endothelial dysfunction,

can limit oxygen and energy substrate availability to the myocardium that is already metabolically inflexible (292-294).

Although endogenous TAG stores contribute to fatty acid supply for β -oxidation and ATP production, exogenous fatty acids are the major source for cardiac fatty acid β -oxidation and the source of endogenous TAG stores, considering the fact that the heart is not a lipogenic organ (1,291). Exogenous fatty acids are delivered to the myocardium either as circulating free fatty acids bound to albumin or packed into the TAG constituent of chylomicrons or very-low-density lipoproteins (VLDL) (291,295). Circulating levels of fatty acids directly affect the rates of their uptake and oxidation in the heart, as well as their storage as endogenous TAG (which can serve as a source of fatty acids for β -oxidation) (1,291). The majority of circulating fatty acids are in the form of TAG in lipoprotein, which requires their hydrolysis into simpler free fatty acids before their uptake into the cardiomyocyte. This occurs by means of lipoprotein lipase (LPL), which is synthesized in cardiomyocytes as an inactive monomeric proenzyme before being transferred to the luminal surface of capillary endothelial cells (ECs) (1,296,297). However, what occurs at the level of trans-endothelial transport of fatty acids remains poorly understood. Our findings presented in Chapter 5 suggest a role for an important known component of autophagy in ECs, ATG7, in fatty acid transport. This may occur through the role of ATG7 in EC autophagic flux in the control of fatty acid delivery to myocardial cells. However, whether ATG7 is involved in some other actions that eventually affect endothelial fatty acid uptake or transport to underlying cells is still a possibility that we could not determine. Regardless, upon deletion of ATG7 in ECs, isolated mouse hearts displayed reduced reliance on palmitate β -

oxidation as an energy source during both insulin stimulation and following induction of ischemia. This was accompanied by decreased TAG content in EC-ATG7^{-/-} mouse hearts. In addition, there was a decline in EC fatty acid binding proteins (FABP 4 and FABP 5) mRNA expression in cultured ECs that were transfected with siRNA against ATG7 as compare to control siRNA.

ECs dynamically form and degrade lipid droplets with corresponding changes in enzymes and proteins involved in TAG synthesis and degradation in response to changes of free fatty acid and TAG levels in the blood (121). This indicates active lipid metabolism in ECs that not only maintains a buffering mechanism of excess fatty acids in the blood and lipid homeostasis inside the EC, but also suggests a key role of ECs in trans-cellular transport of fatty acids from the circulation to adjacent cells such as cardiomyocytes. Although only 30% of the cells of the heart are cardiomyocytes (with 70% being are other cell types including endothelial cells (ECs), fibroblasts, smooth muscle cells, and immune cells (298)), the vast majority of volume and contractile function is attributed to cardiomyocytes (1). Hence, by far the largest energy demand and production in the heart is ascribed to these cells. On the other hand, mitochondrial content of ECs is relatively low and these cells rely heavily on glycolysis for energy production (261). Therefore, the contribution of ECs in coronary vasculature to cardiac energy metabolism, particularly fatty acid β -oxidation and even glucose oxidation is minimal and mostly limited to the delivery of such substrates, among others, to cardiomyocytes. As such, the metabolic rates measured in our isolated hearts largely represent cardiomyocyte utilization of substrates delivered by coronary endothelium.

Autophagic flux is regulated by numerous components in and out of the cell at several steps, ultimately resulting in fine-tuning of this flux to promote cellular survival by carefully adjusting the degree of proteins and organelle disposal (253,254). Dysregulation of cellular autophagy may induce a wide list of diseases including vascular aging, angiogenesis and calcification of the vessel wall (253). A relevant term, lipophagy, refers to the specific degradation of lipids by the autophagic machinery. A recent study discussed a dynamic relationship between lipolysis, autophagy, and mitochondrial fusion existing in mouse embryonic fibroblasts to coordinate the fate of fatty acids, where they are either: i) stored in lipid droplets, ii) transported to mitochondria for oxidation, or iii) transported to autophagosomes for degradation and transport to the surrounding fluid (129). Interruption of the balance seems to cause mishandling of these fatty acids and possible lipotoxicity. In this context, genetic disruption of liver macro autophagy leads to the accumulation of lipid droplets (264). Further, impaired endothelial autophagy markedly increases atherosclerotic burden in a chronic model of lipid excess (ApoE^{-/-} mice) (126). Therefore, endothelial autophagy appears critically important in limiting lipid accumulation within the vessel wall. A recent report from our collaborators on this project demonstrated that intact endothelial autophagy regulates vascular lipid homeostasis (125). After incubating traceable LDL with HUVECs transfected with GFP-LC3, this LDL was detected within GFP-LC3 positive structures whose appearance was consistent with autophagosomes (which was confirmed using gold-immunoblotting electron microscopy) (125). These observations motivated us to examine energy substrate metabolism in EC-ATG7^{-/-} hearts. Our findings suggest impaired endothelial transport of fatty acids to myocardial cells when

autophagy is presumably dysfunctional in ECs. The reduced rates of fatty acid oxidation in EC-ATG7^{-/-} hearts suggest a role of intact endothelial autophagy in cardiac energy metabolism. In ECs, long-chain fatty acids enter into and are handled by cells via transporter proteins including CD36 and fatty acid binding proteins (FABP) (1). FABP 4 and 5 double knock-out mice exhibit perturbed trans-endothelial fatty acid transport with remarkably high glucose uptake in the heart and skeletal muscles particularly during fasting (266). The facts that expression of FABP 4 and 5 was affected by knocking down ATG7 in our ECs and that TAG content in EC-ATG7^{-/-} hearts was decreased, suggest a relationship between ATG7 specifically, or endothelial autophagy in general, and the delivery of fatty acids through FABP 4 and 5 to cardiomyocytes for either storage as neutral lipids (TAG) or catabolism in the mitochondria (i.e. fatty acid oxidation).

7.5 Adropin enhances insulin effects on glucose and fatty acid utilization

Insulin stimulates glucose uptake, glycogen production as well as glucose oxidation (288). The insulin receptor is comprised of 4 subunits: 2 α subunits extending extracellularly and 2 intracellular β subunits (287). Binding of insulin to its binding site at the α subunits elicits autophosphorylation of the β subunits on specific tyrosine residues, inducing a conformational change that enhances the tyrosine kinase activity of the receptor to its downstream adaptor or 'substrate' proteins (287,288). Among these substrates are insulin receptor substrate (IRS) proteins. The phosphorylated tyrosine

residues of IRS represent an interaction points and docking sites for a number of downstream mediator proteins, including phosphatidyl inositol 3 kinase (PI3K) (287). PI3K is a key mediator of insulin effects on glucose uptake and subsequent metabolism. PI3K activity produces phosphatidyl inositol (3,4,5) triphosphate (PIP3) which recruits phosphoinositide dependent kinase 1 (PDK1) to the cytosolic aspect of cell membrane where it can phosphorylate Akt (protein kinase B) which in turn, through phosphorylating and activating AS160 and protein kinase c (PKC) pathways, increases GLUT4 translocation to the cell membrane and thus enhances glucose uptake, as well as affecting other Akt downstream targets such as GSK3 β (287,289). The c-Jun amino-terminal kinase (JNK) inhibitory serine phosphorylation of IRS-1 is known to be responsible for inflammatory-induced insulin resistance, as well as free fatty acid-induced insulin resistance (276,286). Therefore, counteracting this process may enhance insulin signalling and ameliorate insulin resistance. The most direct effect of insulin on fatty acid oxidation is its inhibition of myocardial AMPK activity leading to the increase of malonyl-CoA levels and the resulting inhibition of mitochondrial uptake and oxidation of fatty acids (26,44,299).

While the physiological and biochemical roles of insulin in myocardial cell energy metabolism are well-established, new approaches to stimulate insulin actions are still scarce. In Chapter 5, we have shown that administration of adropin, either by three intraperitoneal injections over 24 hours, or by direct addition to the perfusate of isolated working hearts, elicited alterations in cardiac energy metabolism characterized by enhancement of insulin effects on inhibition of fatty acid oxidation (*in vivo and ex vivo*) as well as stimulation of glucose oxidation (*ex vivo*). The mechanism involved in these

metabolic actions of adropin appears to involve stimulation of insulin signaling and counteracting of JNK inhibitory serine phosphorylation of IRS-1. Although we showed in the heart a similar shift towards glucose oxidation (or at least a decrease in reliance on fatty acids for ATP production) as was shown in previous research in skeletal muscles (192,194), we could not recapitulate the mechanisms proposed to mediate adropin's actions in skeletal muscles. Previously proposed alterations in CD36, CPT I as well as PDK4 and acetylation of PGC-1 α observed in skeletal muscle were not seen in our heart studies. The reason is not clear although it could have resulted from the relatively short period of treatment we used. However, the treatment protocol used in reference (192) was similar to the one adopted by us without reproducing the same 'transcriptional' effects of adropin. It is worth mentioning that skeletal muscles were tested in that study and a possible variable response/mechanism in the cardiac muscle cannot be excluded. The fact that acute addition of adropin to the perfusate of isolated working hearts induced fast and strong responses may suggest existence of an undiscovered plasma-membrane adropin receptor mediating its intracellular actions. GPR19, an orphan G-protein coupled receptor, has been proposed as membrane receptor for adropin in cardiomyocytes (284), while a role of Notch1 signaling has been also suggested (194). Regardless, adropin has shown impressive metabolic effects in our study and deserve further investigation in models of insulin resistance. If successful, adropin or similar synthetic analogues may provide a therapeutic option that promotes insulin sensitivity of the diabetic heart with concomitant improvement of cardiac function.

7.6 Limitations

7.6.1 The isolated working heart

The isolated working heart is an experimental tool that was used heavily in the studies in this thesis to examine cardiac function in parallel with measurements of cardiac energy metabolism. It provides preload and afterload parameters similar to *in vivo* conditions. A global ischemia/reperfusion (I/R) protocol can also be introduced. The perfusate content of energy substrates, addition of treatments, as well as durations can be adjusted as needed to simulate as much as possible physiological or pathological conditions required for the specific study. However, an inherent limitation of this method is that the *ex vivo* hearts are no longer exposed to the conditions they were experiencing *in vivo*. This may be reflected on metabolic rate measurements as not accurately representing *in vivo* metabolic rates. Related to limitations of this system is that in Chapter 5 (EC-ATG7^{-/-} perfusions) due to technical difficulties, we could not readily change fatty acid concentration during perfusion experiments and may have missed the detection of a role of the ATG7^{-/-} endothelium in ‘buffering’ surges of circulating fatty acids as occurs in some physiological/pathological situations. However, this ‘*ex vivo*’ medium can also represent a strength for this technique, as it allows chronic changes in cardiac metabolism to be evaluated in isolation from extra-cardiac physiological/pathological factors. Moreover, it can provide valuable data on direct effects of an acute treatment on cardiac metabolism and function, as what we achieved with *ex vivo* adropin perfusions (Chapter 6). The parameters of *ex vivo* cardiac function, although revealing, are not the same as usually investigated functional parameter for *in situ* hearts, such as in echocardiography. Additionally, only two-substrate metabolic

rates can be assessed during a perfusion experiment, corresponding to the two radioisotopes used (^3H and ^{14}C). Therefore, I used two sets of animals to measure each of the two perfusion protocols in Chapter 6 to yield the desired three metabolic rates: glucose oxidation, glycolysis, and palmitate oxidation. As energy metabolism is directly related to cardiac work, the simultaneous assessment of metabolic rates and cardiac work represent an advantage of this system over some of other more often utilized techniques for energy metabolism measurement such as whole muscle cell homogenates or mitochondrial preparations which suffer serious technical issues regarding disrupted biological membranes, inaccurate metabolite concentrations, and absence of actual workloads.

7.6.2 *In vitro* enzyme activity assays and subcellular fractionation

Our enzymatic activity assays used in Chapter 3 provided different milieu compared to what actually exists at *in vivo* cellular/tissue levels. These include product inhibition, allosteric inhibition/activation, co-factors concentrations, activity of carnitine/acylcarnitine at sarcolemmal and mitochondrial (and possibly on other organelle) membranes, and the use of carnitine and its acyl esters by other reactions. The provision of inhibitory products or any other *in vivo* factors, in isolation or in combinations, in the assay medium is extremely difficult to apply if not impossible. In that sense, such *in vivo* determinants of enzyme activities can never be perfectly represented in *in vitro* assays. Nonetheless, the assays we used utilized buffers offering optimal pH, solubility and unlimited substrates and cofactors, and assessed the activity at linear steady-state velocity that produces considerable concentrations of products in the process thus at least partly simulate *in vivo* conditions.

High mitochondrial breakage constituted a technical disadvantage of Polytron homogenization in the study presented in Chapter 3. Therefore, we adopted different cell permeabilization techniques in the experiments subsequent to Polytron homogenization to increase specificity. Indeed, mitochondrial breakage was lower in Potter-Elvehjem homogenized cardiac tissue and H9c2 cells and further reduced with the milder digitonin permeabilization. The use of CS enzyme as a marker of mitochondrial breakage may have represented a strength to our subcellular fractionation method. Both CrAT and CS associate with the inner mitochondrial membrane with higher ability of CrAT compared to CS which shows limited saturability (236,237). Accordingly, there is a higher probability that a smaller proportion of mitochondrial CrAT than that of CS is released from broken mitochondria during homogenization and centrifugation. Therefore, the calculated (corrected) cytosolic CrAT may have actually been an underestimate of the actual value or that at least the estimation is safely valid.

7.6.3 Representation of cardiomyocyte energy metabolism by H9c2 cells

H9c2 cells are proliferative myoblasts derived from embryonic rat heart ventricle that show a more glycolytic metabolic phenotype compared with primary adult cardiomyocytes (227,228). After differentiation, energy metabolism in these cells becomes relatively more reliant on oxidative mitochondrial metabolism (228). The relatively higher mitochondrial activities of CrAT and CS in differentiated cells, compared to undifferentiated cells (Chapter 3) are consistent with mitochondrial maturity and biogenesis occurring with H9c2 differentiation. However, this is not complete and still not as oxidative as primary cardiomyocytes. Nonetheless, the

availability and feasibility of culturing this proliferative cardiac cell line as well as their metabolic maturity upon differentiation have served our research purposes.

7.6.4 The mouse model, strain-specific differences and genotype characterization

In this thesis we studied energy metabolism in the mouse heart, which when compared to the rat heart is less representative of the metabolic profile of the human heart (21). However, in addition to the availability of genetic manipulation in the mouse, which was used to address the research goals of studies in Chapter 3, 4 and 5, the mouse heart offers some metabolic advantages regarding the assessment of the response to insulin. The augmented responses of glucose and fatty acid oxidation, which resembles the significant responses in humans, allow easier assessment of differences in the effect of insulin on cardiac energy metabolism (300,301). However, using different mouse strains as in Chapter 3 (FVB background for ACC2KO vs. C57BL/6 for HFD mice) may have affected the values measured for metabolic rates as well as malonyl-CoA levels. Differences in metabolic rate are expected among mouse strains (302). These could also possibly exist among genotypes across the three research projects in Chapters 3 to 5 (ACC2KO vs. MCU^{fl/fl-MCM} vs. EC-ATG7^{-/-}). Another limitation of our studies in Chapter 4 (MCU^{fl/fl-MCM}) and Chapter 5 (EC-ATG7^{-/-}) is that within our available techniques, we could not confirm the genotype characterization such as mitochondrial Ca²⁺ currents and impairment of endothelial autophagy, and therefore relied on our collaborators' recent reports which characterized the same models we obtained from them to perform our research.

7.7 Final conclusions

The research in this thesis provides important information regarding the regulation of cardiac energy substrate metabolism at several molecular levels. The research highlights checkpoints in the control of cardiac energy metabolism that can be utilized in the future for the treatment of heart disease. These novel findings suggest that the relationship between glucose and fatty acid oxidation is more complex than we have previously thought. We have found that carnitine acetyltransferase, an important member of the carnitine acyltransferase family, has a small activity in the cytosol of cardiomyocytes that may complete the picture of its already known roles in mitochondrial acetyl-CoA buffering, to be extended to a role in cytosolic acetyl-CoA dynamics. We believe that this could add another integrative part of the Randle cycle inter-relationship between glucose and fatty acid metabolism through linking mitochondrial acetyl-CoA to cytosolic malonyl-CoA control of fatty acid oxidation. We have also been able to show that the proposed concept of mitochondrial Ca^{2+} control of mitochondrial energy production may not be as direct and essential as previously thought. This adds up to our understanding of mitochondrial energy mechanics and therefore underlines the need for continuing research in this field.

We also focused on understanding the control of myocardial energy metabolism by adjacent (coronary endothelium) as well as remote (liver-secreted adiponin) tissue types. We provided novel findings regarding a role of a constitutive biological process in endothelial cells, autophagosome formation, in lipid transport across the endothelial layer. To our knowledge, this is the first research to demonstrate this novel observation linking endothelial autophagy to cardiac energy metabolism. Our data suggest that

targeting vascular physiology, particularly endothelial autophagy, may offer a new approach to normalizing deranged myocardial mitochondrial bioenergetics. The metabolic communication between the liver and the heart in modulating cardiac energy metabolism by adropin is interesting. Adropin and possibly synthetic analogues may provide a promising therapeutic option to improve cardiac insulin sensitivity when insulin resistance is a concern. We speculate that stimulating glucose oxidation through modulating any of the investigated molecular mechanisms may improve cardiac function.

7.8 Future directions

The data presented in this thesis raises the potential for considerable amount of future research. Of importance, more research is required to unequivocally prove cytosolic CrAT localization through, for example, advanced genetic modification of CrAT mRNA to hold traceable markers that can be visually detected within the cytosol while taking into consideration the size of such tags which can confound the results. It remains to be determined if the cytosolic CrAT is directly providing the acetyl-CoA molecules that is used by ACC to produce malonyl-CoA and what can be used as direct inhibitors or activators of CrAT transcription or activity, as well as the metabolic consequences of such interventions.

Of clinical relevance, it is important to examine if our findings on the effects of chronic and acute adropin administration on glucose and fatty acid oxidation in the normal heart can be extended to hearts with insulin resistance such as in *db/db* or diet induced

obesity models. Another important area that requires further investigation is whether adropin is a ligand of a specific undiscovered cell membrane receptor, or if it binds to an already known receptor of possibly similar ligands. We reported in this thesis that acute exposure of the hearts produced significant changes in energy substrate preference. Together with the fact that adropin is a polypeptide that most probably will not easily enter the cell, these findings point to possible receptor-mediated actions of this humoral factor.

It will also help to determine how the cardiac-specific inducible knockdown of MCU enhances cardiac function even in the absence of an ISO challenge. It has been reported that MCU is essential in the acute requirement of energy such as fight or flight situations stimulation (109). However, this is not consistent with our results and therefore the findings presented in this thesis will need to be reproduced *in vivo* and compared to other models of transgenic MCU expression/ deficiency. Currently, there is confusion as to the metabolic and functional consequences of modifying MCU expression/function and future research may provide a clearer image and information on whether this can have direct clinical relevance.

In accordance with trans-endothelial lipid trafficking through autophagic flux, previous studies have provided evidence that in primary EC, LDL stimulates autophagosome formation (125). Research is needed to characterize the link between extracellular LDL, or possibly free fatty acids, and the incorporation into autophagic structures. Despite the fact that in the research presented fatty acid oxidation was not largely decreased by EC-ATG7 deletion under basal conditions, insulin addition elicited significant enhancement of glucose oxidation in such hearts. Therefore, it would be of value to explore the

possible link between insulin and endothelial autophagy in the context of cardiac energy metabolism. In addition, it will also be interesting to test whether strategies for modulating endothelial autophagy have undesirable systemic effects. Another area that will be important to further investigate is what other potential mechanisms govern the endothelial cross transport of fatty acid and glucose to the underlining cardiomyocytes and whether these can be exploited to improve myocardial viability in response to I/R injury.

References

1. Lopaschuk, G. D., Ussher, J. R., Folmes, C. D., Jaswal, J. S., and Stanley, W. C. (2010) Myocardial fatty acid metabolism in health and disease. *Physiological reviews* **90**, 207-258
2. Jaswal, J. S., Keung, W., Wang, W., Ussher, J. R., and Lopaschuk, G. D. (2011) Targeting fatty acid and carbohydrate oxidation—a novel therapeutic intervention in the ischemic and failing heart. *Biochimica et Biophysica Acta (BBA)-Molecular Cell Research* **1813**, 1333-1350
3. How, O.-J., Aasum, E., Kunnathu, S., Severson, D. L., Myhre, E. S., and Larsen, T. S. (2005) Influence of substrate supply on cardiac efficiency, as measured by pressure-volume analysis in ex vivo mouse hearts. *American Journal of Physiology-Heart and Circulatory Physiology* **288**, H2979-H2985
4. Buchanan, J., Mazumder, P. K., Hu, P., Chakrabarti, G., Roberts, M. W., Yun, U. J., Cooksey, R. C., Litwin, S. E., and Abel, E. D. (2005) Reduced cardiac efficiency and altered substrate metabolism precedes the onset of hyperglycemia and contractile dysfunction in two mouse models of insulin resistance and obesity. *Endocrinology* **146**, 5341-5349
5. Liu, Q., Docherty, J. C., Rendell, J. C., Clanachan, A. S., and Lopaschuk, G. D. (2002) High levels of fatty acids delay the recovery of intracellular pH and cardiac efficiency in post-ischemic hearts by inhibiting glucose oxidation. *Journal of the American College of Cardiology* **39**, 718-725

6. Savage, D. B., Petersen, K. F., and Shulman, G. I. (2007) Disordered lipid metabolism and the pathogenesis of insulin resistance. *Physiological reviews* **87**, 507-520
7. Schwenk, R. W., Luiken, J. J., Bonen, A., and Glatz, J. F. (2008) Regulation of sarcolemmal glucose and fatty acid transporters in cardiac disease. *Cardiovascular research* **79**, 249-258
8. Saddik, M., and Lopaschuk, G. (1991) Myocardial triglyceride turnover and contribution to energy substrate utilization in isolated working rat hearts. *Journal of Biological Chemistry* **266**, 8162-8170
9. Murthy, M., and Pande, S. V. (1987) Some differences in the properties of carnitine palmitoyltransferase activities of the mitochondrial outer and inner membranes. *Biochemical Journal* **248**, 727
10. McGarry, J. D., and Brown, N. F. (1997) The mitochondrial carnitine palmitoyltransferase system—from concept to molecular analysis. *The FEBS Journal* **244**, 1-14
11. McGarry, J. D., Mannaerts, G., and Foster, D. W. (1977) A possible role for malonyl-CoA in the regulation of hepatic fatty acid oxidation and ketogenesis. *The Journal of clinical investigation* **60**, 265-270
12. McGarry, J. D., Leatherman, G. F., and Foster, D. W. (1978) Carnitine palmitoyltransferase I. The site of inhibition of hepatic fatty acid oxidation by malonyl-CoA. *Journal of Biological Chemistry* **253**, 4128-4136

13. Paulson, D. J., Ward, K. M., and Shug, A. L. (1984) Malonyl CoA inhibition of carnitine palmityltransferase in rat heart mitochondria. *FEBS letters* **176**, 381-384
14. Dyck, J. R., and Lopaschuk, G. D. (2002) Malonyl CoA control of fatty acid oxidation in the ischemic heart. *Journal of molecular and cellular cardiology* **34**, 1099-1109
15. Schulz, H. (2008) Oxidation of fatty acids in eukaryotes. in *Biochemistry of Lipids, Lipoproteins and Membranes (Fifth Edition)*, Elsevier. pp 131-154
16. Olson, D. P., Pulinilkunnil, T., Cline, G. W., Shulman, G. I., and Lowell, B. B. (2010) Gene knockout of *Acc2* has little effect on body weight, fat mass, or food intake. *Proceedings of the National Academy of Sciences of the United States of America* **107**, 7598-7603
17. McGarry, J. D., Takabayashi, Y., and Foster, D. W. (1978) The role of malonyl-coa in the coordination of fatty acid synthesis and oxidation in isolated rat hepatocytes. *Journal of Biological Chemistry* **253**, 8294-8300
18. McGarry, J. D., Woeltje, K. F., Kuwajima, M., and Foster, D. W. (1989) Regulation of ketogenesis and the renaissance of carnitine palmitoyltransferase. *Diabetes/Metabolism Research and Reviews* **5**, 271-284
19. Saggerson, E. D. (1982) Carnitine acyltransferase activities in rat liver and heart measured with palmitoyl-CoA and octanoyl-CoA. Latency, effects of K⁺, bivalent metal ions and malonyl-CoA. *Biochemical Journal* **202**, 397
20. Abu-Elheiga, L., Almarza-Ortega, D. B., Baldini, A., and Wakil, S. J. (1997) Human acetyl-CoA carboxylase 2 molecular cloning, characterization,

- chromosomal mapping, and evidence for two isoforms. *Journal of Biological Chemistry* **272**, 10669-10677
21. Belke, D. D., Larsen, T. S., Lopaschuk, G. D., and Severson, D. L. (1999) Glucose and fatty acid metabolism in the isolated working mouse heart. *The American journal of physiology* **277**, R1210-1217
 22. Collins-Nakai, R. L., Noseworthy, D., and Lopaschuk, G. D. (1994) Epinephrine increases ATP production in hearts by preferentially increasing glucose metabolism. *American Journal of Physiology-Heart and Circulatory Physiology* **267**, H1862-H1871
 23. Dyck, J. R., Kudo, N., Barr, A. J., Davies, S. P., Hardie, D. G., and Lopaschuk, G. D. (1999) Phosphorylation control of cardiac acetyl-CoA carboxylase by cAMP-dependent protein kinase and 5'-AMP activated protein kinase. *The FEBS Journal* **262**, 184-190
 24. Besikci, A. O., Campbell, F. M., Hopkins, T. A., Dyck, J. R., and Lopaschuk, G. D. (2003) Relative importance of malonyl CoA and carnitine in maturation of fatty acid oxidation in newborn rabbit heart. *American Journal of Physiology-Heart and Circulatory Physiology* **284**, H283-H289
 25. Alam, N., and Saggerson, E. D. (1998) Malonyl-CoA and the regulation of fatty acid oxidation in soleus muscle. *Biochemical Journal* **334**, 233
 26. Gamble, J., and Lopaschuk, G. D. (1997) Insulin inhibition of 5' adenosine monophosphate—activated protein kinase in the heart results in activation of acetyl coenzyme A carboxylase and inhibition of fatty acid oxidation. *Metabolism-Clinical and Experimental* **46**, 1270-1274

27. Lopaschuk, G. D., and Gamble, J. (1994) The 1993 Merck Frosst Award. Acetyl-CoA carboxylase: an important regulator of fatty acid oxidation in the heart. *Canadian journal of physiology and pharmacology* **72**, 1101-1109
28. Lopaschuk, G. D., Witters, L. A., Itoi, T., Barr, R., and Barr, A. (1994) Acetyl-CoA carboxylase involvement in the rapid maturation of fatty acid oxidation in the newborn rabbit heart. *Journal of Biological Chemistry* **269**, 25871-25878
29. Saddik, M., Gamble, J., Witters, L., and Lopaschuk, G. (1993) Acetyl-CoA carboxylase regulation of fatty acid oxidation in the heart. *Journal of Biological Chemistry* **268**, 25836-25845
30. Kurth-Kraczek, E. J., Hirshman, M. F., Goodyear, L. J., and Winder, W. W. (1999) 5'AMP-activated protein kinase activation causes GLUT4 translocation in skeletal muscle. *Diabetes* **48**, 1667-1671
31. Winder, W. (1998) Intramuscular mechanisms regulating fatty acid oxidation during exercise. in *Skeletal Muscle Metabolism in Exercise and Diabetes*, Springer. pp 239-248
32. Winder, W., Wilson, H., Hardie, D., Rasmussen, B., Hutber, C., Call, G., Clayton, R., Conley, L., Yoon, S., and Zhou, B. (1997) Phosphorylation of rat muscle acetyl-CoA carboxylase by AMP-activated protein kinase and protein kinase A. *Journal of applied physiology* **82**, 219-225
33. Dyck, J. R., and Lopaschuk, G. D. (2006) AMPK alterations in cardiac physiology and pathology: enemy or ally? *The Journal of physiology* **574**, 95-112

34. Hardie, D. G. (1989) Regulation of fatty acid synthesis via phosphorylation of acetyl-CoA carboxylase. *Progress in lipid research* **28**, 117-146
35. Hardie, D. G., and Hawley, S. A. (2001) AMP-activated protein kinase: the energy charge hypothesis revisited. *Bioessays* **23**, 1112-1119
36. Hardie, D. G. (2004) AMP-activated protein kinase: the guardian of cardiac energy status. *The Journal of clinical investigation* **114**, 465-468
37. Kudo, N., Barr, A. J., Barr, R. L., Desai, S., and Lopaschuk, G. D. (1995) High rates of fatty acid oxidation during reperfusion of ischemic hearts are associated with a decrease in malonyl-CoA levels due to an increase in 5'-AMP-activated protein kinase inhibition of acetyl-CoA carboxylase. *Journal of Biological Chemistry* **270**, 17513-17520
38. Makinde, A.-O., Kantor, P. F., and Lopaschuk, G. D. (1998) Maturation of fatty acid and carbohydrate metabolism in the newborn heart. in *Molecular and Cellular Effects of Nutrition on Disease Processes*, Springer. pp 49-56
39. Jaswal, J. S., Gandhi, M., Finegan, B. A., Dyck, J. R., and Clanachan, A. S. (2006) Effects of adenosine on myocardial glucose and palmitate metabolism after transient ischemia: role of 5'-AMP-activated protein kinase. *American Journal of Physiology-Heart and Circulatory Physiology* **291**, H1883-H1892
40. Jaswal, J. S., Gandhi, M., Finegan, B. A., Dyck, J. R., and Clanachan, A. S. (2007) Inhibition of p38 MAPK and AMPK restores adenosine-induced cardioprotection in hearts stressed by antecedent ischemia by altering glucose utilization. *American Journal of Physiology-Heart and Circulatory Physiology* **293**, H1107-H1114

41. Russell, R. R., Li, J., Coven, D. L., Pypaert, M., Zechner, C., Palmeri, M., Giordano, F. J., Mu, J., Birnbaum, M. J., and Young, L. H. (2004) AMP-activated protein kinase mediates ischemic glucose uptake and prevents postischemic cardiac dysfunction, apoptosis, and injury. *The Journal of clinical investigation* **114**, 495-503
42. Xi, X., Han, J., and Zhang, J.-Z. (2001) Stimulation of glucose transport by AMP-activated protein kinase via activation of p38 mitogen-activated protein kinase. *Journal of Biological Chemistry* **276**, 41029-41034
43. Yamauchi, T., Kamon, J., Minokoshi, Y. a., Ito, Y., Waki, H., Uchida, S., Yamashita, S., Noda, M., Kita, S., and Ueki, K. (2002) Adiponectin stimulates glucose utilization and fatty-acid oxidation by activating AMP-activated protein kinase. *Nature medicine* **8**, 1288
44. Beauloye, C., Marsin, A.-S., Bertrand, L., Krause, U., Hardie, D. G., Vanoverschelde, J.-L., and Hue, L. (2001) Insulin antagonizes AMP-activated protein kinase activation by ischemia or anoxia in rat hearts, without affecting total adenine nucleotides. *FEBS letters* **505**, 348-352
45. Makinde, A.-O., Gamble, J., and Lopaschuk, G. D. (1997) Upregulation of 5'-AMP-Activated Protein Kinase Is Responsible for the Increase in Myocardial Fatty Acid Oxidation Rates Following Birth in the Newborn Rabbit. *Circulation Research* **80**, 482-489
46. Dyck, J. R., Barr, A. J., Barr, R. L., Kolattukudy, P. E., and Lopaschuk, G. D. (1998) Characterization of cardiac malonyl-CoA decarboxylase and its putative

- role in regulating fatty acid oxidation. *American Journal of Physiology-Heart and Circulatory Physiology* **275**, H2122-H2129
47. Awan, M. M., and Saggerson, E. D. (1993) Malonyl-CoA metabolism in cardiac myocytes and its relevance to the control of fatty acid oxidation. *Biochemical Journal* **295**, 61
48. Goodwin, G. W., Taylor, C. S., and Taegtmeier, H. (1998) Regulation of energy metabolism of the heart during acute increase in heart work. *Journal of Biological Chemistry* **273**, 29530-29539
49. Becker, C., Sevilla, L., Tomàs, E., Palacin, M., Zorzano, A., and Fischer, Y. (2001) The endosomal compartment is an insulin-sensitive recruitment site for GLUT4 and GLUT1 glucose transporters in cardiac myocytes. *Endocrinology* **142**, 5267-5276
50. Postic, C., Leturque, A., Printz, R. L., Maulard, P., Loizeau, M., Granner, D. K., and Girard, J. (1994) Development and regulation of glucose transporter and hexokinase expression in rat. *American Journal of Physiology-Endocrinology And Metabolism* **266**, E548-E559
51. Depre, C., Rider, M. H., and Hue, L. (1998) Mechanisms of control of heart glycolysis. *The FEBS Journal* **258**, 277-290
52. Stanley, W. C., Recchia, F. A., and Lopaschuk, G. D. (2005) Myocardial substrate metabolism in the normal and failing heart. *Physiological reviews* **85**, 1093-1129

53. King, L., and Opie, L. (1998) Glucose and glycogen utilisation in myocardial ischemia—changes in metabolism and consequences for the myocyte. in *Cardiac Metabolism in Health and Disease*, Springer. pp 3-26
54. Panchal, A. R., Comte, B., Huang, H., Kerwin, T., Darvish, A., Rosiers, C. D., Brunengraber, H., and Stanley, W. C. (2000) Partitioning of pyruvate between oxidation and anaplerosis in swine hearts. *American Journal of Physiology-Heart and Circulatory Physiology* **279**, H2390-H2398
55. Stanley, W. C., Lopaschuk, G. D., and McCormack, J. G. (1997) Regulation of energy substrate metabolism in the diabetic heart. *Cardiovascular research* **34**, 25-33
56. Bricker, D. K., Taylor, E. B., Schell, J. C., Orsak, T., Boutron, A., Chen, Y.-C., Cox, J. E., Cardon, C. M., Van Vranken, J. G., and Dephoure, N. (2012) A mitochondrial pyruvate carrier required for pyruvate uptake in yeast, *Drosophila*, and humans. *Science* **337**, 96-100
57. Herzig, S., Raemy, E., Montessuit, S., Veuthey, J.-L., Zamboni, N., Westermann, B., Kunji, E. R., and Martinou, J.-C. (2012) Identification and functional expression of the mitochondrial pyruvate carrier. *Science*, 1218530
58. Randle, P. J. (1986) Fuel selection in animals. Portland Press Limited
59. Sugden, M. C., and Holness, M. J. (2003) Recent advances in mechanisms regulating glucose oxidation at the level of the pyruvate dehydrogenase complex by PDKs. *American Journal of Physiology-Endocrinology And Metabolism* **284**, E855-E862

60. Smolle, M., Prior, A. E., Brown, A. E., Cooper, A., Byron, O., and Lindsay, J. G. (2006) A new level of architectural complexity in the human pyruvate dehydrogenase complex. *Journal of Biological Chemistry* **281**, 19772-19780
61. Holness, M., and Sugden, M. (2003) Regulation of pyruvate dehydrogenase complex activity by reversible phosphorylation. Portland Press Limited
62. Darvey, I. G. (1998) How does the ratio of ATP yield from the complete oxidation of palmitic acid to that of glucose compare with the relative energy contents of fat and carbohydrate? *Biochemistry and Molecular Biology Education* **26**, 22-23
63. Randle, P., Garland, P., Hales, C., and Newsholme, E. (1963) The glucose fatty-acid cycle its role in insulin sensitivity and the metabolic disturbances of diabetes mellitus. *The Lancet* **281**, 785-789
64. Zammit, V. A. (1999) Carnitine acyltransferases: functional significance of subcellular distribution and membrane topology. *Progress in lipid research* **38**, 199-224
65. Vaz, F. M., and Wanders, R. J. (2002) Carnitine biosynthesis in mammals. *Biochemical Journal* **361**, 417
66. Tamai, I., Ohashi, R., Nezu, J.-i., Yabuuchi, H., Oku, A., Shimane, M., Sai, Y., and Tsuji, A. (1998) Molecular and functional identification of sodium ion-dependent, high affinity human carnitine transporter OCTN2. *Journal of Biological Chemistry* **273**, 20378-20382

67. Ramsay, R. R., and Zammit, V. A. (2004) Carnitine acyltransferases and their influence on CoA pools in health and disease. *Molecular aspects of medicine* **25**, 475-493
68. Cordente, A. G., López-Vinas, E., Vázquez, M. I., Gómez-Puertas, P., Asins, G., Serra, D., and Hegardt, F. G. (2006) Mutagenesis of specific amino acids converts carnitine acetyltransferase into carnitine palmitoyltransferase. *Biochemistry* **45**, 6133-6141
69. Jogl, G., and Tong, L. (2003) Crystal structure of carnitine acetyltransferase and implications for the catalytic mechanism and fatty acid transport. *Cell* **112**, 113-122
70. Colucci, W. J., and Gandour, R. D. (1988) Carnitine acetyltransferase: A review of its biology, enzymology, and bioorganic chemistry. *Bioorganic Chemistry* **16**, 307-334
71. Violante, S., IJlst, L., Ruiten, J., Koster, J., van Lenthe, H., Duran, M., de Almeida, I. T., Wanders, R. J., Houten, S. M., and Ventura, F. V. (2013) Substrate specificity of human carnitine acetyltransferase: Implications for fatty acid and branched-chain amino acid metabolism. *Biochimica et Biophysica Acta (BBA)-Molecular Basis of Disease* **1832**, 773-779
72. Hetteema, E. H., and Tabak, H. F. (2000) Transport of fatty acids and metabolites across the peroxisomal membrane. *Biochimica et Biophysica Acta (BBA)-Molecular and Cell Biology of Lipids* **1486**, 18-27

73. Hynes, M. J., Murray, S. L., Andrianopoulos, A., and Davis, M. A. (2011) Role of carnitine acetyltransferases in acetyl coenzyme A metabolism in *Aspergillus nidulans*. *Eukaryotic cell* **10**, 547-555
74. Corti, O., DiDonato, S., and Finocchiaro, G. (1994) Divergent sequences in the 5' region of cDNA suggest alternative splicing as a mechanism for the generation of carnitine acetyltransferases with different subcellular localizations. *Biochemical Journal* **303**, 37
75. Consortium, U. (2012) Update on activities at the Universal Protein Resource (UniProt) in 2013. *Nucleic acids research* **41**, D43-D47
76. Reszko, A. E., Kasumov, T., David, F., Thomas, K. R., Jobbins, K. A., Cheng, J.-F., Lopaschuk, G. D., Dyck, J. R., Diaz, M., and Des Rosiers, C. (2004) Regulation of malonyl-CoA concentration and turnover in the normal heart. *Journal of Biological Chemistry* **279**, 34298-34301
77. Abbas, A. S., Wu, G., and Schulz, H. (1998) Carnitine acetyltransferase is not a cytosolic enzyme in rat heart and therefore cannot function in the energy-linked regulation of cardiac fatty acid oxidation. *Journal of molecular and cellular cardiology* **30**, 1305-1309
78. McGARRY, J. D., Mills, S. E., Long, C., and Foster, D. W. (1983) Observations on the affinity for carnitine, and malonyl-CoA sensitivity, of carnitine palmitoyltransferase I in animal and human tissues. Demonstration of the presence of malonyl-CoA in non-hepatic tissues of the rat. *Biochemical Journal* **214**, 21

79. Muoio, D. M., Noland, R. C., Kovalik, J.-P., Seiler, S. E., Davies, M. N., DeBalsi, K. L., Ilkayeva, O. R., Stevens, R. D., Kheterpal, I., and Zhang, J. (2012) Muscle-specific deletion of carnitine acetyltransferase compromises glucose tolerance and metabolic flexibility. *Cell metabolism* **15**, 764-777
80. Schroeder, M. A., Atherton, H. J., Dodd, M. S., Lee, P., Cochlin, L. E., Radda, G. K., Clarke, K., and Tyler, D. J. (2012) The Cycling of Acetyl-Coenzyme A Through Acetylcarnitine Buffers Cardiac Substrate SupplyClinical Perspective: A Hyperpolarized ¹³C Magnetic Resonance Study. *Circulation: Cardiovascular Imaging* **5**, 201-209
81. Koves, T. R., Ussher, J. R., Noland, R. C., Slentz, D., Mosedale, M., Ilkayeva, O., Bain, J., Stevens, R., Dyck, J. R., and Newgard, C. B. (2008) Mitochondrial overload and incomplete fatty acid oxidation contribute to skeletal muscle insulin resistance. *Cell metabolism* **7**, 45-56
82. Pearson, D., and Tubbs, P. (1967) Carnitine and derivatives in rat tissues. *Biochemical Journal* **105**, 953
83. Lysiak, W., Lilly, K., DiLisa, F., Toth, P., and Bieber, L. (1988) Quantitation of the effect of L-carnitine on the levels of acid-soluble short-chain acyl-CoA and CoASH in rat heart and liver mitochondria. *Journal of Biological Chemistry* **263**, 1151-1156
84. Broderick, T., Quinney, H., and Lopaschuk, G. (1992) Carnitine stimulation of glucose oxidation in the fatty acid perfused isolated working rat heart. *Journal of Biological Chemistry* **267**, 3758-3763

85. Broderick, T. L., Quinney, H. A., Barker, C. C., and Lopaschuk, G. D. (1993) Beneficial effect of carnitine on mechanical recovery of rat hearts reperfused after a transient period of global ischemia is accompanied by a stimulation of glucose oxidation. *Circulation* **87**, 972-981
86. Broderick, T. L., Panagakis, G., DiDomenico, D., Gamble, J., Lopaschuk, G. D., Shug, A. L., and Paulson, D. J. (1995) L-carnitine improvement of cardiac function is associated with a stimulation in glucose but not fatty acid metabolism in carnitine-deficient hearts. *Cardiovascular research* **30**, 815-820
87. Broderick, T. L., Quinney, H. A., and Lopaschuk, G. D. (1995) L-carnitine increases glucose metabolism and mechanical function following ischaemia in diabetic rat heart. *Cardiovascular research* **29**, 373-378
88. Zammit, V. A., Ramsay, R. R., Bonomini, M., and Arduini, A. (2009) Carnitine, mitochondrial function and therapy. *Advanced drug delivery reviews* **61**, 1353-1362
89. Kelley, D. E., and Mandarino, L. J. (2000) Fuel selection in human skeletal muscle in insulin resistance: a reexamination. *Diabetes* **49**, 677-683
90. Kamikawa, T., Suzuki, Y., Kobayashi, A., Hayashi, H., Masumura, Y., Nishihara, K., Abe, M., and Yamazaki, N. (1984) Effects of L-carnitine on exercise tolerance in patients with stable angina pectoris. *Japanese heart journal* **25**, 587-597
91. Xue, Y.-Z., Wang, L.-X., Liu, H.-Z., Qi, X.-W., Wang, X.-H., and Ren, H.-Z. (2007) L-carnitine as an adjunct therapy to percutaneous coronary intervention

- for non-ST elevation myocardial infarction. *Cardiovascular drugs and therapy* **21**, 445-448
92. Canale, C., Terrachini, V., Biagini, A., Vallebona, A., Masperone, M., Valice, S., and Castellano, A. (1988) Bicycle ergometer and echocardiographic study in healthy subjects and patients with angina pectoris after administration of L-carnitine: semiautomatic computerized analysis of M-mode tracing. *International journal of clinical pharmacology, therapy, and toxicology* **26**, 221-224
93. Rizzon, P., Biasco, G., Di Biase, M., Boscia, F., Rizzo, U., Minafra, F., Bortone, A., Siliprandi, N., Procopio, A., and Bagiella, E. (1989) High doses of L-carnitine in acute myocardial infarction: metabolic and antiarrhythmic effects. *European Heart Journal* **10**, 502-508
94. Tarantini, G., Scrutinio, D., Bruzzi, P., Boni, L., Rizzon, P., and Iliceto, S. (2006) Metabolic treatment with L-carnitine in acute anterior ST segment elevation myocardial infarction. *Cardiology* **106**, 215-223
95. Corbucci, G., and Loche, F. (1993) L-carnitine in cardiogenic shock therapy: pharmacodynamic aspects and clinical data. *International journal of clinical pharmacology research* **13**, 87-91
96. DeLuca, H. F., and Engstrom, G. (1961) Calcium uptake by rat kidney mitochondria. *Proceedings of the National Academy of Sciences* **47**, 1744-1750
97. Patron, M., Raffaello, A., Granatiero, V., Tosatto, A., Merli, G., De Stefani, D., Wright, L., Pallafacchina, G., Terrin, A., and Mammucari, C. (2013) The

- mitochondrial calcium uniporter (MCU): molecular identity and physiological roles. *Journal of Biological Chemistry* **288**, 10750-10758
98. De Stefani, D., Raffaello, A., Teardo, E., Szabò, I., and Rizzuto, R. (2011) A forty-kilodalton protein of the inner membrane is the mitochondrial calcium uniporter. *Nature* **476**, 336
99. Marchi, S., and Pinton, P. (2014) The mitochondrial calcium uniporter complex: molecular components, structure and physiopathological implications. *The Journal of physiology* **592**, 829-839
100. Perocchi, F., Gohil, V. M., Girgis, H. S., Bao, X. R., McCombs, J. E., Palmer, A. E., and Mootha, V. K. (2010) MICU1 encodes a mitochondrial EF hand protein required for Ca²⁺ uptake. *Nature* **467**, 291
101. Raffaello, A., De Stefani, D., Sabbadin, D., Teardo, E., Merli, G., Picard, A., Checchetto, V., Moro, S., Szabò, I., and Rizzuto, R. (2013) The mitochondrial calcium uniporter is a multimer that can include a dominant-negative pore-forming subunit. *The EMBO journal* **32**, 2362-2376
102. Williams, G. S., Boyman, L., and Lederer, W. J. (2015) Mitochondrial calcium and the regulation of metabolism in the heart. *Journal of molecular and cellular cardiology* **78**, 35-45
103. De La Fuente, S., Fernandez-Sanz, C., Vail, C., Agra, E. J., Holmstrom, K., Sun, J., Mishra, J., Williams, D., Finkel, T., and Murphy, E. (2016) Strategic positioning and biased activity of the mitochondrial calcium uniporter in cardiac muscle. *Journal of Biological Chemistry* **291**, 23343-23362

104. Denton, R., and McCormack, J. (1990) Ca²⁺ as a second messenger within mitochondria of the heart and other tissues. *Annual Review of Physiology* **52**, 451-466
105. McCORMACK, J. G., and Denton, R. M. (1984) Role of Ca²⁺ ions in the regulation of intramitochondrial metabolism in rat heart. Evidence from studies with isolated mitochondria that adrenaline activates the pyruvate dehydrogenase and 2-oxoglutarate dehydrogenase complexes by increasing the intramitochondrial concentration of Ca²⁺. *Biochemical Journal* **218**, 235
106. McCORMACK, J. G., Halestrap, A. P., and Denton, R. M. (1990) Role of calcium ions in regulation of mammalian intramitochondrial metabolism. *Physiological reviews* **70**, 391-425
107. Williamson, J. R. (1964) Metabolic effects of epinephrine in the isolated, perfused rat heart I. Dissociation of the glycogenolytic from the metabolic stimulatory effect. *Journal of Biological Chemistry* **239**, 2721-2729
108. Diaz-Juarez, J., Suarez, J., Cividini, F., Scott, B. T., Diemer, T., Dai, A., and Dillmann, W. H. (2016) Expression of the mitochondrial calcium uniporter in cardiac myocytes improves impaired mitochondrial calcium handling and metabolism in simulated hyperglycemia. *American Journal of Physiology-Cell Physiology* **311**, C1005-C1013
109. Kwong, J. Q., Lu, X., Correll, R. N., Schwanekamp, J. A., Vagnozzi, R. J., Sargent, M. A., York, A. J., Zhang, J., Bers, D. M., and Molkenin, J. D. (2015) The Mitochondrial Calcium Uniporter Selectively Matches Metabolic Output to Acute Contractile Stress in the Heart. *Cell reports* **12**, 15-22

110. Pan, X., Liu, J., Nguyen, T., Liu, C., Sun, J., Teng, Y., Fergusson, M. M., Rovira, I. I., Allen, M., and Springer, D. A. (2013) The physiological role of mitochondrial calcium revealed by mice lacking the mitochondrial calcium uniporter. *Nature cell biology* **15**, 1464
111. Wu, Y., Rasmussen, T. P., Koval, O. M., Mei-ling, A. J., Hall, D. D., Chen, B., Luczak, E. D., Wang, Q., Rokita, A. G., and Wehrens, X. H. (2015) The mitochondrial uniporter controls fight or flight heart rate increases. *Nature communications* **6**, 6081
112. Yu, T., Hong, H., Yang, J., Gao, Q., and Xia, Q. (2011) Role of mitochondrial calcium uniporter in cardioprotection induced by ischemic postconditioning in isolated rat heart. *Zhejiang da xue xue bao. Yi xue ban= Journal of Zhejiang University. Medical sciences* **40**, 304-308
113. Fernández-Sada, E., Silva-Platas, C., Villegas, C., Rivero, S., Willis, B., García, N., Garza, J., Oropeza-Almazán, Y., Valverde, C. A., and Mazzocchi, G. (2014) Cardiac responses to β -adrenoceptor stimulation is partly dependent on mitochondrial calcium uniporter activity. *British journal of pharmacology* **171**, 4207-4221
114. Holmström, K. M., Pan, X., Liu, J. C., Menazza, S., Liu, J., Nguyen, T. T., Pan, H., Parks, R. J., Anderson, S., and Noguchi, A. (2015) Assessment of cardiac function in mice lacking the mitochondrial calcium uniporter. *Journal of molecular and cellular cardiology* **85**, 178-182
115. Luongo, T. S., Lambert, J. P., Yuan, A., Zhang, X., Gross, P., Song, J., Shanmughapriya, S., Gao, E., Jain, M., and Houser, S. R. (2015) The

- mitochondrial calcium uniporter matches energetic supply with cardiac workload during stress and modulates permeability transition. *Cell reports* **12**, 23-34
116. Rasmussen, T. P., Wu, Y., Mei-ling, A. J., Koval, O. M., Wilson, N. R., Luczak, E. D., Wang, Q., Chen, B., Gao, Z., and Zhu, Z. (2015) Inhibition of MCU forces extramitochondrial adaptations governing physiological and pathological stress responses in heart. *Proceedings of the National Academy of Sciences* **112**, 9129-9134
117. Fong, L. G., Young, S. G., Beigneux, A. P., Bensadoun, A., Oberer, M., Jiang, H., and Ploug, M. (2016) GPIHBP1 and plasma triglyceride metabolism. *Trends in Endocrinology & Metabolism* **27**, 455-469
118. Singh, K. K., Shukla, P. C., Yanagawa, B., Quan, A., Lovren, F., Pan, Y., Wagg, C. S., Teoh, H., Lopaschuk, G. D., and Verma, S. (2013) Regulating cardiac energy metabolism and bioenergetics by targeting the DNA damage repair protein BRCA1. *The Journal of thoracic and cardiovascular surgery* **146**, 702-709
119. Dagher, Z., Ruderman, N., Tornheim, K., and Ido, Y. (2001) Acute regulation of fatty acid oxidation and amp-activated protein kinase in human umbilical vein endothelial cells. *Circulation research* **88**, 1276-1282
120. Dagher, Z., Ruderman, N., Tornheim, K., and Ido, Y. (1999) The effect of AMP-activated protein kinase and its activator AICAR on the metabolism of human umbilical vein endothelial cells. *Biochemical and biophysical research communications* **265**, 112-115

121. Kuo, A., Lee, M. Y., and Sessa, W. C. (2017) Lipid droplet biogenesis and function in the endothelium. *Circulation research*, CIRCRESAHA. 116.310498
122. Jabs, M., Rose, A. J., Lehmann, L. H., Taylor, J., Moll, I., Sijmonsma, T. P., Herberich, S. E., Sauer, S. W., Poschet, G., and Federico, G. (2018) Inhibition of Endothelial Notch Signaling Impairs Fatty Acid Transport and Leads to Metabolic and Vascular Remodeling of the Adult Heart. *Circulation*, CIRCULATIONAHA. 117.029733
123. Murrow, L., and Debnath, J. (2013) Autophagy as a stress-response and quality-control mechanism: implications for cell injury and human disease. *Annual Review of Pathology: Mechanisms of Disease* **8**, 105-137
124. Torisu, T., Torisu, K., Lee, I. H., Liu, J., Malide, D., Combs, C. A., Wu, X. S., Rovira, II, Fergusson, M. M., Weigert, R., Connelly, P. S., Daniels, M. P., Komatsu, M., Cao, L., and Finkel, T. (2013) Autophagy regulates endothelial cell processing, maturation and secretion of von Willebrand factor. *Nat Med* **19**, 1281-1287
125. Torisu, K., Singh, K. K., Torisu, T., Lovren, F., Liu, J., Pan, Y., Quan, A., Ramadan, A., Al-Omran, M., and Pankova, N. (2016) Intact endothelial autophagy is required to maintain vascular lipid homeostasis. *Aging Cell* **15**, 187-191
126. Peng, N., Meng, N., Wang, S., Zhao, F., Zhao, J., Su, L., Zhang, S., Zhang, Y., Zhao, B., and Miao, J. (2014) An activator of mTOR inhibits oxLDL-induced autophagy and apoptosis in vascular endothelial cells and restricts atherosclerosis in apolipoprotein E^{-/-} mice. *Scientific reports* **4**, 5519

127. Settembre, C., and Ballabio, A. (2014) Lysosome: regulator of lipid degradation pathways. *Trends in cell biology* **24**, 743-750
128. Singh, R., and Cuervo, A. M. (2012) Lipophagy: connecting autophagy and lipid metabolism. *International journal of cell biology* **2012**
129. Rambold, A. S., Cohen, S., and Lippincott-Schwartz, J. (2015) Fatty acid trafficking in starved cells: regulation by lipid droplet lipolysis, autophagy, and mitochondrial fusion dynamics. *Developmental cell* **32**, 678-692
130. Allfrey, V., Faulkner, R., and Mirsky, A. (1964) Acetylation and methylation of histones and their possible role in the regulation of RNA synthesis. *Proceedings of the National Academy of Sciences* **51**, 786-794
131. Berger, S. L. (2007) The complex language of chromatin regulation during transcription. *Nature* **447**, 407
132. Saunders, L., and Verdin, E. (2007) Sirtuins: critical regulators at the crossroads between cancer and aging. *Oncogene* **26**, 5489
133. Choudhary, C., Kumar, C., Gnad, F., Nielsen, M. L., Rehman, M., Walther, T. C., Olsen, J. V., and Mann, M. (2009) Lysine acetylation targets protein complexes and co-regulates major cellular functions. *Science* **325**, 834-840
134. Webster, B. R., Scott, I., Han, K., Li, J. H., Lu, Z., Stevens, M. V., Malide, D., Chen, Y., Samsel, L., and Connelly, P. S. (2013) Restricted mitochondrial protein acetylation initiates mitochondrial autophagy. *J Cell Sci* **126**, 4843-4849
135. Finley, L. W., and Haigis, M. C. (2012) Metabolic regulation by SIRT3: implications for tumorigenesis. *Trends in molecular medicine* **18**, 516-523

136. Guan, K.-L., and Xiong, Y. (2011) Regulation of intermediary metabolism by protein acetylation. *Trends in biochemical sciences* **36**, 108-116
137. Verdin, E., Hirschey, M. D., Finley, L. W., and Haigis, M. C. (2010) Sirtuin regulation of mitochondria: energy production, apoptosis, and signaling. *Trends in biochemical sciences* **35**, 669-675
138. Hebert, A. S., Dittenhafer-Reed, K. E., Yu, W., Bailey, D. J., Selen, E. S., Boersma, M. D., Carson, J. J., Tonelli, M., Balloon, A. J., and Higbee, A. J. (2013) Calorie restriction and SIRT3 trigger global reprogramming of the mitochondrial proteome. *Molecular cell* **49**, 186-199
139. Zhao, S., Xu, W., Jiang, W., Yu, W., Lin, Y., Zhang, T., Yao, J., Zhou, L., Zeng, Y., and Li, H. (2010) Regulation of cellular metabolism by protein lysine acetylation. *Science* **327**, 1000-1004
140. Kouzarides, T. (2000) Acetylation: a regulatory modification to rival phosphorylation? *The EMBO journal* **19**, 1176-1179
141. Lu, Z., Scott, I., Webster, B. R., and Sack, M. N. (2009) The emerging characterization of lysine residue deacetylation on the modulation of mitochondrial function and cardiovascular biology. *Circulation research* **105**, 830-841
142. Rine, J., Strathern, J. N., Hicks, J. B., and Herskowitz, I. (1979) A suppressor of mating-type locus mutations in *Saccharomyces cerevisiae*: evidence for and identification of cryptic mating-type loci. *Genetics* **93**, 877-901
143. Riccio, A. (2010) New endogenous regulators of class I histone deacetylases. *Sci. Signal.* **3**, pe1-pe1

144. Lin, S.-J., Defossez, P.-A., and Guarente, L. (2000) Requirement of NAD and SIR2 for life-span extension by calorie restriction in *Saccharomyces cerevisiae*. *Science* **289**, 2126-2128
145. Lin, S.-J., Ford, E., Haigis, M., Liszt, G., and Guarente, L. (2004) Calorie restriction extends yeast life span by lowering the level of NADH. *Genes & development* **18**, 12-16
146. Lin, S.-J., Kaeberlein, M., Andalis, A. A., Sturtz, L. A., Defossez, P.-A., Culotta, V. C., Fink, G. R., and Guarente, L. (2002) Calorie restriction extends *Saccharomyces cerevisiae* lifespan by increasing respiration. *Nature* **418**, 344
147. Anderson, K. A., and Hirschey, M. D. (2012) Mitochondrial protein acetylation regulates metabolism. *Essays in biochemistry* **52**, 23-35
148. Houtkooper, R. H., Pirinen, E., and Auwerx, J. (2012) Sirtuins as regulators of metabolism and healthspan. *Nature reviews Molecular cell biology* **13**, 225
149. Finkel, T., Deng, C.-X., and Mostoslavsky, R. (2009) Recent progress in the biology and physiology of sirtuins. *Nature* **460**, 587
150. Hall, J. A., Dominy, J. E., Lee, Y., and Puigserver, P. (2013) The sirtuin family's role in aging and age-associated pathologies. *The Journal of clinical investigation* **123**, 973-979
151. Matsushima, S., and Sadoshima, J. (2015) The role of sirtuins in cardiac disease. *American Journal of Physiology-Heart and Circulatory Physiology* **309**, H1375-H1389

152. Osborne, B., Cooney, G. J., and Turner, N. (2014) Are sirtuin deacylase enzymes important modulators of mitochondrial energy metabolism? *Biochimica et Biophysica Acta (BBA)-General Subjects* **1840**, 1295-1302
153. Hirschey, M. D., Shimazu, T., Goetzman, E., Jing, E., Schwer, B., Lombard, D. B., Grueter, C. A., Harris, C., Biddinger, S., and Ilkayeva, O. R. (2010) SIRT3 regulates mitochondrial fatty-acid oxidation by reversible enzyme deacetylation. *Nature* **464**, 121
154. Alrob, O. A., Sankaralingam, S., Ma, C., Wagg, C. S., Fillmore, N., Jaswal, J. S., Sack, M. N., Lehner, R., Gupta, M. P., and Michelakis, E. D. (2014) Obesity-induced lysine acetylation increases cardiac fatty acid oxidation and impairs insulin signalling. *Cardiovascular research* **103**, 485-497
155. Hirschey, M. D., Shimazu, T., Jing, E., Grueter, C. A., Collins, A. M., Aouizerat, B., Stančáková, A., Goetzman, E., Lam, M. M., and Schwer, B. (2011) SIRT3 deficiency and mitochondrial protein hyperacetylation accelerate the development of the metabolic syndrome. *Molecular cell* **44**, 177-190
156. Hallows, W. C., Yu, W., Smith, B. C., Devires, M. K., Ellinger, J. J., Someya, S., Shortreed, M. R., Prolla, T., Markley, J. L., and Smith, L. M. (2011) Sirt3 promotes the urea cycle and fatty acid oxidation during dietary restriction. *Molecular cell* **41**, 139-149
157. Bharathi, S. S., Zhang, Y., Mohsen, A.-W., Uppala, R., Balasubramani, M., Schreiber, E., Uechi, G., Beck, M. E., Rardin, M. J., and Vockley, J. (2013) Sirtuin 3 (SIRT3) protein regulates long-chain acyl-CoA dehydrogenase by

- deacetylating conserved lysines near the active site. *Journal of Biological Chemistry* **288**, 33837-33847
158. Mori, J., Alrob, O. A., Wagg, C. S., Harris, R. A., Lopaschuk, G. D., and Oudit, G. Y. (2013) ANG II causes insulin resistance and induces cardiac metabolic switch and inefficiency: a critical role of PDK4. *American Journal of Physiology-Heart and Circulatory Physiology* **304**, H1103-H1113
159. Jing, E., O'Neill, B. T., Rardin, M. J., Kleinridders, A., Ilkeyeva, O. R., Ussar, S., Bain, J. R., Lee, K. Y., Verdin, E. M., and Newgard, C. B. (2013) Sirt3 regulates metabolic flexibility of skeletal muscle through reversible enzymatic deacetylation. *Diabetes* **62**, 3404-3417
160. Laurent, G., German, N. J., Saha, A. K., de Boer, V. C., Davies, M., Koves, T. R., Dephoure, N., Fischer, F., Boanca, G., and Vaitheesvaran, B. (2013) SIRT4 coordinates the balance between lipid synthesis and catabolism by repressing malonyl CoA decarboxylase. *Molecular cell* **50**, 686-698
161. Lerin, C., Rodgers, J. T., Kalume, D. E., Kim, S.-h., Pandey, A., and Puigserver, P. (2006) GCN5 acetyltransferase complex controls glucose metabolism through transcriptional repression of PGC-1 α . *Cell metabolism* **3**, 429-438
162. Dominy Jr, J. E., Lee, Y., Gerhart-Hines, Z., and Puigserver, P. (2010) Nutrient-dependent regulation of PGC-1 α 's acetylation state and metabolic function through the enzymatic activities of Sirt1/GCN5. *Biochimica et biophysica acta (BBA)-proteins and proteomics* **1804**, 1676-1683

163. Scott, I., Webster, B. R., Li, J. H., and Sack, M. N. (2012) Identification of a molecular component of the mitochondrial acetyltransferase programme: a novel role for GCN5L1. *Biochemical Journal* **443**, 655-661
164. Wagner, G. R., and Payne, R. M. (2013) Widespread and enzyme-independent N ϵ -acetylation and N ϵ -succinylation of proteins in the chemical conditions of the mitochondrial matrix. *Journal of Biological Chemistry* **288**, 29036-29045
165. Davies, M. N., Kjalarsdottir, L., Thompson, J. W., Dubois, L. G., Stevens, R. D., Ilkayeva, O. R., Brosnan, M. J., Rolph, T. P., Grimsrud, P. A., and Muoio, D. M. (2016) The acetyl group buffering action of carnitine acetyltransferase offsets macronutrient-induced lysine acetylation of mitochondrial proteins. *Cell reports* **14**, 243-254
166. Kendrick, A. A., Choudhury, M., Rahman, S. M., McCurdy, C. E., Friederich, M., Van Hove, J. L., Watson, P. A., Birdsey, N., Bao, J., and Gius, D. (2011) Fatty liver is associated with reduced SIRT3 activity and mitochondrial protein hyperacetylation. *Biochemical Journal* **433**, 505-514
167. Schwer, B., Eckersdorff, M., Li, Y., Silva, J. C., Fermin, D., Kurtev, M. V., Giallourakis, C., Comb, M. J., Alt, F. W., and Lombard, D. B. (2009) Calorie restriction alters mitochondrial protein acetylation. *Aging cell* **8**, 604-606
168. Pougovkina, O., te Brinke, H., Ofman, R., van Cruchten, A. G., Kulik, W., Wanders, R. J., Houten, S. M., and de Boer, V. C. (2014) Mitochondrial protein acetylation is driven by acetyl-CoA from fatty acid oxidation. *Human molecular genetics* **23**, 3513-3522

169. Sankaralingam, S., Alrob, O. A., Zhang, L., Jaswal, J. S., Wagg, C. S., Fukushima, A., Padwal, R. S., Johnstone, D. E., Sharma, A. M., and Lopaschuk, G. D. (2015) Lowering body weight in obese mice with diastolic heart failure improves cardiac insulin sensitivity and function: implications for the obesity paradox. *Diabetes* **64**, 1643-1657
170. Lai, L., Leone, T. C., Keller, M. P., Martin, O. J., Broman, A. T., Nigro, J., Kapoor, K., Koves, T. R., Stevens, R., and Ilkayeva, O. R. (2014) Energy metabolic re-programming in the hypertrophied and early stage failing heart: A multi-systems approach. *Circulation: Heart Failure*, CIRCHEARTFAILURE. 114.001469
171. Horton, J. L., Martin, O. J., Lai, L., Riley, N. M., Richards, A. L., Vega, R. B., Leone, T. C., Pagliarini, D. J., Muoio, D. M., and Bedi Jr, K. C. (2016) Mitochondrial protein hyperacetylation in the failing heart. *JCI insight* **1**
172. Bedi, K. C., Snyder, N. W., Brandimarto, J., Aziz, M., Mesaros, C., Worth, A., Wang, L., Javaheri, A., Blair, I. A., and Margulies, K. (2016) Evidence for intramyocardial disruption of lipid metabolism and increased myocardial ketone utilization in advanced human heart failure. *Circulation*, CIRCULATIONAHA. 115.017545
173. Karamanlidis, G., Lee, C. F., Garcia-Menendez, L., Kolwicz, S. C., Suthammarak, W., Gong, G., Sedensky, M. M., Morgan, P. G., Wang, W., and Tian, R. (2013) Mitochondrial complex I deficiency increases protein acetylation and accelerates heart failure. *Cell metabolism* **18**, 239-250

174. Vazquez, E. J., Berthiaume, J. M., Kamath, V., Achike, O., Buchanan, E., Montano, M. M., Chandler, M. P., Miyagi, M., and Rosca, M. G. (2015) Mitochondrial complex I defect and increased fatty acid oxidation enhance protein lysine acetylation in the diabetic heart. *Cardiovascular research* **107**, 453-465
175. Fukushima, A., Alrob, O. A., Zhang, L., Wagg, C. S., Altamimi, T., Rawat, S., Rebeyka, I. M., Kantor, P. F., and Lopaschuk, G. D. (2016) Acetylation and succinylation contribute to maturational alterations in energy metabolism in the newborn heart. *American journal of physiology. Heart and circulatory physiology* **311**, H347-363
176. Bers, D. M., Barry, W. H., and Despa, S. (2003) Intracellular Na⁺ regulation in cardiac myocytes. *Cardiovascular research* **57**, 897-912
177. Randle, P. J. (1998) Regulatory interactions between lipids and carbohydrates: the glucose fatty acid cycle after 35 years. *Diabetes/Metabolism Research and Reviews* **14**, 263-283
178. Christensen, N. J., and Videbaek, J. (1974) Plasma catecholamines and carbohydrate metabolism in patients with acute myocardial infarction. *The Journal of clinical investigation* **54**, 278-286
179. Bochaton, T., Crola-Da-Silva, C., Pillot, B., Villedieu, C., Ferreras, L., Alam, M., Thibault, H., Strina, M., Gharib, A., and Ovize, M. (2015) Inhibition of myocardial reperfusion injury by ischemic postconditioning requires sirtuin 3-mediated deacetylation of cyclophilin D. *Journal of molecular and cellular cardiology* **84**, 61-69

180. Porter, G. A., Urciuoli, W. R., Brookes, P. S., and Nadtochiy, S. M. (2014) SIRT3 deficiency exacerbates ischemia-reperfusion injury: implication for aged hearts. *American Journal of Physiology-Heart and Circulatory Physiology* **306**, H1602-H1609
181. Yamamoto, T., Byun, J., Zhai, P., Ikeda, Y., Oka, S., and Sadoshima, J. (2014) Nicotinamide mononucleotide, an intermediate of NAD⁺ synthesis, protects the heart from ischemia and reperfusion. *PloS one* **9**, e98972
182. Atkinson, L. L., Fischer, M. A., and Lopaschuk, G. D. (2002) Leptin activates cardiac fatty acid oxidation independent of changes in the AMP-activated protein kinase-acetyl-CoA carboxylase-malonyl-CoA axis. *Journal of Biological Chemistry* **277**, 29424-29430
183. Reitman, M. L. (2007) FGF21: a missing link in the biology of fasting. *Cell metabolism* **5**, 405-407
184. Scherer, P. E. (2006) Adipose tissue: from lipid storage compartment to endocrine organ. *Diabetes* **55**, 1537-1545
185. Sharma, A. M., and Staels, B. (2006) Peroxisome proliferator-activated receptor γ and adipose tissue—understanding obesity-related changes in regulation of lipid and glucose metabolism. *The Journal of Clinical Endocrinology & Metabolism* **92**, 386-395
186. Kim, J.-Y., Van De Wall, E., Laplante, M., Azzara, A., Trujillo, M. E., Hofmann, S. M., Schraw, T., Durand, J. L., Li, H., and Li, G. (2007) Obesity-associated improvements in metabolic profile through expansion of adipose tissue. *The Journal of clinical investigation* **117**, 2621-2637

187. Morton, G., Cummings, D., Baskin, D., Barsh, G., and Schwartz, M. (2006) Central nervous system control of food intake and body weight. *Nature* **443**, 289
188. Burger, K. S., and Berner, L. A. (2014) A functional neuroimaging review of obesity, appetitive hormones and ingestive behavior. *Physiology & behavior* **136**, 121-127
189. Sakata, I., and Sakai, T. (2010) Ghrelin cells in the gastrointestinal tract. *International journal of peptides* **2010**
190. Schwartz, M. W., Woods, S. C., Porte Jr, D., Seeley, R. J., and Baskin, D. G. (2000) Central nervous system control of food intake. *Nature* **404**, 661
191. LeRoith, D., and Yakar, S. (2007) Mechanisms of disease: metabolic effects of growth hormone and insulin-like growth factor 1. *Nature Reviews Endocrinology* **3**, 302
192. Gao, S., McMillan, R. P., Jacas, J., Zhu, Q., Li, X., Kumar, G. K., Casals, N., Hegardt, F. G., Robbins, P. D., and Lopaschuk, G. D. (2014) Regulation of substrate oxidation preferences in muscle by the peptide hormone adropin. *Diabetes*, DB_140388
193. Kumar, K. G., Trevaskis, J. L., Lam, D. D., Sutton, G. M., Koza, R. A., Chouljenko, V. N., Kousoulas, K. G., Rogers, P. M., Kesterson, R. A., and Thearle, M. (2008) Identification of adropin as a secreted factor linking dietary macronutrient intake with energy homeostasis and lipid metabolism. *Cell metabolism* **8**, 468-481
194. Gao, S., McMillan, R. P., Zhu, Q., Lopaschuk, G. D., Hulver, M. W., and Butler, A. A. (2015) Therapeutic effects of adropin on glucose tolerance and

- substrate utilization in diet-induced obese mice with insulin resistance. *Molecular metabolism* **4**, 310-324
195. Sodi-Pallares, D., Testelli, M. R., Fishleder, B. L., Bisteni, A., Medrano, G. A., Friedland, C., and De Micheli, A. (1962) Effects of an intravenous infusion of a potassium-glucose-insulin solution on the electrocardiographic signs of myocardial infarction: A preliminary clinical report*. *American Journal of Cardiology* **9**, 166-181
196. Horowitz, J. D., Chirkov, Y. Y., Kennedy, J. A., and Sverdlov, A. L. (2010) Modulation of myocardial metabolism: an emerging therapeutic principle. *Current opinion in cardiology* **25**, 329-334
197. Trammell, S. A., Schmidt, M. S., Weidemann, B. J., Redpath, P., Jaksch, F., Dellinger, R. W., Li, Z., Abel, E. D., Migaud, M. E., and Brenner, C. (2016) Nicotinamide riboside is uniquely and orally bioavailable in mice and humans. *Nature communications* **7**, 12948
198. Yoshino, J., Baur, J. A., and Imai, S.-i. (2017) NAD⁺ Intermediates: The Biology and Therapeutic Potential of NMN and NR. *Cell metabolism*
199. Nadtochiy, S., Wang, Y. T., Nehrke, K., Munger, J., and Brookes, P. S. (2017) Nicotinamide mononucleotide (NMN) affords cardioprotection by stimulating glycolysis. *bioRxiv*, 230938
200. Yau, J. W., Singh, K. K., Hou, Y., Lei, X., Ramadan, A., Quan, A., Teoh, H., Kuebler, W. M., Al-Omran, M., Yanagawa, B., Ni, H., and Verma, S. (2017) Endothelial-specific deletion of autophagy-related 7 (ATG7) attenuates arterial thrombosis in mice. *J Thorac Cardiovasc Surg* **154**, 978-988 e971

201. Singh, K. K., Lovren, F., Pan, Y., Quan, A., Ramadan, A., Matkar, P. N., Ehsan, M., Sandhu, P., Mantella, L. E., Gupta, N., Teoh, H., Parotto, M., Tabuchi, A., Kuebler, W. M., Al-Omran, M., Finkel, T., and Verma, S. (2015) The essential autophagy gene ATG7 modulates organ fibrosis via regulation of endothelial-to-mesenchymal transition. *The Journal of biological chemistry* **290**, 2547-2559
202. Menard, C., Pupier, S., Mornet, D., Kitzmann, M., Nargeot, J., and Lory, P. (1999) Modulation of L-type calcium channel expression during retinoic acid-induced differentiation of H9C2 cardiac cells. *The Journal of biological chemistry* **274**, 29063-29070
203. Mittal, B., and Kurup, C. K. (1981) Induction of carnitine acetyltransferase by clofibrate in rat liver. *The Biochemical journal* **194**, 249-255
204. Edwards, Y. H., Chase, J. F., Edwards, M. R., and Tubbs, P. K. (1974) Carnitine acetyltransferase: the question of multiple forms. *European journal of biochemistry* **46**, 209-215
205. Fritz, I. B., Schultz, S. K., and Srere, P. A. (1963) Properties of partially purified carnitine acetyltransferase. *The Journal of biological chemistry* **238**, 2509-2517
206. Chase, J. F., and Tubbs, P. K. (1966) Some kinetic studies on the mechanism of action of carnitine acetyltransferase. *The Biochemical journal* **99**, 32-40
207. Martin, B. R., and Denton, R. M. (1970) The intracellular localization of enzymes in white-adipose-tissue fat-cells and permeability properties of fat-cell mitochondria. Transfer of acetyl units and reducing power between mitochondria and cytoplasm. *The Biochemical journal* **117**, 861-877

208. Linn, T. C., and Srere, P. A. (1979) Identification of ATP citrate lyase as a phosphoprotein. *The Journal of biological chemistry* **254**, 1691-1698
209. Morgunov, I., and Srere, P. A. (1998) Interaction between citrate synthase and malate dehydrogenase. Substrate channeling of oxaloacetate. *The Journal of biological chemistry* **273**, 29540-29544
210. Bradford, M. M. (1976) A rapid and sensitive method for the quantitation of microgram quantities of protein utilizing the principle of protein-dye binding. *Analytical biochemistry* **72**, 248-254
211. Larsen, T. S., Belke, D. D., Sas, R., Giles, W. R., Severson, D. L., Lopaschuk, G. D., and Tyberg, J. V. (1999) The isolated working mouse heart: methodological considerations. *Pflugers Archiv : European journal of physiology* **437**, 979-985
212. Zhang, L., Ussher, J. R., Oka, T., Cadete, V. J., Wagg, C., and Lopaschuk, G. D. (2011) Cardiac diacylglycerol accumulation in high fat-fed mice is associated with impaired insulin-stimulated glucose oxidation. *Cardiovascular research* **89**, 148-156
213. Bligh, E. G., and Dyer, W. J. (1959) A rapid method of total lipid extraction and purification. *Canadian journal of biochemistry and physiology* **37**, 911-917
214. Zhang, L., Mori, J., Wagg, C., and Lopaschuk, G. D. (2012) Activating cardiac E2F1 induces up-regulation of pyruvate dehydrogenase kinase 4 in mice on a short term of high fat feeding. *FEBS letters* **586**, 996-1003

215. King, M. T., and Reiss, P. D. (1985) Separation and measurement of short-chain coenzyme-A compounds in rat liver by reversed-phase high-performance liquid chromatography. *Analytical biochemistry* **146**, 173-179
216. Ussher, J. R., Wang, W., Gandhi, M., Keung, W., Samokhvalov, V., Oka, T., Wagg, C. S., Jaswal, J. S., Harris, R. A., Clanachan, A. S., Dyck, J. R., and Lopaschuk, G. D. (2012) Stimulation of glucose oxidation protects against acute myocardial infarction and reperfusion injury. *Cardiovascular research* **94**, 359-369
217. Benjamin, E. J., Blaha, M. J., Chiuve, S. E., Cushman, M., Das, S. R., Deo, R., Floyd, J., Fornage, M., Gillespie, C., and Isasi, C. (2017) Heart disease and stroke statistics-2017 update: a report from the American Heart Association. *Circulation* **135**, e146-e603
218. Peng, C., Lu, Z., Xie, Z., Cheng, Z., Chen, Y., Tan, M., Luo, H., Zhang, Y., He, W., and Yang, K. (2011) The first identification of lysine malonylation substrates and its regulatory enzyme. *Molecular & cellular proteomics* **10**, M111. 012658
219. Madiraju, P., Pande, S. V., Prentki, M., and Madiraju, S. M. (2009) Mitochondrial acetylcarnitine provides acetyl groups for nuclear histone acetylation. *Epigenetics* **4**, 399-403
220. McGarry, J. D., and Foster, D. W. (1976) An improved and simplified radioisotopic assay for the determination of free and esterified carnitine. *Journal of Lipid Research* **17**, 277-281

221. Wang, Q., Li, S., Jiang, L., Zhou, Y., Li, Z., Shao, M., Li, W., and Liu, Y. (2010) Deficiency in hepatic ATP-citrate lyase affects VLDL-triglyceride mobilization and liver fatty acid composition in mice. *Journal of lipid research* **51**, 2516-2526
222. Poirier, M., Vincent, G., Reszko, A. E., Bouchard, B., Kelleher, J. K., Brunengraber, H., and Des Rosiers, C. (2002) Probing the link between citrate and malonyl-CoA in perfused rat hearts. *American Journal of Physiology-Heart and Circulatory Physiology* **283**, H1379-H1386
223. Costell, M., O'Connor, J., and Grisolia, S. (1989) Age-dependent decrease of carnitine content in muscle of mice and humans. *Biochemical and biophysical research communications* **161**, 1135-1143
224. Chen, J.-F., Liu, H., Ni, H.-F., Lv, L.-L., Zhang, M.-H., Zhang, A.-H., Tang, R.-N., Chen, P.-S., and Liu, B.-C. (2013) Improved mitochondrial function underlies the protective effect of pirfenidone against tubulointerstitial fibrosis in 5/6 nephrectomized rats. *PLoS One* **8**, e83593
225. Baines, C. P., Zhang, J., Wang, G.-W., Zheng, Y.-T., Xiu, J. X., Cardwell, E. M., Bolli, R., and Ping, P. (2002) Mitochondrial PKC ϵ and MAPK form signaling modules in the murine heart: enhanced mitochondrial PKC ϵ -MAPK interactions and differential MAPK activation in PKC ϵ -induced cardioprotection. *Circulation research* **90**, 390-397
226. Kim, S.-M., Kim, Y.-G., Jeong, K.-H., Lee, S.-H., Lee, T.-W., Ihm, C.-G., and Moon, J.-Y. (2012) Angiotensin II-induced mitochondrial Nox4 is a major

- endogenous source of oxidative stress in kidney tubular cells. *PloS one* **7**, e39739
227. Kimes, B., and Brandt, B. (1976) Properties of a clonal muscle cell line from rat heart. *Experimental cell research* **98**, 367-381
228. Pereira, S. L., Ramalho-Santos, J., Branco, A. F., Sardao, V. A., Oliveira, P. J., and Carvalho, R. A. (2011) Metabolic remodeling during H9c2 myoblast differentiation: relevance for in vitro toxicity studies. *Cardiovascular toxicology* **11**, 180-190
229. Fritz, I. B., and Yue, K. T. (1964) Effects of carnitine on acetyl-CoA oxidation by heart muscle mitochondria. *American Journal of Physiology-Legacy Content* **206**, 531-535
230. Pinkosky, S. L., Groot, P. H., Lalwani, N. D., and Steinberg, G. R. (2017) Targeting ATP-Citrate Lyase in Hyperlipidemia and Metabolic Disorders. *Trends in molecular medicine*
231. Idell-Wenger, J. A., Grotyohann, L. W., and Neely, J. R. (1978) Coenzyme A and carnitine distribution in normal and ischemic hearts. *Journal of Biological Chemistry* **253**, 4310-4318
232. Idell-Wenger, J. (1981) Carnitine: acylcarnitine translocase of rat heart mitochondria. Competition for carnitine uptake by carnitine esters. *Journal of Biological Chemistry* **256**, 5597-5603
233. Pande, S. V., and Parvin, R. (1980) Carnitine-acylcarnitine translocase catalyzes an equilibrating unidirectional transport as well. *Journal of Biological Chemistry* **255**, 2994-3001

234. Idell-Wenger, J., Grotyohann, L., and Neely, J. (1982) Regulation of fatty acid utilization in heart. Role of the carnitine-acetyl-CoA transferase and carnitine-acetyl carnitine translocase system. *Journal of molecular and cellular cardiology* **14**, 413-417
235. Zuurbier, C. J., Eerbeek, O., and Meijer, A. J. (2005) Ischemic preconditioning, insulin, and morphine all cause hexokinase redistribution. *American Journal of Physiology-Heart and Circulatory Physiology* **289**, H496-H499
236. D'Souza, S., and Srere, P. (1983) Binding of citrate synthase to mitochondrial inner membranes. *Journal of Biological Chemistry* **258**, 4706-4709
237. Sumegi, B., and Srere, P. A. (1984) Binding of the enzymes of fatty acid beta-oxidation and some related enzymes to pig heart inner mitochondrial membrane. *Journal of Biological Chemistry* **259**, 8748-8752
238. Brownsey, R., Boone, A., Elliott, J., Kulpa, J., and Lee, W. (2006) Regulation of acetyl-CoA carboxylase. Portland Press Limited
239. Folmes, C. D., and Lopaschuk, G. D. (2007) Role of malonyl-CoA in heart disease and the hypothalamic control of obesity. *Cardiovascular research* **73**, 278-287
240. Saggerson, D. (2008) Malonyl-CoA, a key signaling molecule in mammalian cells. *Annu. Rev. Nutr.* **28**, 253-272
241. Xue, B., and Kahn, B. B. (2006) AMPK integrates nutrient and hormonal signals to regulate food intake and energy balance through effects in the hypothalamus and peripheral tissues. *The Journal of physiology* **574**, 73-83

242. Seiler, S. E., Martin, O. J., Noland, R. C., Slentz, D. H., DeBalsi, K. L., Ilkayeva, O. R., An, J., Newgard, C. B., Koves, T. R., and Muoio, D. M. (2014) Obesity and lipid stress inhibit carnitine acetyltransferase activity. *Journal of lipid research* **55**, 635-644
243. Abu-Elheiga, L., Oh, W., Kordari, P., and Wakil, S. J. (2003) Acetyl-CoA carboxylase 2 mutant mice are protected against obesity and diabetes induced by high-fat/high-carbohydrate diets. *Proceedings of the National Academy of Sciences* **100**, 10207-10212
244. Abu-Elheiga, L., Brinkley, W. R., Zhong, L., Chirala, S. S., Woldegiorgis, G., and Wakil, S. J. (2000) The subcellular localization of acetyl-CoA carboxylase 2. *Proceedings of the National Academy of Sciences* **97**, 1444-1449
245. Zhou, L., Huang, H., Yuan, C. L., Keung, W., Lopaschuk, G. D., and Stanley, W. C. (2008) Metabolic response to an acute jump in cardiac workload: effects on malonyl-CoA, mechanical efficiency, and fatty acid oxidation. *American Journal of Physiology-Heart and Circulatory Physiology* **294**, H954-H960
246. Zordoky, B. N., Nagendran, J., Pulinilkunnil, T., Kienesberger, P. C., Masson, G., Waller, T. J., Kemp, B. E., Steinberg, G. R., and Dyck, J. R. (2014) AMPK-Dependent Inhibitory Phosphorylation of ACC Is Not Essential for Maintaining Myocardial Fatty Acid Oxidation Novelty and Significance. *Circulation research* **115**, 518-524
247. Mabrouk, G., Helmy, I. M., Thampy, K., and Wakil, S. (1990) Acute hormonal control of acetyl-CoA carboxylase. The roles of insulin, glucagon, and epinephrine. *Journal of Biological Chemistry* **265**, 6330-6338

248. Heffner, C. S., Pratt, C. H., Babiuk, R. P., Sharma, Y., Rockwood, S. F., Donahue, L. R., Eppig, J. T., and Murray, S. A. (2012) Supporting conditional mouse mutagenesis with a comprehensive cre characterization resource. *Nature communications* **3**, 1218
249. Ni, Y. G., Wang, N., Cao, D. J., Sachan, N., Morris, D. J., Gerard, R. D., Kuroo, M., Rothermel, B. A., and Hill, J. A. (2007) FoxO transcription factors activate Akt and attenuate insulin signaling in heart by inhibiting protein phosphatases. *Proceedings of the National Academy of Sciences* **104**, 20517-20522
250. Taegtmeyer, H., Young, M. E., Lopaschuk, G. D., Abel, E. D., Brunengraber, H., Darley-Usmar, V., Des Rosiers, C., Gerszten, R., Glatz, J. F., Griffin, J. L., Gropler, R. J., Holzhuetter, H. G., Kizer, J. R., Lewandowski, E. D., Malloy, C. R., Neubauer, S., Peterson, L. R., Portman, M. A., Recchia, F. A., Van Eyk, J. E., Wang, T. J., and American Heart Association Council on Basic Cardiovascular, S. (2016) Assessing Cardiac Metabolism: A Scientific Statement From the American Heart Association. *Circ Res* **118**, 1659-1701
251. Brutsaert, D. L. (2003) Cardiac endothelial-myocardial signaling: its role in cardiac growth, contractile performance, and rhythmicity. *Physiol Rev* **83**, 59-115
252. Frangogiannis, N. G., Smith, C. W., and Entman, M. L. (2002) The inflammatory response in myocardial infarction. *Cardiovascular research* **53**, 31-47

253. Nussenzweig, S. C., Verma, S., and Finkel, T. (2015) The role of autophagy in vascular biology. *Circ Res* **116**, 480-488
254. Sciarretta, S., Maejima, Y., Zablocki, D., and Sadoshima, J. (2017) The Role of Autophagy in the Heart. *Annu Rev Physiol*
255. Kheloufi, M., Vion, A. C., Hammoutene, A., Poisson, J., Lasselín, J., Devue, C., Pic, I., Dupont, N., Busse, J., Stark, K., Lafaurie-Janvore, J., Barakat, A. I., Loyer, X., Souyri, M., Viollet, B., Julia, P., Tedgui, A., Codogno, P., Boulanger, C. M., and Rautou, P. E. (2017) Endothelial autophagic flux hampers atherosclerotic lesion development. *Autophagy*, 1-6
256. Singh, K. K., Yanagawa, B., Quan, A., Wang, R., Garg, A., Khan, R., Pan, Y., Wheatcroft, M. D., Lovren, F., Teoh, H., and Verma, S. (2014) Autophagy gene fingerprint in human ischemia and reperfusion. *J Thorac Cardiovasc Surg* **147**, 1065-1072 e1061
257. Hamacher-Brady, A., Brady, N. R., and Gottlieb, R. A. (2006) Enhancing macroautophagy protects against ischemia/reperfusion injury in cardiac myocytes. *Journal of Biological Chemistry* **281**, 29776-29787
258. Park, H.-J., Zhang, Y., Georgescu, S. P., Johnson, K. L., Kong, D., and Galper, J. B. (2006) Human umbilical vein endothelial cells and human dermal microvascular endothelial cells offer new insights into the relationship between lipid metabolism and angiogenesis. *Stem cell reviews* **2**, 93-101
259. Fillmore, N., Mori, J., and Lopaschuk, G. D. (2014) Mitochondrial fatty acid oxidation alterations in heart failure, ischaemic heart disease and diabetic cardiomyopathy. *Br J Pharmacol* **171**, 2080-2090

260. Hardie, D. G. (2013) AMPK: a target for drugs and natural products with effects on both diabetes and cancer. *Diabetes* **62**, 2164-2172
261. Eelen, G., de Zeeuw, P., Simons, M., and Carmeliet, P. (2015) Endothelial cell metabolism in normal and diseased vasculature. *Circ Res* **116**, 1231-1244
262. Liao, X., Sluimer, J. C., Wang, Y., Subramanian, M., Brown, K., Pattison, J. S., Robbins, J., Martinez, J., and Tabas, I. (2012) Macrophage autophagy plays a protective role in advanced atherosclerosis. *Cell Metab* **15**, 545-553
263. Razani, B., Feng, C., Coleman, T., Emanuel, R., Wen, H., Hwang, S., Ting, J. P., Virgin, H. W., Kastan, M. B., and Semenkovich, C. F. (2012) Autophagy links inflammasomes to atherosclerotic progression. *Cell Metab* **15**, 534-544
264. Singh, R., Kaushik, S., Wang, Y., Xiang, Y., Novak, I., Komatsu, M., Tanaka, K., Cuervo, A. M., and Czaja, M. J. (2009) Autophagy regulates lipid metabolism. *Nature* **458**, 1131-1135
265. Smathers, R. L., and Petersen, D. R. (2011) The human fatty acid-binding protein family: evolutionary divergences and functions. *Human genomics* **5**, 170-191
266. Iso, T., Maeda, K., Hanaoka, H., Suga, T., Goto, K., Syamsunarno, M. R., Hishiki, T., Nagahata, Y., Matsui, H., Arai, M., Yamaguchi, A., Abumrad, N. A., Sano, M., Suematsu, M., Endo, K., Hotamisligil, G. S., and Kurabayashi, M. (2013) Capillary endothelial fatty acid binding proteins 4 and 5 play a critical role in fatty acid uptake in heart and skeletal muscle. *Arteriosclerosis, thrombosis, and vascular biology* **33**, 2549-2557

267. Lopaschuk, G. D., Folmes, C. D., and Stanley, W. C. (2007) Cardiac energy metabolism in obesity. *Circulation research* **101**, 335-347
268. Shioda, S., Kageyama, H., Takenoya, F., and Shiba, K. (2011) Galanin-like peptide: a key player in the homeostatic regulation of feeding and energy metabolism? *International journal of obesity* **35**, 619
269. Al Batran, R., Almutairi, M., and Ussher, J. R. (2018) Glucagon-like peptide-1 receptor mediated control of cardiac energy metabolism. *Peptides* **100**, 94-100
270. Ouchi, N., Parker, J. L., Lugus, J. J., and Walsh, K. (2011) Adipokines in inflammation and metabolic disease. *Nature Reviews Immunology* **11**, 85
271. Ganesh-Kumar, K., Zhang, J., Gao, S., Rossi, J., McGuinness, O. P., Halem, H. H., Culler, M. D., Mynatt, R. L., and Butler, A. A. (2012) Adropin deficiency is associated with increased adiposity and insulin resistance. *Obesity* **20**, 1394-1402
272. Altamimi, T. R., and Lopaschuk, G. D. (2015) Diabetes and ischemia: similarities in cardiac energy metabolism. *Heart Metab* **68**, 4-8
273. Yosae, S., Soltani, S., Sekhavati, E., and Jazayeri, S. (2016) Adropin-A Novel Biomarker of Heart Disease: A Systematic Review Article. *Iranian journal of public health* **45**, 1568
274. Ussher, J. R., Baggio, L. L., Campbell, J. E., Mulvihill, E. E., Kim, M., Kabir, M. G., Cao, X., Baranek, B. M., Stoffers, D. A., and Seeley, R. J. (2014) Inactivation of the cardiomyocyte glucagon-like peptide-1 receptor (GLP-1R) unmasks cardiomyocyte-independent GLP-1R-mediated cardioprotection. *Molecular metabolism* **3**, 507-517

275. Gual, P., Le Marchand-Brustel, Y., and Tanti, J.-F. (2005) Positive and negative regulation of insulin signaling through IRS-1 phosphorylation. *Biochimie* **87**, 99-109
276. Aguirre, V., Uchida, T., Yenush, L., Davis, R., and White, M. F. (2000) The c-Jun NH2-terminal kinase promotes insulin resistance during association with insulin receptor substrate-1 and phosphorylation of Ser307. *Journal of Biological Chemistry* **275**, 9047-9054
277. Butler, A. A., Tam, C. S., Stanhope, K. L., Wolfe, B. M., Ali, M. R., O'keeffe, M., St-Onge, M.-P., Ravussin, E., and Havel, P. J. (2012) Low circulating adropin concentrations with obesity and aging correlate with risk factors for metabolic disease and increase after gastric bypass surgery in humans. *The Journal of Clinical Endocrinology & Metabolism* **97**, 3783-3791
278. Jaswal, J., and Ussher, J. (2009) Myocardial fatty acid utilization as a determinant of cardiac efficiency and function. *Clinical Lipidology* **4**, 379-389
279. Iwabu, M., Okada-Iwabu, M., Yamauchi, T., and Kadowaki, T. (2015) Adiponectin/adiponectin receptor in disease and aging. *NPJ aging and mechanisms of disease* **1**, 15013
280. Hall, M. E., Harmancey, R., and Stec, D. E. (2015) Lean heart: role of leptin in cardiac hypertrophy and metabolism. *World journal of cardiology* **7**, 511
281. Kielar, D., Clark, J., Ciechanowicz, A., Kurzawski, G., Sulikowski, T., and Naruszewicz, M. (1998) Leptin receptor isoforms expressed in human adipose tissue. *Metabolism* **47**, 844-847

282. Stein, L. M., Yosten, G. L., and Samson, W. K. (2016) Adropin acts in brain to inhibit water drinking: potential interaction with the orphan G protein-coupled receptor, GPR19. *American Journal of Physiology-Regulatory, Integrative and Comparative Physiology* **310**, R476-R480
283. Hoffmeister-Ullerich, S. A., Süsens, U., and Schaller, H. C. (2004) The orphan G-protein-coupled receptor GPR19 is expressed predominantly in neuronal cells during mouse embryogenesis. *Cell and tissue research* **318**, 459-463
284. Thapa, D., Stoner, M., Zhang, M., Xie, B., Manning, J., Guimaraes, D., Shiva, S., Jurczak, M. J., and Scott, I. (2018) Adropin Regulates Pyruvate Dehydrogenase in Cardiac Cells via a Novel GPCR-MAPK-PDK4 Signaling Pathway. *Redox biology*
285. Win, S., Than, T., Fernandez-Checa, J., and Kaplowitz, N. (2015) JNK interaction with Sab mediates ER stress induced inhibition of mitochondrial respiration and cell death. *Cell death & disease* **5**, e989
286. Hirosumi, J., Tuncman, G., Chang, L., Görgün, C. Z., Uysal, K. T., Maeda, K., Karin, M., and Hotamisligil, G. S. (2002) A central role for JNK in obesity and insulin resistance. *Nature* **420**, 333
287. Chang, L., Chiang, S.-H., and Saltiel, A. R. (2004) Insulin signaling and the regulation of glucose transport. *Molecular medicine* **10**, 65
288. Zhang, L., Keung, W., Samokhvalov, V., Wang, W., and Lopaschuk, G. D. (2010) Role of fatty acid uptake and fatty acid β -oxidation in mediating insulin resistance in heart and skeletal muscle. *Biochimica et Biophysica Acta (BBA)-Molecular and Cell Biology of Lipids* **1801**, 1-22

289. Fischer, Y., Thomas, J., Sevilla, L., Muñoz, P., Becker, C., Holman, G., Kozka, I. J., Palacín, M., Testar, X., and Kammermeier, H. (1997) Insulin-induced Recruitment of Glucose Transporter 4 (GLUT4) and GLUT1 in Isolated Rat Cardiac Myocytes EVIDENCE OF THE EXISTENCE OF DIFFERENT INTRACELLULAR GLUT4 VESICLE POPULATIONS. *Journal of Biological Chemistry* **272**, 7085-7092
290. Kienesberger, K., Pordes, A. G., Völk, T. G., and Hofbauer, R. (2014) L-carnitine and PPAR α -agonist fenofibrate are involved in the regulation of Carnitine Acetyltransferase (CrAT) mRNA levels in murine liver cells. *BMC genomics* **15**, 514
291. Augustus, A. S., Kako, Y., Yagyu, H., and Goldberg, I. J. (2003) Routes of FA delivery to cardiac muscle: modulation of lipoprotein lipolysis alters uptake of TG-derived FA. *American Journal of Physiology-Endocrinology and Metabolism* **284**, E331-E339
292. Egginton, S., Hauton, D., Winter, J., and Evans, R. D. (2013) Individual microvascular units are critical to cardiac performance. *The FASEB Journal* **27**, 898.812-898.812
293. Fang, Z. Y., Prins, J. B., and Marwick, T. H. (2004) Diabetic cardiomyopathy: evidence, mechanisms, and therapeutic implications. *Endocrine reviews* **25**, 543-567
294. Wan, A., and Rodrigues, B. (2016) Endothelial cell–cardiomyocyte crosstalk in diabetic cardiomyopathy. *Cardiovascular research* **111**, 172-183

295. van der Vusse, G. J., van Bilsen, M., and Glatz, J. F. (2000) Cardiac fatty acid uptake and transport in health and disease. *Cardiovascular research* **45**, 279-293
296. Lee, J., and Goldberg, I. J. (2007) Lipoprotein lipase-derived fatty acids: physiology and dysfunction. *Current hypertension reports* **9**, 462-466
297. Pulinilkunnil, T., and Rodrigues, B. (2006) Cardiac lipoprotein lipase: metabolic basis for diabetic heart disease. *Cardiovascular research* **69**, 329-340
298. Tirziu, D., Giordano, F. J., and Simons, M. (2010) Cell communications in the heart. *Circulation* **122**, 928-937
299. Kovacic, S., Soltys, C.-L. M., Barr, A. J., Shiojima, I., Walsh, K., and Dyck, J. R. (2003) Akt activity negatively regulates phosphorylation of AMP-activated protein kinase in the heart. *Journal of Biological Chemistry* **278**, 39422-39427
300. Folmes, C. D., Clanachan, A. S., and Lopaschuk, G. D. (2006) Fatty Acids Attenuate Insulin Regulation of 5'-AMP-Activated Protein Kinase and Insulin Cardioprotection After Ischemia. *Circulation research* **99**, 61-68
301. Ferrannini, E., Santoro, D., Bonadonna, R., Natali, A., Parodi, O., and Camici, P. G. (1993) Metabolic and hemodynamic effects of insulin on human hearts. *American Journal of Physiology-Endocrinology And Metabolism* **264**, E308-E315
302. Faulx, M. D., Chandler, M. P., Zawaneh, M. S., Stanley, W. C., and Hoit, B. D. (2007) MOUSE STRAIN-SPECIFIC DIFFERENCES IN CARDIAC METABOLIC ENZYME ACTIVITIES OBSERVED IN A MODEL OF ISOPROTERENOL-INDUCED CARDIAC HYPERTROPHY. *Clinical and experimental pharmacology and physiology* **34**, 77-80

Appendices

Appendix A: Supplemental Data for Chapter 3

Figure A1. Percentage of mitochondrial breakage in mouse heart ventricular tissue homogenized by either a Polytron or a Potter-Elvehjem homogenizer.

Mitochondrial breakage was assessed using citrate synthase activity leakage to cytosolic fractions, n= 5-14.

Mitochondrial Breakage

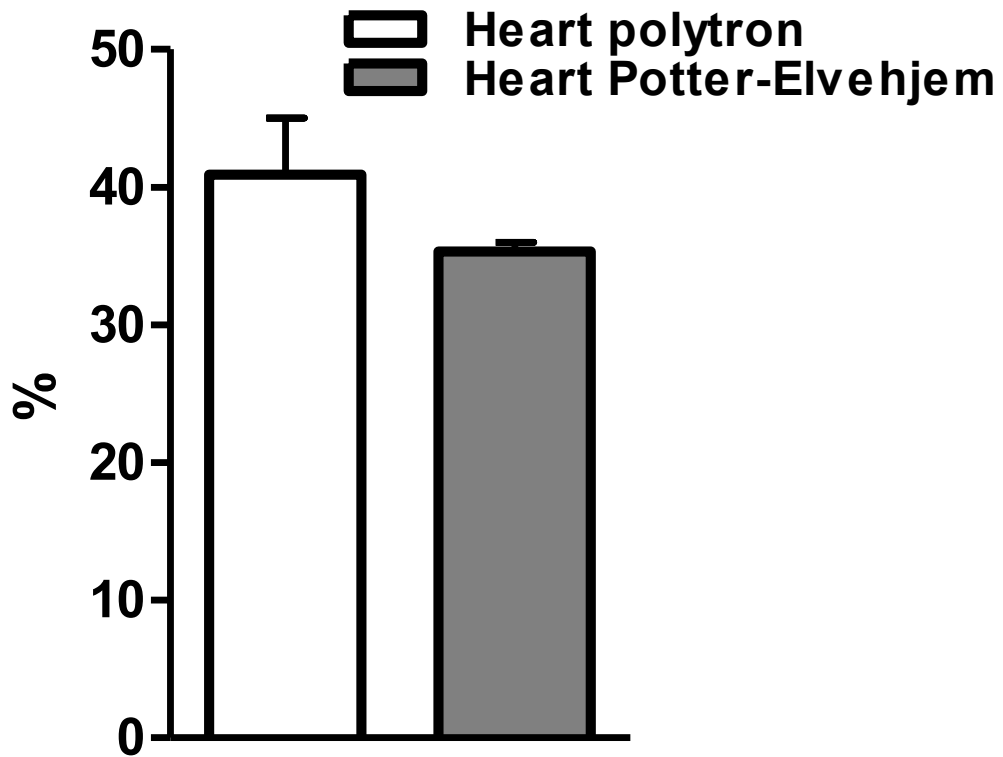


Figure A1

Figure A2. Confocal microscopy images of a frozen section of left ventricular C57BL/6 mouse heart tissue. The presented field shows immunohistochemistry fluorescence of nuclei (Dapi), carnitine acetyltransferase (CrAT), catalase (CAT, a peroxisomal marker), Mitofusin-1 (a mitochondrial marker). Through overlaying the images, CrAT appears to diffusely localize throughout the cytoplasm with a small amount of protein expression residing outside mitochondria and peroxisomes (green colour in the merged image).

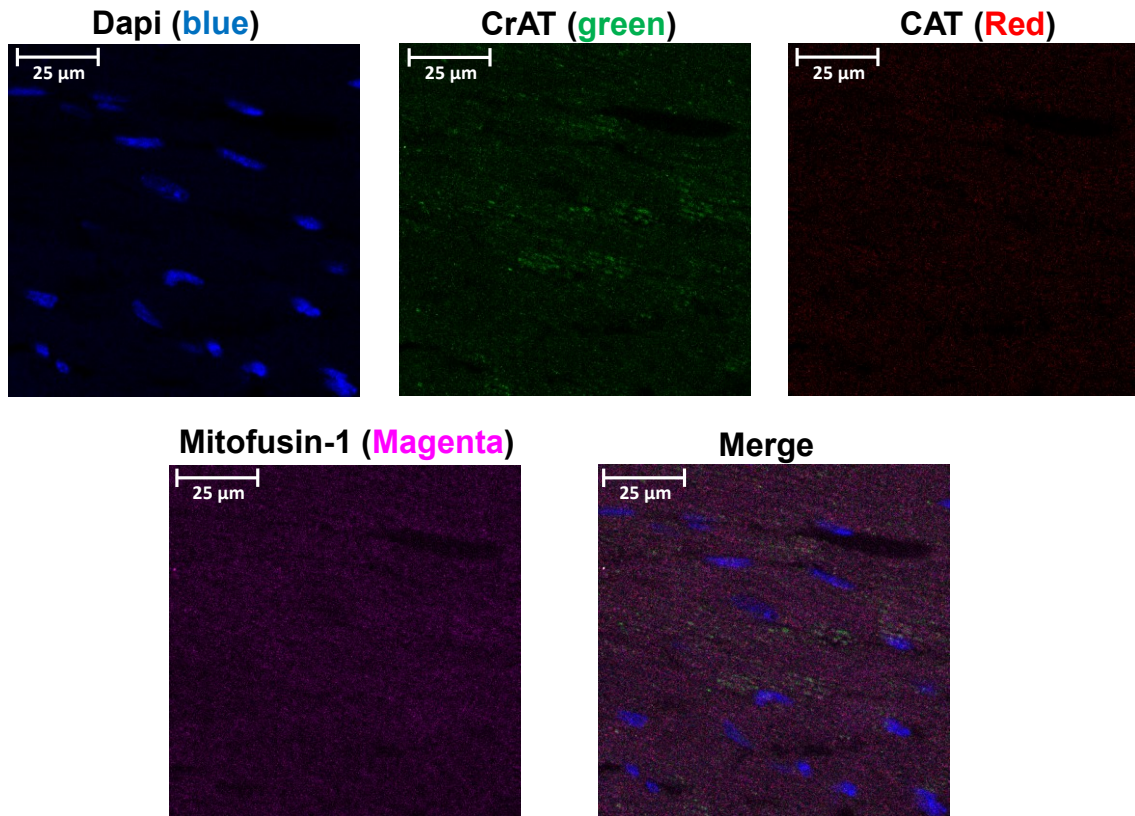


Figure A2

Figure A3. Percentage of mitochondrial breakage in cultured H9c2 cells permeabilized by either a Potter-Elvehjem homogenizer (A), or by digitonin plasma membrane permeabilization (B). Mitochondrial breakage was assessed using citrate synthase activity leakage to cytosolic fractions, n= 3.

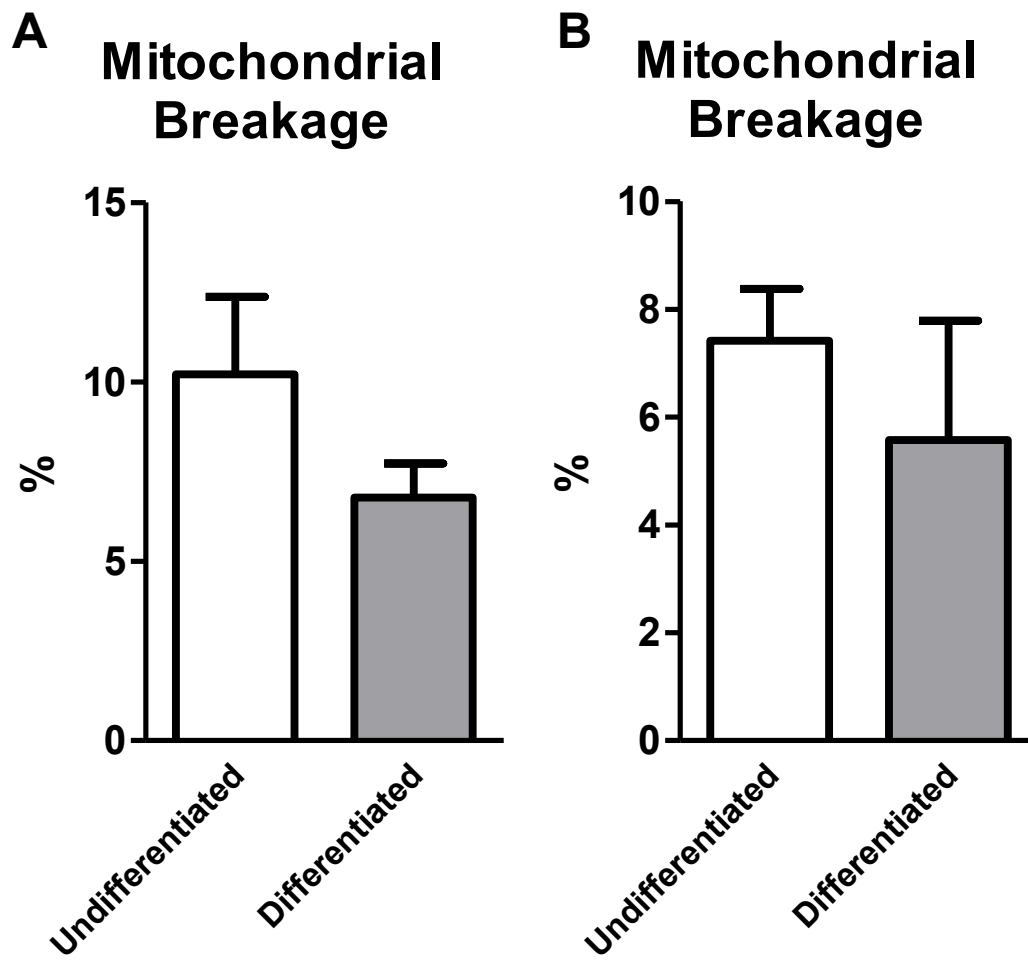


Figure A3

Figure A4. Succinyl CoA levels in heart ventricles of ACC2KO mice as compared to WT controls. Short CoA esters were assessed by UPLC as explained in chapter 2 and 3, n= 6-7.

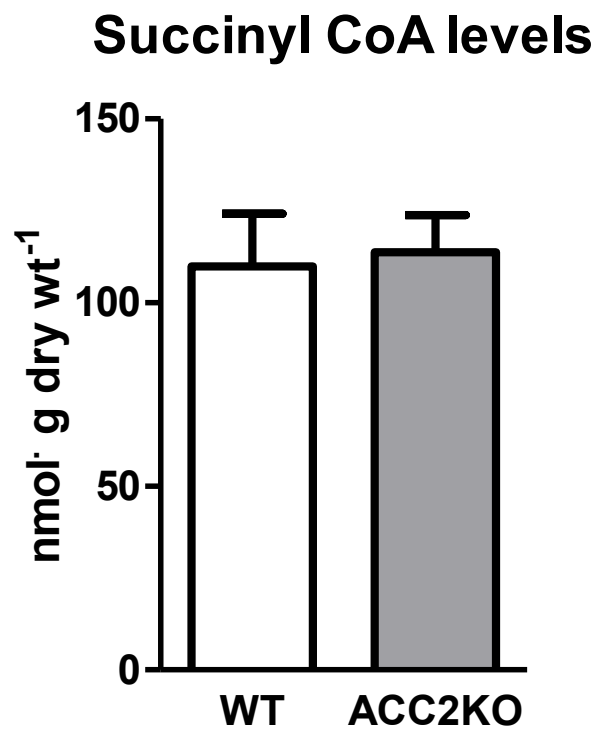


Figure A4

Appendix B: Supplemental Data for Chapter 6

Figure B1. Glucose tolerance test of fasting lean C57BL/6 mice which received three injections of 450 nmol/kg adropin³⁴⁻⁷⁶ or vehicle over 24 hours, n= 7-8.

Glucose tolerance test

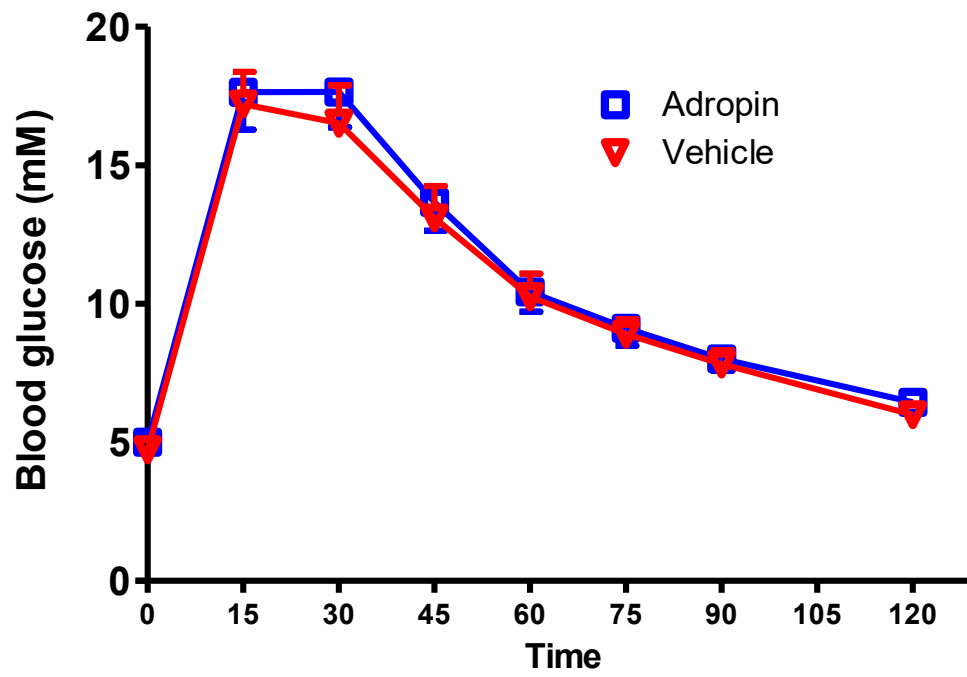


Figure B1

Figure B2. Total protein acetylation (A) and PGC1- α (B) in mouse hearts perfused with *ex vivo* adropin³⁴⁻⁷⁶ (2nM), n= 6.

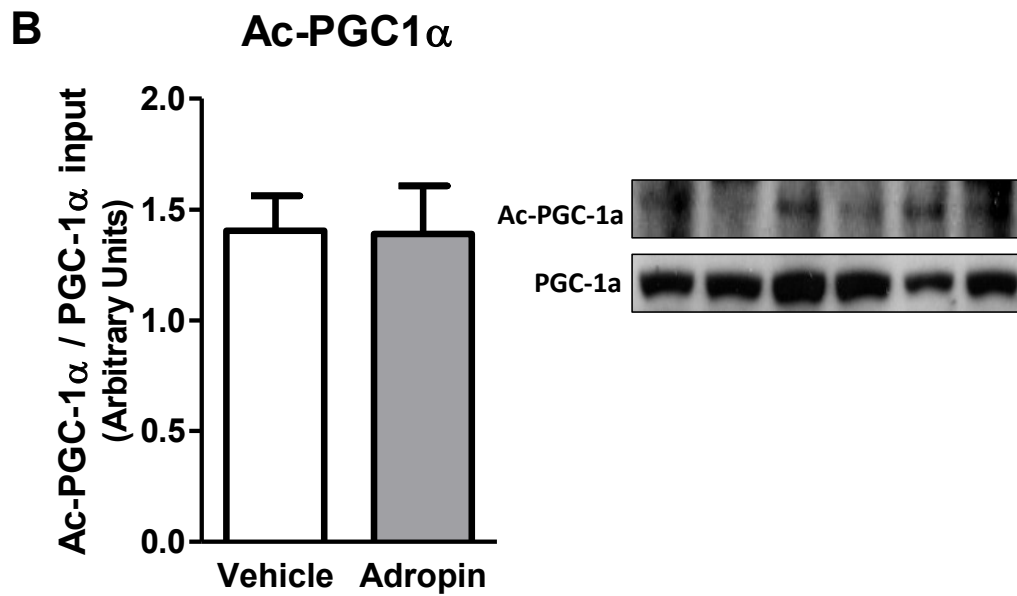
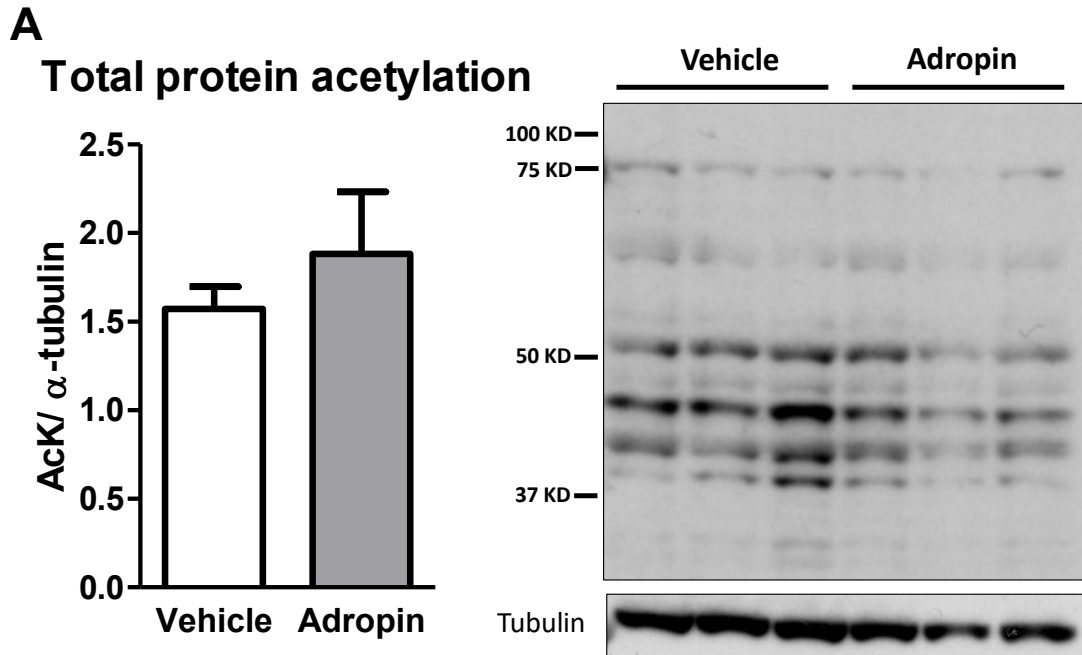


Figure B2